REPORT DOCUMENTATION PAGE

Form Approved
OMB No. 0704-0188

1. AGENCY USE ONLY (Leave blank)	2. REPORT DATE	3. REPORT TYPE AND DATES COVERED
	January 1996	technical

4. TITLE AND SUBTITLE

Tessellator Robot Design Document

5. FUNDING NUMBERS

6. AUTHOR(S)

Kevin Dowling

7. PERFORMING ORGANIZATION NAME(S) AND ADDRESS(ES)

The Robotics Institute
Carnegie Mellon University
Pittsburgh, PA 15213

8. PERFORMING ORGANIZATION REPORT NUMBER

CMU-RI-TR-95-43

9. SPONSORING/MONITORING AGENCY NAME(S) AND ADDRESS(ES)

10. SPONSORING/MONITORING AGENCY REPORT NUMBER

11. SUPPLEMENTARY NOTES

12a. DISTRIBUTION/AVAILABILITY STATEMENT

Approved for public release;
Distribution unlimited

12b. DISTRIBUTION CODE

13. ABSTRACT (Maximum 200 words)

This report documents the preliminary design for a mobile manipulator system to service the Space Shuttle. This document arose from the Mobile Robot Design Course in the Spring of 1991 held at Carnegie Mellon's Robotics Institute. A wide number of issues are addressed including mechanical configuration and design, software and hardware architectures, sensing, power, planning, and a number of design process issues as well. Many comparisons and analyses are presented and much of this work helped formulate decisions and designs in the eventual robot system, and Tessellator.

14. SUBJECT TERMS

15. NUMBER OF PAGES

222 pp

16. PRICE CODE

17. SECURITY CLASSIFICATION OF REPORT	18. SECURITY CLASSIFICATION OF THIS PAGE	19. SECURITY CLASSIFICATION OF ABSTRACT	20. LIMITATION OF ABSTRACT
unlimited	unlimited	unlimited	unlimited

NSN 7540-01-280-5500 Standard Form 298 (Rev. 2-89)

DTIC QUALITY INSPECTED 4

Tessellator Robot Design Document

Kevin Dowling

4 January 1996
CMU-TR-RI-95-43

Carnegie Mellon University

The Robotics Institute

THE ROBOTICS INSTITUTE

Technical Report

Tessellator Robot Design Document

Kevin Dowling

4 January 1996
CMU-TR-RI-95-43

Robotics Institute
Carnegie Mellon University
Pittsburgh, Pennsylvania 15213-3890

Abstract

This report documents the preliminary design for a mobile manipulator system to service the Space Shuttle. This document arose from the Mobile Robot Design Course in the Spring of 1991 held at Carnegie Mellon's Robotics Institute. A wide number of issues are addressed including mechanical configuration and design, software and hardware architectures, sensing, power, planning and a number of design process issues as well. Many comparisons and analyses are presented and much of this work helped formulate decisions and designs in the eventual robot system, the Tessellator.

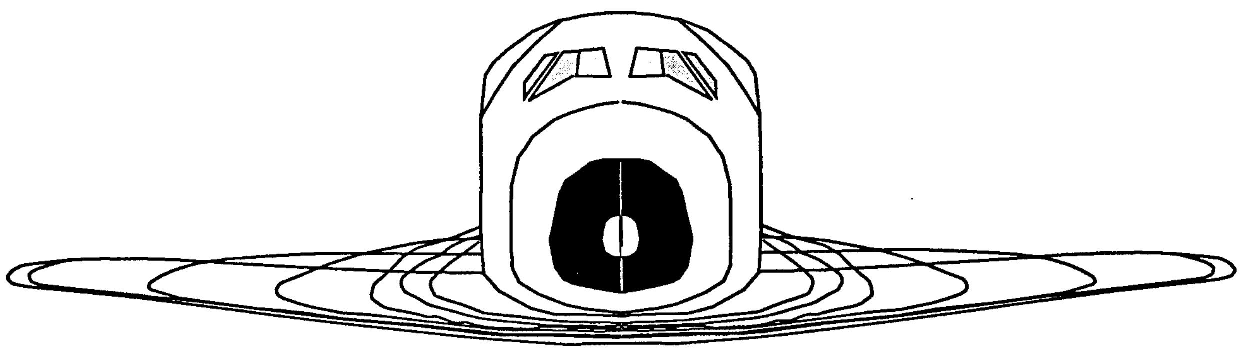

This research was partially supported by NASA NAGW-1175. The views and conclusions contained in this document are those of the authors and should not be interpreted as representing the official policies, either expressed or implied, of NASA or the U.S. government.

Preface

This document arose from the Mobile Robot Design Course in the Spring of 1991 held at Carnegie Mellon's Robotics Institute. Based on an earlier 1990 study, CMU had been awarded a grant to design and build a robot system to service the space shuttle but the funding hadn't arrived by early 1991. This was the first year the mobile robot course had been offered and I saw it as a good opportunity to leverage the activity of a number of students in the Robotics Institute's PhD program into this work.

Tony Stentz, Hagen Schempf, Mike Blackwell, Dave Simon and I designed the course syllabus. We spent the first two weeks covering just the task and facility issues and only then began to work through design issues. Each week individuals or small teams would present the results of their work to the rest of the team and moderated discussions would follow. The class time became a group meeting time to discuss many issues especially those related to integration and design issues. The most productive hours were those outside the class that focused on design issues. From the first day, we felt it was important to capture the ideas and work in a living document and some of the early course work was outlining this report.

This design document reflects the four month activity of the course but doesn't begin to detail the many paths taken, the long discussions and the voluminous material generated. Every one of the students put in an effort far beyond a course of equivalent credit-hours. At the end of the semester the students presented the results of the course to the Institute. This seminar presentation has become a tradition for the design course and a way of marking a milestone for projects that utilize the course.

The document reflects our thoughts and work that spring and many things changed during the summer of 1991 including some vehicle configuration, sensor types and other items. However, the fundamental product, and more importantly, the process of creation came directly from the work shown in this document.

Soon after the course ended, NASA funding arrived and we began a detailed system design. I revisited the document once in a while for a few months, mostly with some cursory edits, but didn't have the time to followup thoroughly. The document lay dormant for several years while Tessellator was being built and through other projects I was working on.

In the fall of 1995, I revisited the document and incorporated changes from several hand-edited copies that I had saved and I then made another complete pass through the document. It was tempting to change details to reflect the eventual design and it was even more tempting to correct ideas and statements that, in later analysis, were faulty. However, I chose to keep the document essentially intact to accurately reflect our thinking in the Spring of 1991.

It's been a wonderful experience.

Kevin Dowling

Acknowledgements

The Design Document was written by the following people:

- Kevin Dowling - Project Leader
- Hagen Schempf - Research Scientist, Group Leader
- Mike Blackwell - Research Engineer, Group Leader
- Tony Stentz - Research Scientist, Course Leader
- David Simon - Teaching Assistant, Group Leader
- Students:
  Vladimir Brajovic, R Coulter, Simon Gatrall, Herman Herman, Goang-Tay Hsu, Sing Bing Kang, Dirk Langer, Bob O'Toole, Ken Rosenblatt, Dan Rossi, Gary Shaffer, Sergio Sedas, Fred Solomon, Hans Thomas, David Wettergreen, Wayne Wong.

This design could not have been created without the input and assistance from Todd Graham at KSC and Bill Spiker at Boeing. The Tessellator system has components from several groups. These are:

- Boeing - Workcell controller.
- CMU - Mobile base, manipulator, navigation system, robot controllers.
- KSC - Program management, liaison to TPS and Safety groups.
- Rockwell - Rewaterproofing tool and associated hardware.
- SRI - Perception for local position registration and anomaly detection.

Other important input came from NASA operations personnel, the end users. As the eventual users of the robot, their input is critical to system use and acceptance.

Followup

Many of the students have gone on to complete degrees and continue their marks on the world:

Dave Simon has completed is PhD and is leading a pioneering medical robotics effort here in Pittsburgh, Simon Gatrall is a lead designer with a west coast firm, Sing Bing is a scientist at DEC research, Bob O'Toole did graduate work at Stanford, further work at CMU and is now at Harvard Medical School, Gary completed his PhD and is a post-doc at CMU, Hans has been working with NASA Ames on several exciting robot missions. Dave Wettergreen is finishing up and will be a postdoc at Ames as well. Sergio finished and taught at Mexico's prestigious Monterrey Tecnologico University and later moved into the private sector with a large robotics firm. All the other students are nearing completion of their degrees and will, without doubt, move into exciting areas in robotics.

1. Introduction

The Space Transportation System (STS) consists of a launch vehicle and orbiter. The orbiters (Atlantis, Discovery, Columbia and Endeavor) are covered with a Thermal Protection System (TPS) consisting of ceramic tiles and blankets that protect the Shuttle from the heat of re-entry into Earth's atmosphere. Maintenance of TPS is laborious and time consuming. Thus, there is considerable interest in methods to assist in this process.

This document details requirements, specifications, rationale, and the design for a robotic system that automates Thermal Protection System (TPS) tasks performed in the processing of the shuttle orbiters. The robot, as envisioned, will be capable of performing tasks that include injection processes and inspection of tile anomalies and defects. The document is a product of a semester-long examination of the problem, applicable technologies and proposes a solution.

The project goal is to design and deploy a robot system in a fast track project for automating specific TPS tasks. This document provides a firm basis for all design decisions in the robot system development and will detail system form and the design process through which it evolved. Questions relating to how the robot system is used and how long they take are outlined in a section on task scenarios. Qualification and certification issues are addressed throughout the document.

It is envisioned that this document will be completed by June of 1991 and our team can go ahead to blueprint, fabricate and assemble the system over the summer months and be testing it by late fall of 1991.

In this section we will provide background for this document, design goals, an outline and acknowledgment of contributors to this design process.

1.1 Background

We assume familiarity with the Orbital Thermal Protection System Automation Study Final Report, October 1990[1]. That study concluded that a number of TPS tasks were amenable to robotic systems. These included rewaterproofing of the bottomside orbiter tiles, surface defect inspection and accurate dimensioning of tile geometries. The study concluded that certain tasks were possible with robotic technologies and were worthwhile for the following reasons:

- **Safety**. Material and chemicals associated with particular tasks are dangerous to humans and require suiting up and the cordoning off of work areas.
- **Time.** It is possible for a single machine to do the work of several people, not only reducing hazard exposures but also man-hours associated with that task.
- **Quality and Reliability**. By providing accurate first pass measurements and verification, rework is reduced. Many of the TPS tasks are characterized by highly repetitive work and the bottomside tile tasks are fatiguing overhead work.

1. Thermal Protection System Process Automation Study Final Report KSC-DM-3491, 1990

- **Paperwork**. The time and paper savings of automating these processes can save many hours and many trees. The incorporation of automated data recording and information transfer will result in high data integrity and the generations of complete and accurate reports.

The report concluded that a number of tasks could be automated without intensive development of new technologies and outlined possible solutions to these tasks. These solutions were preliminary but provided insight to the design issues and possible solutions. The selected processes, tile rewaterproofing and visual inspection, were selected for the following reasons: reduction of orbiter process time, increased quality, the repetitive and fatiguing nature of the process, and existence of required sensor technologies. This document begins where the study leaves off and presents a system design capable of carrying out operations such as inspection and rewaterproofing of tiles.

1.2 Document Outline

The document shows system development from requirements to design:

1) Introduction
    - Overview and background of project and outline of the document.
2) Design Specification
    - Facility, environmental and project constraints relating to robot design.
3) Design Evaluation
    - Criteria are established to compare designs.
    - Based on the specifications, candidate designs are proposed and evaluated.
    - A series of evaluations are followed by a design selection. Detailed and specific analyses are in the Appendices.
4) Task Scenarios
- Given the design selection we answer the following questions:
    - How will the system be deployed, used and stowed?
    - What are the most important considerations in these scenarios?
    - What are estimated times for each activity?
    - What errors might occur and how will they be handled?
5) Configuration Base, Manipulator, Controller, Power
    - The tile robot design.
    - Design details of the mechanics, electronics, actuation, sensing and real-time control.
6) Architecture and Planning
    - Task Controller formulation to handle system interface, planning, execution monitoring and user interface

7) Perception
    - Global and local positioning, safety sensing, and requirements for sensing
8) Conclusion
9) Appendices
    - These are detailed discussions of design issues. For the most part, the main body of the text presents issues and conclusions and the appendices show methods and analyses.

1.3 Design Process

We are planning a 12 month project schedule to develop and build the mobility system. Our first six months of project work are concerned with establishing these issues as well as determining final configuration of the robot. The following period will be the final design, fabrication and assembly of the machine. The last three months are testing and evaluation of the system. This will culminate in an end of year demonstration detailed in the next section.

The first year of design will focus on design and delivery of a mobile base and the design of the appended manipulator.

1.3.1 End of Year Demonstration

The one year development of this project will culminate in a demonstration of a mobile base and elements of overall system capability. The demonstration will use a mock-up of the orbiter underside as the task area.

- The robot will be outside the underside area and the start-up procedure will be demonstrated by an operator.
- The operator will guide the base to the underside using the manual control.
- Maneuverability of the base will be shown through a variety of motion examples.
- Mobile base position will be acquired in the area through a positioning system and the base set-up for beginning task work.
- A camera attached to a fixed platform will digitize an image of the tiles above the base.
- The image will be processed to show extraction of feature information from the tile image. This may be used to demonstrate local positioning capability as well as image analysis for anomaly detection. This work will be done by SRI.
- An autonomous base movement will be made to a new position.
- Several levels of safety will also be demonstrated for obstacle avoidance and system shutdown for a variety of conditions.

Deployment and task sequence are as described in the Task Scenario section. See Figure 1-1 for a plan view of the setup.

Figure 1-1 Demonstration of mobile base and positioning systems

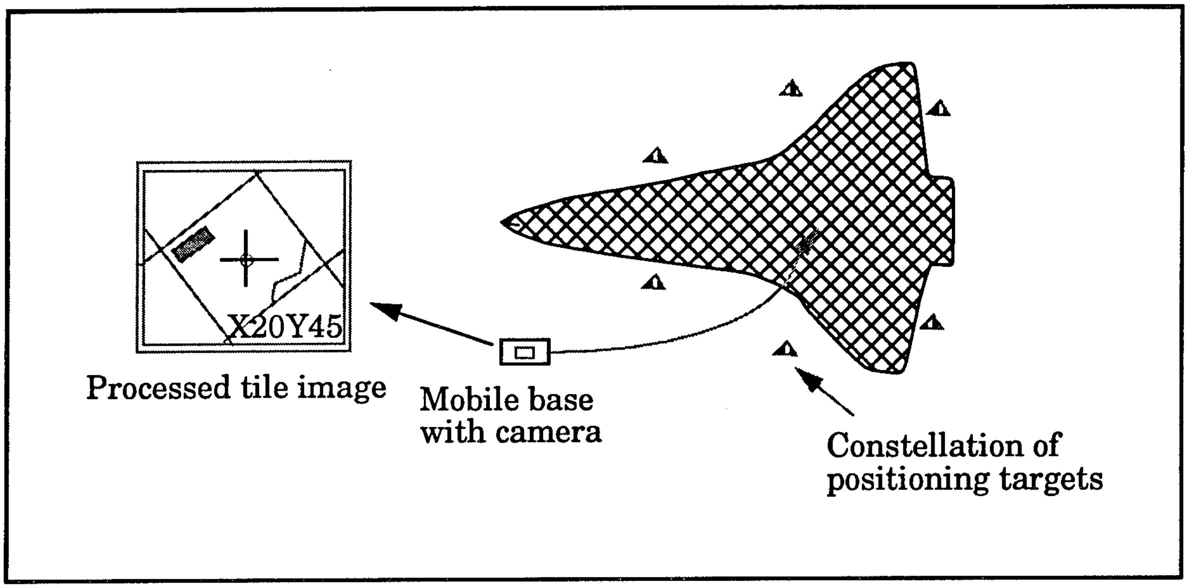

2. Design Specifications and Constraints

This section details system and task specifications for the robot that are configuration independent. These specifications include required capabilities and constraints based on KSC's task needs and facilities and are used to establish a baseline for robot design.

System specifications include:

- Access to greater than 75% of the bottomside tiles. This represents approximately 15,000 tiles.
- Accurately position a tool within a small distance of a hole on a tile. Preliminary accuracies are +/- 3cm base positioning accuracy and +/- 2mm end effector positioning accuracy. Note that while the position of the base must be known to this accuracy, the base does not necessarily have to be placed at that accuracy. Additionally, the size of the eventual tooling nozzle is directly related to the required accuracy. Thus, a large nozzle can reduce positioning needs with respect to a hole. These preliminary figures are based on a 6mm nozzle diameter.
- Autonomous base positioning is desired to facilitate the execution of tasks and reduce manpower requirements and would not require operator intervention. However, supervision may be required for early deployment scenarios due to caution and scepticism by operations personnel.
- Payload for the end-effector is estimated at 25kg. This is based on estimates from Rockwell and SRI. This end-effector includes mounting plate, actuation, valves, injection nozzle, compliance device, cameras, positioning sensors, safety sensing, wiring, and connectors. This does *not* include the wrist mechanism.
- Total rewaterproofing or inspection time is less than 40hrs.This is the current time for three two-man crews to perform rewaterproofing of the orbiter tiles. One of the crew monitors the tiles covered and the other performs the injection. Rough calculations of 20,000 tiles/30 hours. Allowing 2 hours per shift for suiting up, breaks and equipment checks equates to 5.4 seconds per tile. However there are three teams which means a comfortable 16.2 seconds per tile per team. This means the robot system needs to perform the tasks at approximately 40hours/15,000 tiles or 9.6 seconds per tile. To allow for set-up and take down time this time needs to be reduced to about 6 seconds/tile. See Task Scenarios in the following chapter.

2.1 Facility Constraints

Original project requirements specified that the automation of TPS processes should disturb the orbiter flow as little as possible and that extensive facility modifications were not allowable. Any robot which would work with the TPS crew must work in the same environment as they do. The two environments where TPS work takes place are the Mate-Demate Device (MDD) at Dryden and the Orbiter Processing Facility (OPF) at Kennedy Space Center (KSC). There are some common physical constraints between the facilities since they were both designed for easing orbiter access.

Figure 2-1 Plan view of OPF

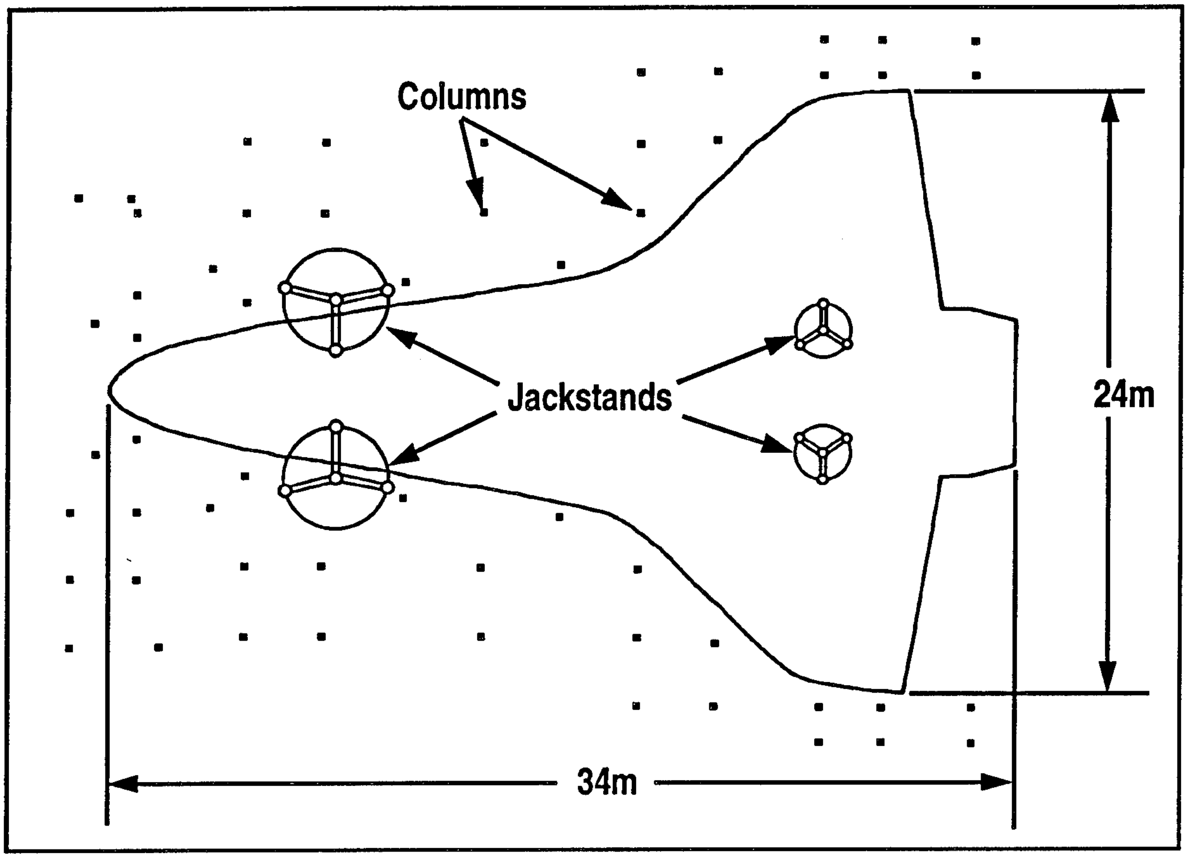

2.1.1 Orbiter Processing Facility

The Orbiter Processing Facility (OPF) is designed to give maximum access to all areas of the orbiter. Work platforms surround the orbiter at various levels and many steel columns support these platforms. Together these platforms and columns and other equipment limit access for a robot vehicle. These structures also dictate upper limits on the robot's size and workspace. The base of the robot must be able to navigate through columns which are approximately 2.5m apart. In order to maneuver around the orbiter, an initial upper bound on the long dimension was determined to be 4.9m. This assumes the ability of the base to turn in place, otherwise a series of "parking maneuvers" is required. This is an upper limit but should not be construed as the only limiting size factor.

The most difficult issue is that the robot must be stowed and lowered to under 1.8m in height to drive under the surrounding OPF platforms. The lowest point on the orbiter in the jacked and leveled position is at 2.9m. The landing gear doors are closed during portions of the time that the robot will be used for TPS tasks. Therefore, those tiles can be rewaterproofed without the robot having to service tiles on the open doors.

The TPS Process Automation Study shows a height of 4.6m to reach the wing tips, which is incorrect. The undersides of the wingtips are actually at 3.9m. The highest bottomside tiles are around the nose, but platform 1, adjacent to the nose, prevents manipulator access to tiles above 4.1m.

Cables and hoses are a common feature of the work area, therefore the robot must be able to overcome 5cm obstacles on the ground without crushing them or causing the system to sway around dangerously near the underside of the orbiter. KSC has affirmed that cable protection in the form of metal channels will be used for the work areas.

The orbiter is supported by jackstands of similar design at both the OPF and the MDD. The front and rear pairs of jackstands are spaced approximately 2.75m apart. We established a clearance distance for the robot by allowing 0.15m on either side. Thus, the robot can have a maximum dimension of 2.45m along the line that joins the jackstands. If the robot shape in plan view is a rectangle, then the long side can be longer than 2.45m and still drive between the jackstands. The upper bound on the long side is limited by constraints in the OPF, and practical concerns of building and transporting a large robot. This is discussed fully in later sections.

Figure 2-2 Elevation view of OPF.

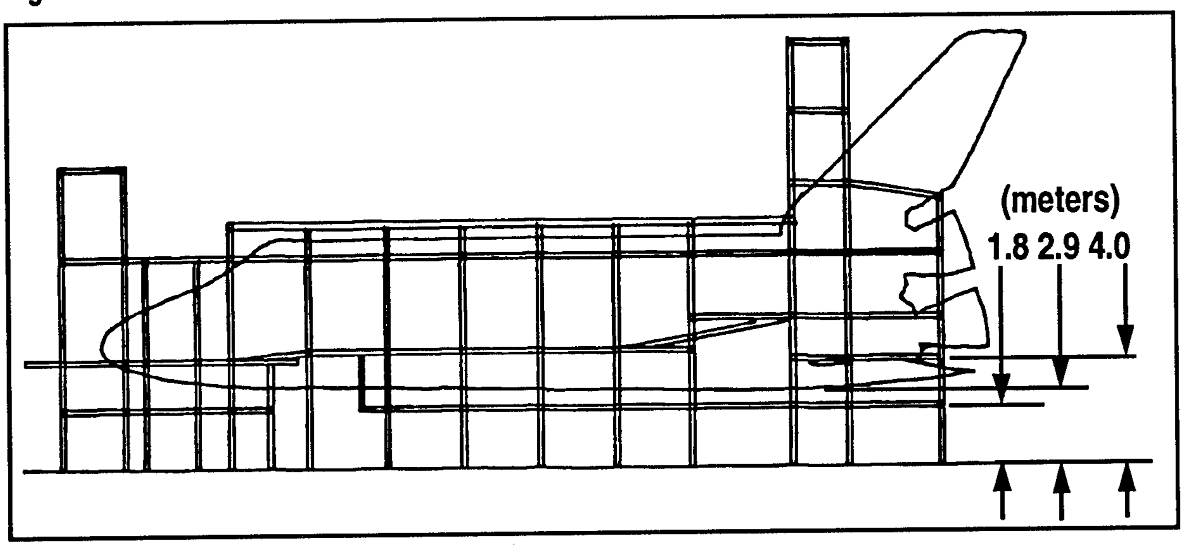

Manipulator Related Aspects

Nearly all the tiles we will service are close to horizontal. See Figure 2-3 on page 16 for iso-contours of the orbiter. For slopes of 45 degrees the highest tiles are 3.9m. T iles higher than 3.9m on the nose are at greater slopes. The only other high slopes are at the wingtips. We detail reasons for limiting slopes in the Manipulation section but will provide some rationale here. The limit of 45 degrees reduces the mechanical complexity of the manipulator and lowers the working height requirements. By reducing mechanism complexity we will be unable to reach only 400 tiles near the orbiter nose. However, a robot which capable of servicing vertical tiles and 4.1m heights would still require clearance from the underside of platform 1, so the loss is less than 400 tiles.

Platform 8 is below the wings at the 2.42m level. It underhangs the leading edges of the wings by about 0.3m and the wingtips by about 0.92m. The leading edges of the wings are covered with Reinforced Carbon-Carbon (RCC) tiles which do not concern this work, but about 200 tiles per wingtip are lost because of the underhanging platform. These tiles are not reachable from below due to clearance and approach problems.

Figure 2-3 Iso-contours of orbiter

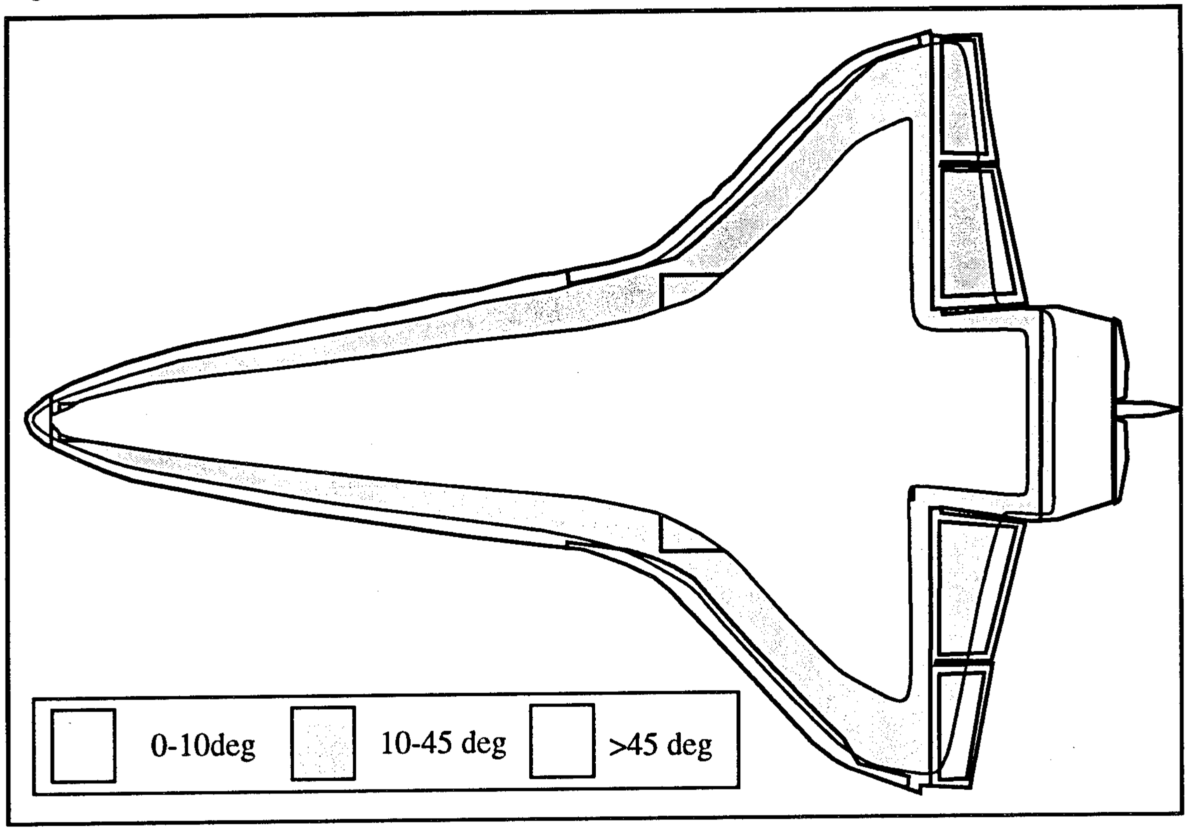

2.1.2 Mate-Demate Device

The Mate-Demate Device, MDD, at Dryden Flight Research Center has better clearance, for the most part, than the OPF. However, the MDD has platforms around the nose and these supports are more constraining than those in the OPF. With the nose landing gear down there is a narrow 1.22m passage between the platform leg and the landing gear. With the landing gear up, the distance between the legs is roughly 3.7m. The position of the orbiter with respect to the ground is specified to be the same as in the OPF. Thus, except for the position of forward platform legs, the MDD can be characterized as a subset of the problems of the OPF.

The MDD does introduce weather and wind factors that are not problems in the sheltered and controlled OPF environment. Wind loads and weather are detailed in NASA Technical Memorandum 82473, *Terrestrial Environment (Climatic) Criteria Guidelines for Use in Aerospace Vehicle Development*, 1982 Revision.

2.2 Environmental and Safety Issues

Following is a list of safety issues and requirements for personnel or equipment operating near the shuttle. The list is by no means exhaustive, and is meant only to highlight some of the most relevant items that will affect the design and use of the tile robot. For a more complete description of these and other relevant items, please refer to the following documentation:

- KSC Ground Operations Safety Plan Vol I, II. Safety Requirements (GP-1098F)
- National Space Transportation System. Limitations for Nonflight Materials and Equipment used in and around the space shuttle orbiter vehicles. (JSC-NSTS 08242)
- Change Sheet for Space Shuttle Ground Support Equipment General Design Requirements (SW-E-0002)
- Procedure for Performance of System Assurance Analysis (DE-P 360)
- Guide for Design Engineering of Ground Support Equipment and Facilities for use at Kennedy Space Center (KSC-DE-512-SM)
- National Space Transportation System, Space Shuttle Ground Support Equipment General Design Requirements (SW-E-0002)
- Thermal Protection System, Material Review Maintenance Procedures (NL0601-9026)
- Thermal Protection System, Standard Maintenance Procedures (ML0601-9025)
- Reusable Surface Insulation (RSI) Acceptance Criteria for Operational Vehicles (ML0601-002)
- Reusable surface Insulation (RSI) Tile Step/Gap Requirements and Acceptance Criteria for Orbiter Operational Vehicles (ML0601-001)

There are a number of additional documents that include requirements for pressurized gas vessels and electrical hazards. Here are some examples of these safety requirements:

Liquids, gases, and materials

There are many flammable and corrosive liquids, gases and materials in continuous use around the shuttle area and great care is taken to eliminate the possibility of explosive hazards. One method limits the amount of dangerous liquid that goes near the shuttle, the other is to eliminate ignition of the liquid via electrical discharges.

The amount of flammable, corrosive and non-flammable liquids in or around the shuttle area is limited to 4oz (30ml). The container must be shatterproof and clearly labeled. The size of the container is specified (30ml flammable, 120ml non-flammable). Additionally, transfer of liquids, such as loading or reloading, in or around the shuttle area is prohibited.

Interestingly, this requirement conflicts with the rewaterproofing chemical storage. The DMES is held in container larger than 30ml. This must be resolved.

Electricity and Electro Static Discharge

A spark can ignite flammable gases, therefore spark generation must be eliminated. Electrical connections cannot be made or broken in proximity to a flammable gas or liquid and all connectors should be designed for one-way-only mating. Electric and electronic equipment must be removed to a safe distance before connections are made.

At 30% relative humidity (RH), Electro Static Discharge can be a problem. All equipment, structures, and personnel must be properly grounded. Signal isolators, power and lines

must be bundled separately to ground. Proper shielding and grounding of power and communication lines is required.

The use of non-conductive materials such as plastics, certain adhesive tapes and polyurethane foam which build up electro-static charge must be avoided.

Spark arrestors, which eliminate arcing, must be included in equipment that operates near the shuttle.

Heat Producing Elements

Heat producing elements must not be left unattended and should not be placed within 3 meters of shuttle vehicle, flammable liquids or explosive materials. This is strange since large heat lamps are used during tiling bonding and curing processes. However, to avoid wrestling with these issues either small halogens or strobes could be used to illuminate camera views.

Radio Emissions

Certain radio frequencies are restricted from certain distance of the flight hardware or launch accessory equipment containing Electro Explosive Devices (EED's)

Portable, hand-held, KSC controlled radio transceivers that operate in the very high frequency (VHF) and ultra high frequency (UHF) ranges cannot transmit over 6.1m.

Mobile, KSC controlled radio transceivers operating in the 170 megahertz range cannot transmit over 15 meters.

Unapproved radio transceivers, Citizen Band and amateur radios cannot transmit over 184 meters.

We are currently examining wireless high speed communications for use with the OPF. One option uses 18GHz frequencies at a very low power level of 25mW. This will be checked to see if wireless data communication is possible in the OPF.

Extraneous Materials

Objects entering the OPF are cleaned before entering the area and equipment must also be checked for excess oil or grease which could cause contamination problems.

Only shatterproof materials can be used. If glass must be used it must be enclosed in a shatterproof container or wrapped with tape to contain pieces if the glass broke. The use of lenses in cameras and other sensors is affected by these specifications. Either an exception to the specifications is made or some style of protected or shatterproof lenses must be used.

Another violation of this requirement can be seen when heat lamps are used to cure re-bonded tiles back to the orbiter. The glass bulbs are exposed. NASA shrugged.

Wind

Operations are restricted or halted when wind speeds are in excess of a recommended range. This is relevant only at Dryden at Edwards Air Force Base. These wind speeds are

detailed in NASA Technical Memorandum 82473. Operations are halted when wind speeds are above 40kph.

Tile Rewaterproofing Operations

Because of the flammability of the injection chemical, DMES, the tile rewaterproofing task requires a part time Safety Professional, an operations task supervisor, and a person from Environmental Health to monitor the concentration of DMES during TPS blanket operations. A control area of 3.0 meters in radius around the injection area must be cleared of people.

Multiple operations will not be performed within the same facility during hazardous operations unless they meet the following requirements:

- Operations can safely and quickly be terminated
- Personnel performing operations are provided a route of rapid exit
- Emergency vehicles must have access in an emergency situation.

Mechanical Design

Lifting equipment should have mechanical stops to preclude exceeding design limitations. Additionally, primary and secondary emergency braking must be provided to prevent drops or load collision in the event of primary brake failures.

All structures must be designed to withstand earthquakes without loss of structural integrity and stability.

Remote stop capabilities must be provided. For example, kill buttons to shutdown system.

Fire Lanes

No operation must block access to fire lanes or incoming and outgoing emergency equipment.

Batteries

During the charging cycle certain batteries, such as lead acid types, generate toxic and corrosive gasses, while others, such as lithium batteries, are subject to leaking. Proper means of ventilation must be provided to exhaust the gasses. Specific NASA documentation describes how to handle a leaking battery. This outgassing effect occurs only during charging operations which are planned to be external to the OPF.

Safety Analysis

System Assurance Analysis (SAA) is used by NASA to identify critical items that may require redesign, as well as catastrophic and non-catastrophic situations which can and should be eliminated via redundant systems or component redesign. SAA is used to assess the risk involved in a current design.

There are seven analyses within SAA:

- Reliability Analysis.

- Critical Assessment
- Failure Mode and Effect Analysis
- Single Failure Point Analysis
- Sneak Circuit Analysis
- Hazard Analysis
- End to End analysis.

Comments and Observations

Due to the number of flammable gasses and liquids that are used in operation such as the rewaterproofing chemical, DMES, NASA is very concerned about potential sources of fire. For this reason, NASA imposes tight constraints on the minimum separation between any flammable element to an electric or otherwise potential spark generating component. This can affect our selection of the robot size, the enclosure and insulation of each of our electro-magnetic components, and the location of the DMES reservoir. There is a clearance of three meters around the DMES application site.

Electromagnetic energy could activate the flight hardware or launch accessory equipment containing Electro Explosive Devices (EED's). This will impose some constraints on the operating frequencies of our design as well as to the degree of EMI shielding that we should provide.

Mechanically, the robot should be designed so that it will not create a hazard in the case of mechanical, electrical or power failure. Besides redundant sensory control, we must consider mechanical means such as cams, brakes, and mechanical stops. Simulation of this can come from a mechanical disturbance of the entire machine.

The robot must be easily removed from the path of emergency equipment. This will be accomplished though use of an operators pendant that shuts down current operation, retracts manipulator mechanisms and allows joystick control of the machine.

2.3 Summary

In summary, the Facility constraints include:

- Required reach of 2.9m to 4.0m
- The system must be retracted to under 1.8m to enter the OPF.
- Width between jackstands is less than 2.45m.
- OPF door access is <3.0m width; < 3.0m height
- Vehicle must overcome 5cm obstacles such as tubing, hoses, wires etc.
- Materials compatibility requirements must be met.
- No hydraulics are allowed due to airborne particulate matter that can affect sensitive hardware in the environment.

- There are a variety of environmental requirements that must be met including temperature, humidity, and wind for each facility.

Project Constraints

- One year from design to demonstration of mobile base and positioning system followed by a year of manipulator implementation and control.

We will meet all regulations and constraints that pertain to the robot system design. However, we have found a number of safety regulations that conflict with current practice and need to resolve these with KSC.

3. Task Scenarios

In this section we present a description of what both the operator and the robot will do in order to service the orbiter tiles. A series of scripts are detailed that show the sequence and times for all actions. Figure 3-1 shows the flow of the basic scenario. The 8-hour work shifts are scheduled into periods of deployment, robot operation (which includes base motion, global positioning, local positioning and tile servicing), and stowage. This basic scenario repeats along ① for each work shift until the orbiter is completely serviced. The development of the scripts is a continuing iterative process that is constantly changing depending on technical and process changes.

Deployment occurs at the beginning of the task scenario with human operators preparing the robot and environment for tile servicing. Robot activities during one work shift require repeated base moves (locomotion), global positioning, local positioning, and tile servicing (manipulation). These repeat along ② for each *area of tiles* within the workspace. Finally human operators stow and secure the robot so that it will be ready for deployment after a period of recharging.

Figure 3-1 Task sequence

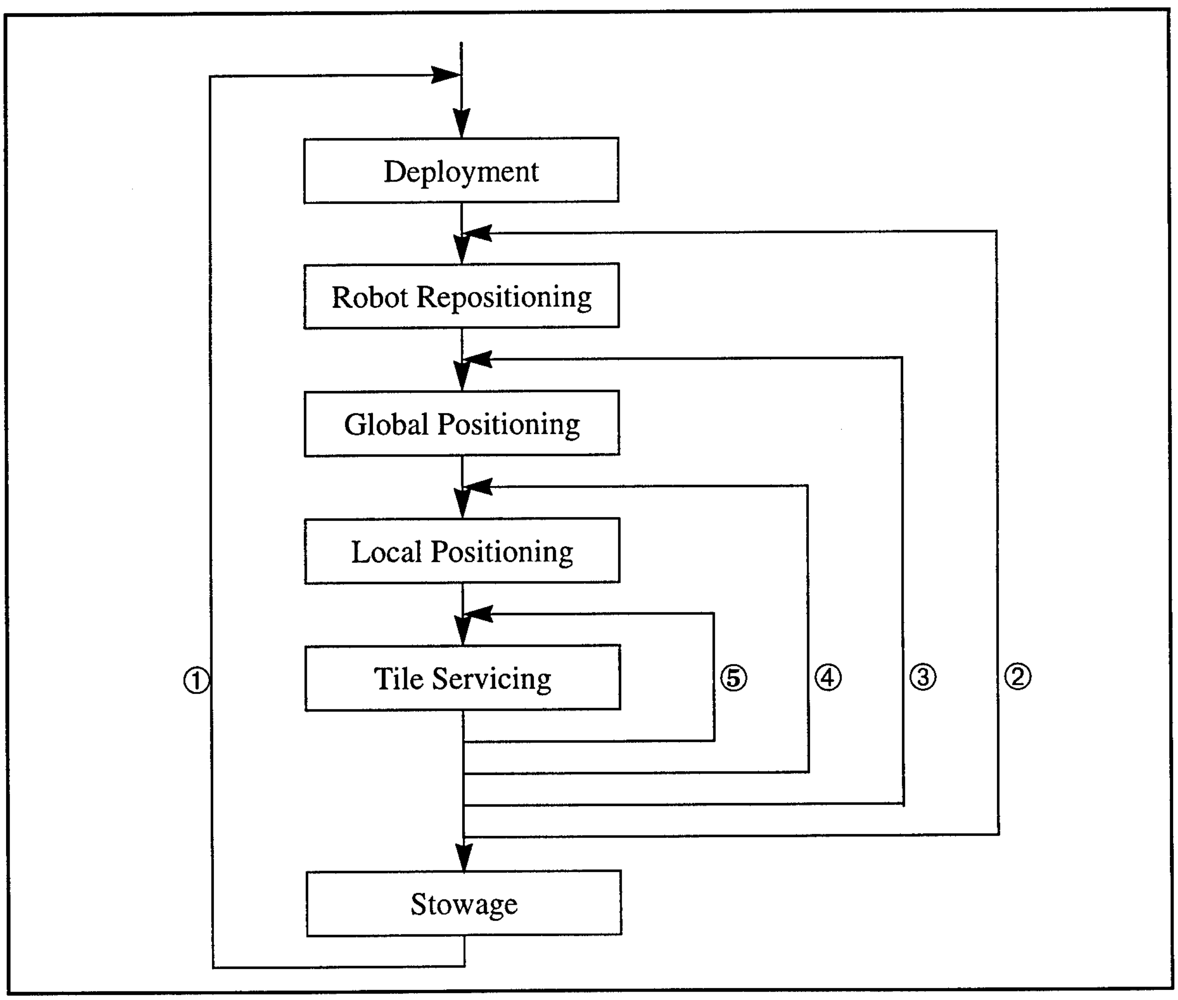

There are several variations of this basic robot operation scenario that are under consideration. The information sequence that flows from global positioning to local positioning to tile servicing must be maintained. Also, global positioning certainly occurs at least once after each locomotion operation. However, it may be possible (although probably not necessary) to repeat global positioning after each tile servicing operation by flowing along ③.

Local positioning is required to localize the end-effector very accurately with respect to shuttle tiles. Local positioning may occur only once per tile servicing, in which case intermediate positions would be extrapolated from known positions and the primary iteration ⑤, or local positioning could occur after every tile is serviced, in which case the iteration flows along ④.

The remainder of this section contains descriptions and discussion of each of the six steps in the task scenario seen in Figure 3-1 and a discussion of error recovery.

Definitions

Some definitions are in order at this point:

- *Workspace* is the area reachable by the manipulator with the base stationary.
- *Work area* refers to the total area coverage by the base in a work shift or session.
- *Region* refers to a subset of the workspace that is used for local position registration.
- *Base Move* is the motion of the robot between workspaces.

3.1 Deployment

Deployment is the process through which the TPS robot system is initialized and positioned to begin working on the orbiter. Deployment occurs once at the beginning of each work shift.

Preparatory actions that occur in previous shifts include recharging the robot batteries, generating work orders, getting flow manager approval, and clearing the workspace for robot activity.

Deployment begins in the OPF Backshop:

1)	Check DMES tank level	15 sec.
2)	Check N_2 tank level	15 sec.
3)	Check battery level	30 sec.
4)	Unplug from battery charger	60 sec.
5)	Power on sensors and actuators	60 sec.
6)	Power on computers (initialization)	300 sec.
7)	Allow controller self-check	300 sec.
8)	Allow mechanical self-check	300 sec.

9)	Check/calibrate tooling package	60 sec.
10)	Check DMES flow	60 sec.
11)	Download task information	150 sec.
12)	Download orbiter information (tile map)	150 sec.
13)	Unplug off-board communications	60 sec.

Transport the TPS robot from the OPF Backshop to the OPF Bay:

14)	Drive robot (100 meters, coarse move speed 0.25 m/sec) OR	420 sec.
15)	Tow or drive robot (100 m, towing speed 2 m/sec) and hitch	300 sec.
16)	Enter through OPF door	300 sec.

Then, once the robot is in the OPF Bay:

17)	Check TPS robot workspace	60 sec.
18)	Activate GPS targets (if necessary)	300 sec.
19)	Verify GPS target	300 sec.
20)	Drive the robot to initial position	300 sec.
21)	Engage stabilizers and perform leveling	30 sec.

The time to deploy the TPS robot, excluding preparatory actions, is estimated at 48.5 minutes (2910 seconds).

In another scenario a complete transfer of tile images is proposed to compare new tile images with old stored images. Physically loading an optical disk for a particular orbiter may be faster and easier than downloading 15,000 images.

3.2 Robot Repositioning

Repositioning the robot involves a sequence of actions that result in the safe locomotion of the base between tile processing areas.

1)	Signal operator (wait for approval to begin locomotion cycle)	(average)60 sec.
2)	Retract and home the manipulator/end-effector	20 sec.
3)	Retract gantry Z-motion to locomotion height	10 sec.
4)	Disengage stabilizers (if present)	5 sec.
5)	Drive the robot base to next position (manual or autonomous)	60 sec.
6)	Engage stabilizers and perform leveling	30 sec.
7)	Extend gantry Z-motion to operating height	10 sec.

The time to reposition the robot from one tile servicing area to another is 3.25 minutes (195 seconds). This operation may involve human operator interaction to approve, supervise and perhaps control (joystick) the motion. Time is reduced by reducing dependence on human operators.

Planning for this locomotion cycle, which includes determination of an obstacle free path, occurs during free computing time in earlier operations so is not included in the time estimate. The global locomotion route (orbiter tessellation with robot workspace) is pre-computed prior to locomotion. The path to the next processing area is determined prior to each locomotion operation. The detection and avoidance of unexpected obstacles occurs concurrently with driving the base and incurs no additional time. The coordination of this planning is discussed in section 6.4 Mobile Base Moves on page 125.

The first locomotion operation following the deployment involves no base motion since the robot is already in position and because a locomotion plan cannot be generated until a global position (the next step) is determined. This may not always be true for different positioning scenarios however, and in that case a base move is made first.

3.3 Global Positioning

Global position is determined through a series of fully automated actions which may include laser scanning, target reading, and computation. The specifics of global positioning are described fully in section 7.2 Global Position Estimation on page 151.

1) Determine global position 1 sec.

No operator actions are required for the TPS robot to determine global position. Global positioning may occur once per base move, periodically during tile servicing or for every tile to be serviced. This frequency of positioning is not yet established.

3.4 Local Positioning

Local position is generated through video image processing of an area of orbiter tiles. The specifics of local positioning are described fully in section 7.3 Local Position Estimation on page 159.

1) Acquire image for positioning 0.1 sec.
2) Determine local position (Average per tile) 3.0 sec.

No operator actions are required for the TPS robot to determine local position.

As noted in the comments to Figure 3-1 on page 23, three scenarios are possible for local positioning. It could occur only once per base move to home the manipulator, it could occur once per region of tiles, or it could occur once for each tile. Only the latter option would not require dead-reckoning and extrapolation of position. The scenario for local positioning is not yet established.

3.5 Tile Servicing

The tile servicing scenario is repeated for every tile in the workspace of the robot. Manipulator characteristics and performance are covered in section 5.3 Manipulator on page 64 and section B. Manipulator Evaluation on page 181. These steps repeat until all tiles in the workspace are processed:

1) Acquire image for inspection 0.1 sec.

2) Extend manipulator/end-effector 0.5 sec.

3) Inject DMES and purge with N_2 3.0 sec.

4) Retract manipulator 0.5 sec.

5) Move manipulator to next tile 2.0 sec.

6) Damp manipulator move 0.5 sec.

Planning for the manipulation cycle (including determination of an order and route of tile processing) is presumed to occur during free computing time in the locomotion cycle and is not included here.

Image processing is needed to extract positions and hole locations using a database of tile information and images. This processing time was established on a per tile basis with 3 seconds as an average upper bound. This is the case if processing occurs on a tile-by-tile basis or if additional processing occurs for a number of tiles simultaneously. This time is not included in tile servicing because it is the result of the local positioning operation described in section 3.4 Local Positioning.

Most frame buffers can capture images in a single frame time which is 1/30 of a second but memory loading will be the bottleneck, so 0.1 seconds is a safe bound on the image acquisition time. However, it may be required to take multiple frames and average them. As as result this time could increase to 0.2 seconds.

Since the end-effector distance to the tile is small the final tooling motion will also be small and quick (about 0.5 sec). Any small translation motions that are required to cover the injection hole occur simultaneously with this motion.

The Rockwell specifications call for a 4 second purge with nitrogen, N_2, after injecting DMES. But only 2 second purge times are actually *required* for purging. Thus, a safety factor of twice the required amount has been spelled out for operations personnel. It may be possible to reduce this required 2 second time with accurate tooling, careful force application and measured timing. In any case, KSC operations personnel have been observed performing the rewaterproofing operation with only a 2-3 second purge time. In this script, a total injection and purge time of 3 seconds is a compromise between the physical requirement and the factor of safety in the Rockwell specifications.

Through careful planning of tile-to-tile motions in the workspace, travel distance can be minimized. For a regular tessellated surface this planning is well understood and can certainly occur ahead of time for any workspace. Thus most, if not all, tile-to-tile motions will be between adjacent tiles (about 15cm) and the move time will average 3 seconds including acceleration, cruising and deceleration for the manipulator mechanism.

Final damping of manipulator motions and stabilizing the end-effector depend on mechanical configuration. Resonances are affected by mechanical structure as are deflections and compliance. For a 1m long pivoting arm these resonances should be small fractions of a second. Thus, with current estimates and no padding, the time may be reduced by as much as 40% for this scenario. See section B.4 Stiffness and Resonances on page 188 for discussion of damping.

The average time to process one tile (not including determining position of the injection hole) is estimated at 6.6 seconds. Evaluating this time is critical because this cycle time dominates the total work time. The work cycle time is multiplied by 15,000 tiles so that if this time changes by only 1 sec/tile then the total work time is changed by (~15000 tiles × 1 sec/tile ÷ 3600 sec/hour =) 4 hours and 10 minutes! As a result, any reduction in this time makes a large difference in total work time.

3.6 Stowage

Stowage occurs at the end of each 8-hour work shift. In the OPF Bay:

1) Drive TPS Robot to final (safe) position	60 sec.
2) Deactivate GPS targets (if necessary)	300 sec.
3) Exit through OPF door	300 sec.
4) Drive robot (100 m, speed 0.25 m/sec) OR	420 sec.
5) Tow robot (100 m, towing speed 2 m/sec) and hitching	300 sec.

Then, in the OPF Backshop:

6) Plug into off-board communications	60 sec.
7) Self-check and shut-down sensors and actuators	300 sec.
8) Self-check and shut down controller	300 sec.
9) Power off	60 sec.
10) Plug into battery charger	60 sec.
11) Battery recharging (8 hours)	28800 sec.
12) DMES refill	1800 sec.
13) N_2 tank refill	900 sec.

Total time, excluding battery charge time, is 90 minutes (5400 sec.). All of these tasks must be performed by the operator. Batteries recharge during the robot's dormant work shift. Thus, the development of a removable battery pack and a means of easily swapping them is of great advantage.

3.7 Exception Conditions

3.7.1 Minor Exceptions

Most processing errors and component failures that occur will result in some time delay in the scheduled processing of shuttle tiles. Processing errors may cause termination of activities but are better characterized as error events that can be detected and recovered from during the task cycle. Each of the possible error modes must be identified and a scenario for resuming normal operations developed. See section 6.5.1 Exceptions on page 135 and section 6.5.2 Exception Handling on page 136 for the design of software to handle exceptions.

The recovery sequence for a processing a minor exception is:

1) Global and local position check
2) Notify operator — Put image, description of problem, all system parameters on queue for operator attention.
3) Wait (if the operator response is necessary)
4) Continue processing

A rough estimate is that on 5% of the tiles the system will fail to inject the tile on the initial attempt[1]. That is, 750 of 15,000 tiles or, for a 40 hour process time, 18.75 failed identifications per hour[2]. If the operator can specify the position of the hole for these tiles concurrent with the processing of other tiles in the workspace then about 18.75 tiles x (6.6 seconds to reprocess - 3.1 seconds not spent processing originally) equals 61 seconds additional per hour that must be spend reprocessing those tiles. An important part of achieving this low failure time cost is that tiles which cannot be processed are sent to the operator for attention and that the operator can determine what to do with the tile before the next base move. For example, pinpoint the position of the insertion hole with a cursor. Note that hole locations are expected to be determined in an initial special pass performed once for each orbiter.

Examples of minor exceptions are:

- Plugged injection hole — the hole can be identified but is blocked
- Indistinguishable injection hole
- Ambiguous single tile discrimination — the system cannot identify the primary or registration tile. This could also indicate positioning error so in addition to the recovery sequence perform a position check.
- Chemical backflow from hole
- Ambiguous position change — could be position system error or slip
- Obstacle precludes motion
- High or continuous rate of processing, planning or calibration exceptions — can become a major exception
- Cameras improperly aligned — difficult to detect
- Camera lens clouded (covered with chemicals)
- Lighting insufficient/saturated
- Power low

1. The 5% comes from an early experiment, by SRI, of the failure rate of the perception system to identify and localize the tile injection hole. It should be emphasized that this is the rate of failure of the first attempt and that in all cases the failure is identified and noted for reprocessing or operator attention.
2. In tile processing scenarios in which groups of tiles are sensed this rate is lower.

Minor exceptions associated with planning include the inability of the planning software to cope with some situations. These exceptions are due to some external influence on the robot that cannot be corrected without additional information and operator assistance. Minor exceptions resulting from wear or calibration problems can be caused by slow deterioration or sudden change of events. They are evidenced by an increasing failure rate by the system.

3.7.2 Major Exceptions

Component failure will likely result in temporary suspension of activities. Some failures can be corrected during processing by restarting, reinitializing or recalibrating. Operating scenarios for process terminating failures and process suspending failures are required to gracefully recover or shutdown from these situations.

The actions of the system in the event of a major exception must occur very quickly and require no initial operator interaction. These actions are encoded directly in the controller which is discussed in section 5.4 Controller on page 97.

1)	All actuators disabled	50 ms.
2)	All brakes locked	500 ms.
3)	Automatic control suspended	50 ms.
4)	Actuated motion killed by expunging all controller command buffers	50 ms.
5)	All incoming automatic commands rejected	10 ms.
6)	Operator notified	500 ms.

Examples of major exceptions:

- Hardware kill signal (heartbeat stops)
- Software kill signal
- Limit switch triggered
- Tilt sensor triggered
- Failure of vacuum system — error achieving vacuum seal
- Failure of injection system (N_2 or DMES)
- Failure of contact sensors — error achieving proper contact pressure
- Controller crash
- Amplifier failure/fault
- Bad encoder readings
- No response to actuation commands
- Manipulator/End-effector forced into contact with tile.
- Insufficient power for commanded task

Again, further discussion of the exceptions can be found in section 6.5.1 Exceptions on page 135.

3.8 Summary

The task scenario for tile processing is the sequence of robot deployment, followed by repeated cycles of locomotion, positioning, manipulation, and finally stowage. This section, the Task Scenario, outlined a script of system operation by decomposing and scheduling each processing step.

We have also been able to characterize operator interaction throughout the process. Operator interaction is *heavy* when the robot is dependent on the external world for information or action. This is the case during both deployment and stowage where data must be transferred and connections must be made and broken. Operator interaction occurs *intermittently* during locomotion and error recovery operations when operations must be facilitated by human intervention. Finally, operator interaction is *light* while the robot is in the autonomous and high speed cycle of tile processing.

Estimated times are roughly 50 minutes for deployment and 90 minutes for stowage. The additional stowage time is due to refills and maintenance at the end of a work shift. Actual work times include base moves between workspaces of slightly over 3 minutes and position determination of only a few seconds. The greatest amount of time in a shift is the tile servicing sequence which is conservatively estimated at 9.6 seconds per tile which includes a 3 second processing time per tile.

4. Design Evaluation

In previous sections we have established a set of requirements based on facilities and task needs and in this section will generate and evaluate designs that are amenable to these. The design ideas were generated through a process of lengthy discussions, enumeration of mechanisms, and thorough investigation of system parameters affected by design choices. This section will conclude with the overall design choice for the mechanism.

In order to comparatively evaluate the designs under consideration, it was necessary to formalize the design evaluation process. The following list outlines the steps which we used to evaluate competing designs.

1) Generate a list of design criteria which are relevant to the designs under consideration. Associate with each criterion on the list a measure of the importance of the criterion to the overall design.
2) For each design under consideration, evaluate the design with respect to each of the criteria on the list generated in step 1. The output of this step is a description of the advantages and disadvantages of each design with respect to the relevant criteria.
3) Based on the results of step 2, select one of the designs under consideration.

We did not attempt to apply this process rigorously, but rather we used it as a guideline for organizing the evaluation process. In particular, the final design decision was not based upon a single number generated as a linear combination of the evaluated criteria. As this chapter will illustrate, most of the designs under consideration differed only slightly when evaluated with respect to the criteria. We believe it is dangerous to rely solely on a mathematical combination of scalar values. Thus, the design selection was ultimately based upon a few of the most important criteria.

The remainder of this chapter presents the criteria that were considered in the evaluation process. This is followed by a description of the candidate designs with an emphasis on how the designs differ with respect to several of the most important criteria.

4.1 Design Criteria

This section presents the criteria which were considered in the design evaluation process. The criteria are divided into three categories: End User Criteria, Performance Criteria, and Design Criteria. Associated with each criterion is a number in parenthesis specifying the importance of this criterion as it relates to the overall design (1= least important, 5 = most important).

4.1.1 End User Criteria

These criteria are related to user satisfaction/acceptance. It provides a focal point for guiding system decisions as well.

- Ease of use during operation (4)
- Reliability (4)

    - Mean Time Between Failure (MTBF)
    - weak links, single point failures
- Supervision/Monitoring (4)
    - operator view of operation
    - operator knowledge of system status
- Deployment (4)
    - required operator interaction -deployment phase
    - setup/takedown time
- Safety (5)
    - failure criticality - potential for human/shuttle damage
    - failure recovery - ease of system removal
- System maintenance (4)
    - serviceability/repair
    - availability of off-the-shelf components
    - modularity

4.1.2 Performance Criteria

These criteria are related to the basic capabilities and functions of the system.

- Maneuverability (3)
    - footprint
    - turning radius
    - ability to straddle obstacles
- Base
    - tip-over stability (5)
    - compliance (4)
    - damping (4)
    - position accuracy (4)
- Arm
    - compliance (stiffness) (3)
    - damping (resonance) (4)
    - position accuracy (4)
- Tile coverage
    - total number of tiles (3)

- number of tiles per move (3)
- Transition time
  - tile to tile (4)
  - base move (3)
- Power consumption/efficiency
  - tethered (1)
  - untethered (3)
- Terrainability (4)
  - ground clearance
  - climb obstacles

4.1.3 Design Criteria

These criteria are related to meta-issues of the design and construction of the system.

- Technical Feasibility
  - critical component precedent (4)
  - critical component analogy (3)
- Scaleability (3)
- Facility modification required / facility access (5)
- Simplicity
  - Assembly (parts count/cost) (4)
  - off-the-shelf components (4)
  - # of DOF's (cost, time,...) (3)
- Packaging/layout/access (4)
- Materials compatibility (5)
- Extensible to other sensing tasks (4)
- Ability to incorporate safety features into design (5)
- Sensing payload/power/cabling (5)
- Calibration (camera/manipulator) (5)

4.2 Design Overview

This section summarizes the major pros and cons of each of the configurations that were considered. All of the candidate configurations consisted of a mobile base with some means of positioning a tool. The two types of mobile base considered were a low-profile base with a single column at its center; and a rectangular "gantry-style" base (an upside-down U-shaped base) with an XY table on top. For use with single-column low-profile

base, three types of positioning means or arms, were considered: a large SCARA manipulator, a small SCARA manipulator, and an articulated Puma-style manipulator. For the gantry-style base, two types of positioning means were considered: a small SCARA manipulator and a Stewart platform.

SCARA refers to a gravity decoupled design that provides selective compliance which is useful for high speed assembly. SCARA stands for Selective Compliance Adaptive Robot for Assembly. Selective compliance is achieved through the use of two rigid planar links and a final vertical motion that is orthogonal to the planar motion and is parallel to gravitational effects.

4.2.1 Candidate Designs

- Mobile base with single column
  - SCARA arm (large)
  - SCARA arm (small)
  - Articulated arm
- Gantry base with x-y platform
  - SCARA arm (small)
  - Stewart platform

Figure 4-1 on page 37 shows a number of candidate configurations. In the upper left is shown an early concept for a walker that clings to the bottom surface via suction. A number of wall-walkers have been made and used for wall-walking and window cleaning. However for reasons of safety, plus results detailed in Tile Coverage and Cycle Time Evaluation on page 40, this configuration is not suitable. In the upper right is shown a typical articulated arm configuration. This is a standard industrial manipulator with a 3 DOF wrist. In the lower left is a Stewart platform which are commonly used for aircraft simulators to provide realistic 6DOF motions. In the lower right is a standard material handling lift using a scissors mechanism.

These and other designs were considered in the course of the design evaluations. In the following sections we will detail advantages and disadvantages of these configurations. For each design we provide a qualitative assessment for particular criteria and brief comments.

Figure 4-1 Candidate designs

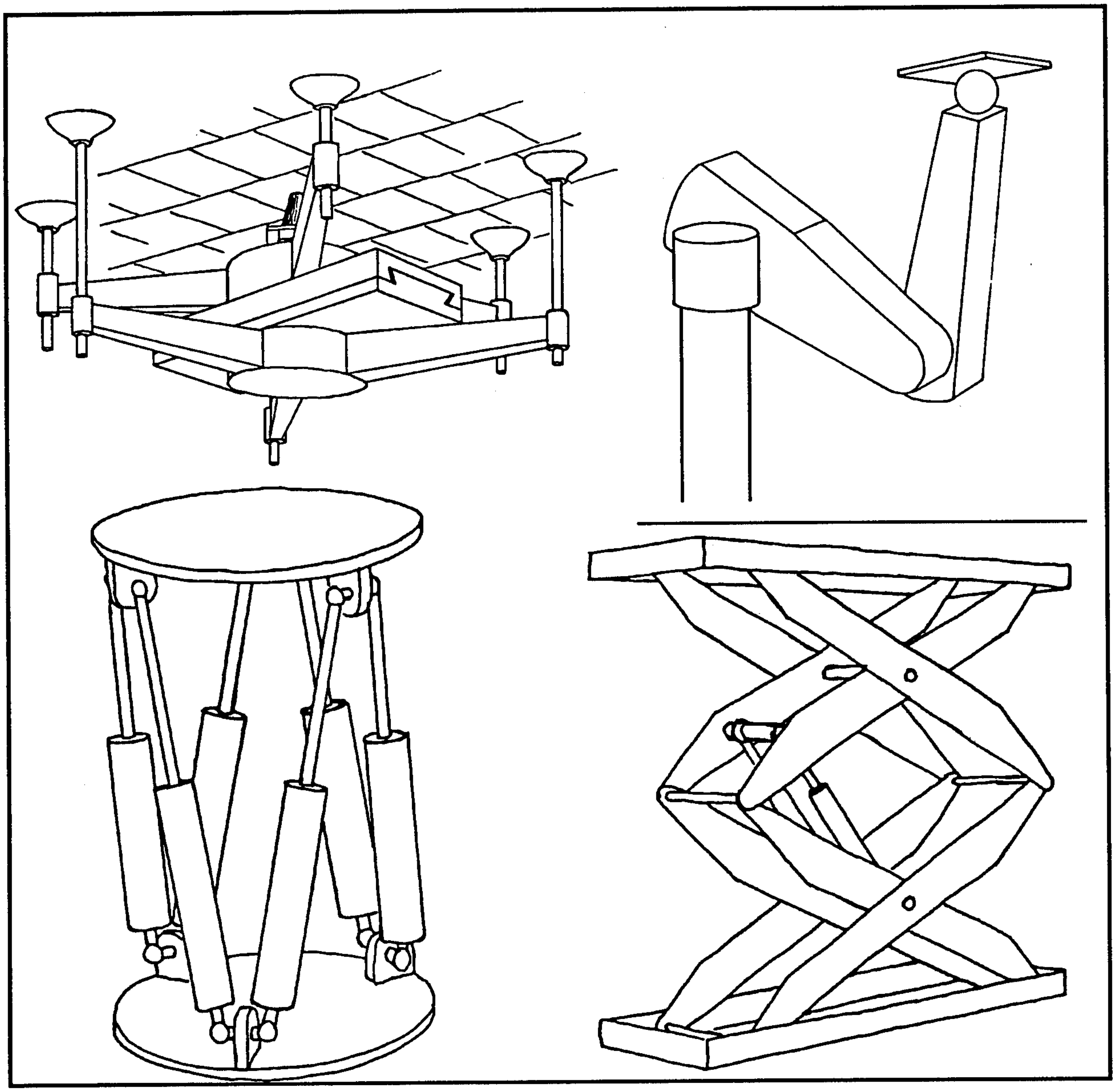

Single-Column Base with Large SCARA Manipulator

This is a 60cm high circular base with a telescoping column at its center. A two-link planar Scara-type manipulator is mounted to the column. The vertical reach of the column would be 4.6m from the ground, and the arm would have about a 1.83m horizontal reach.

- **+** reliability -- relatively few moving parts
- **+** power consumption -- Scara consumes minimal power
- **+** ease of operation -- unobstructed view of end effector
- **+** technical feasibility -- Scara is proven technology
- **+** safety -- low-profile base cannot collide with open landing gear doors

- + transition time -- Scara provides fast manipulator motion
- + high tile coverage
- - technical feasibility -- single-column elevator may be difficult to physically realize
- - safety -- failure of single-column elevator could be catastrophic
- - scaleability -- single column becomes increasingly susceptible to buckling
- - damping -- resonance in structure of elevator and SCARA arm

Single-Column Base with Small Scara Manipulator

This is the same as the above configuration, except the manipulator would have one 60cm link instead of two links, that is, no elbow.

- + reliability -- relatively few moving parts
- + power consumption -- SCARA consumes minimal power
- + ease of operation -- unobstructed view of end effector
- + technical feasibility -- SCARA is proven technology
- + safety -- low-profile base cannot collide with open landing gear doors
- + transition time -- SCARA provides fast manipulator motion
- - technical feasibility -- single-column elevator may be difficult to physically realize
- - safety -- failure of single-column elevator could be catastrophic
- - scaleability -- single column becomes increasingly susceptible to buckling
- - low tile coverage due to size and doughnut-shaped workspace.

Single-Column Base with PUMA-Style Articulated Manipulator

This is similar to the above configurations, except the column is shorter to accommodate the different style of manipulator. The biggest disadvantage of this configuration is the horizontal reach of the manipulator. To access a reasonable number of tiles from one location of the base, the arm has to have several feet of reach. An articulated arm's actuators are vulnerable to gravity when it stretches out horizontally.

- + reliability -- relatively few moving parts
- + ease of operation -- unobstructed view of end effector
- + technical feasibility -- ndustrial arms are a proven technology
- + safety -- low-profile base cannot collide with open landing gear doors
- - safety -- actuator failures in the PUMA could be catastrophic
- - power consumption -- PUMA is much less efficient than the SCARA
- - limited payload at the end effector
- - safety -- manipulator workspace is complex

- calibration - deflections and low-frequency vibrations in the arm could be large
- lower tile coverage -- intersections of sperical workspaces is inefficient.
- transition time -- increased due to larger number of actuators to be servoed
- technical feasibility -- single-column elevator may be difficult to physically realize
- safety -- failure of single-column elevator could be catastrophic
- scaleability -- single column becomes increasingly susceptible to buckling

Gantry-Style Base with Small SCARA Manipulator

The gantry-style base was inspired by commercial straddle cranes. This robot design would consist of an XY table, or gantry, mounted on top of a straddle-crane-like base. A 1-link planar SCARA-type manipulator would be positioned by the XY table.

+ very high tile coverage
+ transition time -- XY table provides fast tile-to-tile motion
+ safety -- humans are below envelope of arm motions and cannot interfere.
+ maneuverability -- manipulators on the gantry-style base can overhang some ground obstacles
+ power consumption -- SCARA consumes minimal power
+ excellent arm positioning accuracy due to XY table
+ technical feasibility -- XY tables and SCARA manipulators have precedent
+ packaging -- a lot of room in the base

- reliability -- more actuators
- ease of operation -- view is obstructed by gantry
- maintenance -- more moving parts
- simplicity -- lots of actuators to control

Gantry-Style Base with Stewart Platform

This is the same gantry-style base, but with a 6 degree of freedom Stewart platform instead of a planar SCARA-type manipulator.

+ transition time -- XY table provides fast tile-to-tile motion
+ safety -- humans are below workspace of arm
+ maneuverability -- gantry-style base can overhang some ground obstacles
+ excellent arm positioning accuracy due to XY table
+ technical feasibility -- XY tables and Stewart platforms have precedence
+ packaging -- a lot of room in the base

- reliability -- more actuators

- ease of operation -- view is obstructed by gantry
- maintenance -- more moving parts
- simplicity -- lots of actuators to control

4.2.2 Preliminary Configurations

We have enumerated the advantages and disadvantages of a number of mechanisms and concluded that two of configurations make the most sense for this problem. They are illustrated below. They are the single-column lift and the X-Y gantry with single-link Scara. We will now examine other issues to help us further decide between configurations.

Figure 4-2 Candidate configurations.

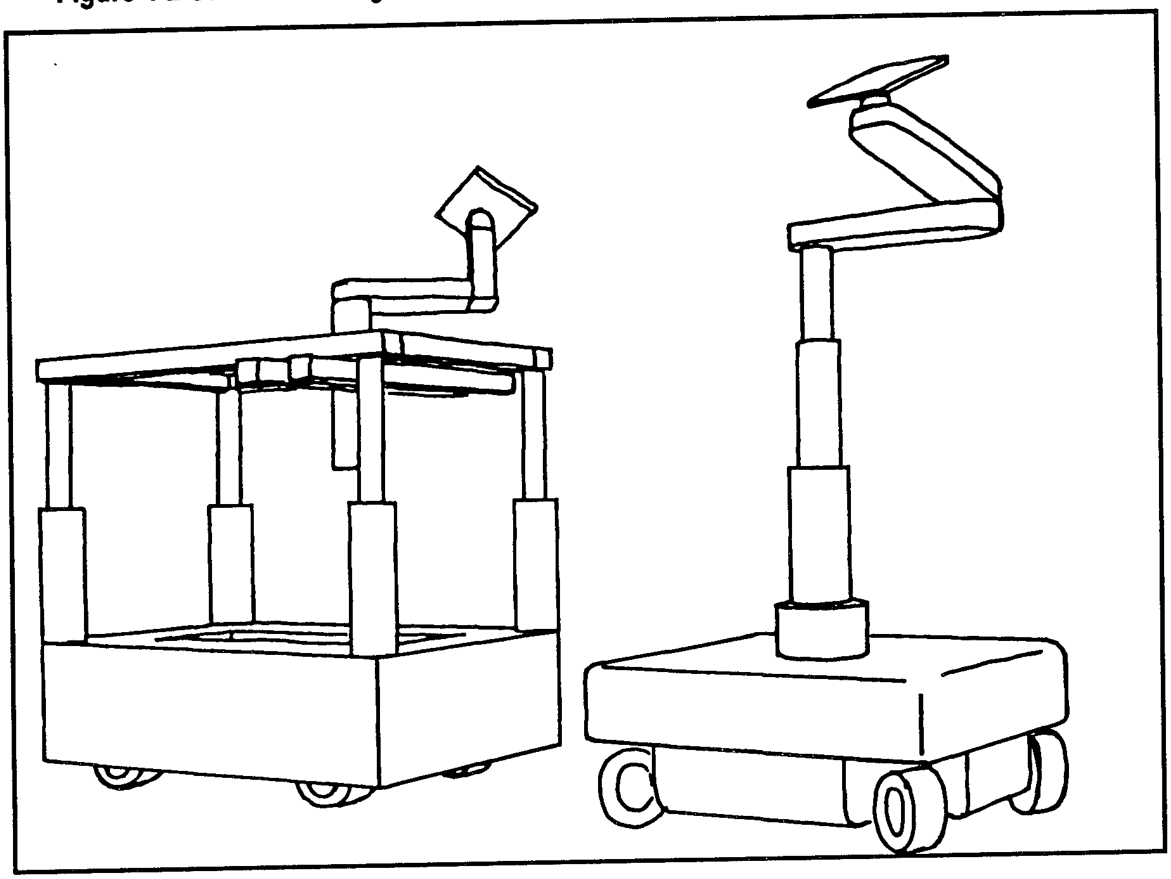

4.3 Tile Coverage and Cycle Time Evaluation

All of the designs under consideration have a mobile base and a manipulator which can service some given number of tiles per base move. It may prove important to determine the effects of a larger or smaller base or a round or rectangular workspace on the total task time. In order to better evaluate the designs we needed more qualitative and especially more quantitative information. We started with hand drawn studies, and ended up with some generalized formulas which helped shape the final design selection.

4.3.1 Base Tessellation Analysis

Base tessellation refers to the tiling patterns of the robot workspace across the total area of the orbiter to be serviced (the task-space). The first important observation about tessellating the workspaces is that there are always some inefficiencies in coverage due to overlap. If the task-space was a regular shape, a rectangle for example, a workspace could be designed to tessellate the task-space perfectly with no wasted moves or overlap. Since orbiter is not a regular shape, and there are many obstacles in the MDD or OPF, it was important to determine the effect of this overlap. We use the term *efficiency* to refer to the ratio of non-overlapped spaces to total area.

Based on our initial understanding of the mechanical constraints and our knowledge from Facility Constraints on page 13, we chose a set of 7 different workspaces to compare. They included 4 different SCARA robots, and 3 gantry robots. The process involved drawing outlines of the workspace on scale drawings of the orbiter outline, trying to tessellate the task-space as efficiently as possible.

Figure 4-3 Sample tessellation

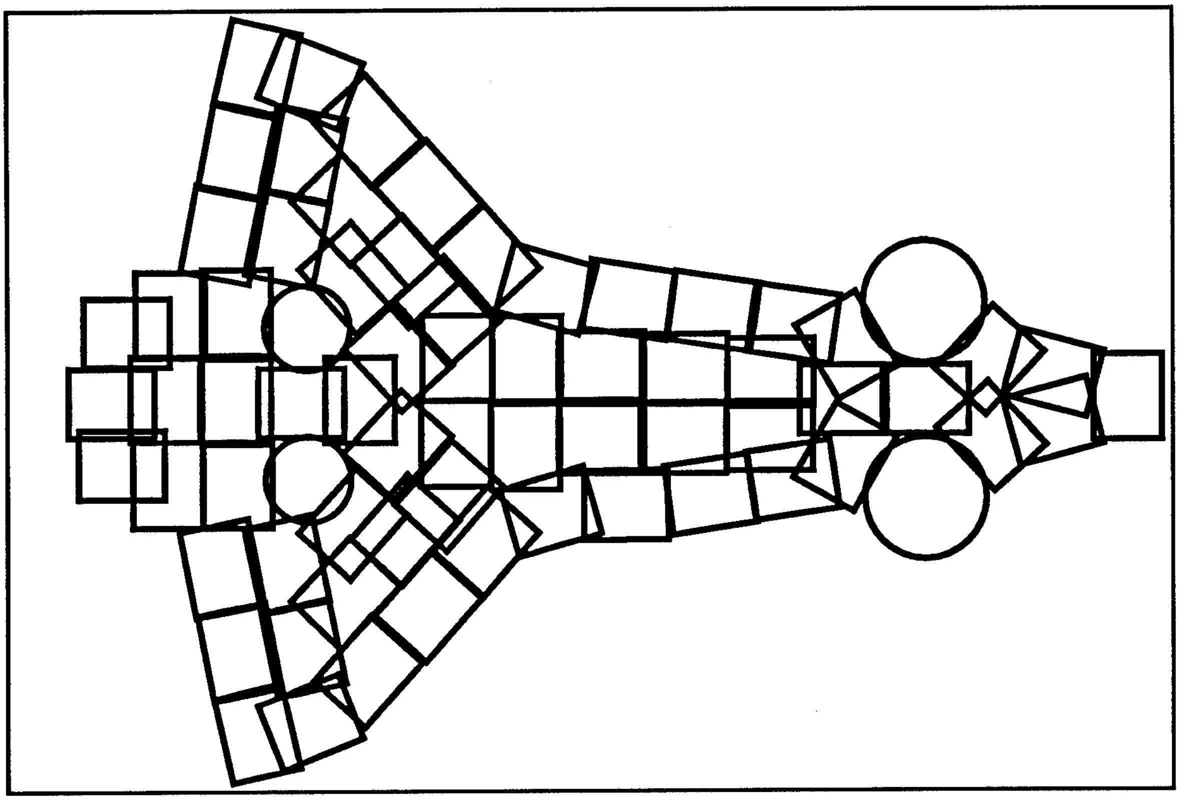

Figure 4-3 shows an example of results we obtained. This figure is for a gantry robot with a 2.5m by 3.0m workspace. Note that in the center, the workspaces can be placed adjacent to each other for minimal overlap. However, almost everywhere else, especially around the jackstands, several base moves requiring overlap are necessary to service as many tiles as possible. Also worth noting is the importance of locating and orienting the base accurately to achieve optimal tessellation. All of the base moves along the edge require careful movement to avoid platforms and columns around the edges. The jackstands are

also tricky to plan around, and they prevent the robot from reaching tiles directly over the jacstand supports. This affects configuration issues such as manipulator over-reach beyond the edge of the base.

The manual studies provided initial estimates of the number of base-moves required for the given configurations. Smaller workspaces require more moves, and a certain amount of overlap is required to tessellate the entire task space. The question is how does this affect total task time?

4.3.2 Timing Analysis

The next step was to develop insight to give total task time based on the configuration. The basic generalization involves viewing the tessellation of a given base as a function of efficiency and workspace. The efficiency is the average percentage of the workspace which can be used during each base move. The following equation describes the relationship between the total time and a given base design's parameters.

Figure 4-4 Relationship between time and efficiency.

T_t = time to service a tile

N_t = number of tiles to be serviced.

B_t = base planning and move time

e = efficiency

N_w = number of tiles in workspace

(3600 is the conversion factor between seconds and hours)

$$\text{Total} = \frac{Tt \cdot Nt + \dfrac{Bt \cdot Nt}{e \cdot Nw}}{3600} \qquad \textbf{Eq. 1-1}$$

While efficiency appears as a variable in this equation, it is really a function of the interactions between workspace and the task-space. Empirical studies gave us a range of efficiencies between 0.55 and 0.67. Logically, a robot which serviced only one tile per base move would have an efficiency of 1.00, however it would require 15,000 base moves. Any robot with a reasonable number of tiles in its workspace will not be 100% efficient due to imperfect overlap of base moves.

Figure 4-5 Total time as a function of efficiency and workspace

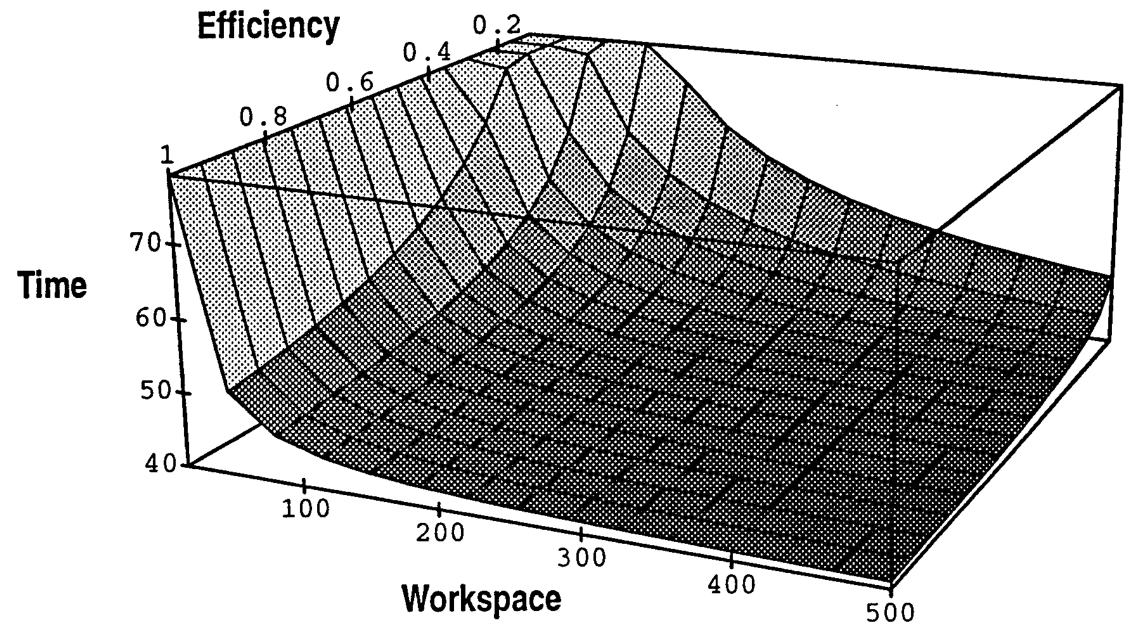

Figure 4-5 illustrates the effect of efficiency and workspace on total process time. Only small workspaces and low efficiencies show a significant adverse effect on the total task time. If the workspace is over 150 tiles the total time is only mildly affected by efficiency. The vast majority of this graph is relatively flat.

The tile servicing time, as discussed in Task Scenario, has a great effect on overall time. Another way of looking at the problem is illustrated in Figure 4-6 which shows that tile servicing time is critical to total task time by comparing the effects of time to service a tile and the time to move the base. With approximately 15,000 tile servicing steps and only a few hundred base moves at most, it is fairly intuitive that this would be the case. However it is important to note that a *reduction of 1 second on the tile time results in an approximate 4 hour reduction in total task time.*

Figure 4-6 Task time as a function of tile and base times

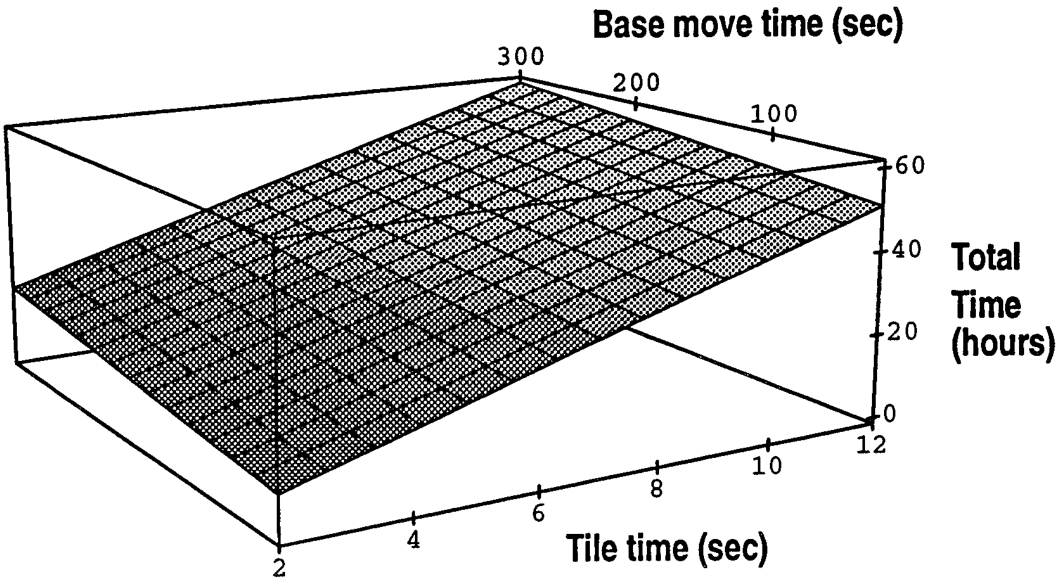

With these results, we have now established a lower bound on the workspace required of the machine to carry out the tasks in the time needed. But there are other factors in deployment and use that can affect the evaluation. From Figure 4-5 we show a general range of useful efficiencies and workspaces. From the manual tessellation studies a conservative efficiency of 0.6 was estimated to be a lower bound and although Figure 4-6 shows that base move time is not as critical as tile servicing time. The base movement time includes some level of human operator interaction.

Base moves and their effect

While it appears that workspace size greater than 150 tiles does not have a strong effect on the overall time, it does affect the number and frequency of base moves. If operators are required to interact every few minutes with the system for monitoring base moves then the attractiveness of the system to users is less than one that needs infrequent attention. A goal of approximately one base move per half-hour was set. Figure 4-7 shows the relationship between moves and workspace size. Once per half hour translates roughly into 80 moves during the course of rewaterproofing the orbiter. This results in a workspace of 300 tiles. A reduction to 250 tiles in the workspace gives 100 moves, or a base move every 24 minutes.

Figure 4-7 Total time as a function of workspace size.

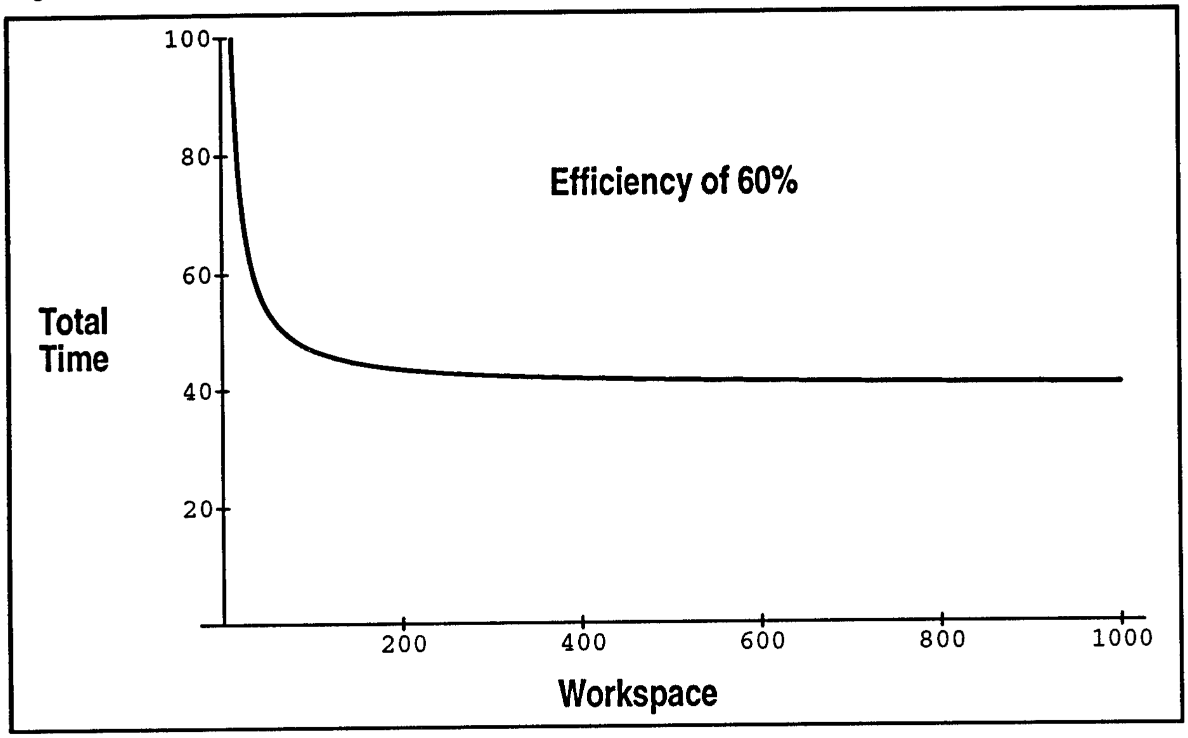

4.4 Manipulator Configuration

The issues of importance in selecting the appropriate kinematic configuration can be split into several clearly identifiable groups. These individual criteria can then be applied to the proposed configuration candidates to distill the most promising design. This section will evaluate each criteria individually and comment on its impact for each of the design candidates followed by a design selection.

4.4.1 Design Criteria Evaluation

The design evaluation criteria are the following:

Workspace (size and uniformity)

The important constraint of maximizing *horizontal* workspace acreage has a drastic effect on the choice of manipulator kinematics. For a given base move, any manipulator configuration should be able to reach the same workspace at any elevation. This criteria directly affects the industrial-arm configurations, as the spherical-like workspace at full extension implies a varying reachable plane for different extensions. A Scara manipulator configuration on the other hand, has a constant workspace independent of elevation - the workspace can be varied by varying the overall reach of the serial-link mechanism.

Complexity (mechanical and control, technical feasibility and precedence)

The inherent complexity of a manipulator design results from interactions of mechanical and control issues. Even though industrial-arms and Scara manipulators have been on the market for years and achieved certain levels of reliability there are clear distinctions one can make at the controller level. The reduced level of controller complexity and reliability

of a non-redundant mechanism, such as a Scara arm, with a lack of multiple solutions for a given endeffector position, has direct advantages in control and planning, and results in additional levels of inherent safety. Whether an industrial-arm, Scara, or Stewart-platform configuration is selected, all technologies have extensive track records and can be deemed suitable candidates. The differing levels of complexity and thus reliability at the mechanical and controller level are understood and solvable.

Mechanical Configuration (size, weight, power consumption, payload and accuracy)

However, very few of the currently available commercial manipulators are suited for the metric of minimizing weight while maximizing reach. Most of the industrial arms, scara and stewart-platform manipulators were built to be stationary devices bolted to the factory floor. As a result, the final manipulator configuration would probably be a custom design. The scara configuration has increased payload and reduced power consumption as compared to a industrial serial manipulator. Since power consumption will have to be minimized a scara would be preferable. The overall accuracy in XYZ-positioning for gravity-decoupled manipulators is usually equal if not better than in other manipulators, where joints have to counter the effects of gravity. Accuracies are comparable for the different proposed manipulator configurations, and are mainly dependent on the overall reach required, since endpoint accuracy is usually determined through angular positioning accuracy.

Safety (of shuttle and operator)

The safety margin of any mechanical device in the face of different failure scenarios is also an important criteria. A power failure requires brakes to prevent uncontrolled motions. A problem with the planner or controller in the case of an industrial manipulator may result in the elbow of the manipulator contacting the tiles on the underside of the shuttle. Even though these may seem to be unlikely scenarios, the possibility for such catastrophic behaviors is always present, and designs have to be judged accordingly, requiring modifications or elimination of a particular configuration.

Maintenance (reliability and availability of generic/custom parts)

As we mentioned earlier, the eventual manipulator configuration will most probably involve a custom design. In order to minimize the cost of parts, machining, and maintenance, the design will have to stress the need for using mature, proven and tested technologies and componentry. The final design will also have to take into account how serviceable the system is, in the event a component fails and needs to be replaced. The replacement will have to be easy and require little time.

Kinematic/Dynamic Behavior (compound motions, kinematics, resonances, damping, speeds)

To position the tooling and sensing in XYZ space with arbitrary orientation, a number of joints need to change position. The degree of position change and the number of joints (degrees of freedom) involved in such 'compound' motions is an indication of the controller and planner complexity. It also affects overall power consumption which we desire to minimize. Such constraints clearly impact the differences between a Puma and a Scara manipulator configuration. The former will always require compound motion for any trajectory and thus consume more energy than the latter. The Scara configuration requires

only planar motions and orientations, thus minimizing overall motion amplitudes, complexity, and total power consumption.

The size and weight requirements for a given manipulator design have to be weighed against the resulting structural and joint resonances which can limit bandwidth and thus system performance. This is extremely important as time lost during motions due to low response times, system damping and overshoot is multiplied by the large number of tiles being serviced. Thus the final configuration will have to consider proper component selection (powerful motors, stiff transmissions), and appropriate sizing (number and length of links) and weight distribution (structural weights and endeffector payload).

4.4.2 Configuration Evaluation

It is important to enumerate the benefits and trade-off between a single-column Scara manipulator configuration, and a four-column gantry single-boom manipulator configuration, as shown in Figure 4-2. The main difference between these two designs, is their reachable workspace. A top view of the area covered by the different configurations is shown in Figure 4-8.

Figure 4-8 Workspace tile coverage

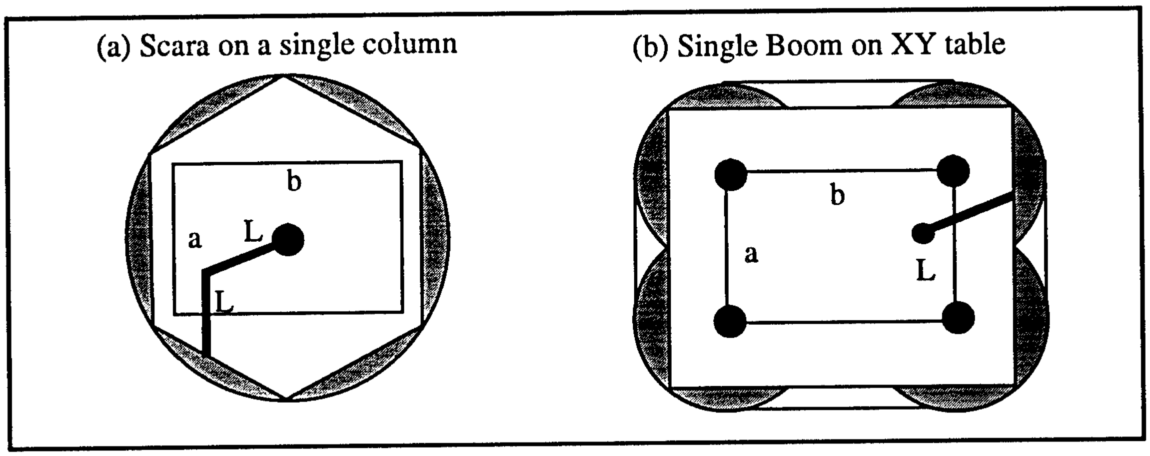

The workspace of the gantry robot clearly depends on the size of the base and the manipulator boom length, while the single column design is only affected by the length of the manipulator itself. The equations for areas covered are:

$$^{SCARA}A_{circle} = 4\pi L^2 \qquad \textbf{Eq. 4-1}$$

$$^{XY}A_{rectangle} = [(a+2L)\ (b+2L) + \pi L^2 - 4L^2] \qquad \textbf{Eq. 4-2}$$

The optimum area coverage for the circular and rounded rectangle workspaces, can be represented by a hexagon inscribed within the circular workspace of the single column Scara workspace, and the largest rectangle inscribed within the rounded-corner rectangle of the gantry workspace (see Figure 4-8). The two equations describing the maximum area covered for a compact tessellation geometry, are given below:

Eq. 4-3

$$A_{optimum}^{hexagon} = 4\eta\pi L^2 = \frac{3\sqrt{3}}{2\pi}4\pi L^2 \approx 0.828 \cdot 4\pi L^2$$

Eq. 4-4

$$A_{optimum}^{rectangle} \approx \{ (a-\sigma) + 2L\sin\left[\operatorname{atan}\left(\frac{b}{a}\right)\right]\} \{ (b-\sigma) + 2L\cos\left[\operatorname{atan}\left(\frac{b}{a}\right)\right]\}$$

Notice that we added a dimensional loss σ to the base dimensions a and b, to account for lost travel within the XY table due to finite shuttle dimensions and terminations. The dimensional loss typically ranges between 0.3m and 0.6m.

Assuming that the area of an average sized tile is about 0.0232 m^2, we can generate a set of plots for tiles covered as a function of individual boom length L, and the total footprint base area of the mobile base (A=ab). In our applications study, we have selected a hexagonal 'packing factor' η=0.828, and a base dimension shortening factor σ=0.5m. The results that were obtained via numerical evaluation, were performed for bases of different total area, with different manipulator lengths. As the use of aspect ratio is not an unambiguous measure, each base area can be achieved in a variety of ways, yielding different a and b values.

From our previous analysis, we will require an area of between 200 and 500 tiles. We then have to decide what dimensions are required to package the necessary components, and what the maximum size frontal and side dimensions can be. Facility passage constraints and maximum allowable turning radius for maneuverability will provide the limiting dimensions. In order to understand this information in a more qualitative sense, consider Figure 4-9:

The uppermost horizontal line, Maximum Arm Length, represents the upper physical limit on total arm length, due to considerations of weight, power, packaging, endpoint positioning accuracy, and bandwidth. The lower horizontal line, Minimum Number of Tiles, represents the lower limit of the necessary number of tiles that need to be covered in each base move. This is needed to reduce an excessive number of base moves and complete the rewaterproofing task within the pre-described time frame. The left vertical line, Minimum Base Size, reduces the available number of configurations by setting a minimum base size in order to properly package all the necessary components (batteries,

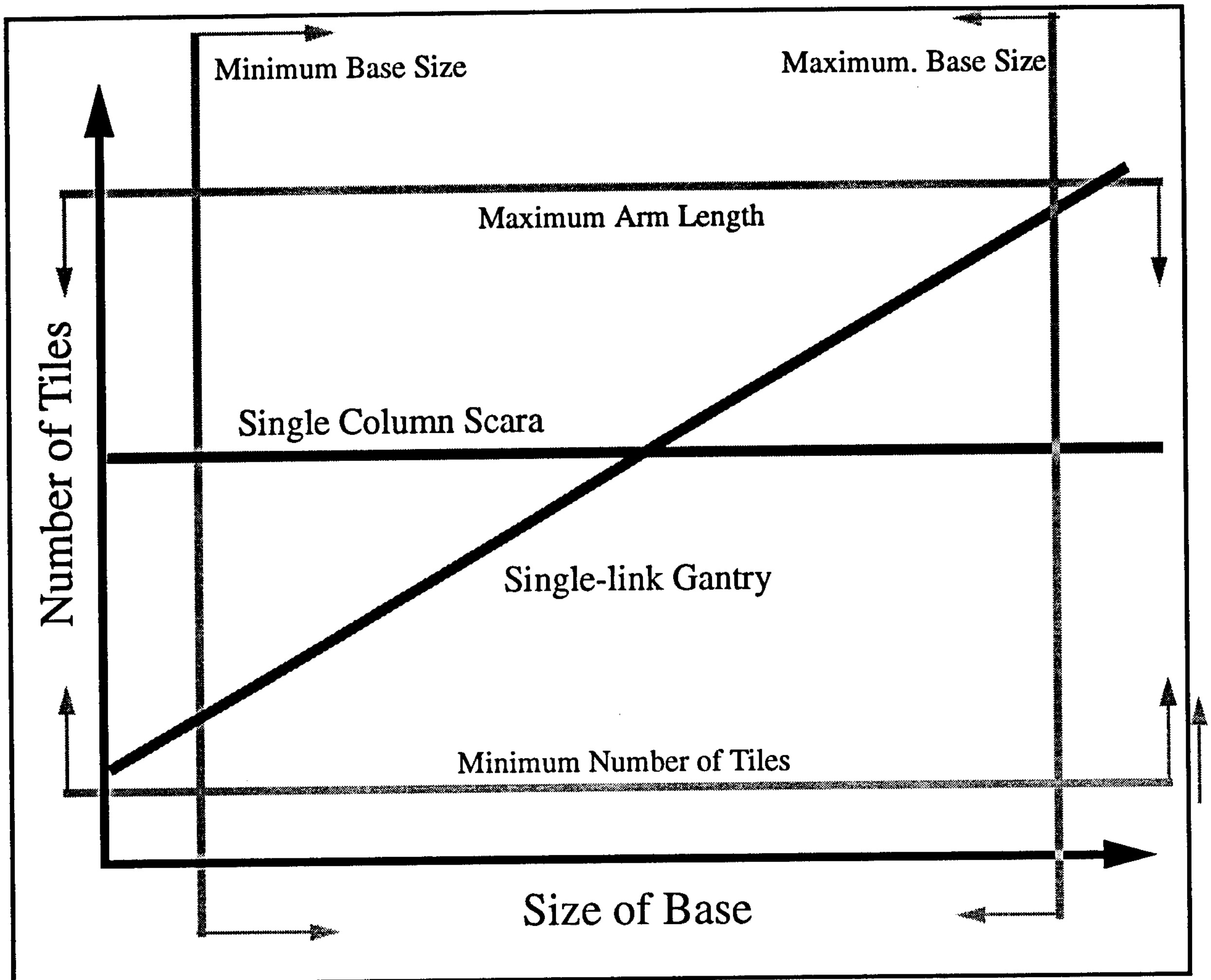

Figure 4-9 A qualitative analysis of constraints and requirements.

computers, amps, DMES, etc.), and create a base with sufficient static and dynamic stability for the elevation and manipulation devices.

The right vertical line, Maximum Base Size, represents the uppermost limit on the total base size which can gain access to the OPF and MDD, and can be easily shipped from site to site. In summary, the graph illustrates that, for a given length boom, that the Scara configuration will reach a fixed number of tiles independent of base size and that the gantry configuration coverage is a function of base size. Therefore at some point, the number of tile processed by the gantry configuration will exceed the Scara configuration. These criteria need to be properly weighed, in order to arrive at the desired final robot configuration. The current analysis has resulted in the selection of the gantry-XY single-boom robot, based on the following:

- The dimensional data obtained from the OPF and MDD floor plans,
- The maximum number of hours available for tile servicing,
- The acreage allowable to the base for shipping, access, and maneuvering within the OPF.

- Manipulator reach within allowed accuracy and bandwidths.

4.5 Configuration Decision

The overall conclusions of this section are that a single-boom manipulator configuration, with properly apportioned horizontal and vertical displacements, coupled to an endeffector wrist with the necessary dexterity, would be the appropriate solution to all the TPS tasks being considered. This design concept addresses all the criteria in the following ways:

It represents maximized inherent safety, it has mechanical precedence and thus represents a mature and reliable technology, consumes minimal power during a service cycle, has the lowest complexity of planner and controller, can be easily maintained, and has favorable dynamic response to accomplish fast tile-to-tile servicing cycle motions.

Based on the pros and cons enumerated in previous sections, the configuration decision was in favor of a gantry-style base with a single-boom manipulator mounted on top of an XY table. The rationale is as follows:

Mobile Base

- Footprint and turning radius can be the same for either base type.
- Straddlability doesn't matter -- it buys you very little and costs structure and additional planning.
- Base stability and terrainability are equivalent for both base types.

Systemic Issues

- Power consumption will be nearly equal to other options although gantry mass may add slightly to the power budget.
- Deployment is nearly identical for both systems. Tether issues affect both base types in the same way. Gantry might obstruct operator's view.
- Total number of tiles processed is nearly equivalent for both base types.

Task Planning

- Number of tiles processed per base move is dependent on manipulator workspace size.
- Total processing time for the underside of the shuttle is primarily a function of manipulator speed. This argues for a smaller manipulator.

Mechanism

- In general, the gantry-type base is stiffer, exhibits higher resonance, and has lower deflections, but only by small factors.
- Single column and planar arm can do the job, but with greater design effort.
- Gantry-style base has a large number of actuators, but many of them occur in symmetrical groups of four.
- End effector requirements are equivalent.

The advantages of the gantry-style base, XY table, single-boom manipulator combination outweighed the drawbacks. The exact dimensions and aspect ratio of the base are yet to be determined but are roughly 2.0m by 2.5m The straddlability capability of the gantry-style base will be traded off for the added rigidity and packaging volume provided by connecting the four corners of the gantry together with a rectangular base.

Importantly, the gantry-style lends itself to application flexibility due to its improved stiffness, speed and payload of the manipulator performing the servicing operations. Figure 4-10 on page 52 shows the current configuration.

Figure 4-10 Final configuration

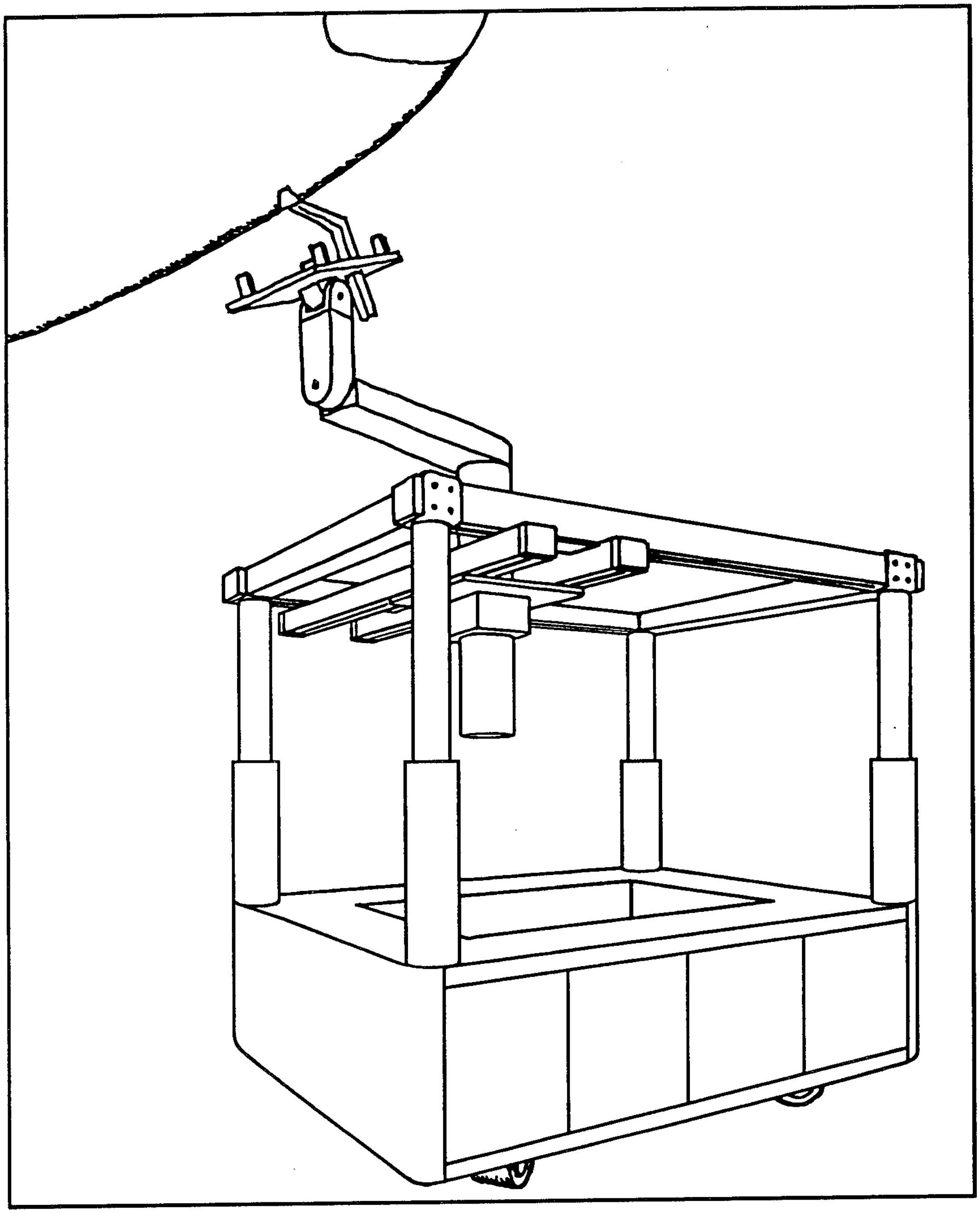

5. Configuration

In previous sections initial specifications were followed by a series of designs that were proposed and evaluated according to many design criteria. In this section we move from the general description of the system to a detailed look at system form and components. The four main subsystems are:

- Base
  The base is developed as a support structure for mobility, manipulation and control. Base issues such as needs for packaging, power requirements, drive and steering configurations and the physical links to other system components are addressed.
- Manipulator
  The base supports manipulation that, in turn, performs the TPS related tasks. The design of this is integral to a number of base issues including support for mechanism and control. Manipulator design is proposed, examined and analyzed for performance.
- Controller
  The vehicle controller executes and monitors a wide variety of tasks including motion control, safety of the vehicle, in addition to proactive and reactive control for the manipulation tasks.
- Power system
  Finally the power system is examined to establish power budgets and volume and weight of the system. Options and decision rationale are outlined for this critical element.

This section provides detailed overview of the system and how we arrived at specific design decisions.

5.1 Vehicle Base Configuration

The mobile base provides vehicle locomotion, packages vehicle subsystems, and gives structural support for the overhead manipulation system. At such an early stage in the design, the payload and space requirements of the mobile base are not settled, but are bounded. Thus, a good estimate of vehicle size and structural requirements can still be obtained.

5.1.1 Base Dimensions

The vehicle size is bounded by facility constraints and required workspace area. The vehicle width is limited by the 2.5m space between the aft jackstands to 2.14m while the collapsed vehicle height must allow entry and exit under 1.84m platform structures.

Design length is primarily limited by maneuverability, since as the length increases the swept volume of the turning vehicle increases. The trade-off is the increased manipulator workspace vs. the loss of vehicle maneuverability. We wish to maximize the workspace of the manipulator, hence maximizing the vehicle length, while preserving the vehicle's maneuverability. This gives high coverage without penalizing agility. As shown in Base Tessellation Analysis on page 41, the lower bound on vehicle length can be established by determining the minimum workspace necessary to complete the tiling operations.This study indicates that a minimum of 150 tiles must be serviced per base move. The difficulty of a large turning machine and the problems of shipping and handling a large machine are recognized and lead to a pragmatic upper bound of about 3m in length.

The base length can be optimized as a function of the maneuverability cost and the total tiling time cost. However, it is difficult to fully assess the cost of maneuverability. We studied the trends of tiling cost to determine whether a suitable upper limit could be established on the basis of this single merit but could not resolve an exact solution.

5.1.2 Drive and Steering Configuration

The base is required to traverse large flat areas at slow speed; there is neither high speed handling nor long duration acceleration requirements for this machine. The Task Scenario scripts detailed short distances of travel. However, transport packaging could involve longer distance traverses, but over distances greater than service distances at KSC or at Dryden it is more practical to haul the machine via some other transport device such as a trailer or lift.

The following list provides initial requirements of the drive and steering units:

- *180 or 360 degree wheel turn-in-place.*The wheel turn requirements reflect the need for omnidirectional steering; we are continuing the steering analysis to determine whether 180 or 360 degree wheel turn is necessary for the desired motions. The zero scrub radius is required to minimize lateral machine motion during wheel turns, which impedes planning and dead reckoning.

- OPF and MDD cables and floor clutter present obstacles up to 5cm in height. Larger obstacles will not be driven over. A means of maintaining wheel contact is necessary to prevent racking (torsional twist) of the overhead XY table as well as dead-reckoned position. This might result in a complex suspension or a rocker arm pivot.
- NASA safety procedures require that no electrical contact be made or broken in the orbiter environment, necessitating the use of *brushless motors.*
- *Encoders* with 12 bit resolution for steer and drive.
- Electrical spring loaded *deadman type brakes.* I.e. Engage when power is off.
- Wheel compliance should be minimized to reduce manipulator settling time. Compliant wheels would introduce extra vibratory modes and settling time.

After an extensive evaluation we settled on an independently actuated configuration utilizing independent wheel steer/drive systems. See Appendix A for a detailed look at the different possible configurations. The final system we have chosen is independently driven and steered wheels.

Independent Drive and Steer

The primary advantage of independent drives is the ability to provide three degrees of motion for the vehicle. Independent steer can provide crabbing motions, rotations, or any rate of curvature. Like the omnidirectional wheel or the synchronous drive with turntable, this configuration can follow any path and rotate along that path. It does not have the climbing limitations of the omnidirectional wheel nor the mechanical packaging issues of the synchronous drive. Another advantage is the redundancy of drive mechanisms. If a drive unit fails the remaining three can still move the vehicle.

The primary disadvantage is the control of the additional actuated degrees of freedom. It is necessarily an overconstrained system. For a 4 wheel steer and drive, a total of 8 degrees of freedom of control are required. Thus, the system is overconstrained by several DOF's and possible control errors will introduce 'floor stretching' or 'isometric exercises' which are internal forces generated through improper control. However, through careful design of geometries even highly overconstrained systems can avoid actuator conflict.

Another disadvantage is difficulty of operator input and control in the absence of computer control between operator and robot. However, through independent mechanical frame to align the wheels and a standard 3DOF joystick this control is acheivable.

Figure 5-1 Independent steer configuration.

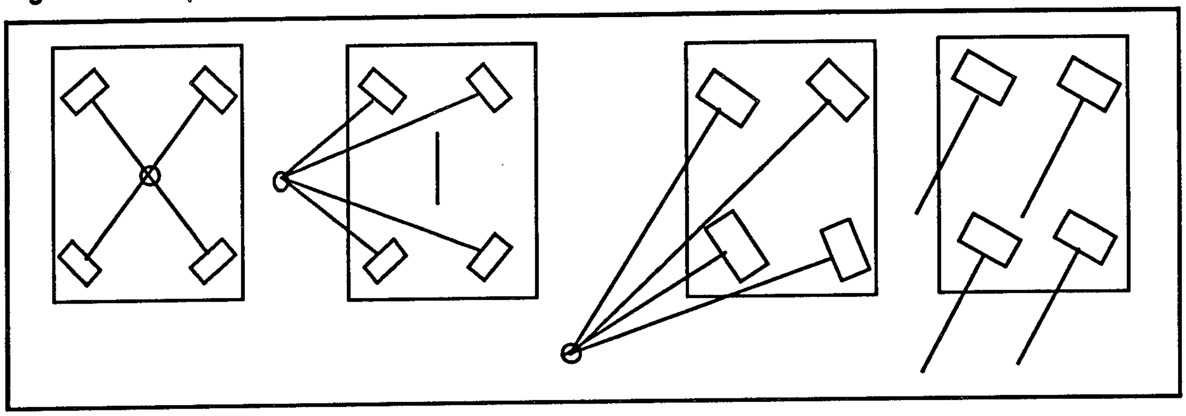

Examples of Precedent Systems

The existence of precedent or analogous mechanisms is required for a project that is fast tracked, otherwise assumptions and errors can lead to project failure.

- Unique Mobility, Englewood, Colorado designed and constructed the Full Mobility Robotic Vehicle Platform (FMRVP) a four drive and steer vehicle with independent suspension.[1] The vehicle is capable of turning while moving in a fixed direction. The FMRVP was developed and successfully tested and then delivered to Missile Command (MICOM) in Huntsville, AL for further evaluation in 1990. A small prototype was also constructed for concept tests.
- Ability Technologies of Spencer Iowa, has constructed mobile base systems utilizing three driven and steered wheels and demonstrated the accurate control of the vehicle from a remote link.
- The CMU Remote Workhorse Vehicle (RWV) is a remote teleoperated vehicle with independent hydraulic steer and drive that can provide control for crabbing, rotation and describing arcs of any radius. However, the Workhorse, while capable of these motions, limited all movement to simple arcs, crab, and rotations in place.

Examples of Analogous Systems

While a number of overconstrained systems have been developed there are several specific and relevant examples worth noting.

- The Carnegie Mellon Planetary Rover program designed and built the Ambler (12 DOF planar motions) which provides body control from 6 legs such that 12 actuated DOF's control 3 body DOF's.
- Construction machines such as rough terrain forklifts and straddle cranes are capable of translation as well as short radius turns through hydraulic control systems.

1. Parish, David W., Development, Test and Evaluation of the FMRVP. AUVS-90 Proceedings, Dayton, Ohio 1990.

Drive and Steer Selection

The many advantages of the fully independent drive and steer outweigh the concern regarding control issues. Concerns of additional DOF cost and time, upon closer inspection, do not greatly impact the design process. This layout involves the replication of four units that are designed once and assembly and packaging are simplified because the units are independent and there are no mechanical linkages between the units. A suspension is necessary for overcoming obstacles if tires are rigid and the independent drive facilitates this since no mechanical coupling is involved.

In addition, off-the-shelf mechanical technology from Automatic Guided Vehicle Systems (AGVS) is available to facilitate development. These are wheel-drive units built by several companies including Schabmuller, Hesselman, and Hurth.

5.1.3 Packaging

Subsystem packaging is one of the form giving parameters of the base design. Packaging issues include mounting, access, and interconnects between units. Current items for packaging include:

- Batteries
- DMES containment and associated filters and plumbing.
- Nitrogen for rewaterproofing and inert pressurizing of base unit.
- Controller cages (base, manipulator, and perception)
- Servoamplifiers
- Power supply and distribution

The open section in the base shown in Figure 5-2 gives several advantages. Maintenance and access are improved to most pieces of equipment is improved, and the space can be used to house sections of the manipulator section while it is not deployed.

Figure 5-2 Base packaging

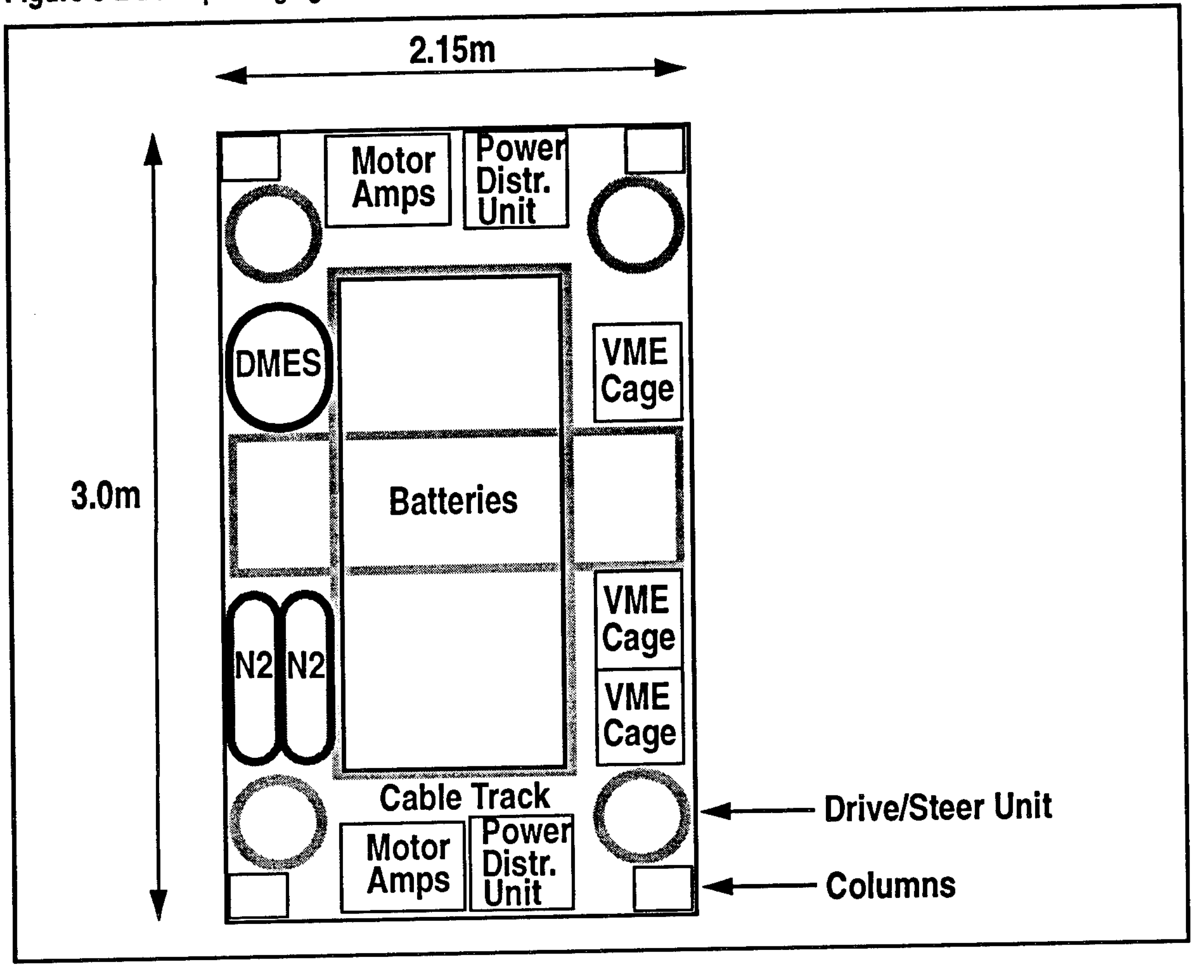

5.1.4 Suspension

A rigid vehicle requires only three planar contacts for determinate stability. The fourth, redundant contact remains in the same plane only on level surfaces. If any one wheel mounts an obstacle, one of the other three wheels will lose contact with the ground. If any two wheels simultaneously mount an obstacle, then it's possible, but unlikely, that no wheel contact is lost.

Thus, in addition to the wheel contact needs, the manipulator table must be isolated from the effects of "racking", a torsional twist caused by uneven structural supports in a rigid vehicle. For example, if one of the four wheels is sitting on an obstacle, then the weight of the machine will impart a torque about the longitudinal machine axis, twisting the plane of the XY table.

It is necessary to prevent either of these two problems from occurring. An unstable vehicle is a risk to the equipment in the facility, including the shuttle. A sufficiently large torque on the manipulator frame could prevent it's motion or cause permanent damage to the robot mechanism or simply make the system inaccurate.

Since the assumption that the vehicle is rigid is not completely true, the structure could be designed with sufficient flexure, so that no ground contact would be lost during obstacle

crossing, or the tires themselves could be made of compliant materials that do not allow loss of wheel contact. Since structural rigidity is crucial to maintaining a short damping time for manipulator motion, the first solution is rejected. Additionally, the weight of the machine and the size of the obstacles makes the second solution intractable.

Durability and structural strength are very important for the robot and any suspension must reflect this. The vehicle will be driven at extremely low speeds and over small obstacles such as cables. There are two candidates to fulfill these requirements. The first design is based on an independent suspension passenger vehicle, and the second suspension is based on those used in agricultural tractors.

If each of the four wheels were coupled to the structure via a spring, then if any one wheel mounted an obstacle, the springs on the four wheels would extend or compress and maintain wheel contact. The suspension spring stiffness is a function of the total vehicle mass, and the equivalent structural stiffness of the vehicle. Our initial estimations indicate that the structural stiffness of the vehicle will be large, and so the spring stiffness can be chosen as a function of the vehicle mass.

The second design consideration is based on a proven suspension used in agricultural tractors. The rear tractor axle is unsprung and the two front wheels are mounted to a single axle that is pinned to a yoke on the tractor body. If any of the four wheels mounts an obstacle, wheel contact is maintained by the rotation of the front axle. Torques cannot be transmitted through the pin joint. See Figure 5-3 on page 59.

There is precedence for the rocker arm suspension design in construction equipment and farm machinery. Farm tractors and front end-loaders use a pinned front axle. The pinned axle front end dominates in heavy earth moving equipment because of its strength. A sprung front end typically does not have the rigidity or strength necessary for such heavy duty work.

Figure 5-3 Rocker arm suspension.

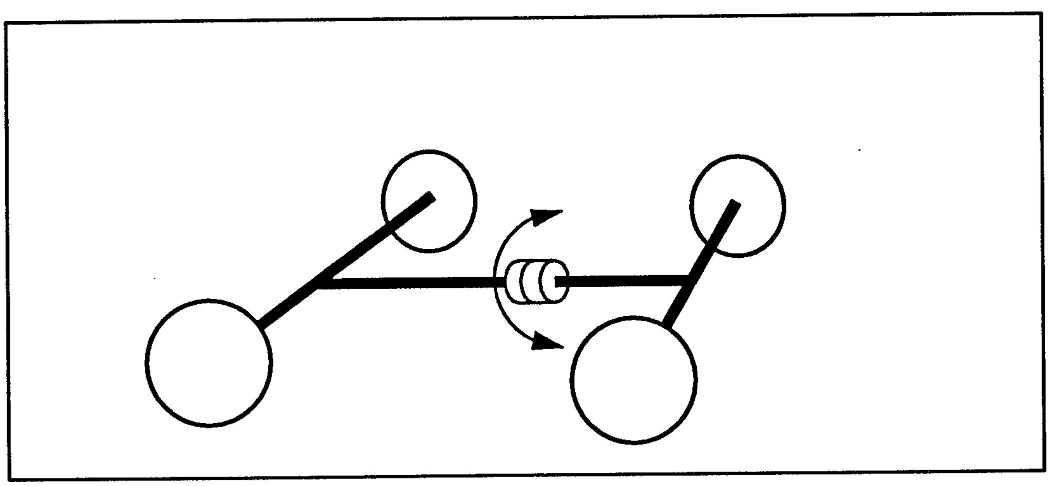

5.1.5 Towing

For emergency situations or possibly for transport without power there is a need to allow towing or pushing of the vehicle. Weight and size may prohibit single person pushing the machine around. It is akin to trying to push and steer a small car by running alongside.

As a result we need to provide a standard linkage for tow such as a trailer hitch or coupling. The machine also needs to be backdriveable to facilitate tow or push. Mechanics of wheel systems should allow passive alignment, like castering or a fixed piece that forces alignment. The need for braking action capability and towing will have to be examined carefully.

5.1.6 Commercial Bases

With general requirements for the base established a survey of commercial units was made to determine relevance and use of these units. Robotic bases and Automatic Guided Vehicles (AGV's) were the subject of our search.

Computer controlled mobile bases are increasingly used in several markets. Cybermotion, Transitions Research and Denning are current vendors. Although the Cybermotion and Denning offer synchronous steer with rotating turrets the mechanics of the drive and steer system consume most of the base volume. Of the two, the Cybermotion base has the superior mechanics and offers accurate dead-reckoning capability. However, the volume and payload considerations for the tile robot, in addition to difficulty of structural add-ons preclude the use of these units. The TRC base provides differential steer and uses AGV wheel drives used in other commercial AGV units, but the TRC frame is primarily designed for research and not heavy duty commercial use. The three companies do not offer the size, packaging and payload necessary for this system.

At first glance, AGV's appear to offer many of the functions necessary in a mobile base. They incorporate a locomotion system emplaced in structure capable of moving heavy loads. We investigated the possibility of retrofitting an AGV for use in the gantry robot design.

AGV's manufactured by the following companies were reviewed: BT Systems, Eaton-Kenway, Caterpiller, Mentor AGVS, Apogee Robotics, Superior Robotic Transporters Roberts Sinto, NDC Automatic Guidance Components, AGV Products, Depotmat, Volvo, and Control Engineering.

The structure of the heavy duty units is typically welded steel tube construction, capable of supporting multiples of our projected loads. However, the majority of these systems use either differential, tricycle or rear-Ackerman type steering. None of these steering systems provide the omnidirectional capabilities required of our system. A retrofit of an AGV would consist of stripping away all non-structural components, and preparing this structure for mating with the upper structural section of the gantry robot. Finally, packaging of controllers, additional batteries, sensing and guidance systems means a lot of redesign and rework.

Economics also enter into the evaluation. Prices for AGV's range from \$50,000 to over \$100,000. At this price level, even with salvageable locomotion, the use of an AGV is not

justified. Time saved in structural design is spent in redesign, and time saved in structural construction is spent in retrofit work. The use of an AGV as a base does not offer time or economic savings due to the amount of rework necessary.

In summary, no current commercial base offers the combination of maneuverability, packaging and cost that warrants their use.

5.1.7 Manipulator Lift Mechanism

The proposed design of the actuator system for the gantry robot is a tube in boom extension system. The total collapsed height of the gantry crane must be less than 1.84m. The manipulator platform must be moved up to a height of 2.75m. The structural stiffness must be sufficient to prevent excessive flex during manipulator motion, and to provide a sufficiently short duration ring out time.

Column synchronization is required both for structural integrity and for accurate alignment of the manipulator to the shuttle surface. A horizontal platform orientation must be maintained as the platform is raised and when the XY table is operating. The OPF floor has some drainage slope which will slightly tilt the base of the machine, and hence the table. In order to level the XY platform independent column control is necessary.

Another method of leveling the XY platform is to level the machine base with stabilizers, and then raise the platform using synchronous actuator motion. Open loop synchronization of the four columns is a significant mechanical problem, requiring the mechanical coupling of actuators with either chains or shafts. In our structural design, the room required for belt or chain passage around the base of the machine would inhibit the packaging of the other base components, and make maintenance and serviceability difficult.

Independent closed loop column actuation is an easier method of ensuring actuator synchronization. By controlling the current flow to each of the motors using the absolute position of the screw shaft as feedback, the columns can be made to raise and lower in unison. Independent feedback from tilt indicators can also be used to raise and lower the platform at a specified attitude.

Some commercial units utilize an electric linear actuator which produces the required stroke and thrust in one package. The system consists of a sealed tube in boom with an internal ball screw actuation system. The actuators can act as a structural column, eliminating the need to design and fabricate the column.

If no commercial components were found to be acceptable a boom over tube column can be custom built for each of the four supporting columns. Figure 5-4 on page 62 shows an example of this. Four linear rails per column maintain colinearity and transfer torque loads during extension. Approximately 30cm of the total 1.84m collapsed height is the XY table and the collapsed manipulator. Ground clearance and lower lateral structure are another 30cm and there is less than 1.2m of column overlap, of which 90cm is needed in extension.

Figure 5-4 Column structure

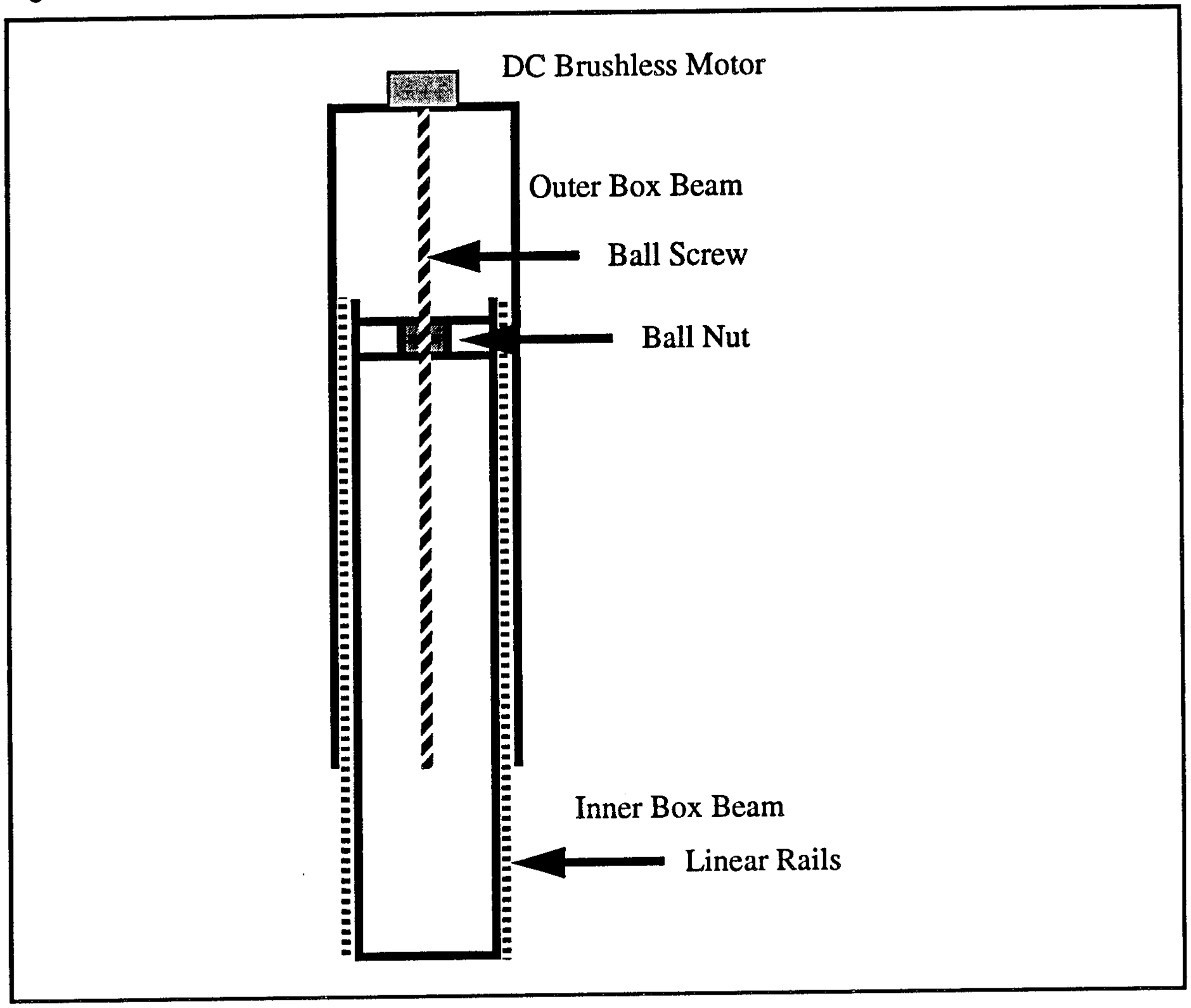

A ballscrew actuator provides lift. A pair of ballnuts are mounted about 30cm apart inside the inner column. The ballscrew runs through these ballnuts up to a servo motor mounted on the top of the outside column.

Other designs have been considered. Multiple side by side rack and pinion stages were considered, as well as a tube in boom assemblies where the inner tube is actuated up and out of the outer tube. This inherently seals the ball screw system inside the column, unlike the rack and pinion and allows the actuating motor to be mounted on the top where it is more easily accessible for maintenance. The rack and pinion design also requires visible lubrication fluids which are not permitted in the OPF unless it is securely covered by a boot or bellows.

5.1.8 Base Structure

The base construction must support the weight of all of the equipment and maintain base rigidity for the overhead manipulator. The current weight budget estimate shows that the batteries are, by far, the biggest weight concern.

The main loads that the base structure will see are:

- 340kg of batteries.
- 230kg distributed among the four columns.
- Forces of the wheel drive units.

These loads induce small structural stresses, which allow construction in lightweight welded aluminum. Aluminum has the additional advantage of corrosion resistance, which is important in the expected operating environments.

5.2 Base Configuration Summary

We've presented a variety of needs for the vehicle base including drive train, suspension, and actuation. For each of these we've shown a number of alternatives and a recommended solution. They are as follows:

- Base Dimensions: 1.8m wide, and up to 2.5m long.
- Packaging: Layout of components shown.
- Drivetrain: All wheel steer and drive.
- Suspension: Rocker arm.
- Base: Custom design, one off or commercial not viable.
- Vertical lift mechanism: A modification of a commercial actuator.
- Base Structure: Aluminum chassis using a welded lattice construction.

5.3 Manipulator

This section details the design selection for the manipulator configuration. It is divided into a number of sections on manipulator components and related topics:

- General Design Requirements
  - Accuracy and positioning
  - Force
  - Safety
  - System
- Manipulator Design Requirements
  - Task requirements
  - Safety Issues
- Endeffector Design Requirements
  - Shuttle proximity and facility requirements
  - End-effector and tooling requirements
  - Tile height and contour analysis
  - Vision sensing requirements
  - Reach and dexterity requirements
- Manipulator and Endeffector Design
  - XYZ mechanism
  - Manipulator kinematics
  - Implementation and packaging
  - Task execution effects and future tasks
  - Wrist and tooling kinematic arrangement
  - An additional DOF
  - Safety-related design
  - Mechanical componentry
- Manipulator System Integration
  - Configuration, dimensions and componentry
  - Power consumption
- Summary

Each section contains several subsections which explore the different criteria and design aspects that are crucial in making the decision. Not only does it expose important issues in the selection process, but also details assumptions and numerical analyses used. We believe this form of presentation is more realistic and revealing than simply stating the final design

decisions and only listing the factors governing the decision. The reader is encouraged to examine the assumptions and numerical justifications.

At the end of each section we have summarized the key points involved in the final design proposal and selection cycle. The section concludes with a presentation of the final configuration, technical implementation details, deployment scenario, timing, and a power consumption analysis.

5.3.1 General Design Requirements

The specific requirements below are based on the tile rewaterproofing task, but should also satisfy the tile inspection task.

Accuracy and Positioning Requirements

- Position endeffector and rewaterproofing tool parallel to tile surface to within 2.5cm from the tile.
- Mechanically position tip of rewaterproofing nozzle to within +/- 0.1 cm of the white circle surrounding the injection hole. White circle is 1 cm in diameter, with the injection hole (0.1cm) anywhere within that circle. The vision system can locate the hole centroid to within +/- 0.1 cm.
- Mechanical accuracies are dependent on local position estimation accuracies and nozzle diameter.
- Transit times from tile to tile are to be minimized. Transition time of 1 sec over 30cm requires a minimum endpoint speed of 30cm/sec.
- Service time per tile will be kept below 10 sec for the entire process.

Force Requirements

- Hold the endeffector with a force necessary to retain shuttle contact during a 3.4 atm nitrogen purge. Necessary contact force depends on nozzle diameter and the gauge-pressure inside the nozzle.
- Manipulator must support an endeffector (tooling, sensing, plates, motors, transmission, etc) to weigh no more than 25 kgs.
- Endeffector must retain a contact force in excess of the backpressure which must not exceed the breaking contact strength of the shuttle tiles of 0.7-1.0 atm.
- Contact force to be controlled by the rewaterproofing nozzle mechanics and electronics.
- Forces and torques exerted on shuttle are to be monitored and used as safety triggers at certain predefined thresholds.

Safety Requirements

- No part of the manipulator is to touch the shuttle tiles other than the end-effector nozzle.
- No large nor fast motions with heavy masses are permitted within 30cm of

the shuttle.

- Each motion is to have several electronic and mechanical contact detection and avoidance sensors. These are to be used in avoiding and detecting imminent contact.
- Mechanical failures and runaways protected through power cutoff and mechanically or electrically induced reaction motions away from the shuttle.

System Requirements

- Minimize continuous power during entire rewaterproofing cycle.
- The manipulator and endeffector is to be easily monitored, reached, and serviced.

5.3.2 Manipulator Design Requirements

Task Requirements

The primary task we are considering for the tile servicing robot is the rewaterproofing of the underside TPS tiles. Other activities include tile inspection, step-and-gap measurement, and charred filler bar inspection. All of these tasks have basically the same dexterity requirements even without knowing details and requirements for charred filler-bar inspection. They require that tooling be accurately positioned normal to the outer shuttle surface, with constrained normal and shear contact forces. This entails reaching the bottom surface of the orbiter, whose height varies between 2.74m and 4.11m above the ground, and whose tangential plane varies between 0^o and 45^o relative to horizontal. Accuracy requirements are 2 mm in position and 1^o in orientation. Orientation and small displacement inaccuracies can be compensated for by mounting contact tooling on passively compliant bases. Such devices can create pure rotations and translations about a fixed point due to forces and torques applied at the interface.

Summarizing, the major requirements for the manipulator are:

- collapsed height of 1.83m
- vertical work range between 2.74m and 3.96m
- highly controllable contact forces (normal and shear)
- +/- 45^o to +/-60^o rotational ranges (pitch and yaw) at full extension
- minimum of five DOF motion (three positional, two rotation)
- 25 kg payload at full extension and rotation
- exert controllable force to keep nozzle in tile contact at 3.4 atm
- monitor and control contact force not to exceed 0.7 atm to avoid tile damage
- move from tile to tile and reorient in less than 2 seconds
- wrist rotate DOF may be necessary for vision sensing system

Safety Issues

We will use electronic obstacle detection and avoidance sensors at the tooling and camera/sensing platforms to monitor endeffectors proximity and orientation with respect to the shuttle tiles. These sensors can be used to properly orient the tooling/sensing platforms and provide continuous monitoring of the local environment. Mechanical safety will be provided in the form of micro-switch 'whiskers' which will be used on the vertical shoulder raise, the sensing/camera platform, and the actual tooling platform. The combination of these sensors will provide several layers of safety that will prevent improper end-effector contact with the shuttle whether computing hardware is operational or not. The mechanical safety level will interrupt power to all critical DOFs and retract the endeffector tooling away from the shuttle through a passive mechanical system.

Since the manipulator arm will be able to extend the endeffector beyond the edges of the base, we will have to provide for some form of collision avoidance sensing and controller scheme. We could combine such electronic sensing schemes as infrared sensors, piezo-electric or capacitive proximity sensors to provide electronic means of detecting and avoiding obstacles. Using mechanical whiskers mounted along the surfaces and edges of the horizontal boom and tooling/sensing plates will provide hardware safety loops in case of computer or controller failure. These hardware safety levels can include tool retraction, disabling motor power and application of brakes on all axes.

Recovery from such scenarios will utilize assistance from an operator, due to the necessity of determining the source of the detected warning or error. The computer will certainly be able to point out the sensor that was tripped and the possible area to investigate, unless the computers are inoperable. Depending on the severity of the detected imminent collision or fatal error, we will provide safe and reliable recovery schemes which will bring the system back on line, under minimal assistance of an operator.

Motors will be protected from runaway by using several position encoding schemes to check their relative operations, while brakes and relays will provide for lock-up in the case of power loss or detection of an unexpected and imminent collision. The choice of actuation and material components will be made to minimize mechanical failure so that no parts or subsystems can inadvertently damage the shuttle. Furthermore, we will minimize the presence of catastrophic single point failures through careful design and inherent sensing/actuation redundancies. If there is a crucial component that has a likelihood of failing, we will identify its most prominent failure modes and provide electronic and mechanic safety levels to safeguard against probable results of component failure. Those components deemed likely to fail during the early stages of the service life of the robot, will be designed to be easily repaired with minimum skills and minimum down-time, with adequate number of spares provided to the end user.

5.3.3 Endeffector Design Requirements

Shuttle Proximity and Facility Requirements

Following is a list of general and specific safety concerns and practices which must be followed by personnel or equipment operating near the shuttle. The list is not exhaustive, and is meant only to highlight some of the most relevant items that will affect the design

and emplacement of the robot. For a more complete description of these and other relevant items, please refer to Section 2.2 "Environmental and Safety Issues" on page 16.

The use of certain materials in the manipulator device will be checked to insure compatibility with environmental conditions such as DMES exposure, wind and sand exposure, and corrosion resistance in a humid and salt air environment. The entire system will also have to provide electric grounding to avoid electro-static buildup that could lead to spark emission during shuttle contact. This implies grounding straps and avoiding materials that can build up electrostatic charge such as plastics or foams. Exposed moving robot parts need to be sealed to avoid entry of contaminants and to prevent exposure of the OPF or the MDD to greases and lubricants. The manipulation device will also have to resist wind exposure at Dryden's MDD such that wing gusts will not disturb the manipulator during a rewaterproofing cycle.

Tile rewaterproofing requires a clear area of 3 meter radius around the operating location, and such procedures require the presence of a part-time Safety Professional, an operations task supervisor, and a person from Environmental Health to monitor the process. New or revised guidelines will have to be drawn up for the use of the robotic rewaterproofing system, as our intent is to reduce the hazards in this operation by removing the human operators.

The mechanical design of the manipulator elements will require mechanical stops and additional braking. This is to avoid collisions with the shuttle tiles if design limits are exceeded or power is lost. We are less subject to such severe constraints, as we will be operating underneath the shuttle, and gravity is in our favor in the event of power failure but brakes and limit-stops will still be appended.

Endeffector and Tooling Requirements

We have listed here in bulletized format those specific requirements currently requested by the endeffector design group from Rockwell International (Revision 02-11-91).

- General
    - System operation in outdoor conditions for future servicing at KSC runway.
    - Temperature, moisture, dust, light, wind conditions
    - Fluid and electrical lines shall remain flexible over the life of the robot.
- Structures
    - Minimize tooling weight to 10 lbs.
    - Components to withstand the inertial acceleration forces.
    - Tooling components to be reliable and easily maintainable.
- Materials and Fluids
    - Materials used shall be resistant to DMES exposure. These include 7075 & 2219 Al, Iconel 601, Stainless Steel, Ti-alloy, and RTV560.
    - Fluid system to be mounted and linked via external hose to the injection

tooling, including gas and electrical cabling.

- Nitrogen pressure supply included in fittings.
- DMES and N_2 supplies to be sized for an entire 8 hr. shift (approximately 10 liters of DMES) and to be supplied with a level detection and monitoring device, while pressure and flow meters monitor the delivery process.
- Nozzle diameter to be 11mm.
- DMES injection of 2ml +/- 1ml at 0.1-0.2 atm followed by a 4 second 3-4 atm N_2 injection.
- Tile sealing pressure not to exceed 0.9 atm to avoid tile surface damage.
- Forces and torques during injection process are monitored at the endeffector.
- Leaks shall be detected and excess DMES will be stored or disposed of at the nozzle.
- Injection nozzle shall be translated no more than 5cm towards contact with the tile surface from a fixed end-effector position.
- Injection nozzle axis shall be perpendicular to the local tile surface normal. Misalignment causes a torque about the tool and sealing of the nozzle becomes inadequate. Proper alignment is essential or that tile is aborted after 2 successive injection attempts.
- A quick-exchange tooling system shall be used to attach/remove the tooling attachment.
- Shuttle, robot base or manipulator vibrations shall not affect the endeffector tooling injection procedure if kept below 0.125mm peak-to-peak at 20 Hz.
- The endeffector system shall be equipped with a manual override capability for start-up calibration and emergency conditions.
- No human exposure to DMES will be allowed
- Lines, reservoirs, and nozzle components that are carrying DMES shall be protected or puncture-proof.
- A dedicated processor will be available solely for the endeffector/tooling process.

This information is obtained from NASA KSC TPS Process Automation Study, Final Report, KSC-DM-3491, other Rockwell Materials Properties Documents and discussions with NASA personnel.

Tiling Height and Contour Analysis

To extract reach and orientation requirements for the overall mechanism and the endeffector, we looked at the overall distribution of isocontours for constant changes in tile centroid elevation and curvature of the orbiter underside. Figure 5-6 and Figure 5-6 illustrate these contours projected on the underside. These distributions and curvatures are important in the design of XY table size, vertical reach, and endeffector sizing.

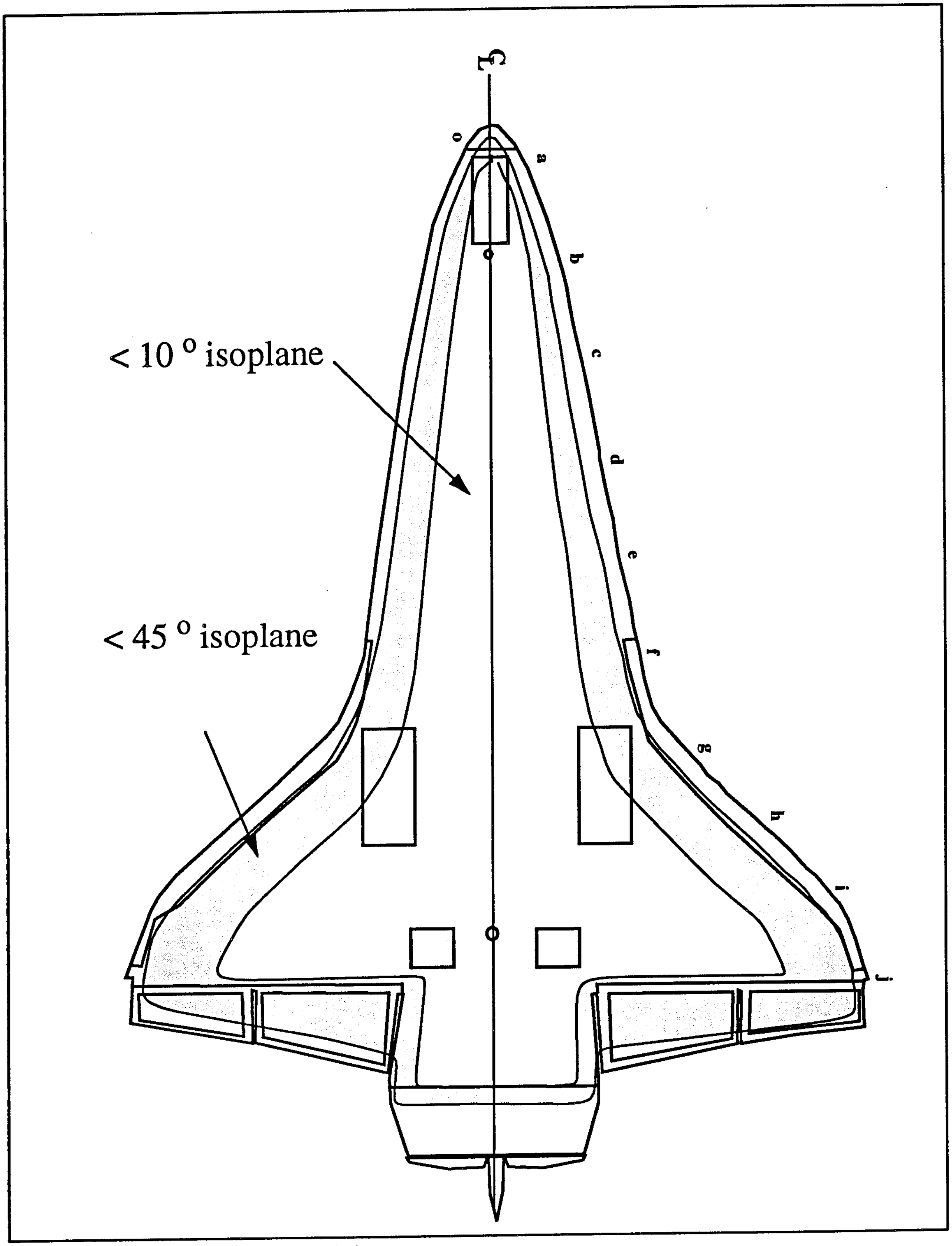

Figure 5-5 Bottomside shuttle iso-contours

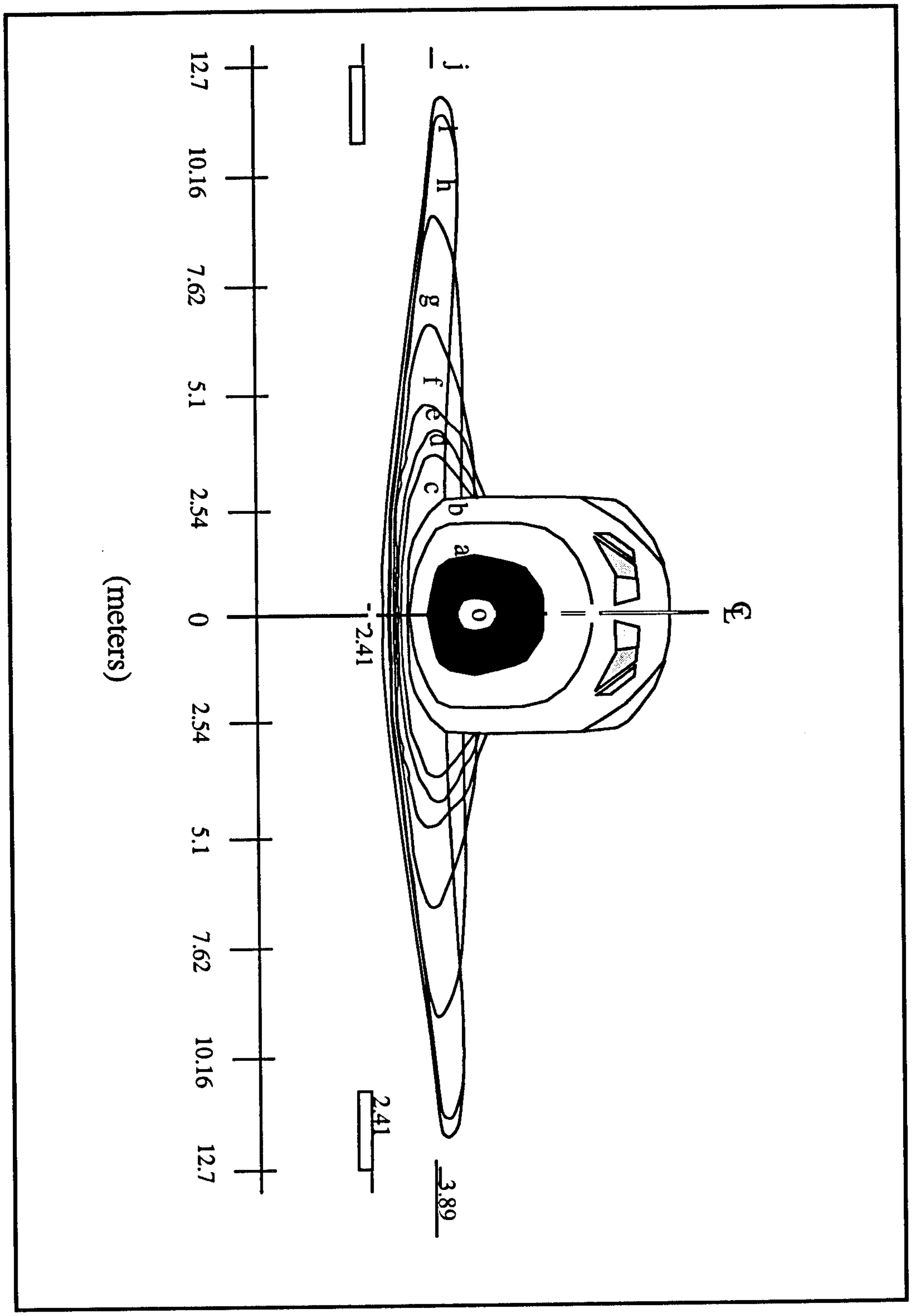

Figure 5-6 Frontal shuttle contours

As can be observed from the figures, the surface area where the tile angles are less than 10° is large and accounts for 60% of the entire underside, while the areas less than or equal to 45° is another 30% of the area, leaving around 10% of tiles with tangent planes between 45° and 90°. The cross-sectional view also shows the height, measured perpendicular to the axis of symmetry of the shuttle, and elevations at 3.0m intervals of the shuttle. In the 0°-10° range, the largest change in elevation is about 0.94m over a 12m distance.

As expected, the changes from 10°-45° are much more rapid along the periphery of the shuttle and the tightest curvature changes occur near the nose of the orbiter.

Figure 5-7 Orbiter cross-section reach dimensions

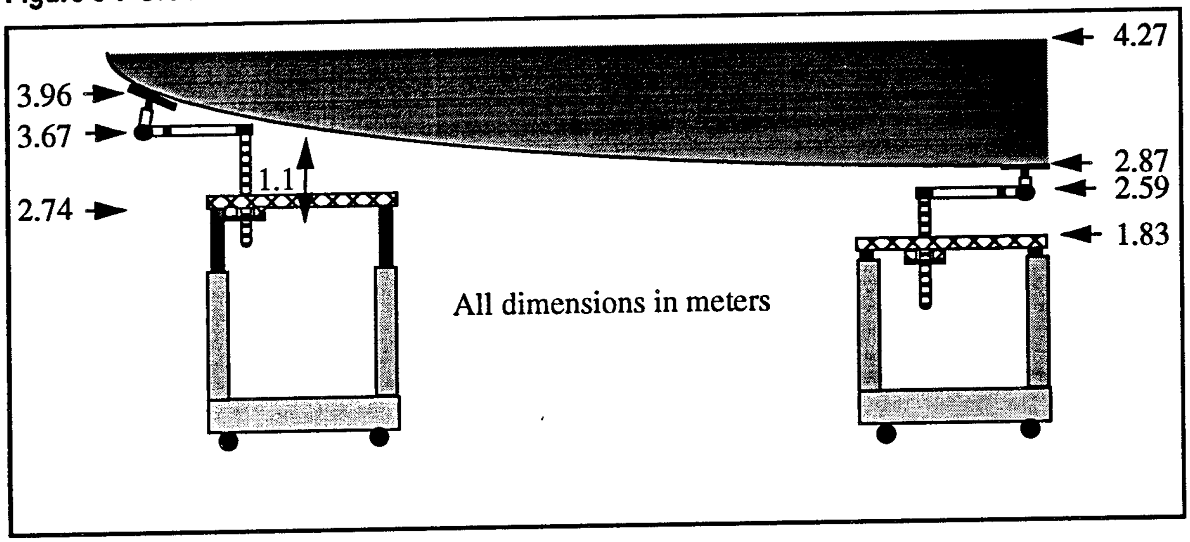

Figure 5-8 Work envelope dimensions

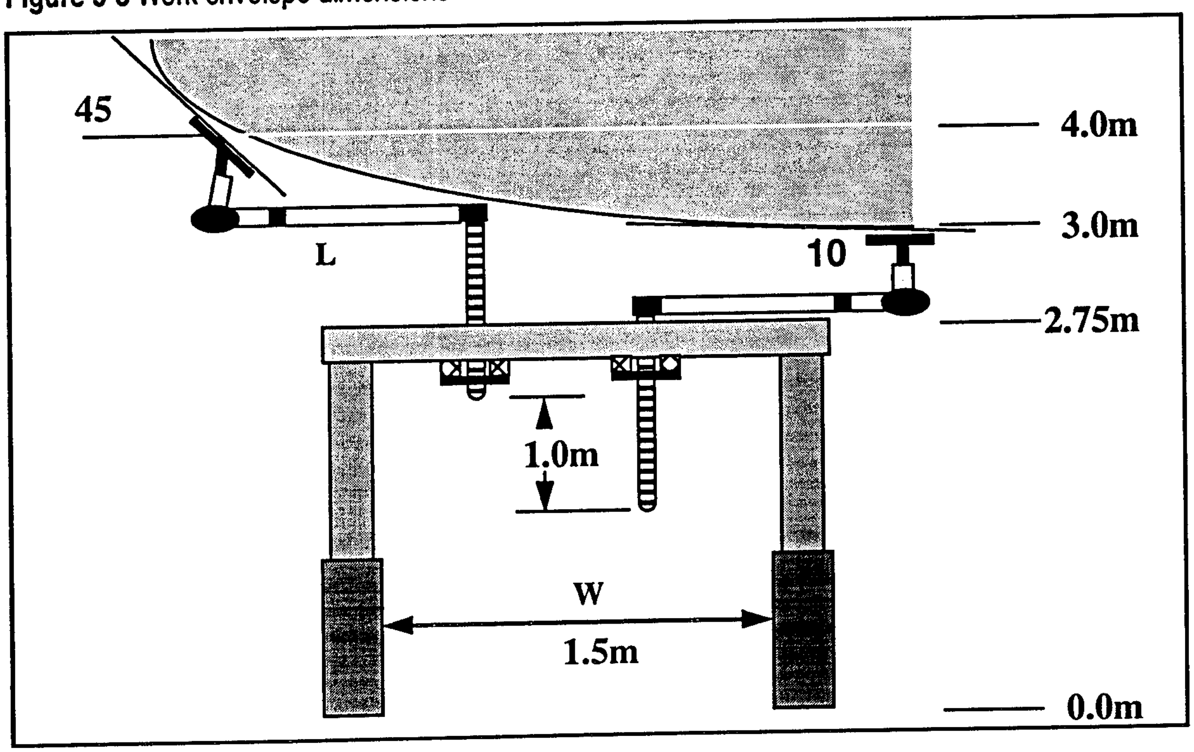

Figure 5-6 and Figure 5-6 are important in deciding the necessary tessellation procedure for the vehicle, especially where reach requirements make it difficult to deploy a long arm from the base. This difficulty is due to relative height requirements and the need to orient the endeffector along the surface normal. To understand the necessary changes in elevation required from this robot, we determined the reach requirements at different locations along the shuttle underside. This allows a decision on extension and reach requirements for each degree of freedom in the vertical gantry extensions, the vertical motion of the boom and endeffector, the length of the boom extension and endeffector geometry. The diagrams illustrate a possible arrangement of work envelope dimensions, allowing a study of reach trade-offs.

The diagram on Figure 5-6 also illustrates the changes in curvature as a function of distance along the shuttle's centerline. Both of these diagrams illustrate a large vertical XYZ table that can extend from 1.83m to 2.75m so the manipulator can reach all tiles properly at all locations under the shuttle. This requirement is shown in Figure 5-7 and Figure 5-8, which show the worst-case scenario of covering tiles that are around the 45^o surface normal range.

In the table below we can see how the shuttle tile tangent planes vary in height as a function of base dimension W and boom length L. We assume we can just reach the 45^o tile and want to reach inward towards the centerline as far as possible (Δ=0.61+(W-1.22)*0.08197+(L-0.5)*0.16; [m]):

Table 1: Vertical excursion required as function of base width and boom length

		Boom length (meters)			
Base W [m]	0.5	0.75	1.0	1.25	1.50
1.22	**0.61**	**0.66**	**0.70**	**0.73**	**0.77**
2.44	**0.71**	**0.75**	**0.79**	**0.83**	**0.87**
3.66	**0.81**	**0.85**	**0.89**	**0.93**	**0.97**

In general, as the width and boom length increase the required vertical excursion also increases. Notice that the base dimension can vary by a factor of two while requiring an additional vertical reach of about 0.25m. This will require that we allow for a vertical Z travel of no less than 0.91m but we will also not need more than 1.22m either.

Vision Sensing Requirements

The main requirements for the vision sensing are stand-off distance, orientation, positioning and calibration accuracies. To view a certain number of tiles in a single image, we need a specific field-of-view and stand-off distance. Even then, large field-of-view optics have a certain amount of distortion, mostly at the edges of the image, which may make part of the image unusable. In Figure 5-9 we have illustrated and also tabulated stand-off requirements subject to linear imaging dimensions and camera optics. The

variables are W=linear dimension of acquired image edge, d=stand-off distance of camera lens from shuttle surface, and α=lens angle of camera.

Figure 5-9 Vision system standoff requirements

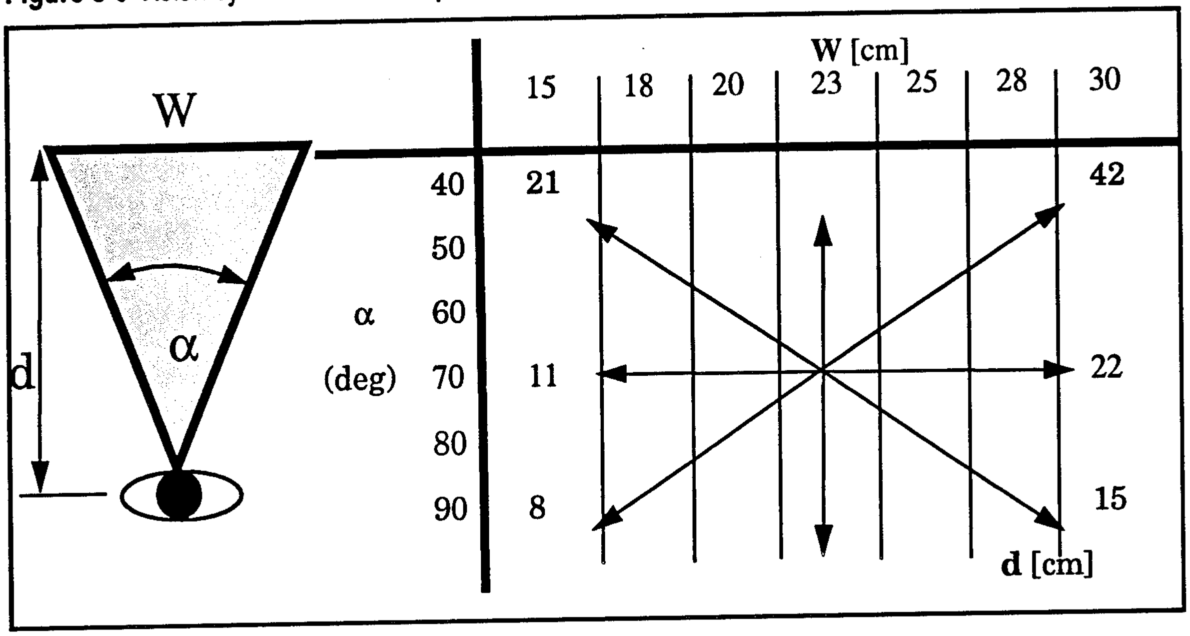

The width of the captured image may only need to be W=15cm wide for a single tile, but we may want to capture at least 4 tiles in an image for navigation purposes, which requires that W be 0.3m. These are requirements that will have to be distilled from the vision sensing and recognition criteria.

Reach and Dexterity Requirements

Reach requirements for the manipulator to position the endeffector are one element of the design. It is necessary to attach a horizontally moving boom of some appreciable length where the length can be between 0.5 and1.5m. to allow sufficient tile coverage.

As shown in the previous section we need to approach the tile surface along the surface normal with respect to the injection point to insure that only one motion, normal to the surface, is necessary. This positioning requirement results in a minimum 5 degree of freedom (DOF) system:

1) Longitudinal x-position along the centerline of the shuttle
2) Orthogonal y-direction perpendicular to the centerline
3) Vertical height z
4) Wrist/elbow pitch
5) Wrist/elbow roll to align the longitudinal axis of the injection nozzle with the local surface normal.

Additionally, vision processing requires the full 6DOF to align new and old images[1]. The rewaterproofing process does not require this rotation as the system is not concerned about orientation along that axis. On the other hand, the vision system may require aligning cameras on the tool plate along a coordinate frame specified within the plane tangent to the tile surface. If such a rotational degree of freedom is necessary for vision purposes, it is more appropriate to mount it as close as possible to the distal link. Mounting it on the elbow would not be appropriate since we only care about orienting cameras. If there are any future servicing tasks that require this orientation capability, it would not be complicated to add.

5.3.4 Manipulator and End-Effector Design

XY Horizontal and Lift Mechanism

The XYZ table positions the manipulator arm in the XY plane and allows the end effector to be positioned in the Z-plane. The exact stand-off distance is yet to be determined and is driven by the requirements of the vision system. For the linear X,Y and Z drives we considered two types of drive mechanisms: ball screws and timing belt drives. The detailed numerical tables and system parameters are tabulated in Appendix B under Manipulator XY Table.

The main advantages of a ball screw linear drive are good accuracy, high stiffness, and good load bearing capability. A ball screw linear drive can be driven open loop (without position feedback) with great accuracy and even better repeatability. However, a high pitch ball screw will also backdrive in a controlled manner in the event of a motor failure. By simply changing the pitch on the ball screw the device can be made non-backdriveable and thus power consumption can be drastically reduced during 'static moves'. However, ball screw linear drives are expensive, especially in the size ranges that we are considering. Ball screw and linear bearing supports are steel to provide rigidity. To minimize the deflection of the bearing races, a horizontally mounted ball screw drive would have to be supported for most of its entire length.

The timing belt linear drive is less accurate than a ball screw linear drive due to the compliance of the timing belt and backlash of the gear-pulley drive mechanism. However, this shortcoming can be corrected through the addition of a high resolution linear optical encoder to provide feedback to the motor controller. The timing belt drive will also be much lighter than a ball screw drive. The structural support components can thus be made out of aluminum instead of steel. These drives are also readily available in long lengths at less expense than comparable ball screw drives. Timing belts are usually reinforced with multiple steel-wire cables to provide the tensile strengths, while indexing is done through plastic ribs along the belt itself. Belt failure is an important consideration, especially if used in the vertical motions.

Timing belt linear drives were selected for the XY portion of the horizontal positioning table because of their long lengths, high speed capabilities, medium to high accuracies, reduced weight, and moderate costs, the advantages of linear belt drives far outweigh their

1. Requirement arising from discussions with SRI.

disadvantages. Possible belt failure in the XY plane will not be catastrophic, since we will have two sets of belts which act as a redundant pair. Such a failure can be easily detected with a linear encoder mechanism and thus be easily monitored. A ball screw linear drive has been selected for the Z axis, due to its ability to sustain larger loads, choice of backdriving efficiency, and the unlikelihood of catastrophic failure and easy safing in case of failure.

A preliminary design of a ball screw driven XY table was conducted using "Thompson" brand components. A double shaft system was used for the X and Y stages. Standard Rc60 case-hardened shafts were used for bearing ways, and Thomson 25mm by 25mm ball screw assemblies were used. Since the loads would cause excessive deflection of the bearing races, aluminum rectangular supports are used under each shaft. The supports are 89mm square aluminum tubes, with a 6mm wall. To protect the bearing surfaces, protective bellows are used to cover the bearing races even though these reduce stage travel. A stainless steel lead screw using a helically threaded round shaft would be required in the final system. Stage deflections were calculated assuming a beam supported, but not fixed, at both ends and a load at the center.

Comparison of the timing belt XY table and the ball-screw XY table reveals that the ballscrew tables have greater travel distance, weigh less, and have less deflection.

Figure 5-10 Three axis gantry system

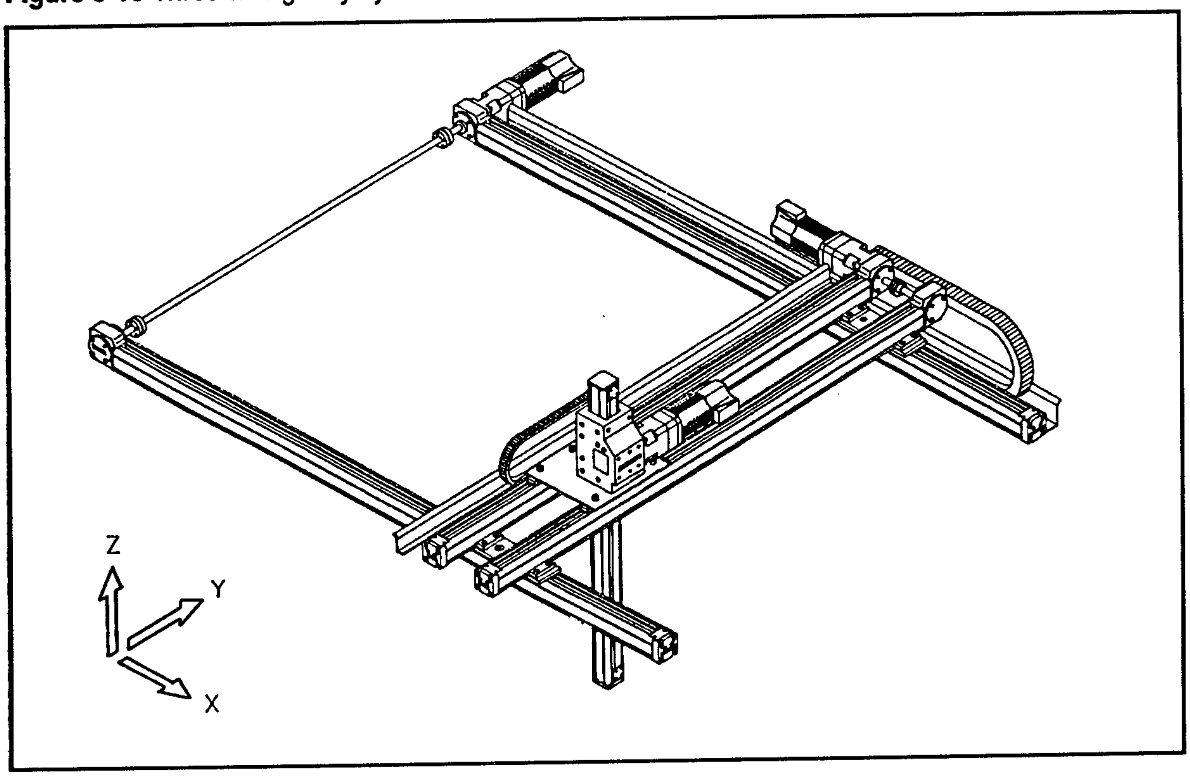

The overall dimensions of the XY table are dependent on the base size. The main disadvantage with such systems is the loss of work envelope due to carriage length, supports and other mechanisms. We have provided a table in Appendix B. that illustrates this by listing different base sizes, XY table dimensions and travels, that result in a given

tile coverage. To cover at least 150 tiles, some form of horizontal boom or extension will be required at the end of the Z axis to extend the workspace, possibly even reaching over the base footprint. The length of overreach will depend on the size of the base, and whether servicing tiles above jackstands is important. We have listed the required arm length to cover 150 tiles for each base size selected for the XY unit. The associated weights and costs are also listed for comparison purposes. The vertical deflections of the unsupported rail lengths are small, as calculated by equations supplied by the manufacturer, and can be minimized even further by reducing the unsupported length through gussets or support along the entire railing.

The final system configuration can thus be summarized to be:

- XYZ Linear Positioning Device
- Use of a lead-screw or belt-driven XY table stage will have to be decided based on materials compatibility, required accuracies, service life, weight and cost. Several manufacturers were identified including Hauser for a belt-driven design, and Thompson or Warner for ball-screw designs. Cost is comparable, but there are also time and weight considerations. Materials compatibility studies are currently underway for the belt-driven unit.
- The vertical Z travel in the XY table will be a lead-screw driven unit, powered and safed by conventional means including brakes, redundant sensors, non-backdriveable transmissions, etc. A non-backdriveable unit relies on the internal system friction to keep the unit in place when power is lost, thereby avoiding damage to the system.

Figure 5-11 Tile-normal configuration.

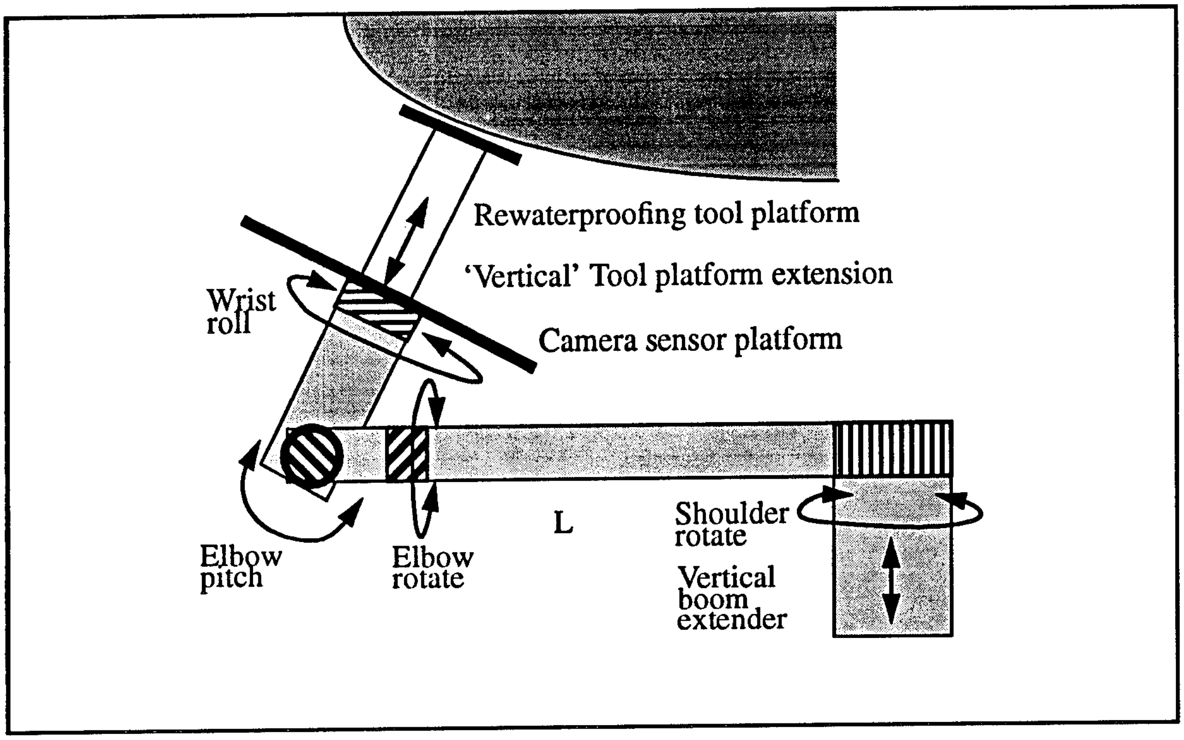

The requirement to create a stiff, fast and safe manipulator has resulted in reduction of individual motions for a four-column gantry elevator and vertical boom elevation, by adding some additional 'vertical' extension at the endeffector. The main design alternatives for possible manipulator configurations that were considered in this study, are sketched out in Figure 5-11, Figure 5-12, and Figure 5-13.

One manipulator configuration would have a short extension as a forearm, after a 2 (or 3) DOF elbow which would be at the end of the horizontal boom. Such a configuration is shown in Figure 5-11. We term this configuration *tile-normal.*

Another way to apportion the additional vertical reach in the true (world-frame) z-direction, is to add the travel at the end of the horizontal boom, bringing a 2 DOF wrist close to the tile surface to perform the rewaterproofing (Figure 5-12). This configuration is termed *vertical-normal.*

A compromise configuration between the tile- and vertical-normal, uses a vertically fixed extension, with an added 2 or 3 DOF wrist attached at the end. This wrist can position a sensing and tooling plate with the proper orientation to the tile. A small and lightweight linear actuator could extend the rewaterproofing nozzle over a 0.1m travel towards and away from the shuttle tiles. The configuration is shown in Figure 5-13, and is termed Vertical-tile-normal.

Figure 5-12 Vertical-normal configuration

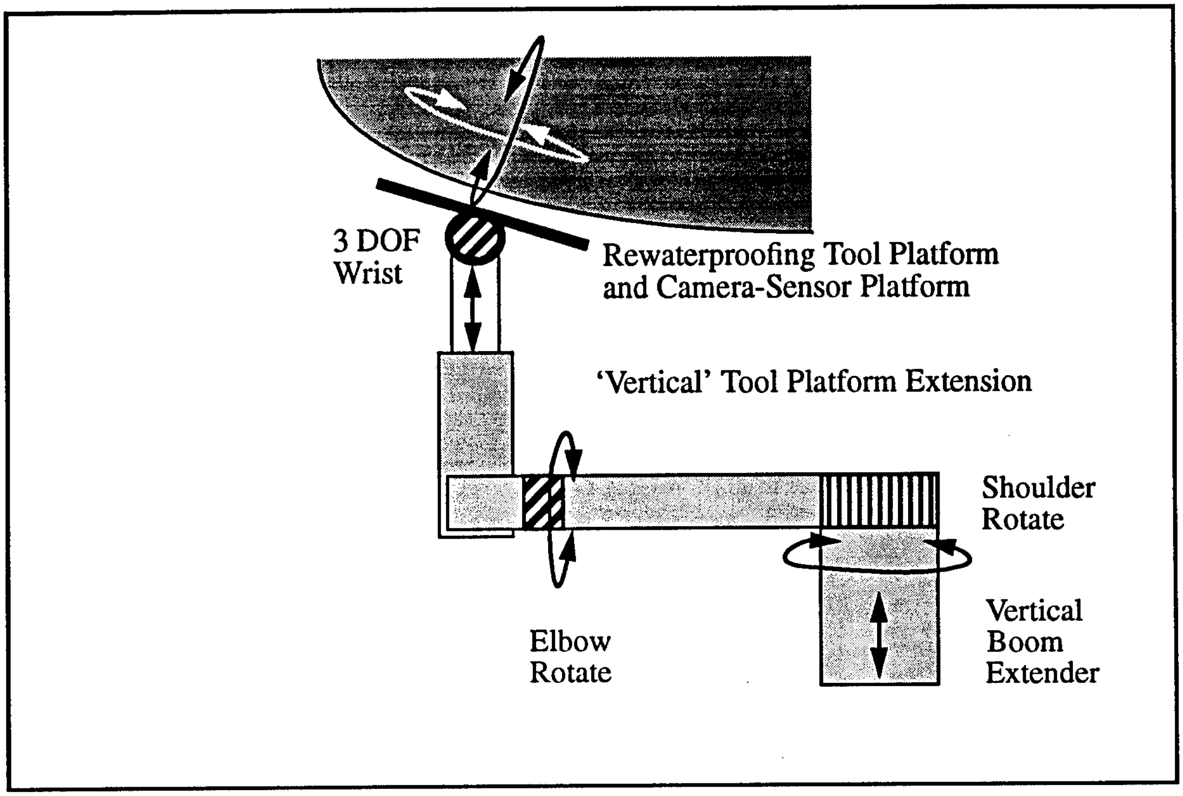

Figure 5-13 Vertical-tile-normal configuration

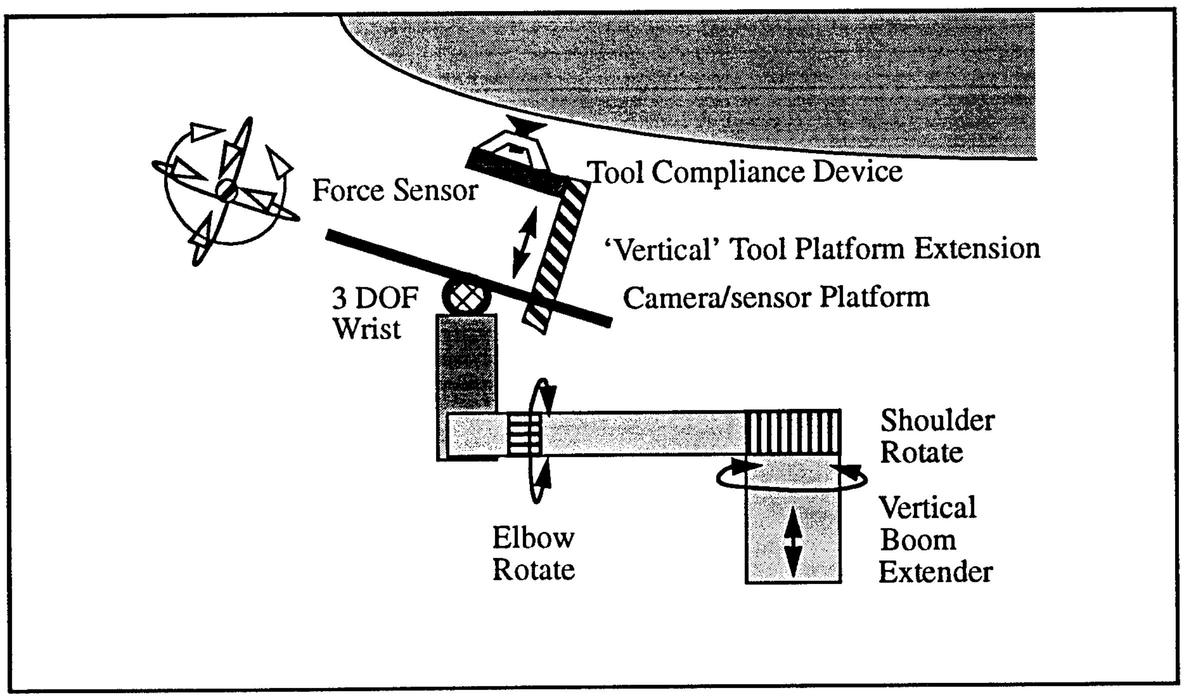

All of the manipulator designs incorporate a forearm roll-joint used only for stowing the endeffector. Each of these three designs will have to be evaluated in terms of its overall length, mechanical feasibility, planning requirements, ease of control, and packaging.

We are favoring the vertical-tile-normal design due to several reasons, which are briefly summarized here, and analyzed in more detail in the sections to follow. Notice that in the vertical-tile-normal design we have retained the fixed vertical arrangement at the elbow, while still incorporating an elbow joint for stowage and deployment only. The advantage of this configuration is that we now have minimized boom and extension lengths by packaging the 2 or 3 DOF wrist into the vertical elbow extension or forearm. This gives more room for packaging than the vertical-normal design and retains the split between camera/sensing and tooling platforms. Any additional sensors can be mounted to the sensing platform and can be positioned in any of the 2 or 3 DOF orientations allowed by the wrist.

The final vertical extension is now solely responsible for deploying the tooling normal into close proximity to the tile surface. We have limited the mass and size of objects that are less than 2.5cm to the shuttle. A force sensor is located at the base of the tooling hardware to monitor interface forces and torques and we can use it as another level of force monitoring and control between the tip of the rewaterproofing endeffector and the tile surface.

During the rewaterproofing task, the only actuator that has opposing forces or control, is the vertical tool extender. All other actuators, providing the orientation alignment is correct, are lightly loaded. The exceptions are the gravity torques from the sensing plate and hardware, vertical extender and tooling on the wrist mechanism. The challenges in this design are the packaging of the wrist mechanism, and the compact and high dynamic fidelity implementation of the vertical tool extension mechanism.

The choice between the three different candidates is governed by several criteria and numerical differentiators. Below we have given the list that comprises all the aspects to differentiate between these configurations. The goal of the list is to show all of the different issues involved in endeffector design to justify the selection of the final design configuration. To motivate the items in that list, we first explore the overall requirements for the endeffector.

Manipulator Kinematics

The three design options differ somewhat in the actual dimensions necessary to service identically located tiles. Figure 5-14 depicts two different manipulators servicing the same tile, and the associated link dimensions and extensions required from each configuration. Notice that the vertical-tile-normal configuration is not included. Since differences between its dimensions and those of the vertical-normal configuration are small.

The equations that govern the required vertical and horizontal dimensions and extensions are as follows:

$$\Delta L = (h_1 + h_2) \tan\alpha \qquad \textbf{Eq. 4-5}$$

$$L_2 = L_1 + \Delta L = L_1 + (h_1 + h_2) \tan\alpha \qquad \textbf{Eq. 4-6}$$

$$\Delta E = \frac{1 - \cos\alpha}{\cos\alpha}(h_1 + h_2) \qquad \textbf{Eq. 4-7}$$

$$E = \frac{h_1 + h_2}{\cos\alpha} \qquad \textbf{Eq. 4-8}$$

Figure 5-14 Manipulator and endeffector reach requirements

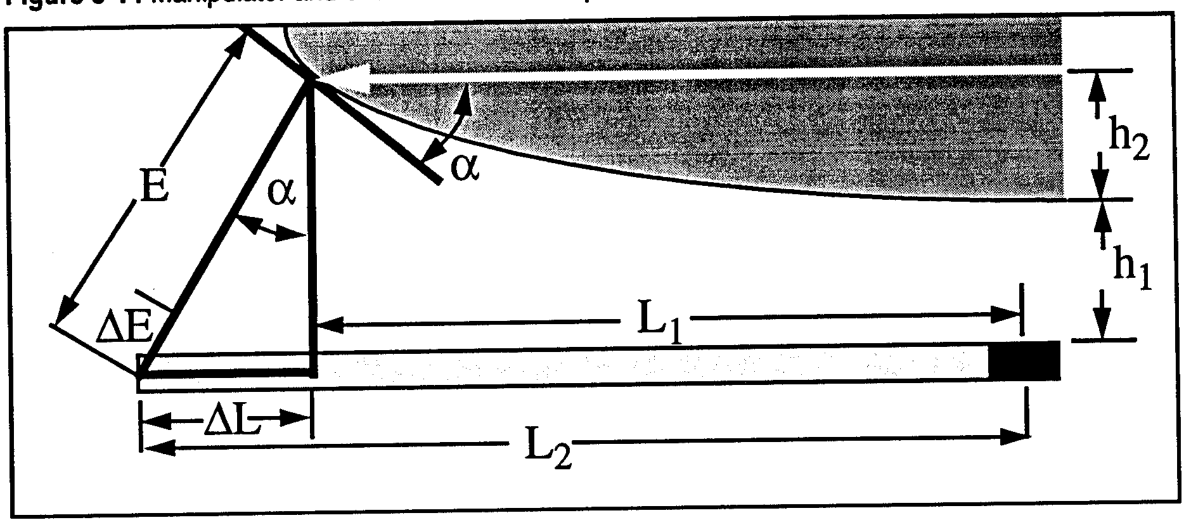

To reach the same tile, the tile-normal design (Figure 5-11) requires an additional horizontal boom length of $(h_1+h_2)\tan\alpha$. The standoff of the horizontal boom-top h_1, and the height differential of the tile distribution h_2, are thus crucial dimensions. In the case of $\alpha=45^o$, the extra boom length (or displacement) is exactly the sum h_1+h_2. In the case of $\alpha=60^o$, the extra boom length (or displacement) is 1.732-times the sum h_1+h_2. The additional extension required (ΔE), is also a factor of the sum h_1+h_2. For $\alpha=45^o$, the additional vertical extension is 0.41-times the sum h_1+h_2, while for $\alpha=60^o$, the additional vertical extension is exactly the sum h_1+h_2.

The most drastic extensions and changes in elevation required are due to the nose area and the leading edges of the wings. A more detailed analysis for reach, stand-off and other necessary dimensions is outlined in a later section describing the necessary degrees of freedom and reaches at a variety of different shuttle locations.

These considerations are important as they dictate the overall boom length, shuttle safety standoff distance, rewaterproofing tool dimensions, and eventually the number of tiles reachable above a certain angle of tangent plane. A clear numerical differentiation can not yet be made and these issues are unresolved.

The three design options differ in the computation of the kinematics and inverse kinematics. In the tile-normal design we can move the actuators and maintain the intersection of all three axes of rotation around a common point. This common point has to be positioned at the point where the perpendicular vector from any tile and the plane described by the horizontal boom intersect. Subsequent elbow pitch and roll motions will align the endeffector extender with the surface normal, leaving the wrist rotate/roll the option of aligning the sensing and/or tooling plates.

The vertical-normal design requires only that the end of the horizontal boom be positioned at the intersection of the gravity vector going through the tile contact point location of the surface normal, and also the horizontal plane described by the horizontal manipulator boom. The vertical-tile-normal design would have a 3 DOF wrist on a fixed vertical extension, which then aligns a linear actuator to bring the tooling close to the shuttle. The only difference from the vertical-normal design is that the center of rotation of the wrist itself must be positioned anywhere along the vector normal to the tile surface injection point.

The differences in forward and inverse kinematics between these schemes are small and well understood. The eventual design decision will mainly be affected by the following criteria:

- Horizontal boom length
- Endeffector compressed and extended lengths
- Required shuttle stand-off distances
- Reach necessary along surface normal
- Power consumption during a rewaterproofing cycle
- Complexity of technical implementation and component packaging
- Safety margins
- Approaches required to avoid excessive contact forces

Implementation and Packaging

To implement each design, factors such as weight, size, and the ability to package it appropriately will be addressed. The vertical-normal configuration will require at least a 2 DOF wrist and designing or buying commercially available units will be expensive. For the tile-normal design, the different DOFs can be simply generated using available components and be shifted away from the endeffector, closer to the shoulder. Additionally all rotational axes should meet in a single point to ease inverse kinematics calculation and planning. If a third rotational degree of freedom is required, it can be easily mounted to the sensing or tooling platform due to the reduced size and inertia requirements.

The vertical-tile-normal design also requires careful design of the 2 or 3 DOF wrist mechanism. The advantage over the vertical-normal configuration is that we have substantially more space in the fixed vertical section of the forearm. This allows simpler packaging of transmissions, motors, encoders, even though the overall wrist design is not necessarily simple. Avoiding singularities, achieving large ranges of motion, maximizing power output, and achieving good positioning accuracies are just some of the stringent criteria the final design will have to meet.

The overall weight of the different options is equivalent, but even if the weight of the tile-normal design is larger, its weight is distributed closer to the shoulder and does thus not have to be carried by the vertical extension actuator. To stow the vertical-normal design endeffector within the base we will add a joint to move the endeffector upwards for deployment or downwards into the XY table plane for stowage. The two designs do not differ with respect to stowage. The main difference lies in the location of the two essential rotational motions required for alignment with the local tile surface normal. Similar arguments can be made for the vertical-tile-normal configuration.

Task Execution Effects

The tile-normal design facilitates the vision sensing and rewaterproofing task combination, since we can take an image while we proceed to approach the tile surface. In the vertical-normal design we first have to take an image at a proper stand-off distance with the proper orientation, after which we have to perform a compound motion to approach the tile and inject the chemical. Such a design requires extra motions and will likely have a longer cycle time per tile. The vertical-tile-normal design only performs one simple motion to align the camera axis with the surface normal of the tile being inspected.

All three designs require compound motions if the perpendicular orientation of the tooling plate has to be continually servoed. The current plan calls for use of the global robot position estimate, tile image registration for accurate local positioning, and the tile database for each orbiter, to compute the orientation and location of the surface normal for each tile serviced. Since there will invariably be inherent positioning errors, we may have to actively servo to the proper orientation if the errors are excessively large and cannot be compensated by the compliance in the nozzle and endeffector. The need for servoing and the achievable accuracy using piezo-electric sonars will have to be determined during the experimental phase of the manipulator design program.

To control contact forces the tile-normal design is likely to have better performance, as the vertical actuation can be made backdriveable and thus more responsive also due to reduced weight at the tip of the endeffector. This feature means more accurate and better force control response. Contact forces can then be monitored with a simple load cell. The use of a wrist force sensor for the vertical-normal design is more complicated, since we need to measure all three force vectors to measure the true contact force and then decide on corrective action. Any corrective action will have to be performed by a set of compound motions using all degrees of freedom except for the vertical gantry extension. Such a scenario is undesirable, and is not required by the tile-normal or the vertical-tile-normal design. We only have to use the extension normal to the tile surface to control force interaction for both of these designs.

The addition of a tool interchange adapter or other hardware required near the endeffector would add little weight and is necessary for both systems anyway. Excessively bulky or heavy hardware could always be mounted on the horizontal boom extender, as long as it meets the 1.83m height criteria for system stowage. This approach would allow for a minimum distribution of mass at distal manipulator locations, thus increasing control fidelity and bandwidth.

Future Tasks

Since we want to do more than visual inspection and rewaterproofing we will have to insure that the design will be able to fulfill future requirements, such as those imposed by step-and-gap measurements and charred filler-bar inspection. Any task involving contact and re-orientation requires a wrist-roll actuator if the sensing and tooling are separated. This additional actuator could be very light and compact without adversely affecting the overall system. Such additional actuation would not be necessary in the vertical-normal design, as it may have a third wrist DOF for the vision sensing system. Currently then, the design will include a third DOF as a wrist-roll, so that future sensors or tools can be mounted to the adapter plate without additional actuation.

The ability to change the endeffector tooling is equivalent for all three designs. The ease of access to the sensing and tooling platform for the tile-normal design, makes such a feature quite desirable for all other designs. The reduced space taken up by each tool is beneficial for the vision system, as it will always be in the same position for viewing the tile surface.

It is premature to consider a tool exchanger design, as we have not finalized the rewaterproofing tool design, nor do we have the requirements for future tooling devices for this robot. As each of these open questions are answered we will resolve the tooling exchange design to suit the intended tools.

Wrist and tooling kinematic arrangement

The robot wrist has two or three rotational DOF's and a single prismatic DOF. This scheme was adopted, in contrast to a conventional spherical wrist, because of the dexterity requirements of the servicing tasks. With a single prismatic joint that raises tooling into shuttle contact, a safety margin is gained since only one joint must be servoed. A conventional, industrial-style, revolute-joint manipulator requires all six DOF to be simultaneously servoed, increasing the likelihood of damage to the tile surface in the event of servo error. Such a scheme would also require complex force-control loops and force sensing. A single axis motion greatly simplifies sensing and control requirements. A functional sketch of the basic required functionality of the wrist mechanism is shown in Figure 5-15.

Figure 5-15 Robot wrist design concept

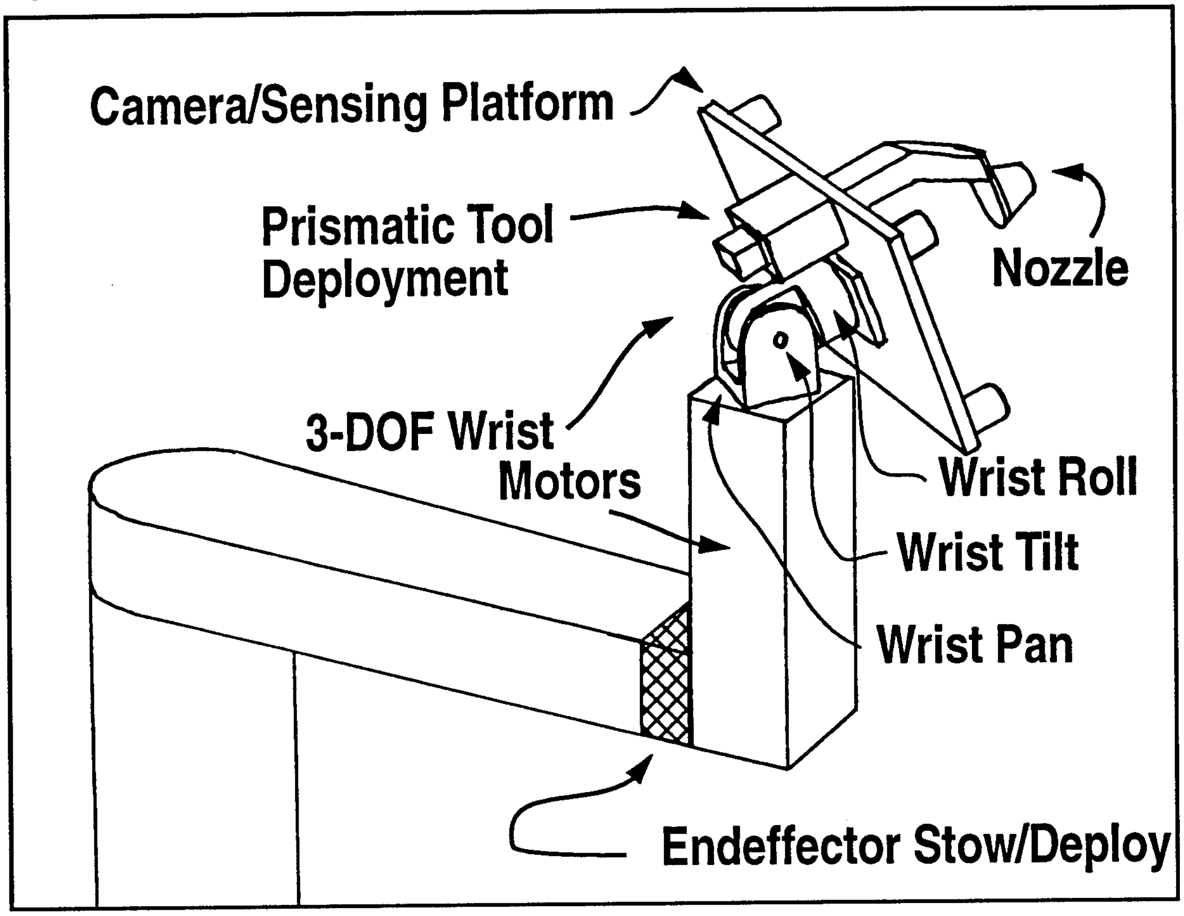

As shown in Figure 5-16 a single tile rewaterproofing scenario would consist of a combined gantry and shoulder motion to position the rotational joints along the given tile's surface normal. The location of the 'elbow' joint lies at the intersection of the tile surface normal and the horizontal plane described by the rotational plane of the horizontal boom (point X in Figure 5-16). The two or three rotational joints are then used to orient the tooling and optical sensing hardware, an image of the tile(s) is taken, and the tooling is then raised to close proximity with the shuttle surface by the prismatic forearm. Custom tooling actuation then raises injector hardware into contact with the tile. The forearm is then retracted and the cycle repeats.

The two essential tooling rotations are to change the elbow pitch angle to the value of the angle α sustained between the horizontal boom and the projection of the normal vector into the vertical plane, and an elbow roll by the angle β inscribed by the vertical through the intersection point and the projection of the tile normal into the vertical plane perpendicular to the horizontal boom vector. A rotational orientation γ about the vector $\bar{v}$ is only necessary to orient the camera sensing hardware - and possibly any future sensing and tooling devices.

Figure 5-16 End effector inverse kinematics

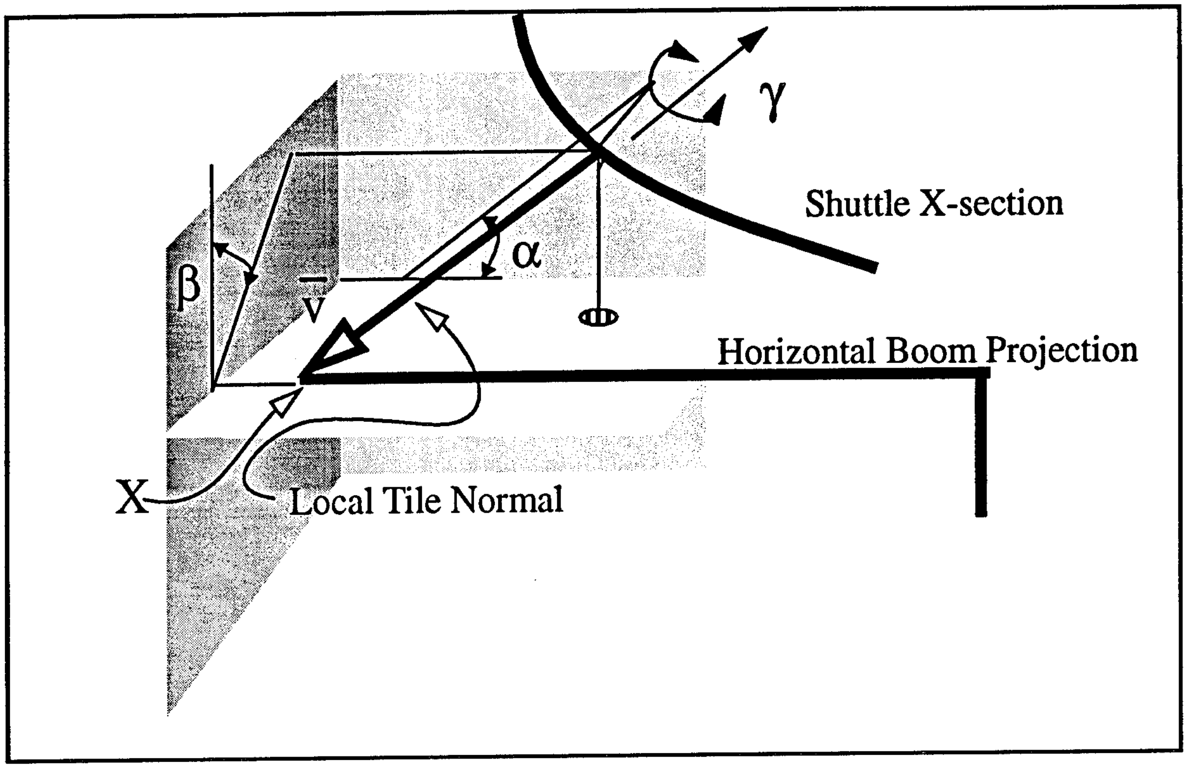

Since the motions provided by the vertical column member and the forearm extension are redundant, it is important that they be proportioned properly to achieve the required dexterity. The most dexterous motions are required when the manipulator must service tiles on the outside edge of the shuttle's bottom surface. This requires that the arm reach "over", and then rotate to the most extreme angles α and β encountered in servicing. The vertical column is kept some safe distance away from the closest orbiter tiles in this scenario. This stand off distance, along with boom length, determine how long the forearm extension must be in order to reach the shuttle. The worst-case curvature in the shuttle bottom occurs in the nose area and all along the leading/outer edges of the shuttle. Since boom length is somewhat fixed by mechanical and minimum required tile coverage constraints at around 1 meter in length, the worst-case curvature causes a 0.31m change in height over the boom length. Since the forearm is inclined at 45^{o}, this means that the forearm must have 0.46m of stroke in order to service the high-curvature tiles.

With the forearm extension decided upon by worst case curvature, we can now determine what stroke range is required by the vertical member. Since the maximum stroke of the gantry lift mechanism has been set at 2.74m to avoid collision between it and the shuttle, this will require at least 0.92m of stroke in order to service the highest tiles. To service the lowest tiles, a combined gantry lift and vertical column move will be necessary. Since the gantry must collapse to a 1.83m height to enter the work area, the vertical column would require a minimum extension of 0.46m to service low tiles from this gantry height.

The rotational motion can be implemented using a variety of schemes. The key requirements are to reduce the moving masses and to limit rotational inertia around the vertical column. Harmonic drives are light and compact, but can have some backlash and

appreciable compliance. They do not stand up well to wear and overloading, but they do offer the largest torque to weight ratio available with any known transmission. Dojen cycloidal cam reducers offer zero backlash with extreme stiffness, yet at a penalty of medium weight. The Dojen cycloidal cam reducer seems to offer the perfect compromise between size, accuracy, and durability, despite the extra added weight. The prismatic forearm can be built using ball-screw actuation, rack and pinion, cables, or chain drives. The final design will largely depend on the configuration of the rewaterproofing tool being designed by Rockwell International.

In the event of a tooling failure, the tooling plate may be lowered to a working height by retracting it downward and lowering the plate using the forearm. If a servoing error occurs during operation, vertical motion can be immediately halted by halting the forearm motion. For added safety, the forearm motion can be implemented using a highly backdriveable transmission system or ball detente to physically limit and control contact force. Obstacle detection and avoidance can be implemented electronically using piezo-electric or infrared sensors and mechanical limit switches that trigger upon contact in the event of controller runaway, power failure or computer failure.

An Additional DOF

Another important consideration is the addition of a limited degree of vertical motion along the manipulator arm, in order to:

1) reduce the vertical travel of the main vertical linear extension at the shoulder of the manipulator,
2) to increase the acreage of tiles reachable with tangent to planes larger than 45^{o}, and
3) to reach into areas that are not readily accessible due to obstructing platforms or workstands.

Such a scheme would allow for a substantially longer boom, anywhere from 1 meter to 1.5 meters, with a rotational pivot included somewhere along the arm. Another added benefit of adding such an extra DOF would be the reduction of required horizontal boom length as it would enable the elbow joint to be placed anywhere along the vector normal to the tile. This joint would only be used in areas of increased curvature or obstacles, while being completely unused for 60% of the low curvature shuttle surface. The added mechanical complexity is small, but there are added component costs in addition to reliability and failure issues.

Several kinematic arrangements and mechanical implementations are depicted in Figure 5-17.

Figure 5-17 Concepts for increased manipulator reach and dexterity

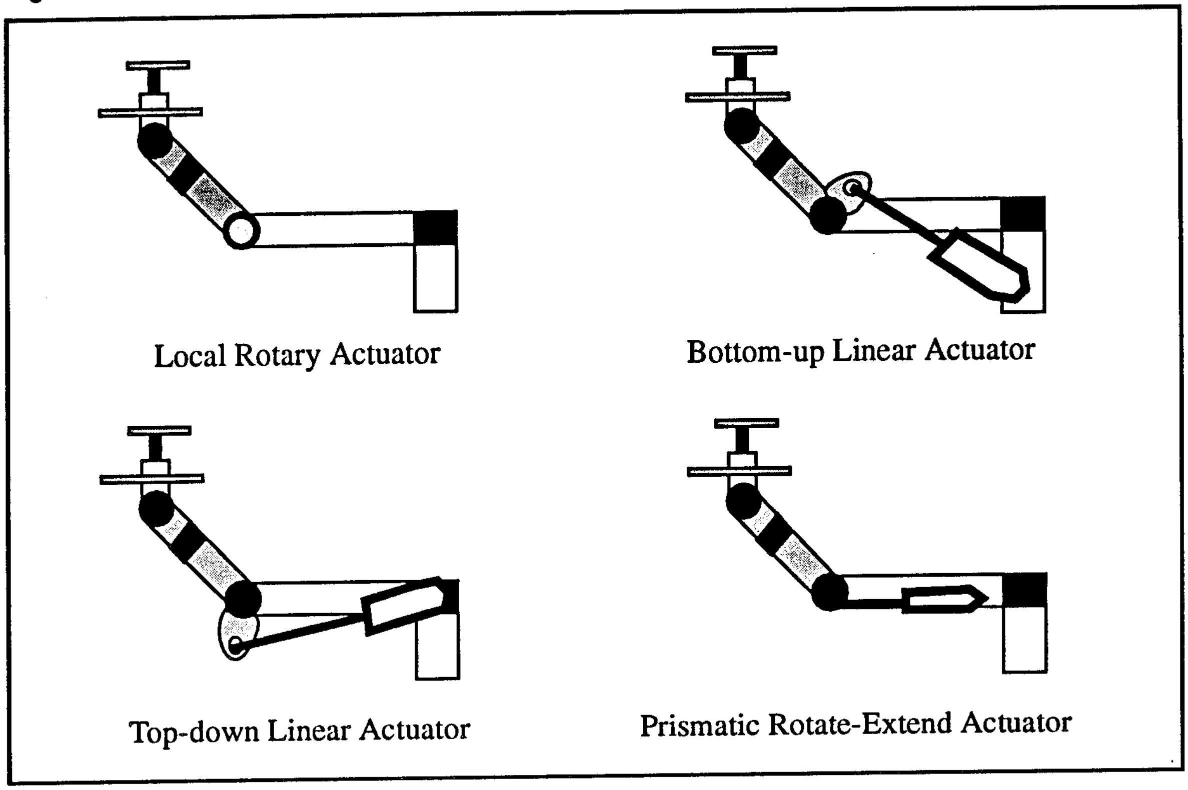

Each of these solutions has benefits and drawbacks. The overall requirements of such a joint are:

1) that it be stiff,
2) consume little power, i.e. self-locking, with no need for rapid dynamic moves,
3) not affect the packaging and stowed profile,
4) have sufficient reach and rotation to alleviate vertical stand-off requirements on the vertical shoulder travel,
5) that it maximize horizontal tile coverage,
6) increase the tangent plane reach of tiles,
7) and be able to circumvent work platforms and other obstacles at different heights (reach between platforms and shuttle surface).

The addition of this extra DOF will have to be evaluated if all the requirements listed are met. Otherwise, reduced horizontal boom length may be necessary. Incorpoation of this additional DOF will be affected if we do *not* service tiles at the nose, wing edges or around the jackstands. If this is the case then the added joint is not really necessary.

We concluded that for a typical 1m to 1.5m long boom, the overall difference in height h_2 is at least 0.56m but no more than 0.89m. See Figure 5-14. The extreme value of 0.56m occurs along the periphery of the shuttle contour, while the 0.89m difference is present over the nose-cone. The added stand-off distance of the vertical travel should be at least 0.13m, thus making the necessary vertical reach even greater. To resolve this question, we

have depicted the servicing scenarios for different locations along the shuttle contour in Figure 5-18, allowing us to explore required lengths and offsets. The governing equations are also given below.

Figure 5-18 Manipulator reach and dimensional study

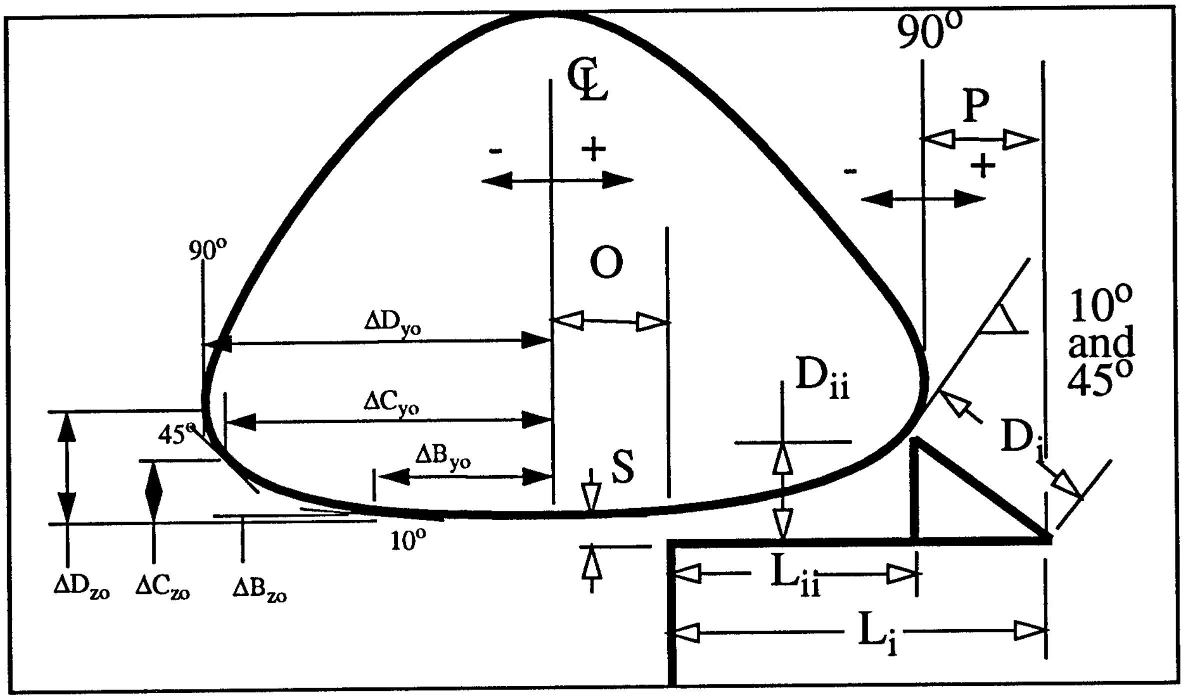

$$D_{ii} = S + \{\Delta B_{zo}, \Delta C_{zo}\}$$ **Eq. 4-9**

$$D_i = \frac{D_{ii}}{\operatorname{acos}\{10°, 45°\}}$$ **Eq. 4-10**

$$S = L_{ii} = given$$ **Eq. 4-11**

$$L_i = L_{ii} + D_{ii}\tan\{10°, 45°\}$$ **Eq. 4-12**

$$O = \{\Delta B_{yo}, \Delta C_{yo}\} - L_{ii}$$ **Eq. 4-13**

$$P = \{\Delta B_{yo}, \Delta C_{yo}\} + (L_i - L_{ii}) - \Delta D_{yo}$$ **Eq. 4-14**

NOTE: ΔB_{yo}, ΔC_{yo}, ΔB_{zo}, ΔC_{zo}, and ΔD_{yo}, are all as defined in the KSC TPS Processing study.

The approach is to determine, for vertical stand-offs of 0 to 0.30m and link lengths L_{ii}, the necessary dimensions O, D_{ii}, D_i, and L_i for the two tangent plane locations of 10^o and 45^o at different locations along the perpendicular to the shuttle's centerline. These are locations a through j on Figure 5-6.

An analysis of the shuttle cross-sections reveals some interesting results for different locations along the shuttle. We have included in Section B.9 "Reach and Dexterity" on page 207, a list of the most interesting points and the relative dependent (D_i, L_i, O, P) and independent variables (X, S, L_{ii}).

The data representation in Appendix B is summarized here:

- A comparison of the protrusion distances P for the two different designs indicates that to reach the 45^o tile tangent plane requires excessive reach outside of the shuttle footprint which would not be possible in certain locations in the OPF. The protrusion distances are between 2.5 and 30cm in the forward nose section, but extend to between 45 and 75cm around the main fuselage sections (location **d**). This is the least accessible area due to the jackstands and low side platforms.
- To provide some stand-off distance S for safety purposes, the length of the endeffector extension D_i lies between 28cm and 120cm for the 45^o tangent plane. Such lengths are excessive. Even for S=0 at the 45^o tangent plane, this dimension can lie between 28cm and 76cm. Such lengths are unreasonable and prohibit the tile-normal design. The region where this is most pronounced is section **d**, along the main fuselage of the shuttle. This location is next to the forward shuttle jackstands, allowing little room and maneuverability.
- The standoff distances required for the vertical-normal design lie between 2.5 and 30cm for zero standoff distances (S=0), and from 30cm to 70cm for 30cm standoffs. The vertical-tile-normal design will lie somewhere between these two regimes, indicating that the reaches required are mechanically achievable and feasible. These two designs, shown in Figure 5-12 and Figure 5-13, can achieve reasonable standoff distances around 15cm, without requiring excessive reaches at the endeffector.
- The selection of a maximum reach of around 45cm at the endeffector should be possible with the vertical-normal and vertical-tile-normal designs, giving enough camera/sensor platform offsets to the tile surface, while allowing for enough reach to place the tooling platform near the shuttle tiles.
- The previous analysis assumed that the horizontal boom was about 1.25m long, which represents an extreme case. If a shorter boom length can be used, the above restrictions would be relaxed even further. Thus, if longer boom lengths are required, only the designs depicted in Figure 5-12 and Figure 5-13 are possible candidates.
- If tiles with a higher curvature need to be serviced in the future, the vertical-

normal and the vertical-tile-normal designs can be easily adapted to do so. However, there will be limits due to obstacles outside the shuttle footprint and less standoff distances due to excessively long horizontal reaches. Such situations would require a shorter horizontal boom, or the addition of an added degree of rotational freedom about the longitudinal horizontal boom axis, deploying an forearm section as shown in Figure 5-17.

Safety-related Design

To provide a maximum of inherent, active, and passive levels of safety, the endeffector design has to fulfill certain criteria. We wished to reduce the speeds and inertias of mechanisms near the shuttle. The tile-normal design (Figure 5-11) differs from the vertical-normal design (Figure 5-12), in that it does not require the entire sensing and tooling to be deployed close to the shuttle. A certain amount of stand-off from the tiles is required for the vision system and a certain angle of (controlled) incidence for lighting and cameras is crucial. Placement of the sensing plate at a fixed distance away from the tile surface, but normal to the tile, makes this an inherently safer arrangement. The vertical extension is then only used to bring the actual tooling to within 5 cm for the injection process to begin. In the case of the vertical-normal design, the entire sensing and tooling arrangement needs to be brought next to the shuttle tile and oriented properly, all within a 5cm distance from the tile surface.

The possibility of tile damage due to erroneous control signals is magnified by the inertia and dimensions of the entire sensing/tooling arrangement. This includes the injection nozzle, proximity sensors, cameras, lighting, and mounting plate. Any vertical extension at the endeffector does not bring the injection nozzle closer to the injection hole, as such a move, even if the orientation is perfect at the endeffector, requires compounded motions from the horizontal boom and xy table. Angular reorientations during such moves are usually also necessary, as the final orientation can not be accurately determined until the tip is almost over the injection hole. Such motions and re-orientations are also required by the tile-normal design. Even if they are larger motions, they occur at a safe distance away from the shuttle. The vertical-tile-normal design incorporates the best features of each design, making standoff distances for vision and lighting systems easy to achieve, reducing contact inertia and maximizing standoff distance to the shuttle.

We will provide electronic safing features such as piezo-electric proximity sonars that are good from 1cm to 15 cm with better than 1 mm accuracy, and mechanical switches. The sensors can be used to halt the entire mechanism, alert the operator, and even initiate safety moves which immediately retract the final vertical tooling extension away from the shuttle. These safety features can provide safety features even in the case of controller failure. In the case of power failure we will use brakes on all major motions, while providing for sufficient backdriveability to retract the final vertical extension at the endeffector.

Mechanical Componentry

The mechanical components proposed in the different designs are commercially available, and their reliability is assured through several prior and/or analogous systems having been built and tested to date. This design also has many custom features to it which requires us to incorporate those components into an appropriate design. Packaging the individual

components such as motors, transmissions, brakes, bearings, supports, etc. into a compact and serviceable package will be the major design challenge.

The use of commercially available zero backlash transmissions such as harmonic drives or cycloidal cam reducers, coupled to brakes, will provide for a reliable and readily available actuator package. Brushless motors will be used and controlled with several sensors. Bearings will be selected based on tolerances, loading and environmental condition. Elements such as connectors and cabling will be selected based on their environmental specifications. Materials used for structural elements and sealing will be selected based on both environment requirements and limitations imposed by the use of DMES. Certain materials that will be used are not yet tested for DMES exposure and need to tested.

5.3.5 Manipulator System Integration

Configuration, Dimensions and Componentry

We propose as a final configuration an XY table with a vertical deployment of a fixed length rotating horizontal boom, with a pitch/roll elbow and small linear actuator at the endeffector to deploy the tooling next to the shuttle tiles. A sketch of the final system configuration for manipulation is depicted in Figure 5-18.

The configuration would include an XY table with an aspect ratio of about 1.28, dimensions 2.74m by 2.13m, with aluminum extrusions holding carriages actuated by timing belts, powered belt-pulleys, extremely low backlash planetary gears and brushless DC motors. Brakes will be included in these two DOFs to reduce the possibility of damage in the event of an emergency. The total weight of this XY positioner is estimated at around 135 kg, including hardware to reduce the unsupported length of the extruded aluminum sections.

The vertical z-motion from within the XY table will have a reach of 0.91m, and be actuated by a non-backdriveable small-pitch ball-screw arrangement. This stage is estimated to weigh no more than 35 kg, and will also be powered by a brushless DC motor. All components will be either anodized aluminum, or stainless steel (ball-screw, bearings, rails, etc.). This DOF will be called the *vertical shoulder lift.*

The rotational shoulder axis will use an extremely stiff, zero backlash cycloidal cam reducer, powered with a brushless DC motor, and supplied with a simple rotary brake at the motor input shaft. Due to cabling constraints the rotational range of motion on this shoulder joint will be no more than 405°, limited by hard mechanical stops. The entire actuator will be packed on the top of the vertical shoulder lift mechanism, so that when the manipulator is in its stowed position, the rails of the XY table will be the highest point on the system and will not exceed 1.83m. Structural material will be aluminum, with sealed stainless double-sided slim-line thrust bearings to support the cantilevered load of the horizontal boom and the endeffector. This joint will weigh no more than 25kgs, and will be called the *shoulder rotate.*

Figure 5-19 Proposed manipulation design concept

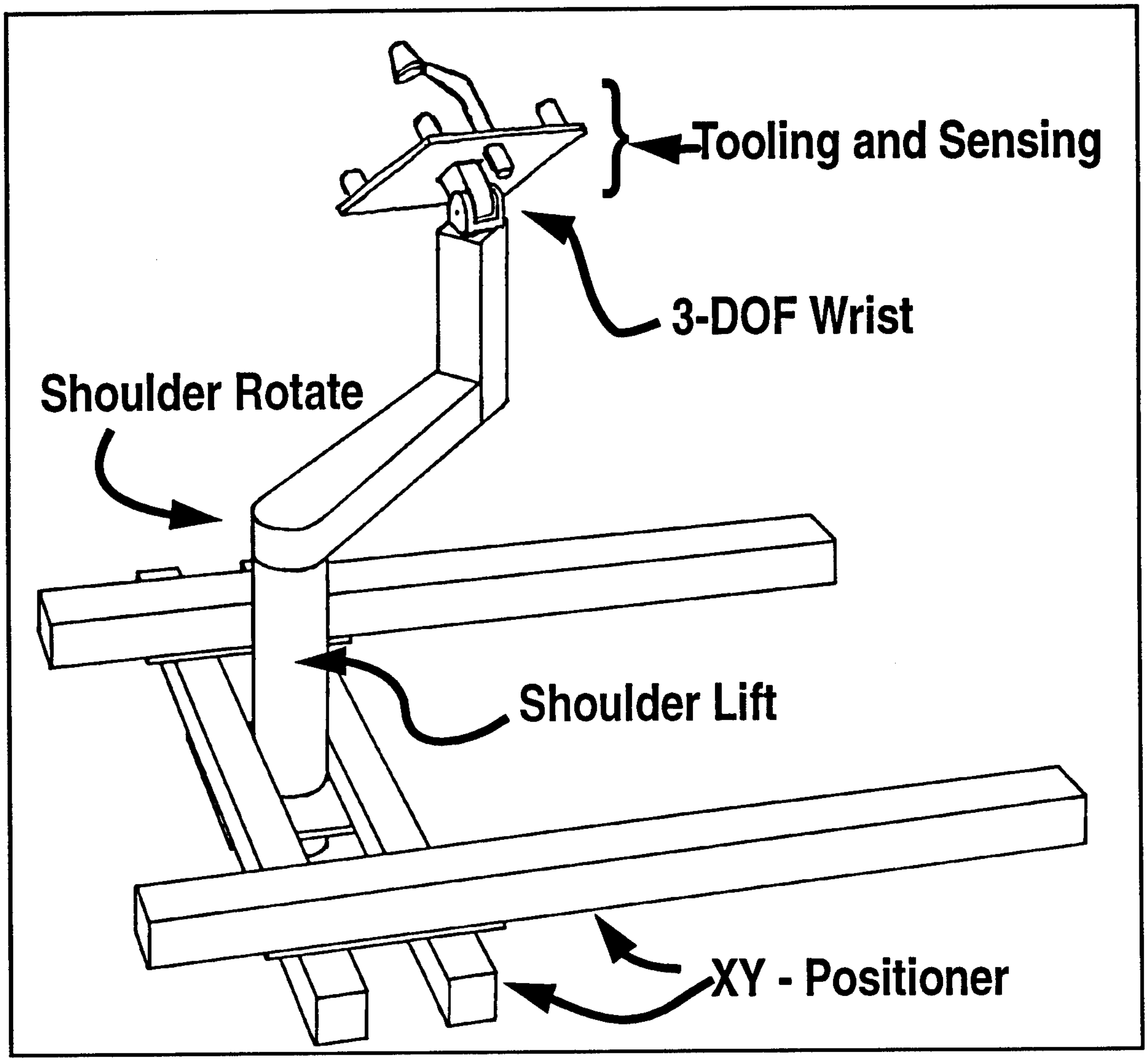

The fixed-length horizontal boom will be about 1.25m long and be made of rectangular aluminum tubing to maximize structural rigidity and minimize deflections at the endpoint. The hollow structure can hold the elbow actuation. This boom will weigh no more than 20 kgs and be called the *horizontal boom.*

The alignment of the sensing and tooling will be achieved with a 2 DOF pitch/roll elbow attached to the horizontal boom. The elbow roll, aligned with the longitudinal axis of the horizontal boom, will have a full 360^0 rotation in order to reach all possible tile and allow for stowage of the endeffector below the XY table plane. We intend to use a high stiffness, low backlash cycloidal cam reducer, driven by a brushless DC motor and secured via a brake. This joint will be completely packaged within the horizontal boom. The elbow pitch will consist of a similar actuator arrangement, and have a rotational axis perpendicular to the elbow roll, with a range of 270^0 to allow complete tile reach, stowage and sensing/ tooling inspection by the operator. These two DOFs will be packaged and assembled into a

single machined elbow joint element to be fastened to the horizontal boom. This package will not weigh more than 25 kgs, and will be called the *pitch/roll elbow joints*.

The endeffector consists of a sensing platform fixed to the elbow-pitch joint, and will deploy the tooling to within 2.5cm of the shuttle tiles. The tooling will sit on a separate plate attached to the end of a linear tool deployment actuator. The linear deployment actuator will have a compressed length of about 0.30m, with a total stroke length of around 0.15m. It will be housed within the elbow pitch structure, and comprise a high pitch ball screw arrangement coupled directly to a brushless DC motor and a small brake. This linear actuator will be highly backdriveable and be used for rapid deployment, position/contact-force servoing, and rapid retraction in case of an emergency or imminent collision. Materials will be aluminum and stainless steel.

An additional DOF for camera platform rotation is needed and will use a brushless DC motor worm-gear arrangement on the sensing platform or an added DOF within the wrist. This gives the sensing/camera platform the ability to rotate about the long axis of the linear actuator axis which also coincides with the tooling symmetry axis for repeatable and consistent tile viewing. The weight of the end-effector, including a 5kg tooling device, interface plates, cameras, lights, force sensor, and related hardware, is no more than 25 kg. The assembly will be called the *sensing/tooling deployment endeffector.*

The entire horizontal manipulator boom, elbow, sensing and tooling endeffector surfaces will be covered with piezo-electric and/or infrared proximity sensors for collision detection and avoidance. We will also use mechanically cantilevered limit switches to protect all components from collision and prevent damage to the shuttle by using them as triggers to relays for power cut-off and brake engagement. The conceptual design is depicted in Figure 5-18.

Power Consumption

To determine a baseline for the energy requirements of the vehicle, a power study was conducted for a the servicing cycle. Most manipulator power will be expended raising and lowering the tooling to and away from the tiles. Thus, the mass being moved should be reduced as much as possible. This argues for a separation of tooling and sensing platforms so the final operation moves only the tooling required for rewaterproofing and not the additional sensors and platforms. The actual stroke of the end-effector vertical positioner has a very small effect on power consumption. The power draw is about 275 Watts continuous. This part of the service cycle is also the one with the largest sustained power draw between base moves. Raising the tooling draws about 50% more power than lowering it, but both levels are about 40 to 80 Watts.

The wrist mechanism is estimated to consume no more than 50 Watts continuously during the entire tile service cycle. This is because the wrist supports only the weight of the sensing/tooling platforms which does not represent a large gravity load. The contact forces/torques due to shuttle contact should be small and lie on a vector that intersect the wrist rotation axes thus representing no net load on the mechanism itself. Locking motions to save power are feasible but not desirable due to safety concerns about having rigidly locked mechanisms in contact to the tiles.

Translating the XY table and/or rotating the boom require an much less power than the tooling extension, around 30 to 60 Watts. Even if peaks were required, consumption levels can be kept well below 100 Watts for the 2 second duration of the move.

Quiescent servoing power draw of continuously servoed actuators that experience counter-forces and torques are limited to the shoulder and the XY table. The current assumption is that they will not draw more than 25% of their maximum rated loading, which would add 25 to 50 Watts during the rewaterproofing cycle. The vertical Z-motion of the manipulator should contain a non-backdriveable transmission to reduce the power draw during the entire service cycle to a minimum. The addition of a brake could reduce this steady-state power draw further. This is important since the power level required to hold the entire manipulator assembly against gravity would dwarf other power consumption in the system. It follows that tile coverage in high curvature areas should use a minimum number of vertical extensions to reduce power consumption.

The overall continuous power budget is around 250 to 300 Watts, with a factor of safety of 1.5. The largest power draw will occur in the areas of increased curvature which represent only 30% of the shuttle tile surface, while the power draw for the remaining 70% of the tile surface should be much lower at about 200 to 300 Watts. See Appendix B for more detail.

5.3.6 Summary

The manipulator design of choice is the vertical-tile-normal design (Figure 5-13), due to its ability to incorporate all the advantages of both of the other designs, without any of their disadvantages. The important issues and conclusions are summarized here:

- The design is an integrated endeffector with camera, sensing, and tooling positioning device.
- The endeffector will require small orientation changes over more than 60% of the shuttle underside tiling. This is due to the relatively flat underside of the orbiters. The 30% remaining tiles will require at most a +/- 45^{o} orientation in pitch and yaw.
- The most compact, power-efficient and safety conscious endeffector solution calls for the separation of camera/sensing platforms which must be oriented in all 3 DOFs and the tooling endeffector.
- The tooling will be raised from the camera/sensing platform to close proximity to the shuttle tiles and allow the rewaterproofing process to proceed. This configuration also seems to offer a higher degree of extensibility to future sensing and TPS servicing tasks including step-and-gap measurement, and charred filler-bar inspection.
- The forward and inverse kinematic problems for such endeffectors are well understood and are not subject to any singularities with our positioning mechanism in the workspaces that we need to cover.
- Obstacles such as work platforms will require that the arm either have a natural 'upward bend' to it, or be actuated to achieve that elevation along a circular path, if hard-to-reach areas such as shuttle wing edges and the nose-cone area.

- Safety considerations include selection of electronic and mechanical means of obstacle detection/avoidance proximity sensors. Such sensors will be used to detect surfaces, with an ultimate safety level provided by mechanical triggering of 'whiskers' that cut off power and enable a hardware-controlled emergency retraction of tooling away from the shuttle. The goal is to never improperly contact any shuttle tile, human operators or facility structure.
- Maintaining contact, controlling contact forces, and providing safety and redundancy levels during the rewaterproofing process requires that forces and torques be measured and controlled at distinct locations: the tool-tip extension, and the tooling extension deployment actuator. The combination of dynamic response and sensor fidelity can be addressed by dividing this control and monitoring between the manipulator and tooling devices.
- Mechanical components are commercially available with additional design and component generation required in the areas of redundant and fault-tolerant motors and controllers, sufficient safety margin in actuator selection and integration design phases, endeffector 3 DOF wrist packaging and the vertical tooling extension mechanism. The focus is on reducing weight, complexity and size, while maximizing accuracy and bandwidth for force control.

The overall system depicted earlier represents an initial conceptual/kinematic design concept which we have attempted to arrive at using logical, numerical, and task-driven reasoning. It represents the most feasible and realistic design proposed to perform the types of tasks that are required. Many trade-offs had to be made with respect to power, reach, dexterity, mechanical precedence, cost, implementation and design overheads, and other less tangible but important criteria. This design represents the best compromise arrived at using all the design and selection criteria.

As more detailed critical reviews occur, and additional information is obtained from all teams involved, this design will mature to the stage that we will be able to detail it at a different level. The separate dimensions for the different motions is dependent on the reaches and dimensions arrived at in other sections. But overall this design calls for about a 2.74m x 2.13m XY table, with a 0.91m vertical Z-motion inside the XY gantry, raising a 1m long horizontal boom carrying a 3 DOF roll/pitch/yaw wrist at its end. The endeffector consists of a camera/sensing platform kept at a minimum standoff distance of 0.2m away from the shuttle tile surface, and is coupled to a tool extension device, 0.15m long, that raises the tooling nozzle-tip 5cm to the shuttle tile. This will allow the manipulator, if the XY table is raised by 1m, to service all tiles that have a tangent plane with less than 45^o. This restriction implies 15,000 tiles can be serviced, excluding a small number, less than 500, on the landing gear doors and around the jackstands. The design of the manipulation system is also amenable to future sensing or positioning tasks.

5.4 Controller

The controller is a layer of electronics and real-time computing hardware that lies between the high-level computing and the sensors and actuators. The high-level computing passes motion commands or status requests to the controller, and in response the controller moves actuators or acquires data from sensors. The controller also includes a safety circuit that reacts to error conditions and joysticks that allow the operator to move the robot manually. Figure 5-20 shows the relationship of the controller to the rest of the robot.

This section first describes the requirements imposed on the controller, then translates the requirements into a design. Interestingly, we found that the design of the controller is more constrained than most of the other subsystems in this robot, because most of the structure of the controller is dictated by the subsystems that it controls.

Figure 5-20 Role of the controller

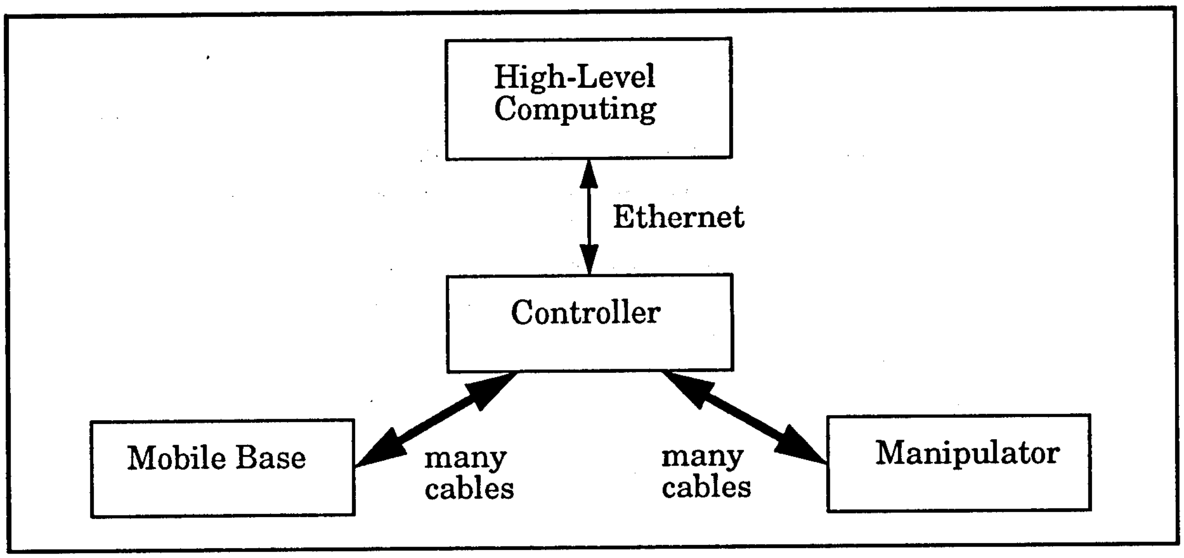

5.4.1 Requirements

Specifics of all requirements for the controller will be discussed in the following sections.

Functional

- Control of all mobile base and manipulator actuators
- Computer-aided joystick for complex motions.
- Safe and timely transitions between operation modes (auto, manual, kill)
- Joystick control with hardware only.
- Acquisition of health/status/safety data from sensors

Global

- Minimal power consumption

The first two functional requirements necessitate real-time computing capability in order to coordinate several actuators. The last three functional requirements do not depend upon

real-time computing capability, but do require specific hardware. This allows some control of the vehicle without computing.

5.4.2 Hardware

Since there are two mechanical subsystems, the mobile base and manipulator, that require the same functionality from the controller, we have chosen to split the controller into two physically separate, but similar, real-time systems. The rest of this section will describe one of these systems; the other system is identical except for the number of motion control cards and the number of input and outputs. The general structure of the real-time system appears in Figure 5-21.

Figure 5-21 Real-time system overview

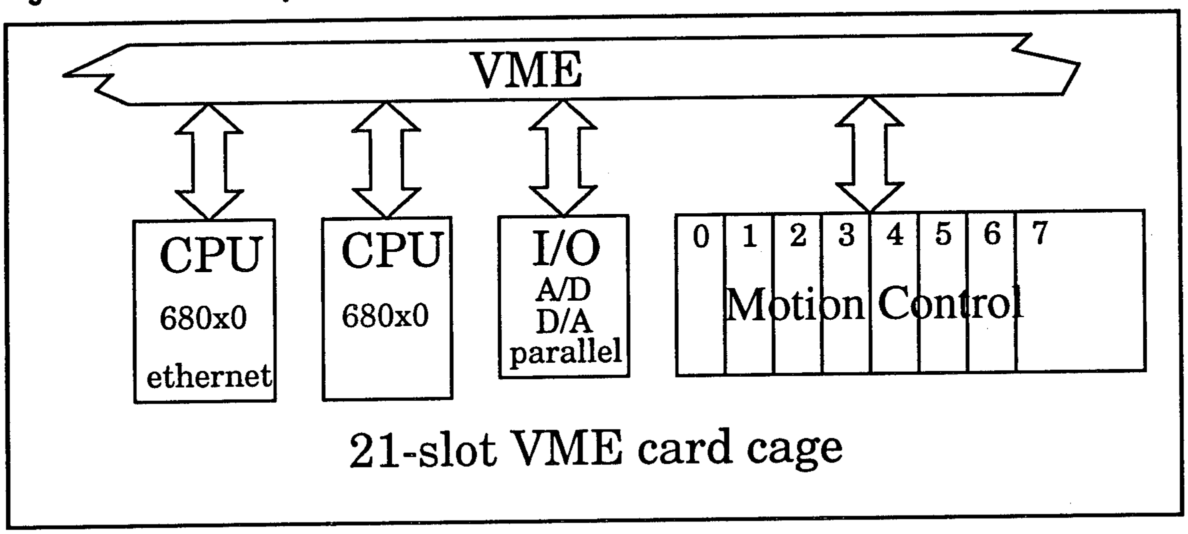

The real time control system is a VME/VxWorks based system with two CPU boards, one board to handle I/O, and several motion control boards (one board for every six actuators). VME is a type of computer bus; VxWorks is a real-time kernel and real-time software development environment. A VME/VxWorks based system was chosen for several reasons:

- VME is an industry standard.
- There is a multitude of off-the-shelf VME components available.
- CMU experience in building VME/VxWorks based controllers.

All of these factors reduce development time by capitalizing on the experience of the team.

There are two CPU's: one is dedicated to motion control and the other monitors status, processes safety sensor data, and warns the high-level computing of unusual situations. There are two basic requirements for the CPU boards:

- At least one of the CPU's must have an ethernet interface to communicate with high-level computing.
- Both CPU's must be supported by VxWorks.

With these constraints in mind, there are several boards under consideration at this time. All are based on one of the 680x0 series microprocessors, have at least 1 Mbyte of RAM, run at a speed of at least 20MHz, and cost somewhere between $2000 and $4000. A number of commercial boards are currently under consideration. Comparisons include specifications such as speed, memory, I/O capabilities, power draw, form factor etc. All of these boards are supported by VxWorks, and have been used by Carnegie Mellon in the past. A major advantage of one manufacturer, Dynatem, is that they are especially power frugal, consuming only 10 to 20% of the power of their counterparts.

The choice of motion control cards is perhaps the most important, since there are approximately 24 actuators to be controlled. There are two motion control boards currently under consideration: one is a two-axis board manufactured by Creonics and the other is a six-axis board from Precision Micro Control. The latter costs less per axis, requires less power per axis, occupies fewer slots in the card cage, and provides the ability to replace unused axes on a board with different modules such as digital I/O. The advantage to using the Creonics boards is that Carnegie Mellon has experience using them, but the difference in price alone might justify going with the new product. The Creonics option is twice the cost of the other.

It may not be necessary to involve motion control boards for actuator control. We are currently examining the possibility of using the CPU boards to run all of the servo-loops. A major advantage is the cost, space, power, cooling and parts count that results from a large number of motion control boards.

There is a need for I/O capabilities such as digital I/O for switching devices on and off, and A/D for joystick inputs. There will be numerous other inputs from as yet unspecified sensors. As soon as the configuration of the robot resolves more completely, we can choose the appropriate I/O capabilities. For now we can leave room in the card cage and a power budget for additional boards. As noted in Figure 5-22, both real-time systems will be housed in separate 21-slot VME card cages, which will leave room for several additional cards.

A summary of a tentative form of the real-time computing appears in Figure 5-22. This combines both the mobile base controller and the manipulator controller.

Figure 5-22 Real-time boards

Manufacturer	Component	Quantity	Power
Dynatem	DCPU30-10F CPU	4	5W
Dynatem	DLAN Ethernet Controller	2	4W
Dynatem	DANA12 I/O board	2	11W
PMC	DCX-VM100 motion control board	5	15W
Dawn VME	VMEBP21-J1J2R backplane	2	n/a
Dawn VME	VME-CC3-6U160-21 card cage	2	n/a
Total			125W

Safety Circuit

In addition to the real-time boards the TPS robot controller will contain a custom safety circuit board that monitors for emergency conditions and maintains system safety. All control signals going to the robot base, manipulator and end-effector must pass through the safety circuit. Depending upon the current system state the control signals are passed or blocked.

Figure 5-23 Safety circuit stages

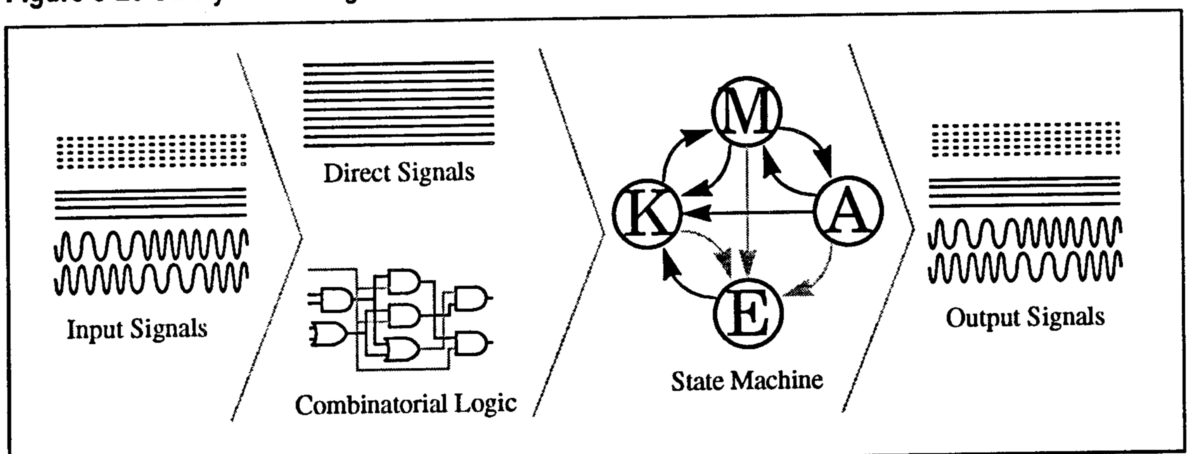

The safety circuit contains a *state machine* that can be in: Auto, Manual, Kill or Error states. The current state is determined by combinatorial logic and direct signals from a number of inputs to the circuit. The state changes in the safety circuit are generated by the control signals, sensor signals and interrupt signals. Specific examples include: limit switches, interrupts, amplifier faults, operator kill/enable signals, and a controller heartbeat.

The system is always powered up in Kill mode. In Kill mode, motion control signals are blocked from going to motor amplifiers. This insures that all motions are disabled. The robot actions and reactions (corresponding to control signals and sensor signals) must be

monitored at a high frequency for error conditions. All error conditions send the circuit back to Kill mode.

The operator must physically switch the circuit into Manual mode. In this state, the operator can drive the joints manually and can obtain status information from any of the sensors. However, the controller cannot command the robot to perform actions autonomously.

The operator must switch the circuit from Manual mode into Auto mode. In the Auto state the software controller is running the robot and commands generated autonomously by the planners are sent to the actuators. The controller heartbeat is a periodic signal that the controller generates while in Auto mode. If the controller should crash, the heartbeat will go away and the safety circuit will automatically switch to Kill mode and shut the robot down.

The Error state catches any anomalous or simultaneous state changes and immediately shifts the circuit into Kill.

The safety circuit is the ideal place to implement a hardware joystick because it is located between the amplifiers and the controller. The hardware joystick generates/moderates current signals directly to the amplifiers. This allows operators to move the robot with all computing powered down. The hardware joystick operates when the robot is in Manual or Auto mode. It can be as simple as switches that drive each motor with perhaps a potentiometer to adjust rate.

5.4.3 Software

The controller software is conceptually decomposed into four functional blocks. There are controller actions that deal with the base, the gantry, the manipulator and the various sensors. (See Figure 5-24.)

Figure 5-24 Conceptual decomposition of the controller software

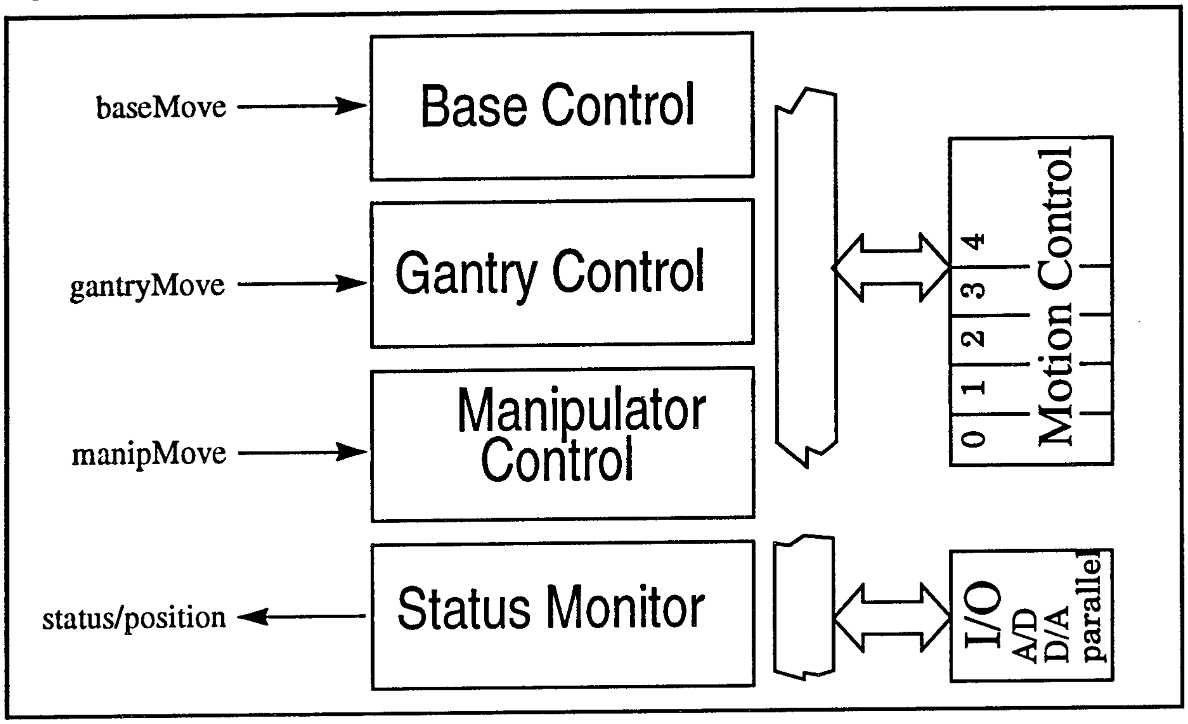

The controller instruction set is decomposed into these four blocks because each represents a conceptually and temporally distinct unit. The base move command initiates the driving between goal positions. Wheel motion is monitored and integrated over time to dead reckon the position of the robot. If an external positioning system is incorporated its estimate of position during the base move can be used to improve the accuracy of the base move. Initially base move commands will specify either linear translation with a given heading or they will specify a rotation in place (point turn).

The motion command for the gantry is used to specify the absolute position of the gantry along its available travel. The gantry height is measured with absolute encoders so positioning at an exact location is trivial.

The manipulator motion commands specify all the manipulator joint angles. The controller interpolates all joints simultaneously from the current configuration to the specified configuration. If intermediate positions or non-linear interpolation of the joints is required then multiple motion commands must be used.

The controller supports position queries of all degrees of freedom in the robot. Queries for the base, gantry and manipulator position are distinct but all work by either reading encoder values or, in the case of dead-reckoned or incrementally encoded values, retrieving the most recent stored values.

The control also supports additional commands, for example the actuation of simple tool motions. These instructions will become more concretely defined as the robot configuration and functionality is finalized.

Commands

Currently there are two types of instructions: commands and queries. Commands request the robot to perform some action, such as moving the manipulator. Queries request information from the controller like the position of the gantry.

The TPS robot controller handles the following commands:

- **baseMove({Δx,Δy,$\Delta\Phi$}1,...,{Δx,Δy,$\Delta\Phi$}n) returns: Success/Failure**

  The baseMove command is used to drive the TPS robot to some new position and orientation that are referenced relative to the current position (i.e. in the robot frame of reference). Locomotion along a complex task is accomplished by commanding a series of base moves. X and Y specify the position while θ is the orientation of the wheels with respect to the base and Φ is the orientation of the base with respect to the world.

- **gantryMove(z) returns: Success/Failure**

  The gantry move command is used to specify the elevation (z) of the gantry platform. It is given as an absolute z in the robot reference frame and the controller servos the gantry to that value.

- **manipMove({x,y,z,θ,ϕ,α,β,μz}1,...,{x,y,z,θ,ϕ,α,β,μz}n)**
  returns: Success/Failure

  The manipulator move command servos all joints (linearly) from the current position to the position specified (absolutely in the manipulator frame of reference). The arguments refer to individual joints of the manipulator.

- **injectTile() returns: Success/Failure**

  The inject tile command causes the controller to send a signal to the tile waterproofing end-effector package. This package contacts the tile and injects the DMES and N2 into the tile. The end-effector package is not controlled by the robot controller but is treated as a "black box".

- **reset() returns: Success/Failure**

  The reset command is used by the higher level planners to tell the controller to stop any motion and flush any queued commands. In addition, if an external source of position information is available, the dead-reckoned position estimation will be reinitialized with this new information.

- **halt() returns: Success/Failure**

  The halt command tells the controller to stop all motions, engage brakes, and flush all queued commands. Additionally, a signal to the safety circuit sends the robot from Auto mode into Kill (disable) mode.

The state of the tile inspection robot must be monitored on three levels, distinguished by time-scale and criticality. The actions and reactions (corresponding to control signals and sensor signals) must be monitored at a high frequency for *emergency* conditions. At a lower frequency, the state of the system must be watched for *warning* conditions. Current

status information will be requested by planning processes, control processes and human operators.

Warning conditions are handled within the controller by monitoring various sensors signals. This monitoring is done by software and no additional circuitry is required. The controller monitors signals from various peripheral devices usually by polling devices periodically. Typical inputs include: air sampling, power level, fluid levels, and clock. Typical outputs are: low battery warning, nearest obstacle, and waiting-for-operator warning.

State monitoring and requests for *status* information are also accomplished by controller software because the acquisition and processing of this information requires real-time interaction with sensors and devices. A dedicated process of the controller will be the health/status monitor. The controller must respond to various status requests and these will generally be asynchronous requests from the planning process that can be handled at low priority. This includes reading encoders to determine positions of actuators, generating dead-reckoned position estimates, reading current levels of power and supplies.

The design of the status monitoring portion of the controller is related to architecture issues, as such it will continue to evolve as the architecture evolves. The TPS robot controller handles the following queries:

- **basePosition() returns: x,y,Φ**

  The base position query reports the best estimate of the location and orientation of the TPS robot base using dead-reckoned and external positioning information.

- **gantryPosition() returns: z**

  The gantry position query responds with the current elevation of the gantry in the robot reference frame.

- **manipPosition() returns: {x,y,z,θ,ϕ,α,β,μz}**

  The manipulator position query causes the controller to determine the current joint positions via encoder readings and report the current manipulator configuration.

- **status() returns: {s1,...,sn}**

  The status command returns the full suite of status information. Although all variables are not yet known this will include readings such as temperature, battery level, and fluid levels.

At least two joysticks are required for the robot. A hardware joystick and a software joystick. The hardware joystick is part of the safety circuit. (See Safety Circuit on page 100.)

Complex motions can be accomplished through a software intermediary between the operator and the controller. A software joystick can provide this for deployment of the robot or in close quarters. The software joystick will be more elaborate than the hardware joystick since it will coordinate and combine multiple actuator motions in a single joystick. For example, the software joystick may allow the operator to drive the robot as an Ackerman steered device or as an omni-directional device. The manipulator may be controlled with many degrees-of-freedom moving simultaneously. The software joystick

will only operate in Auto mode, in which higher level commands can be handled by the controller. The joystick input will be interpreted by the controller into command signals to the actuators just as it does when interpreting commands from the planners.

5.5 Human Interface

Operator interaction and notification require a user interface that is informative and useful during the course of the shift. Display and human interfaces would include high resolution flat panel displays due to concerns about CRT's in the OPF. Image display to closely monitor processing and task performance. Primarily, the interface will supply graphic indications of vehicle status and task performance. See Section 6 for a variety of descriptions of how the interface will be used during operations.

5.6 Power System

A common requirement of all components of the robot system is power. As discussed in the following section, tetherless operation of the vehicle is highly desirable. Since facility constraints preclude motor/generator power systems due to exhaust, batteries or fuel cells are the most viable alternatives for self-contained power. After examining the technological risk of using fuel cells in this application, batteries were chosen as the best self-contained power system for the vehicle.

This section first discusses the tethering issues before delving into the selection of the type of battery to be used as the main source of power and subsequently, the determination of the battery pack configuration based on estimated power needs. The general power distribution scheme is then described in Section 5.6.8.

5.6.1 Tethering Issues

A tether can provide substantial advantages to the configuration of a design but at the same time can result in disadvantages to planning, dedicated personnel or really bad failure modes. This section addresses and examines these trade-offs.

Tether Advantages

The primary benefit of a tether is the unlimited time and high wattage that direct connection can provide. As a result, there are follow-on benefits to weight and volume because battery packaging is eliminated. Tethered option allows the spooling of communications and allowing off-board computing resources thus further reducing on-board packaging requirements.

Tether Disadvantages

Batteries may still be required for travel between the storage facility and the Orbiter location unless towing is provided. See Towing on page 60. If a small battery pack is used the system would still need to supply several hundred watts over an hour period. One hour is a rough figure given distances of parking lot travel and delays during transit. Battery weight and volume would be cut by more than half over the untethered system but would still require charging cycles and monitoring. Another possibility is to tow a small battery trailer, which would be left near the OPF access door for the out of building excursions.

Tether management is another significant issue. Tether winding and spooling can be done on-board but this negates much of the weight and volume benefits. If spooling is off-board then personnel are needed to observe and follow to insure cords do not rub and catch on platform columns and other OPF obstacles.

There are additional considerations of motion planning with the tether tail. Proximity does not allow all possible base motions unless closely supervised by personnel. CMU examples include the Terregator, Locomotion Emulator, and Ambler where dedicated personnel observe and interact with the tether to insure against run-over. Run-over is fatal and results in potential sparking and shorting of power systems. Even in the hands of experienced operators, experiences with Terregator even resulted in "catch-22" situations where the machine was atop the cord it had just pulled out and no power available to move it.

Additional cords and extensions will introduce some complications regarding additional cables strewn across OPF. Motion of the tether must also be carefully monitored to insure against interference with personnel and workstands.

Spools and off-board resources complicate transport between buildings and facilities requiring more personnel attention and complicating debugging work. Untethered operation has great benefit to a self-contained system and increased mobility.

The additional mass of the power system is beneficial to the stability of the system if the upper part of the robot is the same in both the tethered and untethered cases. Preliminary calculations show that the battery mass is more than sufficient for this requirement.

5.6.2 Battery Comparisons

For the following comparisons between various types of batteries, some of the values computed are based on these assumptions:

- Operating time of 10 hrs.
- Operating voltage of 96V.
- Maximum total energy consumption of 7.5 kWhrs. (average power consumption of 750 W over 10 hrs.)

Note that the total energy consumption figure was later revised, with the actual figures presented in subsection 5.6.5. The figures above are used solely for the purpose of comparing the various types of batteries considered.

Lead-acid Battery

Among the lead-acid batteries produced by various manufacturers (Power-Sonic Corp., Sonnenschein Batteries, Inc., KW Batteries, Yuasa Battery Co., Ltd., TS Batteries Ltd.), the best battery found in terms of specific energy and safety is that manufactured by Power-Sonic Corp. Some characteristics of its highest capacity battery (Model PS-12800) are:

- 12 V, 80 Ahr (20 hr rating), 72 Ahr (9 hr rating)
- 8 batteries occupy ~0.1 m^3, weight 185 kg with a total stored energy of 7.68 kWhr (20 hr rating)
- Specific energy of ~42.2 Whr/kg
- Charging time is ~10 hrs. with a charging current of 0.1C. 1C is equivalent to the current rating of the battery. For an 80 Ahr battery, 1C = 80 A.
- Cycle service life of ~400 (discharge depth of 50%) and ~200 (discharge depth of 100%). For these figures, the minimum capacity is 80%.
- Cost is about $0.15 per Whr. Each battery costs $147.50.
- It is a retained or absorbed system, and has an internal process which recombines gases emitted, referred to as the "O_2 cycle." The batteries are designed so that the negative electrode has more capacity than the positive electrode. Any oxygen

generated during charging (within capacity) reacts with the sponge lead of the negative plate, thus preventing hydrogen from being generated. This is patently an advantageous feature. There is a pressure relief valve to release any excess gases.

- The maximum current per battery is 800 A. This means that the maximum instantaneous power for 8 batteries is 8x12 Vx800 A= 76.8 kW.

Nickel-Cadmium (Ni-Cd) Battery

Two companies which produce this type of battery are Sanyo Electric Co., Ltd. and Panasonic Industrial Co. The battery with the highest capacity (1.2 V, 20 Ahr) is manufactured by Sanyo Electric Co., Ltd. However, to achieve the required stored energy of 7.5 kWhr, over 300 batteries will be required. Unlike lead-acid batteries, Ni-Cd batteries cannot be configured in parallel. In addition to its higher cost, four times more expensive than lead-acid batteries, there is also the problem of polarity reversal. Polarity reversal occurs whenever a cell overdischarges, reverses polarity, and charges up with the current from other cells, which can result in cell damage.

Silver-Zinc and Silver-Cadmium Batteries

One manufacturer which produces these types of battery is Yardney Technical Products, Inc. These batteries are capable of extremely high discharge rates, and are very reliable. However, they are prohibitively expensive; they are ~20 times more costly than lead-acid batteries of comparable capacities. The high price is primarily due to the silver component.

Nickel-Zinc Battery

Electrochimica Corp. produces this type of battery. Nickel-Zinc battery technology is relatively new; a paper which describes this battery was published only in 1989[1]. The highest capacity quoted is 300 Ahr, with specific energy of 77 Whr/kg. The price is estimated to be ~3 times that of the lead-acid batteries.

5.6.3 Battery Recommendation

In light of the data gathered on the various types of battery, the recommended type is the lead-acid battery. The reasons for this choice are:

- Lead-acid technology is more mature.
- Its cost is significantly lower.
- It is rugged and reliable (for example, lead-acid batteries can be totally discharged without long term damage.)

Despite the revision in the average power requirement figure, lead-acid batteries are still the best choice as the self-contained power source.

1. Reisner, D., and Eisenberg, M., "A New High Energy Stabilized Nickel-Zinc Rechargeable Battery System for SLI and EV Applications," SAE Tech. Paper 890786, Int'l Congress and Exposition, Michigan, 1989.

5.6.4 Power System Monitoring

In order to function properly, the mobile robot system needs to constantly check its residual power capacity. If lead-acid batteries are to be used, merely tracking the battery pack voltage will not yield a reliable indication of the amount of power discharged.

A better method is to integrate the discharge (load) current over time from the beginning of operation. This can be achieved by using a Hall effect sensor and op-amp circuitry.

5.6.5 Power Budget

In order to determine the total power budget of the robot, and thus the number of batteries required, it is necessary to examine the power requirements of every subsystem of the robot. The sources of power consumption on the robot are:

- Base mechanism
- Manipulator mechanism
- Controller, CPU and I/O boards
- Computing required for planning
- Perception computing and tooling mechanism

The rest of this section details the estimated power consumption for each of these subsystems. The overall power requirements for the robot are then derived to determine the total number of batteries necessary to accomplish a single shift, 10-hour mission.

Base Power Requirements

The breakdown of power consumption for the base configuration is as follows:

- Steering and Drive (4 amplifier drivers): 500 W (ave.), 1500 W (peak, for a few secs.), 0 W (standby off)
- Large vertical motion actuators (2 amplifier drivers): 500 W (peak, for 15 secs.), 26 W (standby on), 0 W (standby off)
- Stabilizers (4 amplifier drivers): 600 W (peak, for a few secs.), 52 W (standby on), 0 W (standby off)

Note that each amplifier driver has a quescient power of about 13 W. To reduce energy consumption while the base is parked, the amplifier drivers and motors are powered off (with motor brakes locked). Since the mobile robot is expected to position its base 15 times in each shift, the energy expended is:

- Deployment (in and out of the facility)
    - The expected total time for the robot to move to the OPF Bay from the OPF backshop is 12 mins. To cater for uncertainties and possible delays (due to obstacles, for example), the time of 15 mins. is taken in the calculation. The total energy expended is (500 W x 15 mins. + 1500 W x 5 secs.) x 2 = 255 Whrs.
- 15 base moves

- Driving and steering: (1500 W x 5 secs. + 500 W x 2.5 mins. + 200 W x 0.5 min.) x 15 = 370 Whrs.
- Big Z-motion: (26 W x 3 mins. + 500 W x 15 secs.) x 15 = 51 Whrs.
- Stabilizing: (52 W x 2.5 mins + 600 W x 15 secs. + 200 W x 0.5 min.) x 15 = 95 Whrs.

- The expected total energy used is 771 Whrs.

The approximate power consumption distribution over time is depicted in Figure 5-25, and it can be easily seen that the maximum instantaneous total power is about 1600 W for ~5secs.

Figure 5-25 Power distribution versus time for the base

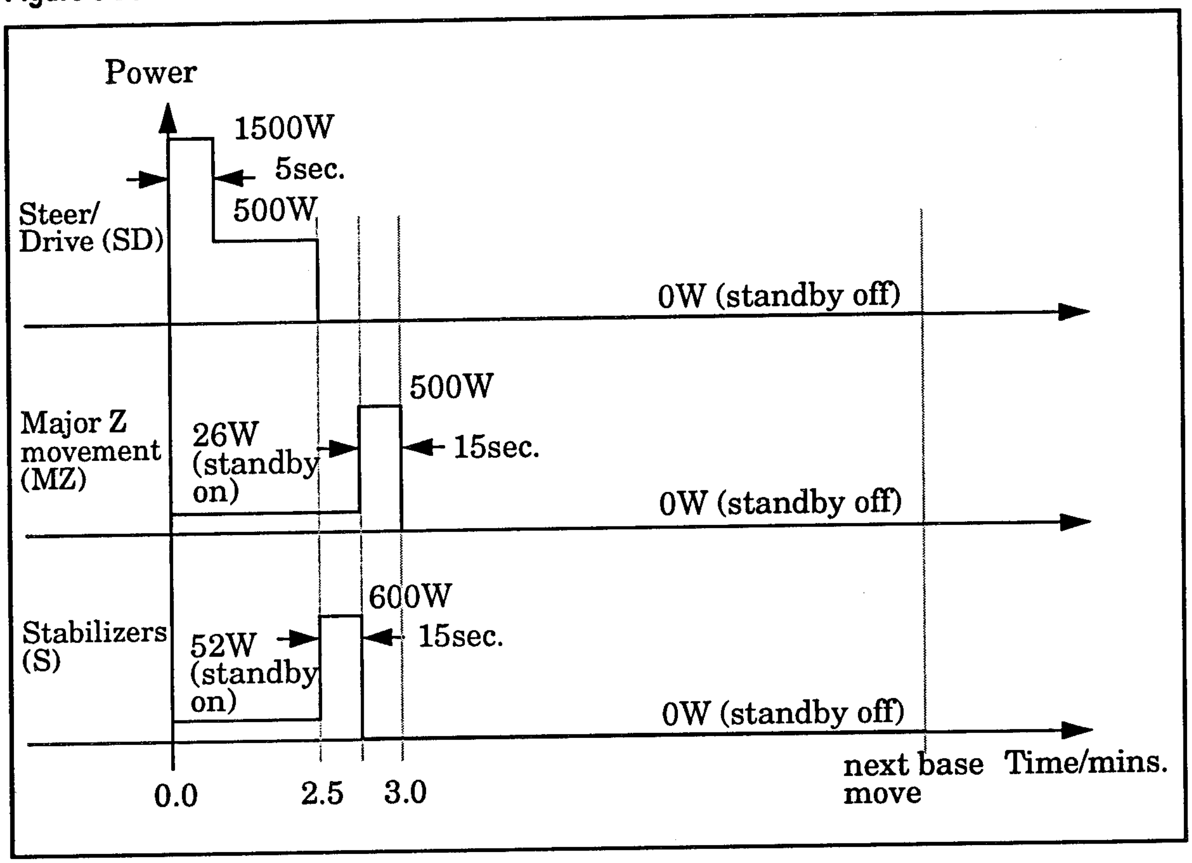

Manipulator Power Requirements

The estimated time spent between tiles is 9.6 secs. The power distribution over time is shown in Figure 5-26. The energy required for an estimated number of 180 tile-to-tile moves per base move and a total of 15 base moves per shift is (13.3 W x 3.1 secs. + 269.0 W x 3.5 secs. + 161.3 W x 0.5 sec. + 13.3 W x 2.5 secs.) x 180 x 15 = 823 Whrs. The maximum instantaneous power is 269 W for 3.5 secs. per cycle.

Note that the power distribution depicted in Figure 5-26 does not include the power consumption during the occasional global and local positioning activities. These times are small and insignificant compared to the total manipulator activity times and can be ignored

in the power estimation. The influence of reduced timing in the tool positioning during the waterproofing process (assuming that the number of tiles processed per shift remains the same) is substantial. A decrease by 1 sec. in this activity results in the reduction of power consumption by 269.0 W x 1.0 sec. x 180 x 15 = 202 Whrs. per shift.

Figure 5-26 Power distribution versus time for the manipulator

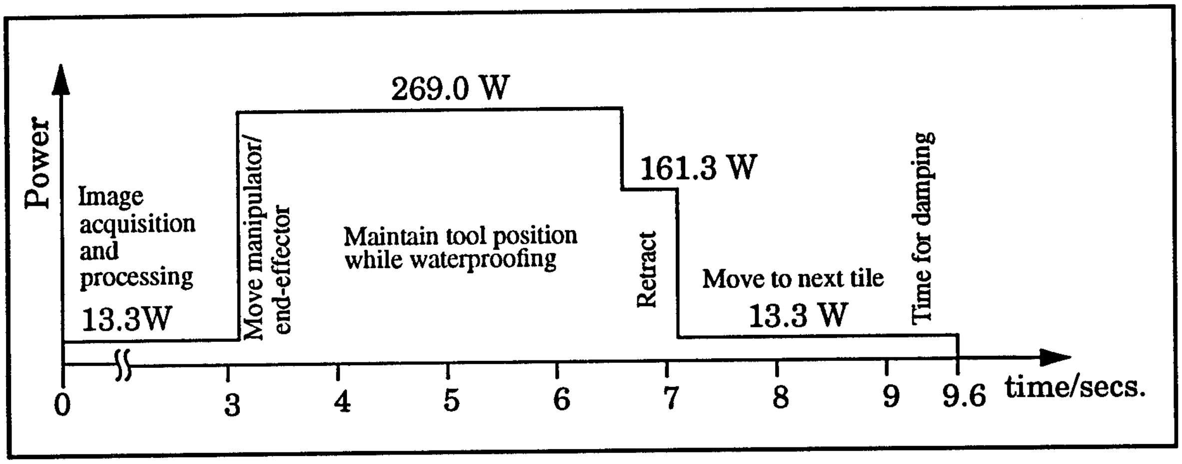

Controller Power Requirements

The following is the breakdown of the estimated power consumption. Note that the peak, average and standby power requirements are approximately the same, since this system is always operating in a steady state.

- 5 motion controller boards: 15 W x 5 = 75 W
- 4 CPU's: 10 W x 4 = 40 W
- 2 I/O boards:10 W x 2 = 20 W

The benchmarks for the CPU and I/O board power estimation are the Dynatem low-power counterparts which consume only 5 W each (the figure of 15 W is used in the above calculations to account for ethernet controllers and possible additional hardware). The total power requirement is thus 135 W, which translates to the energy requirement of 1.35 kWhrs.

Planning and Architecture Power Requirements

For the two CPU's (with memory and disk drives) dedicated to planning, the estimated power consumption is 80 W x 2 = 160 W. The energy required for the duration of the work-shift is 1.6 kWhrs. The Sun SPARC-2 CPU is used as the reference.

Perception and Tooling Power Requirements

The breakdown of the power requirements is:

- 40 long-range sonars: 0.5 W x 40 = 20 W
- 37 short-range sonars: 0.5 W x 37 = 18.5 W
- 4 light curtains: 20 W x 4 = 80 W

- Laser range-finder: ~50W
- Camera: ~10W each x 4 total (SRI estimate) = 40W
- Illumination: 60 W
- Computer hardware (2 CPU's, 8 I/O boards): 10 W x 10 = 100 W (again the Dynatem hardware is considered)
- Waterproofing tool: power consumption is not currently known, but is expected to be small.

A conservative initial estimate for the perception and tooling modules is 400 W. Thus the energy required for the 10-hr. operation is 4.0 kWhrs. Note that the components for the perception and tooling have not been finalized as of this date. Illumination is currently unknown. If high intensity incandescent lighting is required this estimate could become significantly higher.

Total Power Requirements

The total energy requirement for the entire system is 771+823+1,350+1,600+4000 = 8,544 Whrs. The maximum instantaneous power occurs during the initial period of the base move, and is 1,600+13.3+135+160+400 W = 2309 W.

Taking a safety margin factor to be 1.2 and the desired residual capacity to be 10% at the end of the 10-hr operation, the energy rating of the battery pack is

$$\frac{1}{0.9} \times 1.2 \times 8544\text{Whrs} = 11.40\text{kWhrs} \qquad \textbf{Eq. 5-1}$$

5.6.6 Battery Pack

Several important figures for the Power-Sonic lead-acid battery are as follow:

- 12V, 80 Ahr. (20 hr. rating), 72 Ahr. (9 hr. rating). For a 10-hr. operation, the capacity of 75 Ahr. is taken.
- Maximum discharge current: 800 A. For each battery, this yields a maximum instantaneous power of 12 Vx800 A = 9600 W (for a short duration only).
- Dimensions: 30.5cm (length) x 16.8cm (width) x 23.9cm (height over terminal) (12.0" x 6.6" x 9.4")
- Weight: 22.7 kg. (50.0 lb.)

Based on the current average power requirement estimates, the number of batteries required is 11,400 Whrs / (12 V x 75 Ahrs) = 12.7. The operating voltage of 96V is to be used for two reasons: it is suitable as motor and motor amplifier input supplies, and it is not too high to be significantly unsafe. The choice of the operating voltage necessitates the choice of the number of batteries to be a factor of 4. Hence, a conservative number of 16 is chosen. For this battery pack, the total space occupied is 0.196 m^3, and total weight is 363.2 kg.

5.6.7 Battery Charger

Many battery chargers reviewed do not have the capacity to charge the resultant battery pack configuration. In addition, it is desirable for the battery charger to take as its input supply the single-phase 120 VAC power line as three-phase systems may not be available in the facility. The recommended choice which satisfies both requirements is the Hobart Accu-Charger HFF Series Single Phase Model (HFF48S25) distributed by Battery Systems, Inc. Some of its features include suppression of initial current surges and low electrical and audible noise.

Figure 5-27 Power distribution system

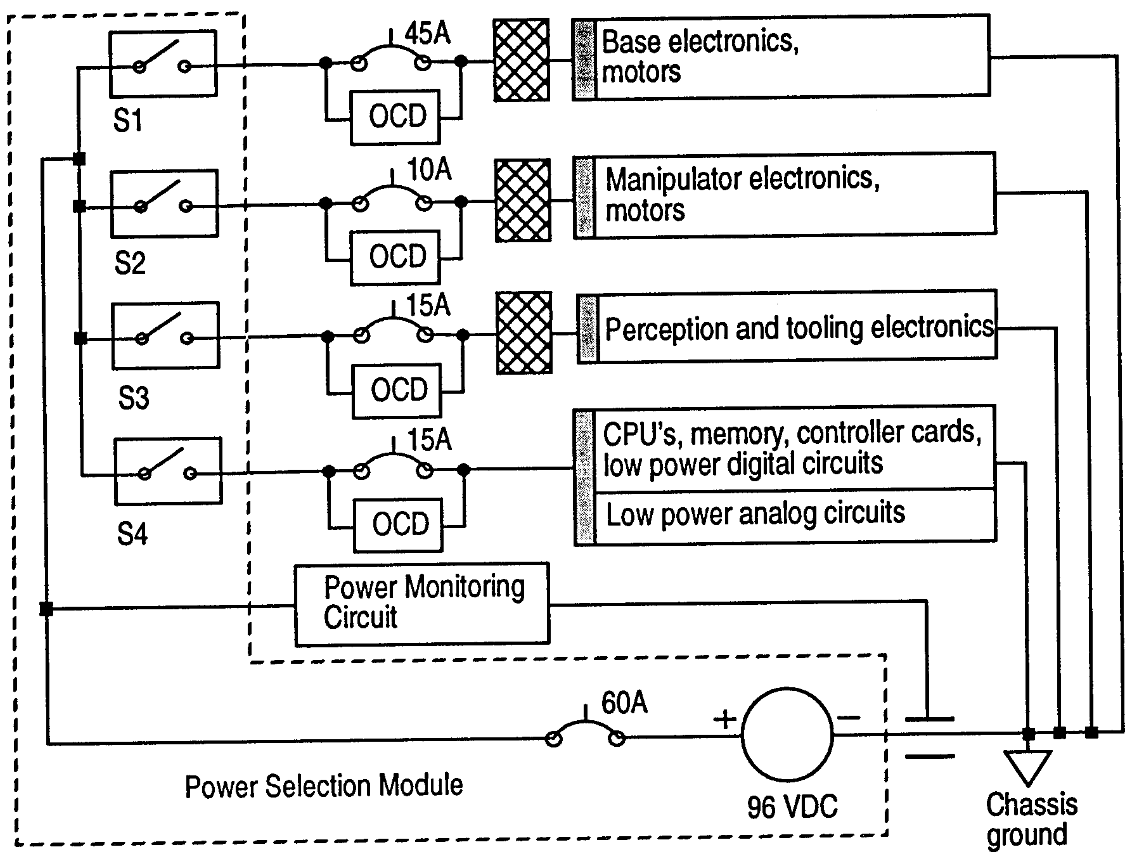

Notes:
1. All circuit-breakers are of a "slow-blow" type.
2. OCD = open-circuit detector circuit.
3. ☒ = computer-controlled switch. The planner can cut power to the various subsystems via this switch.
4. ▯ = DC-DC converter. Each subsystem has its own DC-DC converters.
5. The 96VDC supply either comes from the battery pack (normally so) or from a regulator whose input is an external 120 VAC single phase line.
6. It may be necessary to have two separate power lines for the base electronics due to the possible unavailability of relays with the required high current rating.
7. S1-S4 are switch modules.

5.6.8 Power System Distribution

From the battery pack, power is distributed to the following subsystems:

- CPU's, memory and controller cards, low power digital and analog circuits
- Tooling electronics
- Manipulator electronics and motors
- Base electronics and motors

Figure 5-27 shows the overall distribution scheme.

Power Selection Module

The 96 VDC supply normally comes from the on-board battery pack. However, there will be provisions for an alternative power input via an external 96 VDC power supply to be used in exceptional cases. The detailed circuit is presented in a separate paper.

5.6.9 Summary

The type of battery best suited for the on-board power source is the lead-acid battery. Not only is its technology proven and mature, it is also relatively cheaper, and rugged and reliable. Based on power requirement estimations of each of the major subsystems of the mobile robot, 16 lead-acid batteries (12 V, 80 A-hr rating) are required to power the entire system for the 10-hr. operation per shift. For this battery pack (with operating voltage of 96 V), the total space occupied is 0.196 m^3, and total weight is 363.2 kg.

6. Architecture and Planning

Software architecture is the framework for organizing a large software system, addressing such issues as modular infrastructure, information flow between modules, allocation of computing resources, execution monitoring, and system control. The architecture and software design presented in this section is derived by modeling the body of software as a black box. The functionality of the software is specified, followed by the inputs such as operator commands, sensor readings, heartbeats and outputs such as base actuation commands, arm actuation commands, and graphical displays. For each I/O signal, the bandwidth, frequency, and maximum permitted latency are identified. An attempt is made to resolve any assumptions; those remaining are listed below.

The flow of control through the system is detailed, and functional building blocks to perform the task are identified. These building blocks are interconnected to form the "architecture" of the system. This software architecture is mapped onto a hardware configuration, and the flow of data through the system is analyzed to ensure that all I/O requirements can be met.

The final architecture specification is dominated by a single thread of control. At any point in time, the system is performing a single task (e.g., moving the base or arm). There are no complex interactions between concurrent modules requiring a separate conflict resolution mechanism. Concurrent flow is present (e.g., obstacle detection and health monitoring), but these processes can be modelled as interrupts to the main thread. Based on performance requirements, it is determined that four CPUs should suffice for the hardware configuration: one for the main control flow, one for the obstacle detection and monitoring processes, one of the user interface and one for the external database.

The section is organized as follows. First, the assumptions and requirements for the system are presented. Second, an overview of the control flow through the system is given. Third, the base move flow is detailed. Finally, the tile-to-tile flow is detailed. The table of input and output signals in the system is listed in Appendix C.

6.1 Assumptions

The assumptions made for the robot and the environment in this software system are as follows:

- One manipulator per robot.
- One end effector per manipulator.
- No pipelining of tile servicing operations, i.e. we will not be interleaving multiple tasks.
- All dynamic obstacles are either humans or human controlled machines.
- A planar representation of the workspace volume is adequate, which means that any obstacle in the workspace can be modeled by its projection to the floor plane.
- Accurate tile database. This is necessary to avoid ambiguity between tiles.

- Accurate facility database. This will be used for obstacle avoidance.

6.2 Functional Requirements for the Software

This section describes the functional requirements for the TPS robot software system and the resulting software system architecture for the robot. Since safety is one of our main concerns, we put special emphasis on the error detection and handling in designing the software system architecture.

The major functional requirements for the software system are:

- Control the mobile base, the manipulator, and the end effector.
- Generate a coverage plan for servicing all accessible tiles.
- Detect and avoid obstacles, both on the ground and in the manipulator workspace.
- Monitor health of the vehicle and its subsystems, and respond appropriately to problems as they arise.
- Update the tile database with current information.
- Provide a graphical interface for a human operator.

The functional requirements can be mapped naturally into five different functional blocks:

- Planner/high-level controller: this module generates the coverage plan in the form of a sequence of base positions. This coverage plan can be computed prior to deployment. The actual path for the base and the manipulator are generated during the operation itself. The resulting path will be sent to the low level controller which will servo the actuators of the robot to follow the desired path.
- Obstacle Detection module: this module warns the planner if there are any unexpected obstacles in the vicinity of the robot. The input for this module comes from the perception subsystem. It is then processed to determine if any detected object is not present in the facility database and therefore may represent an unexpected obstacle.
- Health monitoring module: this module monitors the condition of the software and the hardware of the robot and responds appropriately to any problems as they arise. The low level part of this module is actually part of the low level controller. This allows the low level controller to react immediately to critical errors without communication delays or having to rely on other modules, including the health monitoring module itself. Such critical errors include encoder and actuator malfunctions and a missing heartbeat from one of the other modules.
- User graphical interface: this module presents the human operator with information regarding the robot and the ongoing operation in a graphical form. This information includes the present health status of the robot, the currently planned activities, the current position of the mobile base and manipulator, and the status of the tile servicing operations. It also provides the interface for teleoperation of both the mobile base and the manipulator. The teleoperation can be done at several levels of abstraction. At the highest level, the operator simply

provides a goal location and the planner generates a path to reach that goal. At an intermediate level, the operator may directly specify the path which the vehicle or arm is to follow. At the lowest level, the operator controls the robot through joysticks which generate the control signals for the actuators. This user interface will require a communication link between the robot and the external computer. The link should be reliable but it can be a low bandwidth link (~2400 bps).

- Database module: this module supplies all the information that is needed for the task and stores all the important information that is obtained during the task. An example of the information that is needed for the task is the tile map. Some of this data, for instance the tile map, are already available from the Enterprise system, which is a NASA database on the space shuttle. The data that needs to be stored includes the tile images and the status of each tile. Because of the large bandwidth that is required, this database will be downloaded onto an on-board disk during the deployment phase, and updated information will be uploaded at the end of a work shift, prior to stowage. Downloading changes instead of complete descriptions will same a great deal of time.

In Figure 6-1 the above five modules are mapped into the four blocks with the darker color, which are the external database module, health monitoring module, user interface module and the combined planner and obstacle detection module. The planner/high-level controller and the obstacle detection module are grouped in the same module, since conceptually obstacle detection is an integral part of the planner/high-level controller. The other modules are the perception module and the low level controller module. The perception module processes the input from the sensors for various purposes such as end effector positioning and tile inspection. This is explained in more detail in section 7. on page 143. The last module in Figure 6-1 is the low level controller for the actuator. This module is explained in detail in the configuration section 5.4 on page 97.

Figure 6-1 also shows the links between modules that are necessary to fulfill the functional requirements for the software and only the major links are shown here. In addition to these major links there are also other links between the modules. For example: there is a link between every module and the health monitoring module, which are used by the health monitoring module to monitor the heartbeats of the whole system.

To determine the number of processors needed and to identify possible system bottlenecks, the data flow through each inter-process communication link was analyzed. For every type of information that flows between the modules, we determined the bandwidth requirement, expected frequency and necessary reaction time. By analyzing this data and taking into consideration all processes that have to be executed concurrently it was determined that four processors would be sufficient to implement all the dark colored modules in Figure 6-1 and guarantee reaction time. The planner runs on one processor while the health monitoring subsystem and the obstacle avoidance subsystem run on a second processor. The other two processors are used for the user interface and the external database. The user interface will be implemented on an off-board graphics workstation. Point-to-point communications will be used between modules so that the planning module does not become a bottleneck which may impair reaction time. A system such as EDDIE (Efficient Distributed Database and Interface Experiment) will be used[1]. EDDIE has been used for

communication between modules on the CMU Navlab and provides a flexible and efficient language for establishing inter-process communication for distributed systems.

Figure 6-1 The software system architecture

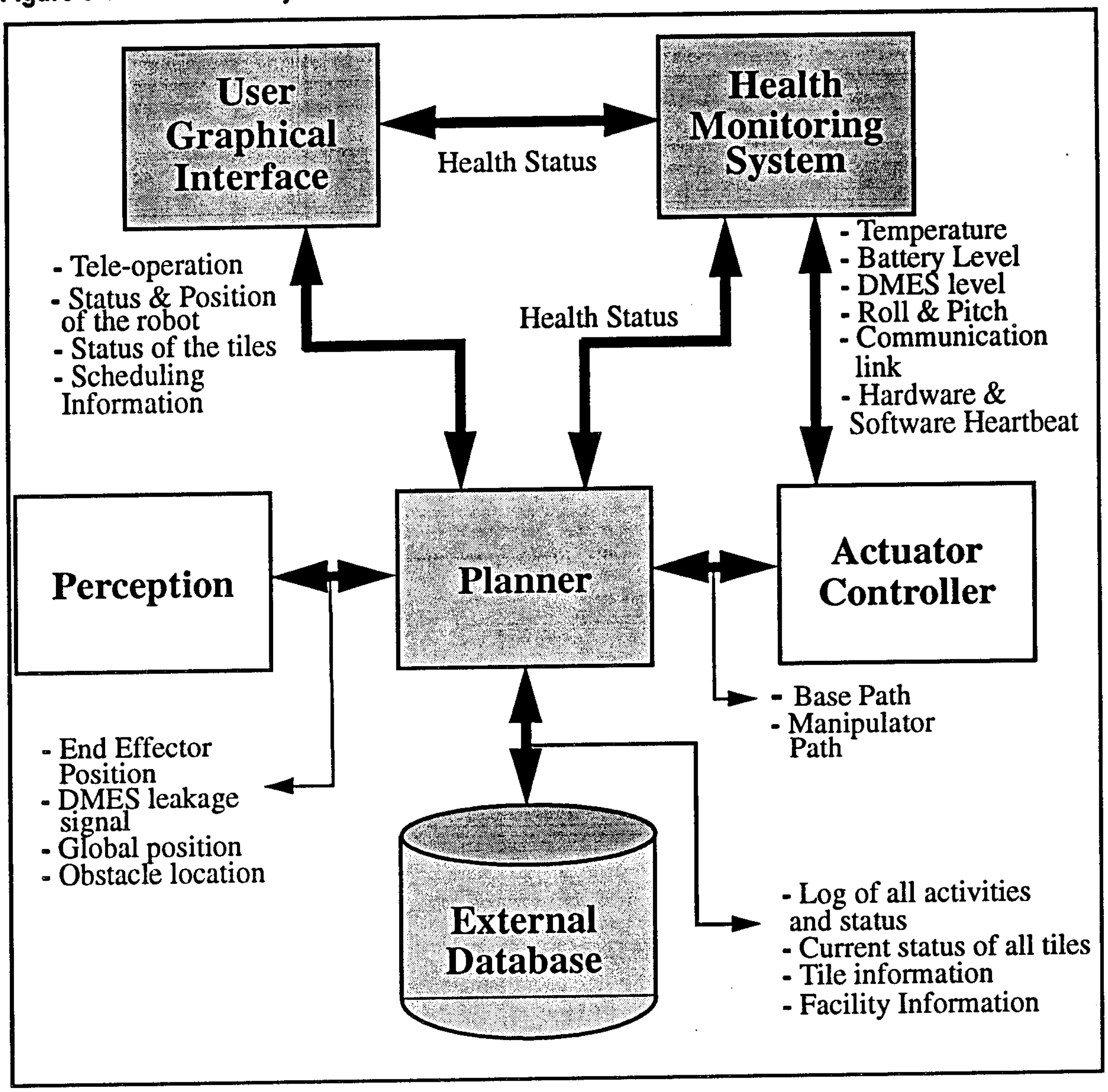

6.3 Operation Flowcharts

This section describes the control flow in the three main concurrent processes, which are the planner/high-level controller process, the obstacle avoidance process, and the health monitoring process. The flowchart for the main operation planning loop is shown in Figure 6-2, and Figure 6-3 illustrates the obstacle avoidance flow of control. The following three subsections give a detailed explanation of the control flow in each of the three loops.

1. J. Gowdy and C. Thorpe, "The EDDIE System: An Architectural Toolkit for Mobile Robots", Robotics Institute Report, Carnegie Mellon University, Pittsburgh, PA, February 1991.

6.3.1 Main Operation Loop

Figure 6-2 shows the main thread of control for the robot. Since this is just a general overview of the control flow, no exceptions or failures are shown here. They will be discussed in detail in section 6.4 on page 125 and section 6.5 on page 134.

Here are the steps in the main loop:

1) Get task commands from user: In this step the operator inputs the goal for the robot through the user graphical interface. The goal can be to inspect and rewaterproof the tiles in a certain area of the shuttle. The operator can also input constraints and preferences that will be used by the planner when it generates the coverage plan. Although the coverage plan may be precomputed it is not a lengthy computing intensive task. Since we may have to replan for obstacles or changes in work schedule the system should be able to generate this plan. The constraints can prohibit the robot from working in certain area at a certain time, while a preference might be used, for example, to force the robot to work on the badly damaged tiles first.

2) Generate coverage plan: The planner generates the coverage plan for the robot which takes into consideration the input from the operator (goals, constraints and preferences), the work schedule near the shuttle, and the shuttle configuration. These first two steps can be executed prior to the deployment of the robot.

3) Move to the home position: The robot moves to the starting position under the first area of tiles to be serviced. The robot must already be in the deployment mode and located under the shuttle. This move is done using dead reckoning with continuous feedback from global position verification.

4) Service one tile: In this step the robot starts inspecting and rewaterproofing the tiles. A more detailed description of this operation and subsequent operations during tile servicing is found in section 6.5 on the tile servicing loop.

5) Move to the next tile: The robot moves its end effector to the next tile. If there are no more tiles in the workspace then check if this is the last workspace. If this is the last workspace then go to step 7 (Go home). Otherwise go to the next step.

6) Move to the next workspace: The robot moves to the next workspace along a planned trajectory according to the coverage plan. This move is done using dead reckoning with a continuous feedback from the global positioning system. After this step go to step 4 (Service one tile).

7) Go home: The robot has finished its goal and goes back to its home position which is defined by the operator.

As seen above, the main control flow is quite simple. Complications arise when a failure or an exception occurs in one or more steps (e.g., what will happen if the robot can not go to the next workspace due to an obstacle). As mentioned above, the exceptions will be discussed in the section for the base move and tile servicing loop. In general, when an exception or a failure occurs the robot will immediately store the current state of the robot and the operation into a permanent storage system so when the exception has been handled the robot can resume its operation without having to restart from the beginning.

During the operation, the operator may need to interrupt the operation. He or she can do so by forcing the robot to go into the pause state. The pause state is explained in section 6.3.3 on page 121. After forcing the robot to go into the pause state, the operator can load a new command for the robot.

Figure 6-2 Main operation loop

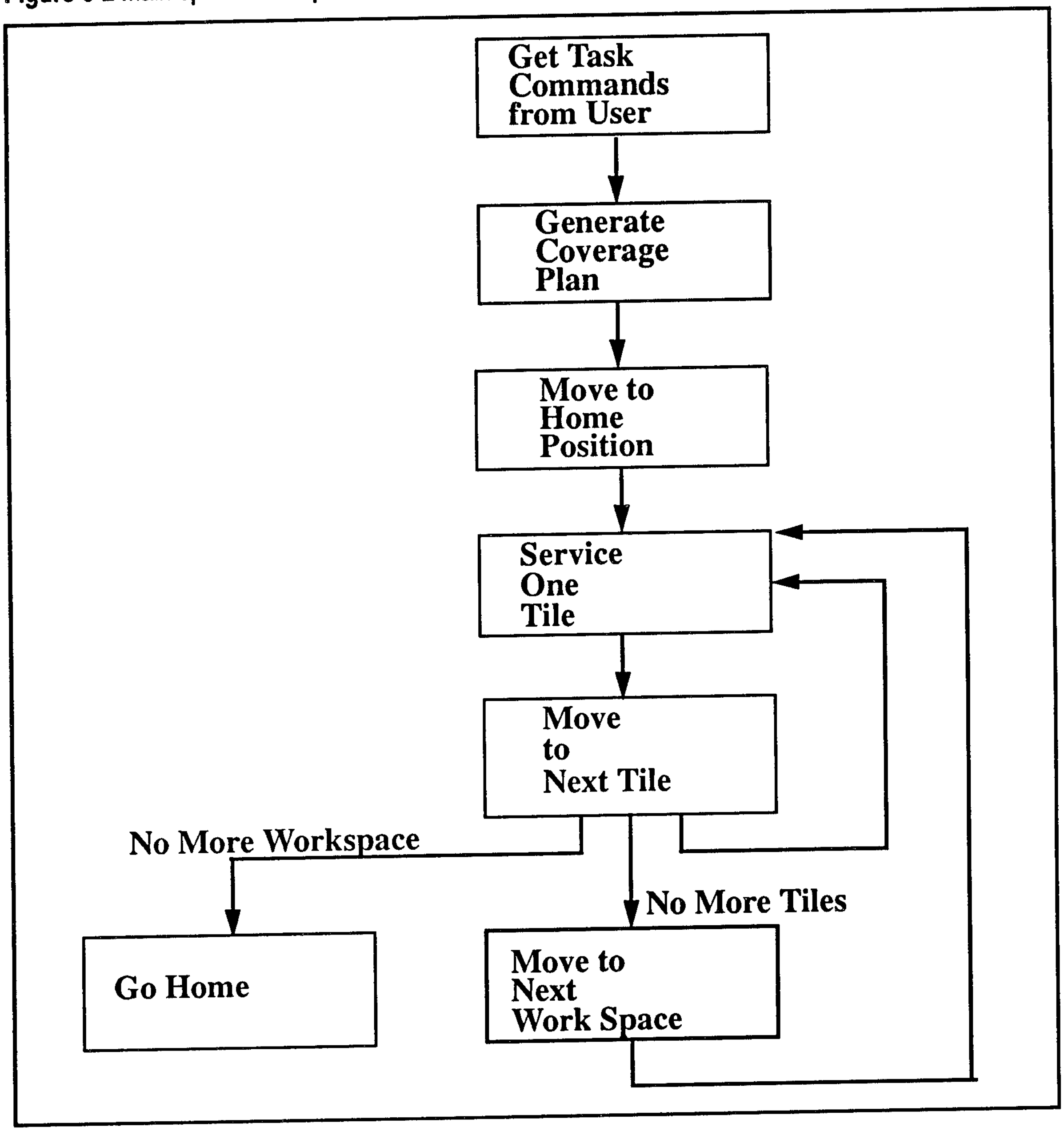

6.3.2 Obstacle Avoidance Loop

The control flow for the obstacle avoidance loop is shown in Figure 6-3. The important thing to notice is that the way obstacles are handled depends on the state of the robot and the type of obstacles.

Figure 6-3 Obstacle avoidance loop

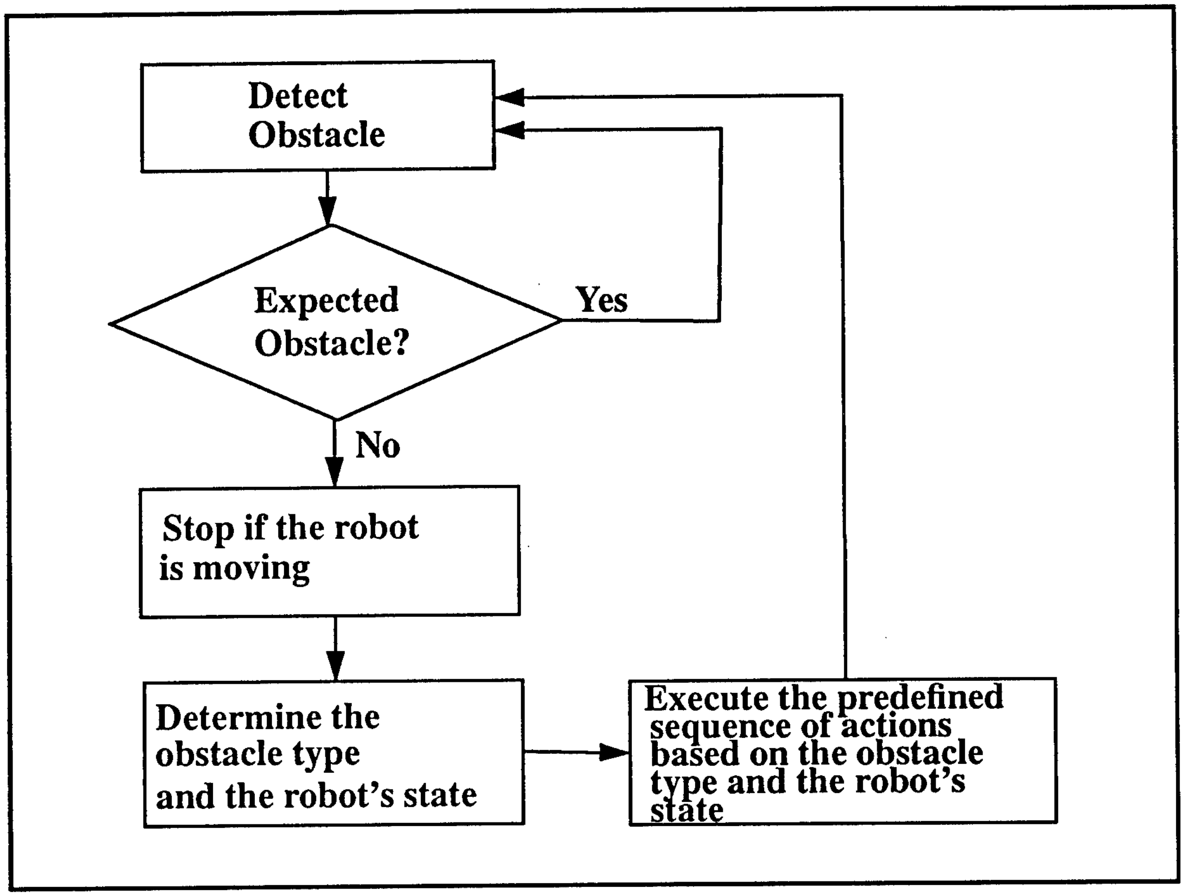

The obstacle detection process runs concurrently with the planner process. When it detects an obstacle it obtains the location of the obstacle to determine whether it is expected or not. If it is unexpected then the robot stops and determines whether it is a dynamic or static obstacle. Then it gets the current state of the robot. Depending on those three variables, the type and location of the obstacle and the state of the robot, the obstacle detection process determines which sequence of predefined actions to take. On most occasions this sequence of predefined actions just interrupts the planner and supplies information regarding the obstacle. The planner then decides what action to take. Again, this will be elaborated in the sections for the base move and the tile servicing loop (section 6.4 on page 125 and section 6.5 on page 134).

6.3.3 Health Monitoring Loop

The health monitoring subsystem is one of the most important parts of the whole system due to the critical nature of the task. It is very important that the robot can detect any internal malfunction as soon as possible to prevent damaging action by the robot. This is the reason for a separate concurrent and continuous process for the health monitoring system. To further improve the safety of the robot, a combination of hardware and software monitoring is employed. The hardware monitoring system is used at the lowest level to safeguard against any software failure. For example, the whisker in the manipulator is electronically connected to a disable switch, so if the manipulator touches anything

accidentally, it will be stopped at once. In addition to faster reaction time, this gives the robot the capability to handle critical errors even when the central health monitoring system is down. This multiple layer of safety mechanisms is employed for all critical and potentially damaging errors, thus greatly reducing the risk of accidental damages. The main control flow for the health monitoring system is shown in Figure 6-4.

Figure 6-4 Health monitoring loop

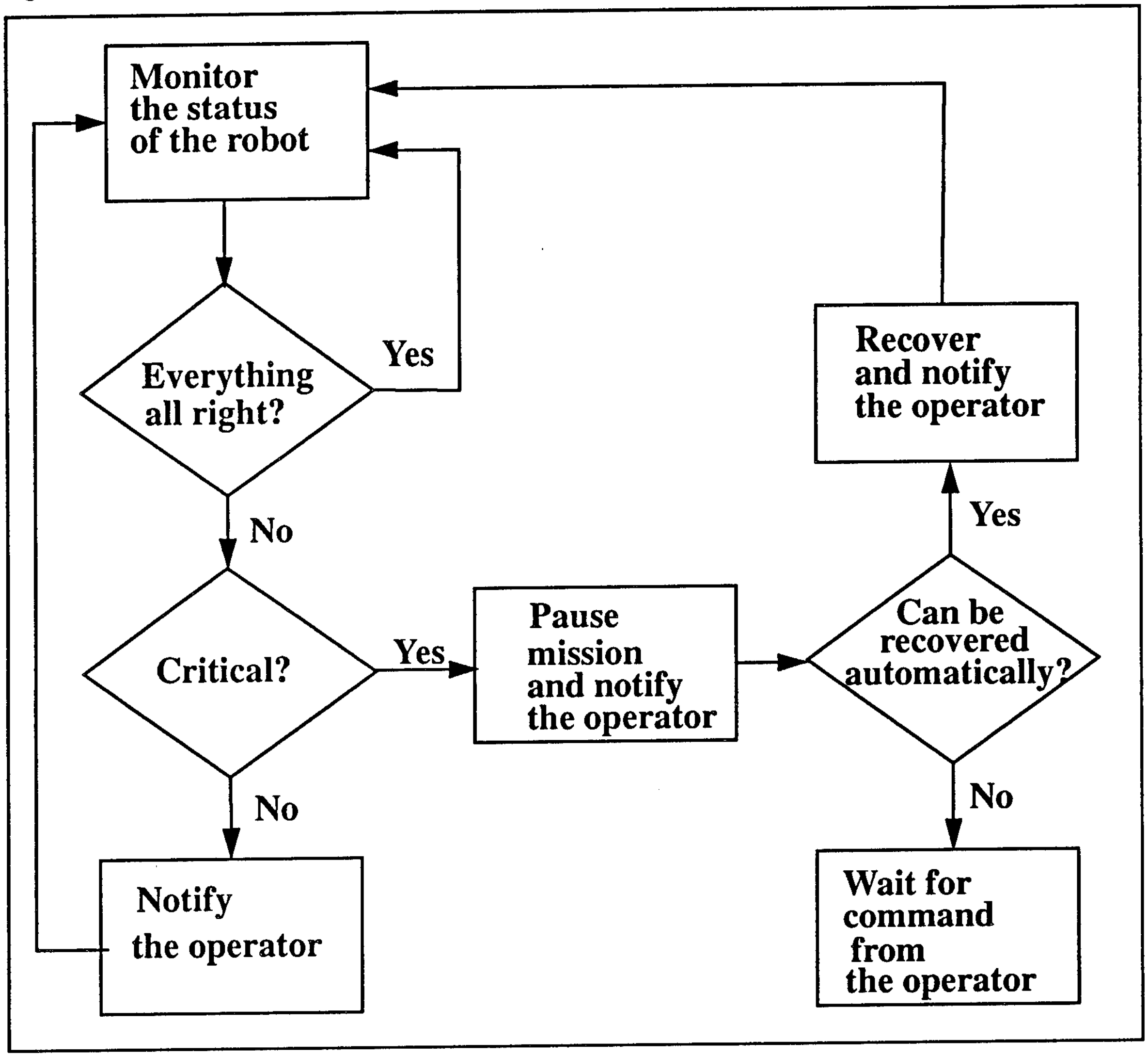

As the flowchart shows, depending on how severe the system fault is, one of the following two actions is taken:

- Pause: Stop moving base, retract arm, save state, notify operator, and check if the robot can recover from the error automatically. If it can and the error is not fatal, the robot will recover automatically, otherwise it waits for the operator. The operator then has a choice of resuming or aborting the operation. He can also send a new command to the robot. This command can be a diagnostic command that helps the operator pinpoint the problem. Examples of the failures that cause the robot to pause:

    - Failed communication link
    - DMES supply depleted
    - Critical battery level
    - Problem with hardware or software heartbeat
    - Excessive roll or pitch for long duration (e.g., caused by a flat tire or obstacle)
    - Internal temperature above safety threshold
    - Encoder error
    - DMES injector problem
    - DMES leakage
    - Exceeding quota of recoverable errors
- Notify: Notify operator of anticipated problem. Examples of the failures that cause this action:
    - Low DMES level or projected shortage of DMES
    - Low battery level or projected shortage of power
    - Internal temperature above warning threshold
    - The number of recoverable errors rises above normal

Independent of how severe the system fault is, the state of the robot and the status of the operation is saved every time a system fault is detected. The status of the operation includes all the information and status of the ongoing operation (e.g., which tiles have been serviced and the tile images). By doing this the operator can resume the operation after fixing the problem without having to redo operations.

Additionally, there are two types of system faults depending on how they are detected. One type of system fault can be detected simply by monitoring the states of some sensors (e.g., temperature, heartbeat and power). This type of error is detected by the low level controller and is reported to the health monitoring module, which in turn notifies the planner and the user interface module. The other type of system fault can not be detected just by simply monitoring these sensors. For example, the individual sensor readings might be correct but are inconsistent with each other, or the robot makes the same trivial error very often. The small error itself might not be enough to cause any concern but the frequency of the errors might indicate that something is really wrong. Calibration error is one example of this type of error.

As mentioned previously, the operator can interrupt the operation by sending an interrupt signal to the robot. This signal forces the robot to go into the pause state from which an automatic recovery is not possible. Once the robot is in the pause state, the operator can load a new command. Since the command can be anything, this interrupt facility enables the operator to abort, pause, or modify the operation when it is needed. This can be

especially useful since the operator might be able to foresee a problem that might arise in the future and by modifying the planned operation the problem can be circumvented.

6.4 Mobile Base Moves

In order to service all accessible tiles, the mobile base must move from place to place to provide access to various areas for the manipulator and end effector. A tile coverage plan is first generated based on the tile database and scheduling constraints. The tile coverage plan consists of a sequence of goal locations which the mobile base must visit. As one area of tiles is being serviced, a plan for moving the base to the next goal and a plan for accessing the tiles in that area can be made based on the latest information available. Figure 6-5 illustrates this process of generating the coverage plan and then visiting each work area and servicing the tiles in that area. The cycle completes when the shift has ended or when all tiles have been serviced.

Figure 6-5 Mobile base move overview

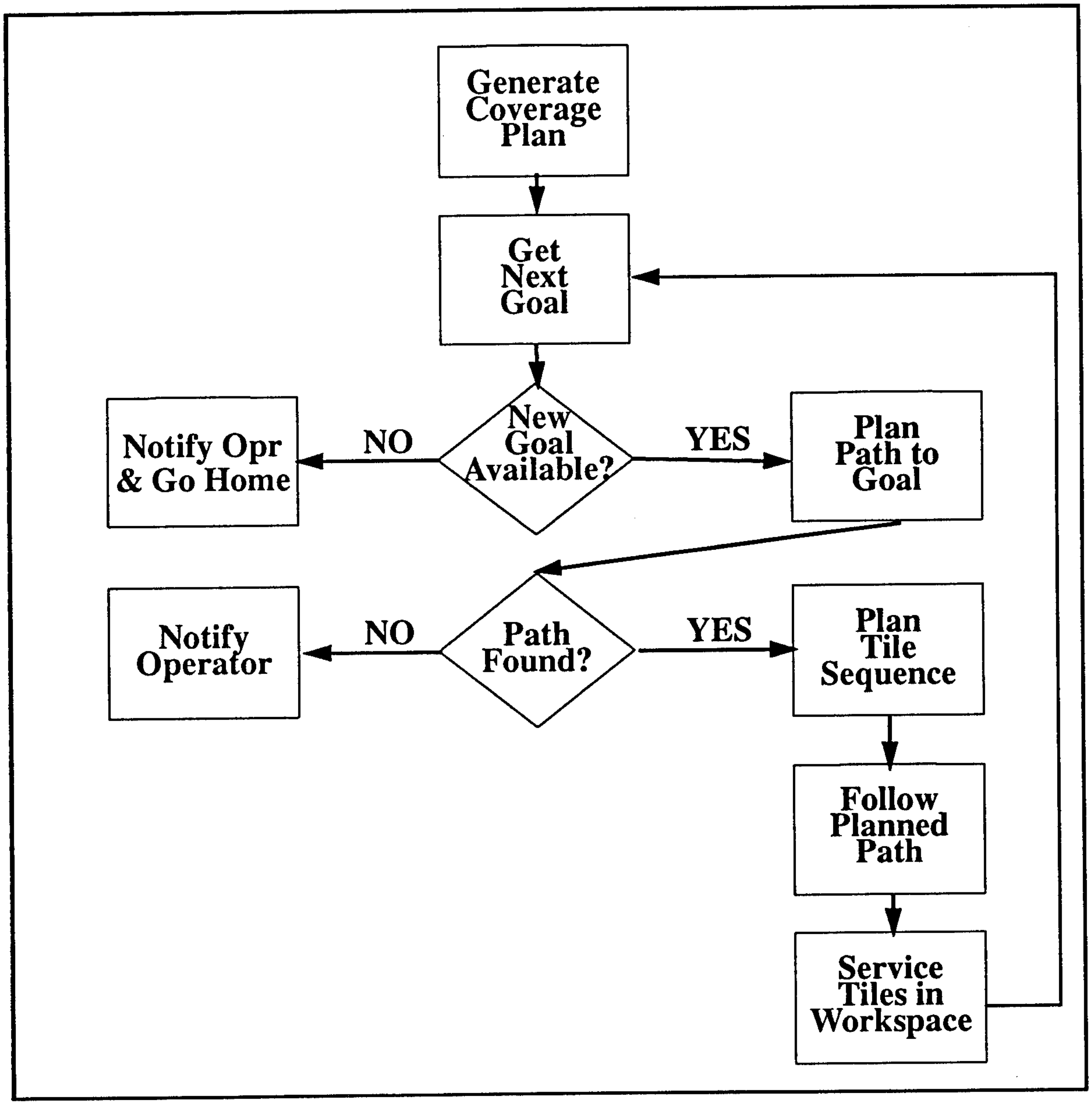

In this section, we will first describe the inputs and outputs of the tile coverage planner. Then the sequence of events involved in moving from one goal to the next is detailed. Next, the actions taken in response to detected obstacles, both static and dynamic, are described. Finally, the user interface which allows an operator to move the mobile base from a remote station is outlined.

6.4.1 Tile Coverage Planning

Before tile servicing operations can begin, it is first necessary to produce a plan for moving the base from area to area so that all tiles to be serviced during a shift can be accessed. Thus, the portion of the orbiter where TPS work will be carried out must be divided into manipulator workspace areas. A workspace area is defined as the area reachable by the end effector with the mobile base parked at a particular location. The movement of the X-Y table creates a rectangular workspace area, and the addition of the area reachable by the manipulator reaching beyond the gantry boundaries yields a somewhat larger rectangle whose corners are slightly rounded (due to the circular manipulator workspace).

The inputs to the tile coverage planner are the tile database, the areas of the orbiter available for TPS work during a given shift, a work schedule detailing the time and location of other ongoing operations, and mission specifications entered by the operator such as priorities to certain areas.

The tile coverage planner then generates a tessellation of the TPS service areas into manipulator workspace areas, as shown in Figure 6-6. There is a small amount of overlap between workspace areas in order to ensure that tiles on the boundary of a workspace are fully accessible and to compensate for the rounded corners of the workspace area. The black areas in the figure indicate obstacles known from the database, and the gray areas indicate areas where other work is scheduled. The coverage plan also indicates an efficient order in which the workspace areas are to be visited, as indicated by the sequence of arrows originating from the home position. Associated with each workspace area is a goal location at which the mobile base is to be stationed in order to provide access to the tiles in that area.

Figure 6-6 Tile coverage plan

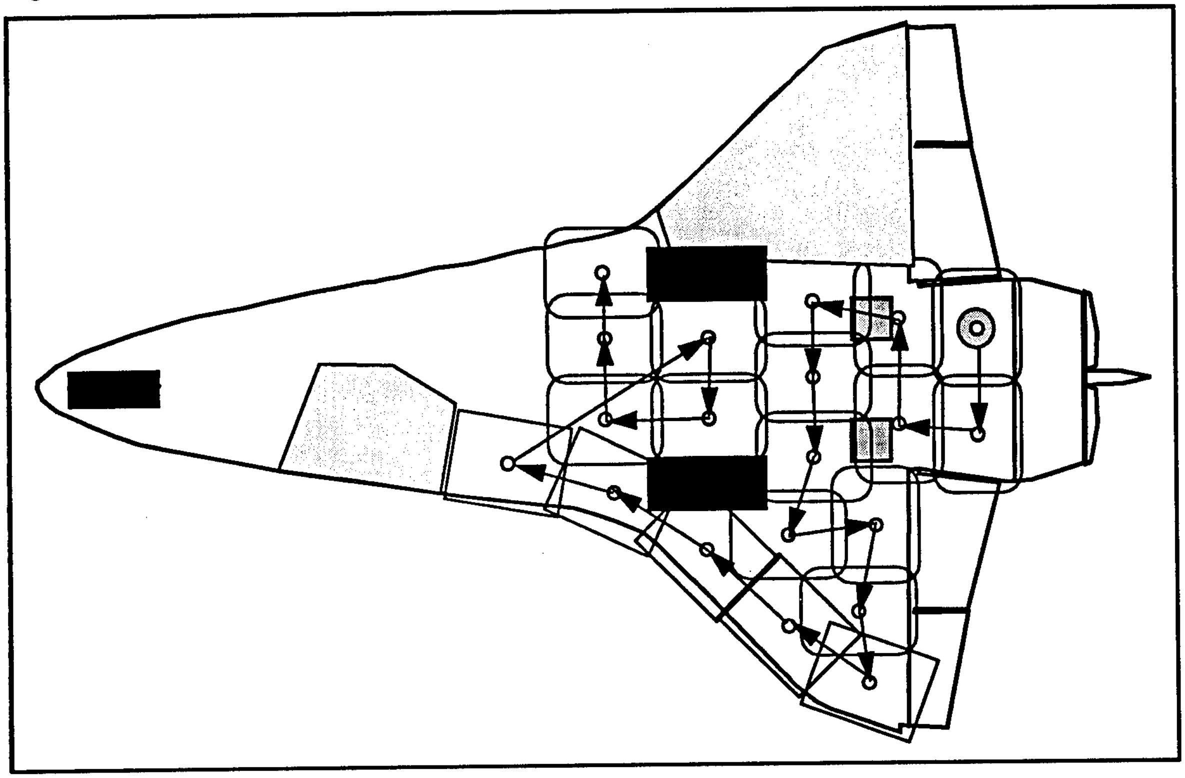

6.4.2 Path Planning

During tile servicing operations, the mobile base must move from one workspace area to the goal location of the next area to be serviced. To this end, a path to the next goal is planned while the tiles in the current workspace area are being serviced.

The path planner plans routes between consecutive goals based on *a priori* knowledge of obstacles. Maps of the facility and shuttle provide the location of objects such as jackstands, workstands, and landing gear doors. These maps can be updated during the course of a work shift as new information is made available to the operator, or when the operator is notified of unexpected obstacles detected by the vehicle sensors.

The planned paths will consist of sequences of linear motions, with base rotations occurring only when the vehicle is stopped at the vertex of two such line segments. Although the steering mechanism allows arbitrary motion in the plane, we have restricted ourselves to these simplified paths for the following reasons:

- Simplified planning.
- A finite sequence of these moves can provide a piecewise linear approximation to any spatial curve to an arbitrarily small error.
- The area is amenable to these types of moves since there are no curved corridors.
- The moves are predictable and easily monitored by a human.
- Tire slippage is minimal and symmetric, thus improving dead reckoning.

The independent steering mechanism allows travel in any direction, so that the vehicle base can be in any orientation regardless of the current direction of travel. This allows the base to navigate obstacles in whatever orientation provides the most clearance, and allows lateral movements for negotiation of tight spaces. Thus, the base can be positioned by first orienting in free space and then sliding into the goal location.

When work in the current workspace area has been completed, the manipulator arm is retracted, the gantry lowered, and the preplanned path is followed to the next goal location, where the gantry is raised again to the appropriate height and work in that area proceeds. This iterative process is depicted in Figure 6-7. The planned path is sent to the controller as a sequence of commands of the form baseMove(Δx, Δy, 0) for linear translations and baseMove(0, 0, $\Delta\theta$) for rotating in place (see Section 5.4 for a description of the controller command set). The desired relative base motions are achieved using the vehicle's global positioning system as described in Section 7.2. This will result in the placement of the mobile base within 3 cm of the desired goal location, which is sufficient to unambiguously distinguish one tile from another based solely on their locations in the tile map.

Figure 6-7 Mobile base move loop

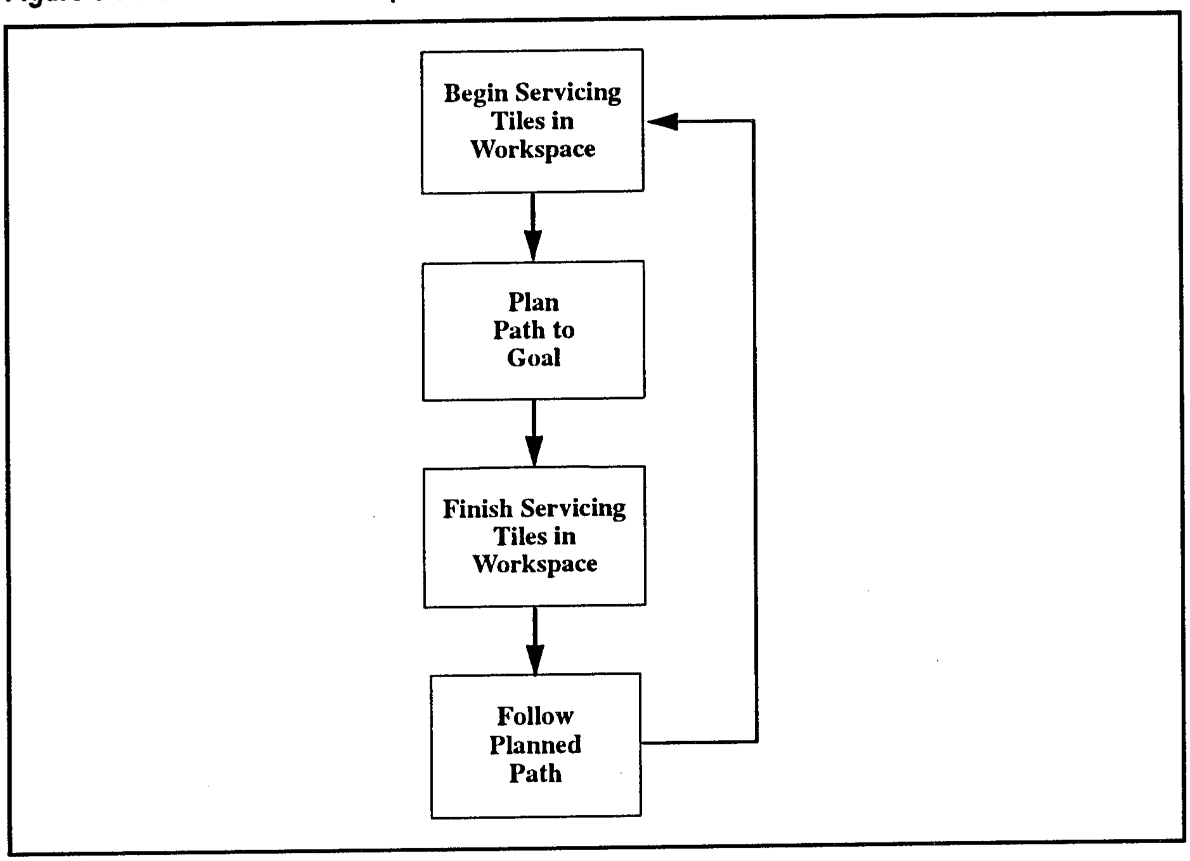

6.4.3 Unexpected Obstacles

When an obstacle is detected, it is compared against the database to see if it was expected and thus accounted for in the preplanned path. If the obstacle is not in the database and lies along the desired path of the vehicle, then the first response is to stop moving.

The reasons for halting the vehicle are:

- Allows for easy disambiguation between static and dynamic obstacles
- Dynamic obstacles are human or human-operated, let them avoid the robot
- Can more accurately pinpoint location before replanning
- Frees planner from real-time constraints
- Stopped time insignificant relative to total shift operations time

Once the vehicle has halted, the sensor readings are monitored for change to determine whether or not the object in question is moving, and the appropriate set of responses is selected for each case.

Static ground obstacles

The detection of an unexpected obstacle occurs asynchronously within a separate process, and an interrupt is signalled, forcing the planner into the state labelled as "Halt Vehicle" in Figure 6-8. At this point, the vehicle stops and the operator is notified. The sensors will simply provide information regarding the presence of an obstacle and its approximate distance and orientation from the vehicle, but cannot be used to accurately determine the location or shape of the obstacle. The operator may indicate that no obstacle is present and instruct the planner to continue along the planned path, or the operator may enter the new obstacle into the database and instruct the planner on how to proceed. The operator is presented with the following six options (illustrated in the figure by dashed lines):

1) database updated (new obstacle entered or old obstacle removed), plan new path
2) mark workspace as inaccessible and go on to next one
3) replan tile coverage with new obstacle in database (probably local patch to plan)
4) follow path specified by operator (after verification)
5) skip this workspace for now and come back to it later (obstacle may be gone by end of shift)
6) ignore obstacle, continue along same path (in cases such as a false sonar return or if the obstacle has been removed)

Figure 6-8 Handling an unexpected static obstacle

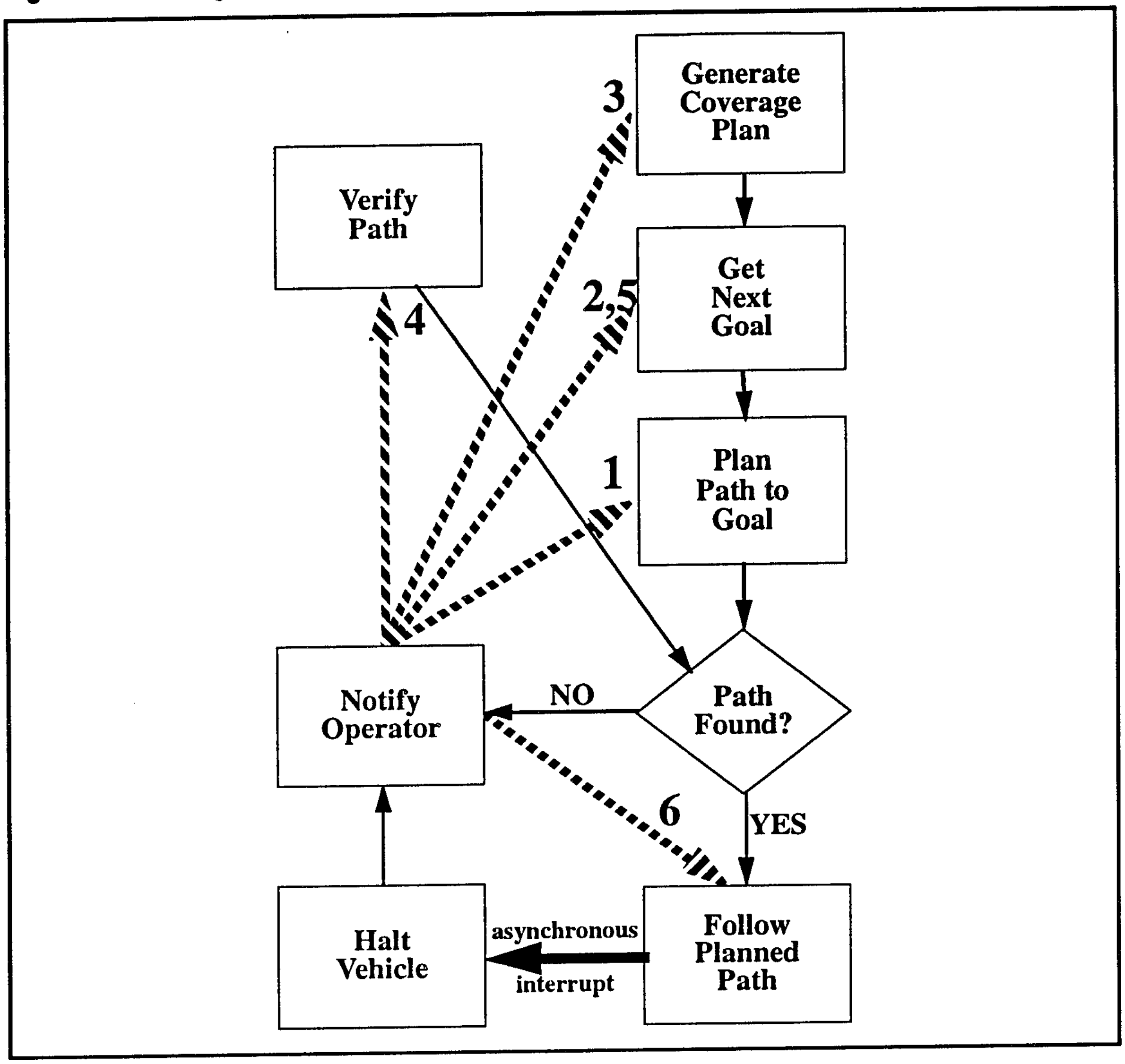

To illustrate this process, consider the situation illustrated in Figure 6-9. The robot has finished servicing those tiles in the workspace areas shown with a gray dot in the center. The vehicle is enroute to the next goal location, indicated by the thick circle, when it encounters an unexpected obstacle. The vehicle halts immediately at the location represented by the filled in circle, and notifies the operator that it has detected the presence of an obstacle at the point symbolized by the 'X'. The operator observes that there is indeed an obstacle there, and enters it into the map database. A new path is then planned to reach the desired goal location, and normal operation resumes. The controller is sent a new set of baseMove commands which override those issued at the onset of the current repositioning maneuver. Once the vehicle has established itself at the goal and tile servicing has commenced in that workspace area, the planner adapts the tile coverage plan to account for the previously unknown obstacle.

Figure 6-9 Replanned path around unexpected obstacle

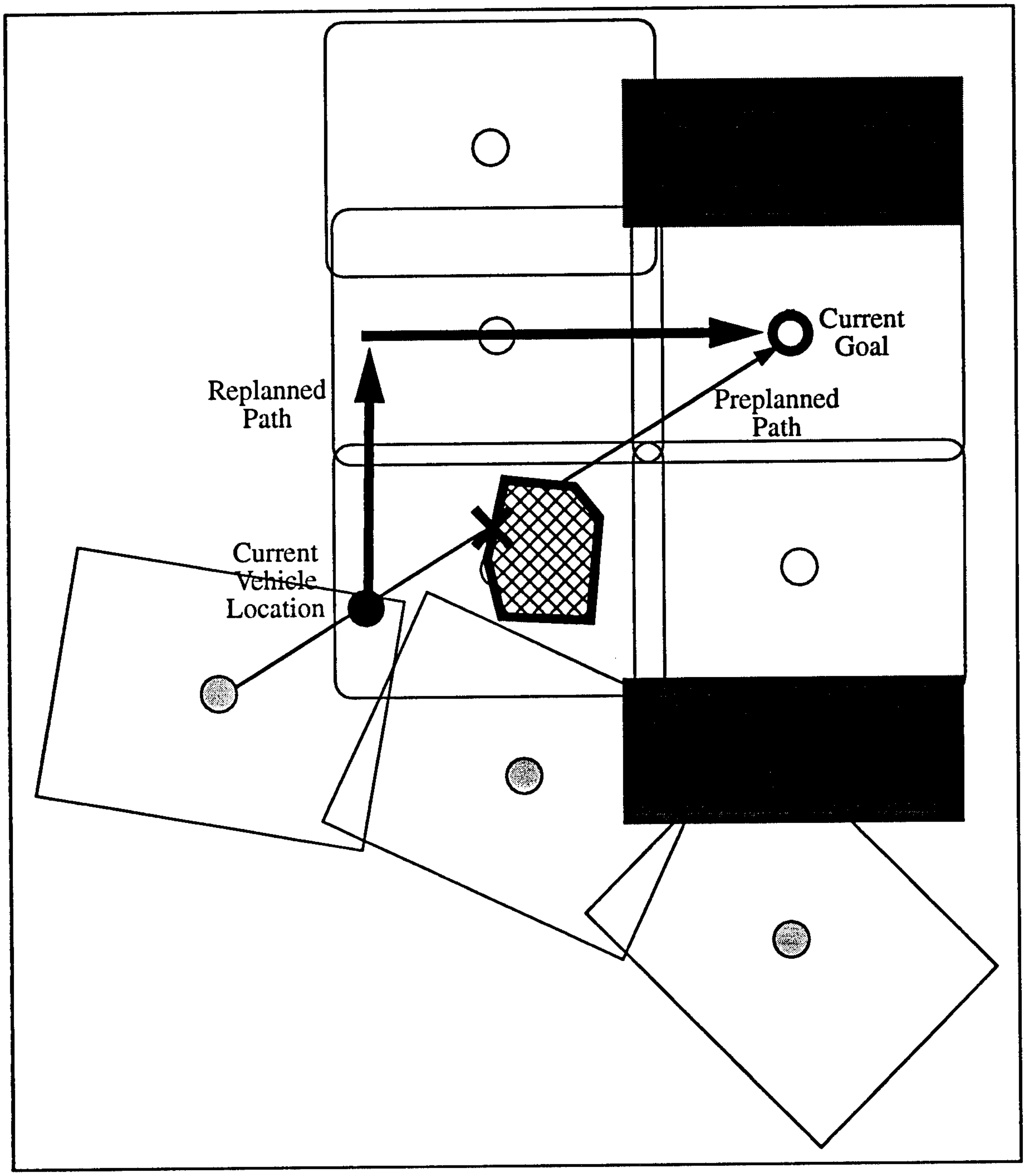

Dynamic ground obstacles

Once the vehicle has halted and the operator has been notified of the presence of an obstacle, it may easily be determined if the obstacle is dynamic by observing whether or not the measured distance to the object is changing significantly (i.e. not small measurement fluctuations which may be due to noise). If the obstacle is moving, the following actions are taken:

1) Determine if the dynamic obstacle is a threat
(e.g. distance < threshold and distance is decreasing)

2) If the obstacle is determined to not be a current threat, continue to monitor its motion and await permission to proceed from the operator

3) If the obstacle is determined to be a threat:

   a) sound an alarm

   b) retract arm if not in home position

   c) wait until obstacle is gone or stopped

   d) if obstacle stops and further base motion is still required, treat it as a static obstacle as described above

6.4.4 User Interface

The operator may at times decide to override or alter the plans of the system. One such time would be when the system explicitly requests operator assistance, as was the case when a path to the current goal could not be found. Other times would be when an error or inefficiency is detected by the operator, or when an update must be made to the schedule or obstacle database. The two types of plans involved in mobile base moves are the tessellation of the serviceable tiles into workspace areas and the planning of paths between the goal points of successive workspace areas. It is first necessary to provide the operator with a display of the computer generated plans and databases, and then provide a means for the operator to change or override those plans.

Tile Workspace Tessellation Plan

The operator will be provided with a graphical display of the bottom side of the orbiter, generated from the tile database. The operator can then input mission specifications to be considered in planning the tile workspace tessellation. Scheduled work on various parts of the orbiter can be entered by using a mouse (or other graphical input device) to indicate the area in question, and the keyboard can be used to enter the times for which other personnel have scheduled the area, as well as any other ancillary information the operator may choose to enter into the record. The operator may also wish to indicate areas which the robot should give priority to and service early in the shift, for example if an area has been observed to have sustained damage or if there are anticipated scheduling conflicts. This information may also be entered into the system by a combination of mouse and keyboard input. If the operator should choose to perform the tile workspace tessellation manually, he can do so by using the mouse to "rubber stamp" a template of the manipulator workspace over the area of the orbiter to be serviced during the shift. Commands for adjusting the size and shape of the template will also be provided. This method may also be used after the automatic generation of the tessellation plan, should the operator wish to manually adjust only a portion of that plan. The resulting display is as shown in Figure 6-6.

Path Plan

When the vehicle is about to commence a base move to the next workspace area, the operator will be provided with a graphical display of the planned path overlaid on an

outline of the orbiter. All permanent obstacles such as jackstands and columns will also be displayed, as will all other known obstacles entered into the database earlier in the shift by the operator or by the perception system. At any time, the operator may indicate the presence of previously unknown obstacles, or he may remove obstacles from the database that are no longer present. If desired, the system can await approval of the planned path by the operator before commencing motion. If the operator should ever choose to manually specify the path to be followed, he may click on waypoints and create a piecewise linear path for the vehicle to follow. The planner will then verify that the path does not intersect with any known obstacles, and proceed to follow that path. Figure 6-9 provides an example of how such a display might appear.

6.5 Tile Servicing Loop

This section depicts the process to service the tiles inside the workspace of a given base position. First, the main flow of the tile servicing loop is delineated. Second, the possible exceptions during the flow are described. Third, the remedial actions for the exceptions are detailed. Finally, the user interface is presented.

Main Flow of the Tile Servicing Loop

As shown in Figure 6-10 on page 134, the main flow for tile servicing can be divided into five major steps. A detailed description of each step follows:

Figure 6-10 Flow for tile servicing and possible exceptions.

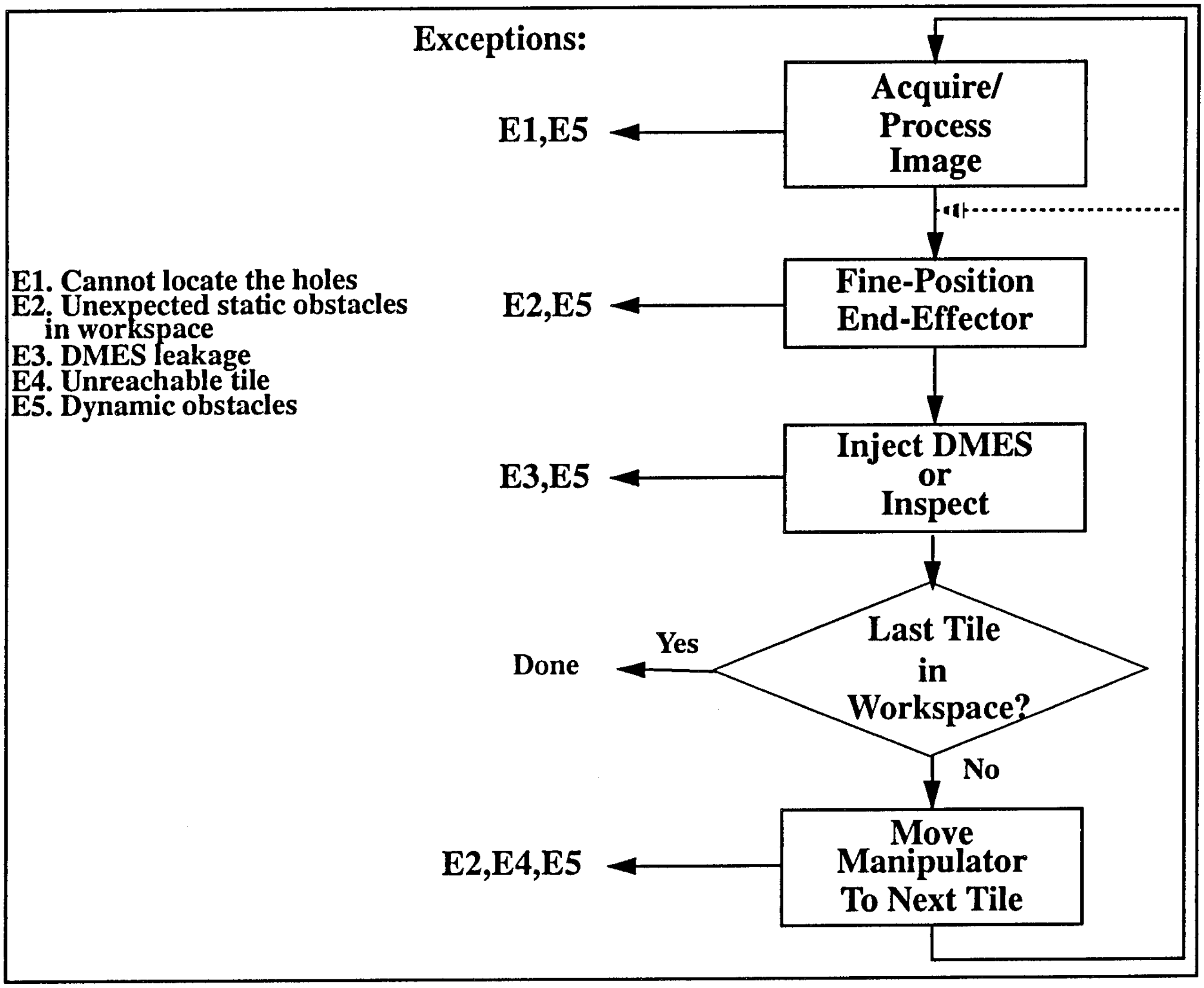

1) Acquire/Process image:

   a) Get the image of the tile(s) to be processed.

   b) Process image to find the injection hole position(s) and verify the tile identity.

2) Fine-position end-effector:

   a) Plan path for alignment.

   b) Execute the path.

3) Inject DMES or perform inspection actions.

4) Move manipulator to next tile:

   a) Retract the end-effector.

   b) Make sure a planar scan of the workspace has been captured recently for obstacle detection.

   c) Confirm the path to next tile.

   d) Move manipulator to next tile position.

   e) Damp manipulator motion.

It is assumed the image acquired in step 1 covers only the tile to be serviced. Tile servicing efficiency can be increased if the image can cover several tiles at a time. In this case, step 1 need only be done if the information of the tile to be immediately serviced is not obtained yet. In the extreme case, if the field of view of the camera system can cover the whole workspace and the accuracy and resolution is sufficient, it is possible to move step 1 out of the loop and do the process only once for each workspace covered by a single base move (as shown in broken line). Also, if the task to be performed is only re-waterproofing and the XY-table dead-reckoning is accurate enough, step 1 need not be done at all. (Refer to Section 7.3 Local Position Estimation on page 159 for more details)

6.5.1 Exceptions

There are several exceptions that can occur during the normal operation specified in the main flow. The possible causes for individual exceptions are described below:

1) Cannot locate the hole(s):

   - Transient sensor noise.
   - Positioning mechanism malfunction.
   - Large area of tiles damaged.
   - Calibration problem.
   - Beyond the algorithm limit.
   - Vision system malfunction.

2) Unexpected static obstacle(s) in the workspace:

   - Transient sensor noise.
   - Planar scan sensor malfunction.
   - Actual obstacle(s).

3) DMES leakage:

- Crack on the tile.
- Erroneous hole location.
- Injector failure.
- Manipulator/end-effector failure.

4) Unreachable tile:
   - Obstacle(s) in the way.
   - Coverage planning error.
5) Dynamic obstacle(s):
   - Transient sensor noise.
   - Real dynamic obstacle(s).

6.5.2 Exception Handling

The general guideline for exception handling is to reduce human intervention by automatic recovery from those exceptions, if possible, while maintaining safety. The general step-by-step procedure for exception handling in the tile servicing loop is given below (Figure 6-11):

1) Pause the operation if it is a severe system malfunction.
2) Pause the operation if the symptom is frequent and not automatically recoverable.
3) Recalibrate the sensing system if the symptom is frequent and the exception may arise from miscalibration.
4) Resort to secondary method of measurement, if any.
5) Call the operator for help if it is in interactive mode.
6) Otherwise, just skip the current tile, label it as unserviceable and move on to the next one.

When an operator is called for help, (s)he always has the options to abort the whole task or some part of the process. And, the operator can interrupt the process at any moment, once (s)he finds something unusual happens. Those missed tiles will be either revisited later or just reported and ignored, depending on the operator's choice.

The detailed description of the remedial actions to be taken when an exception occurs is as follows:

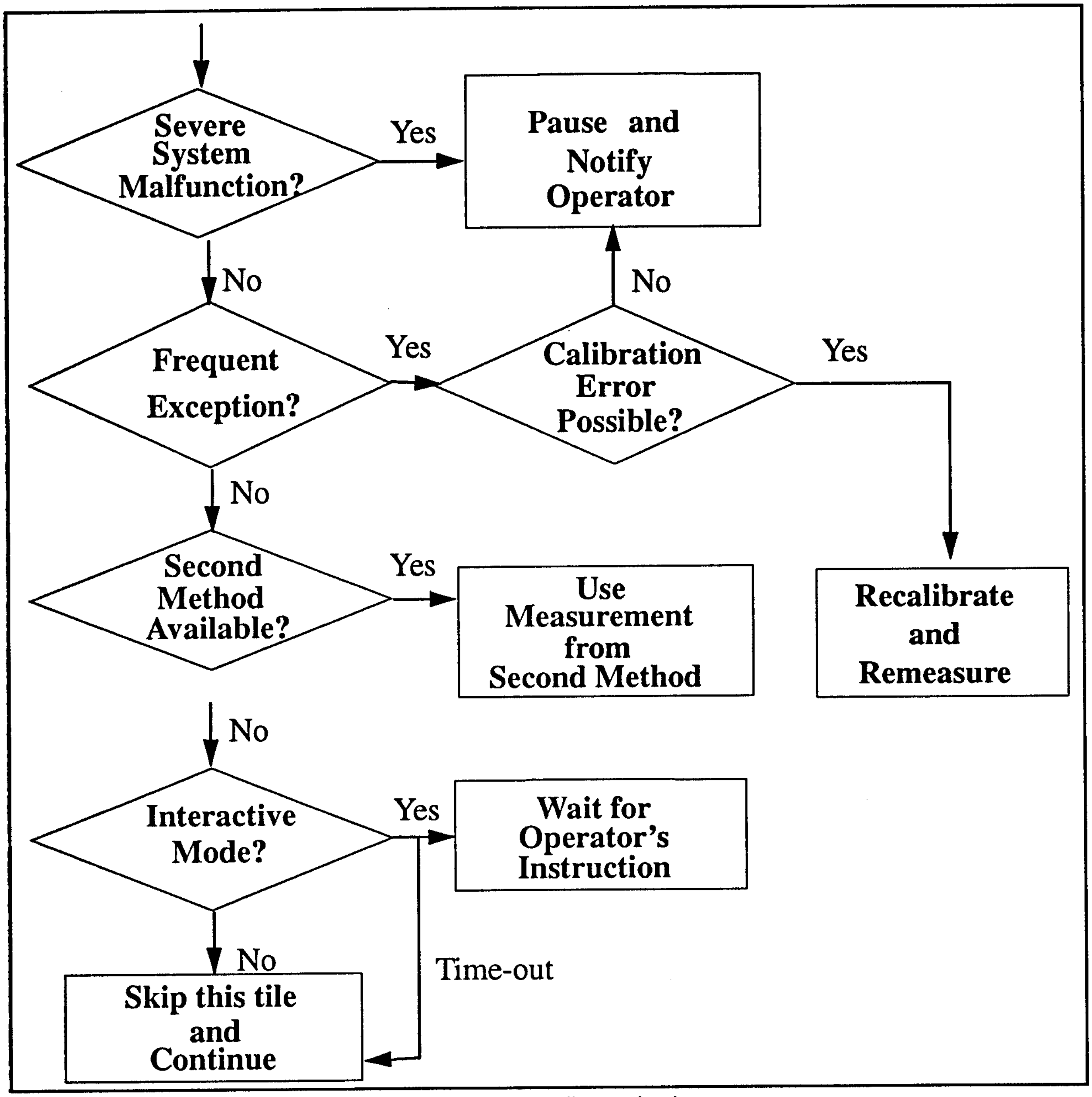

Figure 6-11 General exception handling in tile service loop

1) Cannot locate the injection hole(s):

   a) First assume the cause is transient sensor noise, take a second image and redo the processing.

   b) If it is a recurrent exception, assume a calibration error and recalibrate the camera automatically.

   c) If it still doesn't work, invoke a secondary method (e.g. tile ID recognition) to either identify the tiles to help locate the injection hole(s) or directly find the hole(s).

d) If the injection hole(s) still cannot be found, make sure that there are no large areas of tiles damaged. If this is the case, just report the situation and continue to work on next tile.

e) Otherwise, ask the operator's assistance to locate the holes.

f) If no operator response is detected within a preset time or if the operating mode is not interactive, skip the current tile and go to the next one.

g) If problems occurs frequently for both primary and secondary method, assume a severe system malfunction, notify the operator, and abort the task.

2) Unexpected static obstacle(s) in the workspace:

a) Get sensor information again to confirm the existence of obstacles.

b) If the obstacles still exist, plan a new path to move around the obstacle.

c) If the problem recurs very often, assume severe sensor error and abort the task.

3) DMES leakage:

a) Check the tile image to find cracks. If there is any crack found near the hole, report the defect and continue to the next tile.

b) Otherwise, assume the hole was missed and use the secondary method to locate the hole. If the position found is different from the previous one, redo the injection for the new location.

c) If leakage becomes a chronic symptom for the primary method of hole-locating, switch to the secondary method and report the error.

d) If the hole found in the primary and secondary methods is the same, assume injector or manipulator/end-effector error, notify the operator, and abort the task.

4) Unreachable tile:

a) Try to include this unreachable tile in a workspace that has not been visited yet so that it can be serviced later.

b) Check if it is caused by blocking obstacles.

c) If it is not caused by obstacles, mark the tile as unable to be serviced and report the situation for later debugging of the coverage planner.

d) Continue to work on the next tile.

5) Dynamic obstacle(s):

a) Pause the operation and take a second set of sensor data to make sure of the existence of the dynamic obstacle(s).

b) If it is due to transient noise, continue the operation.

6.5.3 User Interface

The requirement for the user interface needs during the tile servicing loop can be divided into two cases:

1) During normal operation:
   - Camera image of the tiles.
   - Planar scan of the workspace.
   - Configuration of the manipulator and end-effector.
   - Status of plan execution.
   - Coverage plan in the workspace.
   - Indication of the tile to be (or being) serviced on the tile map detailing successful rewaterproofing or anomalies detected.
2) Exception handling:
   - Operator can set the operation mode to be interactive or batch. Under batch mode, when the tile or the injection hole cannot be located, the robot will report the situation and continue to work on the next tile. It will then be the operator's decision whether to re-visit those unprocessed tiles later.
   - Operator can get direct control of the manipulator and end-effector at different levels. At the lowest level, the commands are directly sent to the controller without planner verification. At the highest level, only a goal position is required and the planner will do the planning and control.
   - Operator can help identify the tile by clicking in the tile map when the tile identification algorithm/sensor fails.
   - Operator can help locate the injection hole position by clicking in the tile image when a hole locating exception occurs.
   - Operator can abort the task or any part of the task during an exception.

Figure 6-12 Status for the tiles in workspace

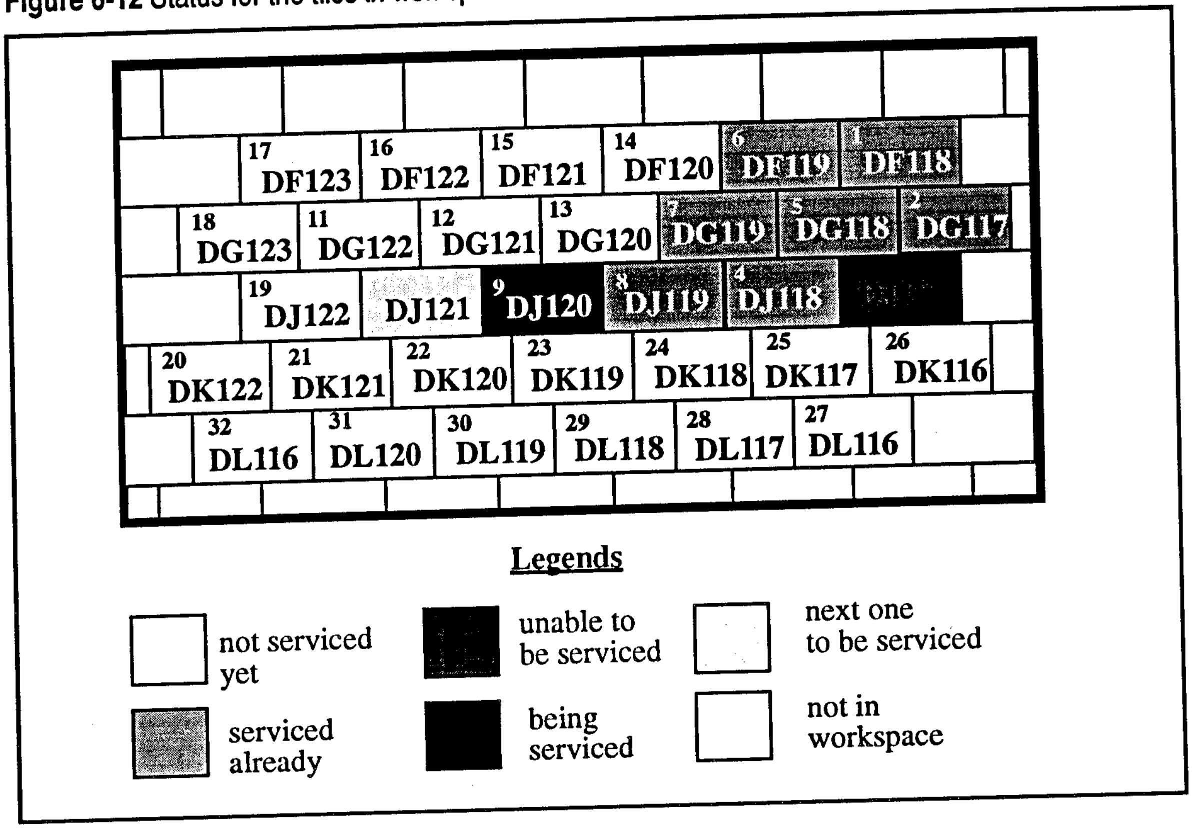

Figure 6-12 shows the mock-up user interface to display the coverage plan for the workspace being serviced and the status of the execution. Tiles in the workspace are colored to reflect their status. Tile identification numbers are shown inside the tile map. The small upper left number in a tile shows the sequence number for execution in a workspace run. Figure 6-13 is a mock-up display to show the planar scan result of the obstacle detection sensor superimposed with those expected obstacles derived from the database. It can be used by the operator to either monitor the workspace or debug.

Figure 6-13 Plan view of the workspace

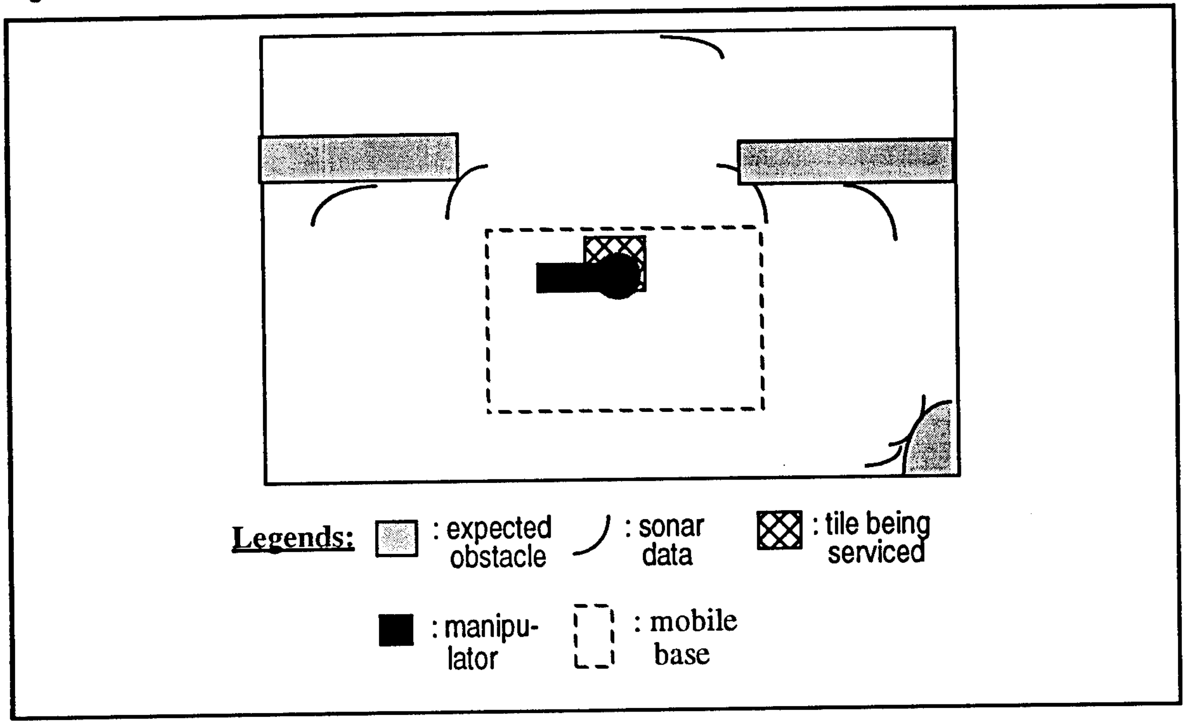

6.6 Summary

The architecture of the software system was found to be dominated by a single thread of control. There are other concurrent processes besides the main thread, but they all can be modelled and handled as interrupts to the main thread. This software system model enables us to simplify the design process by avoiding the problem of complex interactions between concurrent processes.

There are three main functions that are executed in the main thread of control. The first function is coverage plan generation. This coverage plan is used to determine the base moves of the robot. The second function is the base move from one workspace to the other. This function forms an outer loop for the third function. The third function is the tile servicing operation. This is executed in a loop until all the tiles in a workspace area have been serviced.

The two other concurrent processes are health monitoring and obstacle detection. These two processes are considered very important since safety is our main concern in designing the software system. By implementing them as separate processes that continuously monitor the state of the robot and its surroundings, the robot is able to react immediately to any exception that might occur, including planning errors. These two modules also have a direct connection to the low level controller so that they do not depend on the other modules in an emergency situation, and so that an immediate response can be assured.

During base moves the robot might encounter an unexpected obstacle in its path. If this happens, the robot will first halt, and then determine if the obstacle is dynamic or static. If it is dynamic then the robot waits for the obstacle to get out of its path, on the assumption that dynamic obstacles are either humans or human-driven vehicles, and are therefore

capable of avoiding a stationary vehicle. For static unexpected obstacles, the operator must update the database, and may then choose for the area to be avoided or for a new path to the goal to be generated which accounts for the updated obstacle information.

There are also many exceptions that can arise during the tile servicing loop. Many of these exceptions are related to the injection process, e.g. the injection hole can not be found or there is excessive DMES leakage. Other exceptions may be caused by obstacles in the workspace or a malfunction of the manipulator, in which case damage could result. Multiple layers of safety protection are used to safeguard against such possibilities. The lowest layer takes the form of force sensors and mechanical sensors (such as whiskers) that are connected directly to the actuator controller, thus enabling a fast response if the manipulator touches something unexpectedly or exerts too much force. The higher layers use readings from multiple sensors integrated over longer periods in order to detect problems such as calibration errors or to anticipate future problems such as a low battery level.

Another important functionality of the software system is to provide the user interface. For safety and flexibility, the operator is able to monitor the whole operation through the graphical user interface, and interrupt the process at any time. Among other things, the user interface displays the tile coverage plan, the path that the robot will take, the current location of the base and the arm, the health status of the robot, and the status of the tiles. In addition, the operator can also play an active role in controlling the robot. This teleoperation can be done in several levels. In the lowest level the operator can control the actuators directly using a joystick, and in the highest level the operator issues high level commands such as to go to a certain workspace. The operator can also intervene in handling exceptions. This is possible because the operator is always notified when an exception occurs, regardless of whether the robot can recover automatically or not.

7. Perception

This chapter addresses design issues related to the perception subsystem. The perception effort can be divided into three problems as follows:

- *global position estimation* - Where is the mobile base with respect to a reference frame attached to the facility or the shuttle?
- *local position estimation* - Where is the manipulator's end effector with respect to a reference frame attached to a shuttle tile or a group of shuttle tiles?
- *obstacle detection* - Are there objects in the vicinity of the vehicle? If so, what is the approximate location of the nearest point of the object?

An important distinction between global and local position estimation is suggested by their names; measurements associated with each system are performed with respect to either a global or a local frame of reference. Another distinction between these two systems is the level of accuracy associated with their respective estimates. Global position estimation is expected to provide coarse estimates, while local position estimation is expected to provide fine estimates.

An additional perception problem is the inspection of shuttle tiles. This problem can be defined as follows: given a set of tile measurements, determine whether the tile is sufficiently damaged or blemished to require additional attention. For the purposes of this design document, we have ignored the tile inspection problem. We assume that this problem is being studied in detail by the perception group at SRI. When information regarding the tile inspection system is received from SRI, that information will be added to an appropriate section of this chapter.

The intent of this chapter is to outline design issues which relate to each of the three perception problems defined above. In section 7.1, we present an overview of the position estimation problem and outline issues which influence the design of both the global and local components of this system. In section 7.2, we evaluate several global position estimation systems with respect to criteria such as accuracy, cost, ease of deployment, etc. We identify the leading candidate system for the job of global position estimation and discuss attributes of this system in detail. In section 7.3, we describe two complementary approaches to the local position estimation problem. One approach is based upon a static "look and move" type control strategy, while the other is based upon a dynamic visual servoing approach. In section 7.4, we discuss issues involved in the design of the obstacle detection system. In particular, we provide information on various sensors which are being considered for obstacle detection, and outline an initial design of this system.

Figure 7-1 Reference frames for position estimation

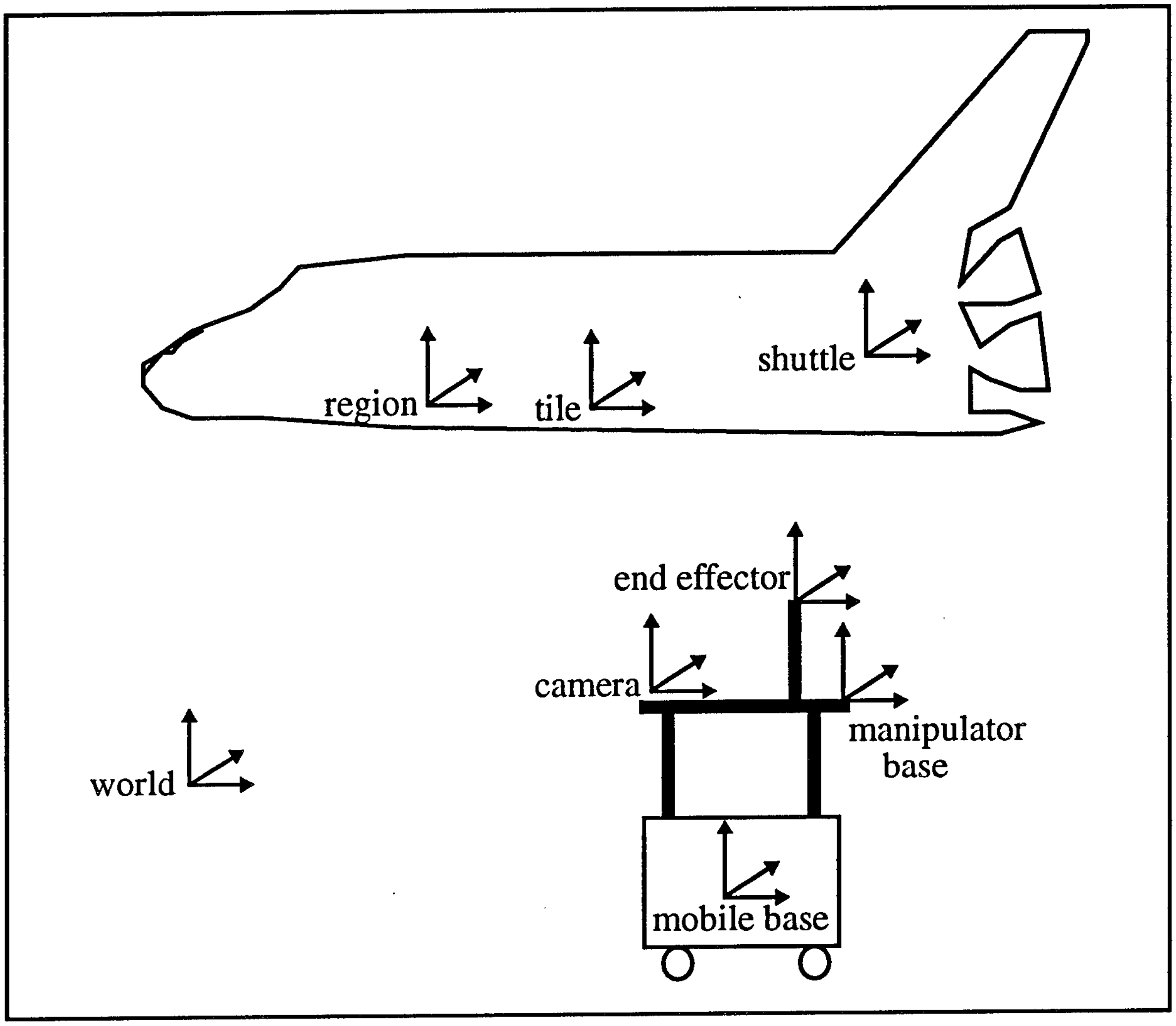

7.1 Position Estimation Overview

Figure 7-1 illustrates several reference frames which are relevant to the position estimation problem. Each of these frames represent a coordinate system which is rigidly attached to one of the indicated bodies. The world frame is attached to a fixed point within the facility and is used as the origin for all world relative databases. The shuttle frame is attached to a fixed point on the shuttle and is used as the origin for all shuttle relative databases (i.e.: tile database). The tile frames are actually multiple frames attached to each tile on the shuttle. These frames may be useful for recording local tile information, such as hole centroid locations. The tile region frames are also multiple frames which define groups of shuttle tiles. A tile region is a small number of tiles (roughly 5-50) which are defined relative to a common reference frame. The rationale for defining tile regions is that small tile databases can be built with much smaller position uncertainties than a single large database. The mobile base frame is affixed to a point on the mobile base structure. The manipulator base frame is attached to the base of the manipulator and is the point from which kinematic control of the end effector is derived. The end effector frame is attached to the last link of

the manipulator and is used to specify tool locations. The camera frame is attached to a reference point on the camera.

Figure 7-2 Global position estimation

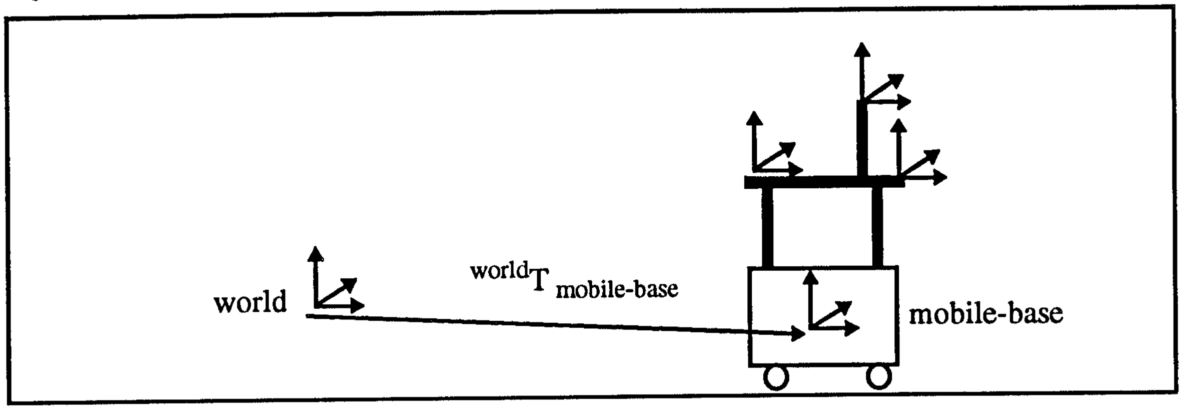

The global position estimation problem, as depicted in Figure 7-2, is to determine a coarse position estimate for the mobile base in the world reference frame, or more formally, ${}^{world}T_{mobile\text{-}base}$.[1] An alternate formulation of the problem is to estimate the position of the mobile base in the shuttle reference frame. We defer discussion of this alternate formulation until section 7.2. The global position estimate will be used as feedback to the mobile base for the purposes of navigating along pre-planned trajectories. Accuracy requirements for global position estimation are specified by two primary factors. First is the need to follow pre-planned trajectories accurately enough to avoid collisions with fixed, known obstacles in the environment. Second is the requirement that global position estimation must provide accurate enough data to position the mobile base within the tolerances required for local position estimation to operate. We are currently evaluating each of these requirements in order to determine the accuracy which will be required of global position estimation.

We have identified at least one global position estimation system which is capable of providing accuracies on the order of a centimeter. For the purposes of positioning the robot's end effector to rewaterproof and inspect the tiles, however, it will be necessary to perform a more accurate position measurement. While the global positioning problem is concerned with locating the mobile base in the world reference frame, the local positioning problem is concerned with locating the manipulator's end effector relative to either a single shuttle tile or a group of tiles. Currently, there are two basic approaches to the local position estimation problem which are under consideration. Both of these approaches use video images of the shuttle tiles to derive the high accuracy position data required.

1. We assume that the global position estimation system is mounted on the mobile base, and not on a point further up the kinematic chain (i.e. on top of the gantry). This assumption does not affect the generality of the discussion.

Figure 7-3 Local position estimation

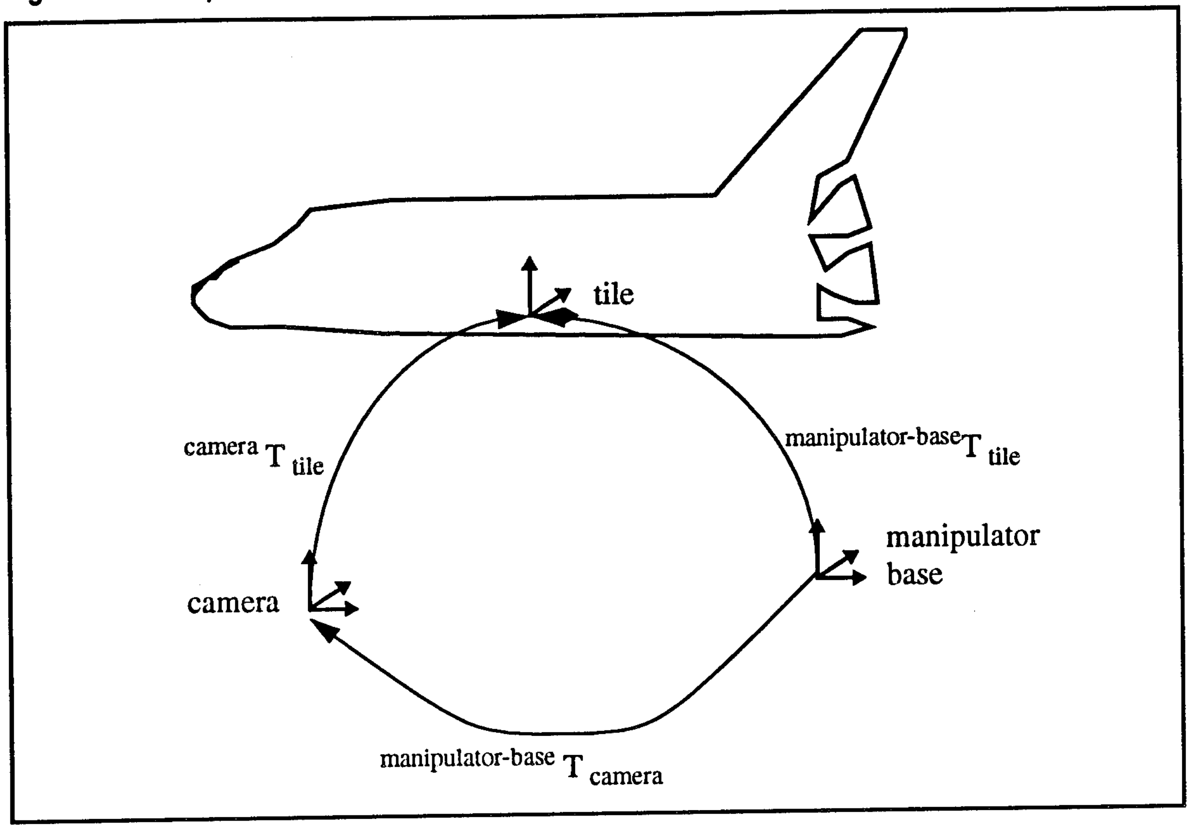

The first approach is illustrated in Figure 7-3. The goal of local position estimation is to determine the location of a tile relative to the manipulator base, ${}^{\text{manipulator-base}}T_{\text{tile}}$. Since this transformation can not be measured directly, it is necessary to infer it based upon the two other transformations shown in the figure. This can be seen in the following equation:

$$ {}^{\text{manipulator-base}}T_{\text{tile}} = {}^{\text{manipulator-base}}T_{\text{camera}} \cdot {}^{\text{camera}}T_{\text{tile}} \qquad \textbf{Eq. 6-1} $$

The term on the left hand side is the unknown transformation which we are trying to identify for the purposes of local position estimation. The first term on the right hand side is the location of the camera specified in the manipulator base reference frame. The measurement of this transformation is often referred to as *camera calibration*. Under ideal circumstances, ${}^{\text{manipulator-base}}T_{\text{camera}}$ will remain constant, and therefore it is only necessary to perform the measurement once. In practice, however, small variations in this transformation require camera calibration to be repeated periodically. The technology for performing camera calibration is well understood[1], and the resulting accuracies will likely be well within acceptable tolerances. The second term on the right hand side of Eq. 6-1 is

1. Tsai, R.Y., "A Versatile Camera Calibration Technique for High-Accuracy 3D Machine Vision Metrology Using Off-the-Shelf TV Cameras and Lenses", IEEE Journal of Robotics and Automation, Vol. RA-3, No. 4, August 1987

the result of the sensing operation and specifies the location of a tile in the camera reference frame. We are currently investigating an approach for performing this tile localization which matches tile features extracted from an image to corresponding features in a tile model. Details of the approach are discussed in section 7.3

For a variety of reasons, it may be desirable to use information from a *group* of tiles to perform the tile localization discussed above. As we suggested earlier, a tile ***region*** is a small group of tiles which is referenced to a common local origin. Tile region databases could be constructed using data from the main tile database. However, rather than referencing all shuttle tiles to a single origin, each tile region would have its own local origin. Except for this change in reference frame, the data in the region databases would be identical to the data in the main database. The rationale for this approach is based upon an analysis of position errors in the main tile database.[1] Based on this analysis, we have determined that tile position errors in the main database tend to be highly dependent upon the region in which the tile is located. Thus, two adjacent tiles in the database are likely to have highly correlated position errors with respect to the common reference frame. For the purposes of local position estimation, however, we are only concerned with the location of one tile with respect to another over a small region of tiles. Thus, we can reduce the positioning errors discussed above by constructing local region databases.

The local position estimation scheme of Eq. 6-1 can be modified to use tile regions. Rather than matching image features from a single tile to the model, we may decide to match image features from several tiles. In terms of Eq. 6-1, the only change would be that the measurements are with respect to the origin of a tile *region,* as seen in the following equation:

$$^{\text{manipulator-base}}T_{\text{region}} = {}^{\text{manipulator-base}}T_{\text{camera}} \cdot {}^{\text{camera}}T_{\text{region}} \qquad \textbf{Eq. 6-2}$$

There are several advantages of this approach. First, it provides a larger number of tile features for the purposes of matching the image to the model thus increasing the robustness of the correspondence. Second, it reduces the number of sensing operations required since a group of tiles are being localized simultaneously. By parallelizing the tile localization process, it is no longer necessary to individually locate every tile before the tile is processed. A disadvantage of this approach results from the decrease in spatial resolution required to image several tiles at once. This decrease in resolution may have an adverse effect on the accuracy of the position estimate.

1. See Appendix L "Tile Centroid Measurements" of the Orbiter TPS Automation Study Final Report.

Figure 7-4 Derivation of end effector control

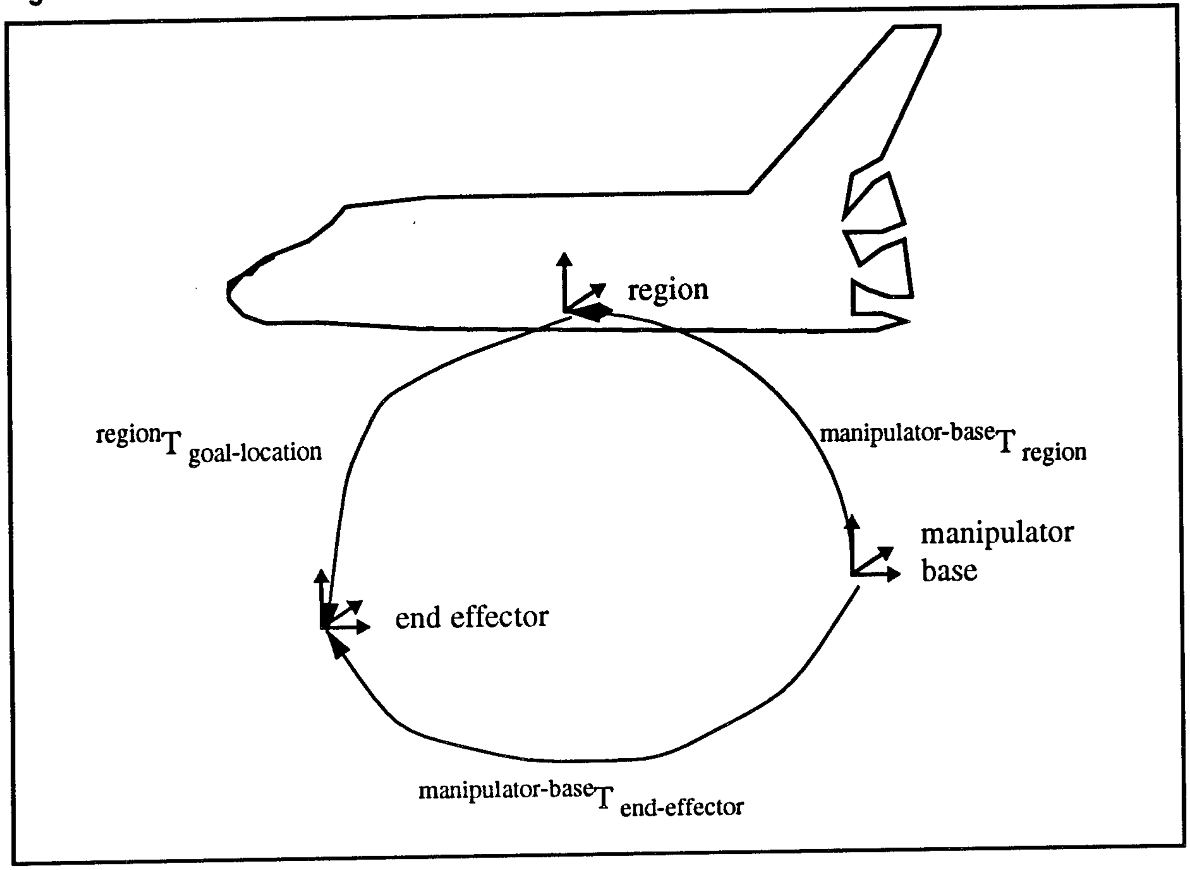

Based upon the framework developed above, a possible scenario for operation of the TPS robot is as follows. Using data from the tile database and the current global position estimate, a path planner would generate a mobile base trajectory to a specified tile region. The mobile base would execute this trajectory using global position estimates to ensure that the path is being properly tracked. Once the goal location is reached, local position estimation would take one or more images for the purposes of calculating ${}^{manipulator\text{-}base}T_{region}$. Thus, it would only be necessary to measure this transformation once per tile region. At this point, kinematic control of the manipulator would be derived as shown in Figure 7-4. The goal of this process is to determine the end effector transformation, ${}^{manipulator\text{-}base}T_{end\text{-}effector}$, required to position the end effector in a specified location relative to the tile region reference frame. This is seen below in Eq. 6-3:

$$ {}^{manipulator\text{-}base}T_{end\text{-}effector} = {}^{manipulator\text{-}base}T_{region} \cdot {}^{region}T_{goal\text{-}location} \quad \text{Eq. 6-3} $$

The left hand side of this equation is the commanded end effector location which is being derived. The first term on the right hand side is the local position estimate derived in Eq. 6-2. The second term on the right hand side is the end effector *goal location* which specifies the *desired* end effector position relative to a tile region. This transformation,

${}^{region}T_{goal\text{-}location}$, is generated by a manipulation planner which uses tile database information and knowledge of its current task goals to select the desired end effector location. Once ${}^{manipulator\text{-}base}T_{end\text{-}effector}$ has been calculated using Eq. 6-3, the end effector can be moved into position, and the tile can be serviced. Every tile within the specified tile region would be serviced in this manner. For each tile, the manipulation planner would generate a (possibly precomputed) transformation, ${}^{region}T_{goal\text{-}location}$, and the end effector location would be computed using Eq. 6-3. It is important to note that the local position estimate, ${}^{manipulator\text{-}base}T_{region}$ is only calculated once per tile region.

In the mode of operation described above, it is not necessary to use information from every tile within a region in order to generate the local position estimate for the region. In fact, it is expected that information from only a small number of tiles will be required to generate the local position estimate for the entire region. This feature is especially useful in situations where tile image features are not easily found. For example, tiles in which robust image features could not be extracted due to outgassing patterns could be handled in this manner. Similarly, tiles which are visually occluded by a nearby workstand could also be handled with this technique. In this mode of operation, manipulator trajectories would be planned using information from the tile database and the local position estimate generated using adjacent tiles.

In order for the local position estimation approach to be used without additional sensing, the resulting accuracies must be within acceptable limits. There are many factors which affect this accuracy. In each of the above equations, there will be uncertainties associated with the information on the right hand sides. When the elements of the right hand sides are combined, the associated uncertainties will propagate to each of the left hand sides.[1] The magnitudes of these uncertainties, as well as the effects of the propagation will determine whether or not this local position estimation approach is successful. In particular, the uncertainties associated with the following sources of information will need to be assessed:

Tile databases

- location of rewaterproofing hole with respect to tile vertices
- location of tile vertices relative to a tile region of fixed size
- location of tile vertices relative to the shuttle frame

Manipulator

- kinematic accuracy over a given operating region

Perception

- transformation between the camera and the manipulator base
- transformation between the camera and a tile region

As we have noted, a primary advantage of the above local position estimation approach is that external sensing operations are minimized since ${}^{manipulator\text{-}base}T_{region}$ is calculated only once per tile region. Thus, it is advantageous to make tile regions as large as possible.

1. Smith, R., Cheeseman, P., "On the Representation and Estimation of Spatial Uncertainty", International Journal of Robotics Research, Vol. 5, No. 4, 1987

Unfortunately, a variety of factors limit the size of tile regions, including: accuracy of tile database information, maximum standoff distance, required image resolution, and manipulator accuracy. We are currently studying each of these issues in order to estimate tile region size. In the worse case scenario, the tile region would need to be shrunk to a single tile in order to realize required accuracies. In the best case scenario, a tile region would span an entire X-Y table workspace, and calibration would only be performed on a portion of the workspace. It is expected that selection of an appropriate tile region size will not occur until hardware has been built and empirical studies can be conducted.

In the event that the above local position estimation scheme does not provide sufficient accuracy, an additional scheme is currently being evaluated. While the above approach can be classified as a static "look-and-move" type strategy, the second scheme is based on a dynamic visual tracking approach. In this approach, the location of the rewaterproofing hole would be sensed, and this information would be incorporated into a high speed servoing loop. Since the dynamic servoing approach would only operate over a small region, it would probably be initialized using the local position estimation approach discussed above. One main difference between these two approaches lies in the accuracy requirements. Since the control loop would be closed at a much lower level in the dynamic tracking approach, the reliance upon the "feed-forward" information sources (tile database and manipulator accuracy) are not as severe. Some details of this local positioning approach are discussed in section 7.3.

Additional study is required of many of the issues outlined in this section. The remaining sections in this chapter discuss some details of global position estimation, local position estimation, and obstacle detection. While considerable thought has gone into the ideas presented in these sections, empirical testing will ultimately be required in order to determine the viability of many of these ideas.

7.2 Global Position Estimation

7.2.1 System Comparison

The following list provides an overview of systems available for global position estimation. Advantages and disadvantages of each system are discussed.

Beacons

These systems are based on triangulation using microwaves or infrared. Several transmitters are mounted in the facility. A receiver is mounted on the robot.

+ Accurate positioning (m - cm range)
  Off the shelf systems available
  Proven technology in marine systems

- Interference with other equipment in KSC
  Interference from metallic objects (scaffolds)

GEC bar code reader

This system uses a 1D laser to perform a 360 degree scan of the environment in a horizontal plane. Bar coded, retro-reflective targets are mounted at various points in the world. The system reads these bar codes and uses stored target position information to compute its position using triangulation.

+ Accurate (cm range)
  Range up to 15 m from a given target
  Uses multiple targets for redundancy
  Off the shelf system available

- Targets may be occluded
  Moderately expensive

Laser range finder

A laser scanner is used to measure the range from the robot to distinct fixed features like landing gear or jack stands. Position is computed by triangulation.

+ Accurate (cm range)
  No artificial targets required

- Ambiguity among features
  Features may be occluded.
  No known commercial systems

Camera

A camera can be used to detect artificial or natural features in the environment.[1] These features may be either active or passive. Positioning is achieved either by using a wide field of view and tracking distinct features, or by using a telephoto view and counting transitions between tiles from a known initial position.

+ Inexpensive

- No known commercial systems
  Natural features may be ambiguous.
  Development could be difficult
  Recovery difficult if position is lost in tile counting approach.

Dead Reckoning

Using gyros, accelerometers, and wheel encoders a coarse position estimate can be derived. Encoders will provide a reasonable estimate of distance traveled. Gyros will provide accurate heading information.

+ Simple
  Inexpensive

- Error accumulation with time.

Floor Based Position Estimation

An optical sensor may be used to detect painted floor patterns, or alternately a magnetic/inductive sensor may be used to detect metal pins embedded in the floor. Patterns could be installed in a grid pattern, and dead reckoning could be employed between grid points.

+ Inexpensive
  Proven technology.

- Modification to KSC required.
  Paint may get erased.
  Accurate global position available only at discrete points.

7.2.2 Proposed System

At the current time, the leading candidate for global position estimation is a triangulation based bar code laser scanner system. Sensors for dead reckoning will also be used as an additional source of position information.

System Components

The system described here was originally developed by GEC and is currently marketed by Caterpillar. A very similar system was recently also introduced by Denning Robotics. Both systems consist of a base mounted laser scanner which sweeps 360° in a horizontal plane. Retroreflective bar coded targets are mounted in the environment, and have to be surveyed

1. Natural features are those which occur naturally in the environment (e.g. jackstands, shuttle tiles). Artificial features are man-made targets which have been introduced into the environment for the purpose of position estimation.

accurately during the installation process. The scanner measures the azimuth angle at which it sees a target and the position is computed by triangulation using a minimum of two targets. Since targets are coded, each target can be unambiguously distinguished

Figure 7-5 Bar code scanner configuration.

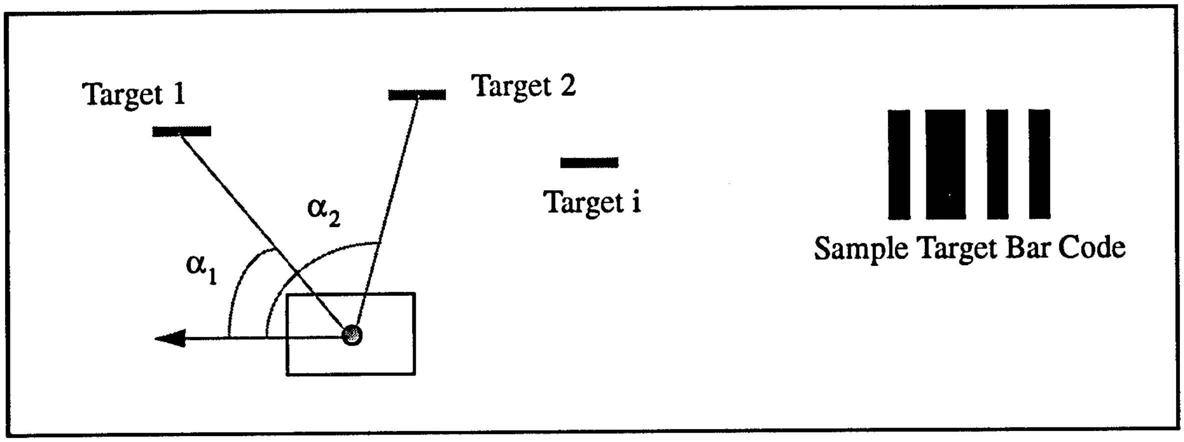

Sources of error in this system are:

- Uncertainty in target location
- Divergence of the laser beam
- Angular resolution of scanner

Information from dead reckoning and target detection can be combined by a navigation module in order to increase the accuracy and reliability of the system. The navigation module outputs current vehicle position and orientation. One advantage of this approach is that information from either dead reckoning or bar code scanning can be used stand alone.

Figure 7-6 Navigation module

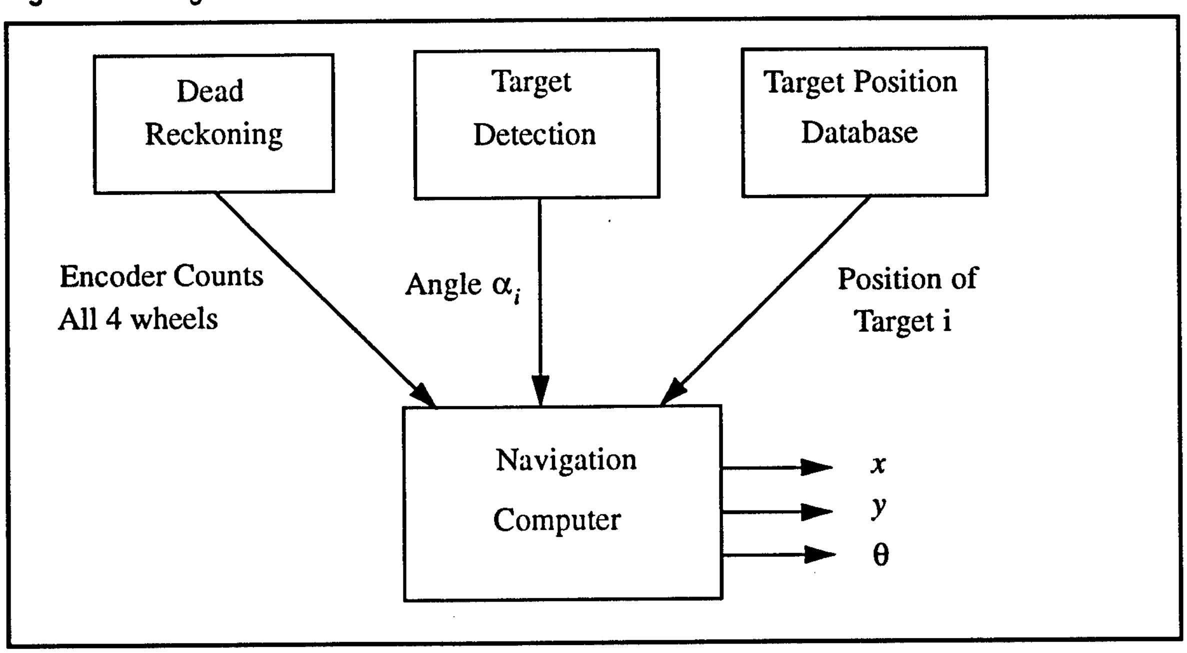

The combination of dead reckoning and target detection information can be achieved using several approaches which differ in complexity and accuracy. In the simplest approach the scanner needs only one target. The angle to the single target is measured from two different positions, while dead reckoning provides the distance travelled between the two positions. Using this information, the position and orientation of the vehicle can be calculated. Since the information provided by dead reckoning is only the relative position between successive positions, global error accumulation is avoided.

For the proposed configuration, however, we assume that there will always be at least two targets in view. Hence we could employ a more accurate method. Each scan from a fixed position provides a position estimate which is accurate to within the scanner's limits. Dead reckoning is used between scans to update the vehicle position and discarded when a position is available from the scanner. Vehicle motions during a scan should be of no concern because of fairly slow base moves. If it proves to be necessary, dead reckoning can be used to compensate for vehicle motion during a scan. Again, global error accumulation due to dead reckoning is avoided since the position estimate is reset after each scan.

The third approach uses a Kalman Filter for combining information sources to predict the current vehicle position. Assuming that reliable error models are available, the accuracy of the position estimate should be significantly better using this approach.

Figure 7-7 Kalman filter approach to navigation

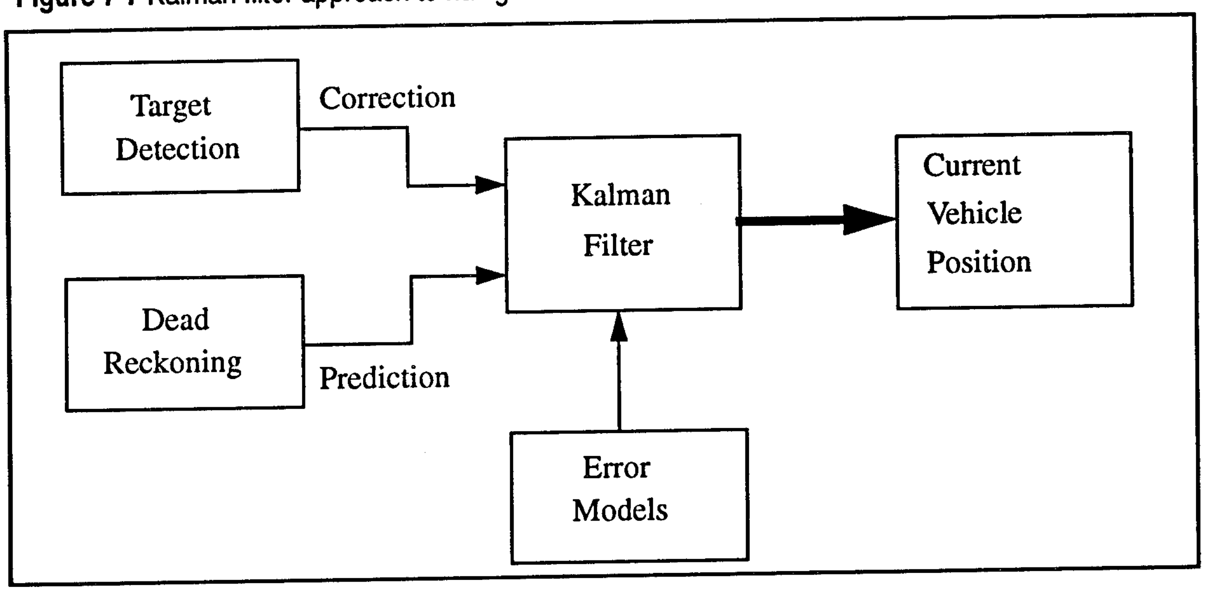

Technical Specifications

Following are some technical details of the GEC bar code scanner:

- Angular resolution: 1024 encoder counts, multiplied by 16 in software to increase the resolution. In practice this leads to an angular resolution of approximately 0.05°
- Position accuracy when using the Kalman approach described above: ~ 1 cm.

- Laser: Class 1, eye safe, weak intensity so that only highly reflective surfaces will be seen by the scanner.
- Range: 15 m with retroreflective targets. As discussed below, the Denning system can increase its range by using active targets.
- Footprint of laser beam at 15 m: ∅10 mm
- Output from scanner head (RS 422 interface, 0-5 V level):
  - **a)** Marker (1 per rev.)
  - **b)** Counts (0 - 1023 from encoder)
  - **c)** Binary code from target

The scanner revolves at 2 rev. per sec. Sectors of the scan in which a potential target can appear are estimated. By taking measurements only within these sectors, noise and spurious returns from false targets are reduced. By using a more powerful laser diode it would be possible to increase the range and still keep the system eye safe. The DENNING system may also use active targets which can be deployed in addition to the passive retroreflective targets. The active targets operate by detecting the sweeping scanner beam which triggers the generation of a pulse sequence from a laser diode. From the scanning head's perspective, there is no difference between the signal emitted by the active target and the one reflected by the passive target. Therefore the scanner does not need to distinguish between active or passive targets. For active targets, the attenuation of the signal is proportional to $distance^2$ as opposed to $distance^4$ for the passive ones. The advantage of using active targets is thus increased range and noise immunity.

Target and Scanner Placement

The targets used for the GEC sensor can be mounted either directly on the shuttle, or on fixed structures within the facility. As we noted above, the location of the targets must be known with a high degree of precision. For this reason, an advantage of facility mounted targets is that they can be mounted once, surveyed, and then left in place. Shuttle mounted targets, however, must be remounted and possibly resurveyed for each shuttle flow. Thus, if shuttle mounted targets are used, it will be very important to have a simple, fast, and temporary method for mounting targets at fixed points on the shuttle. In addition, target surveying would need to be performed quickly and accurately. Shuttle target mounting is further complicated due to the sparsity of suitable target attachment locations.

The maximum dimensions of the work area of the robot beneath the shuttle is ~34 m by ~25 m. When mounting targets, as few changes as possible should be made in the OPF. The primary candidates for facility based target mounting points are therefore the columns supporting the work platforms around the shuttle. In particular, those columns which are closest to the shuttle and are unobstructed by other structures in the facility would provide the best mounting points (see Figure 7-8). The height at which targets can be mounted depends on:

- The height of the scanner on the robot (> 0.5 m and < 2.7 m)
- Considerations of eye safety, i.e. average human height (> 1.8 m)

- Height of shuttle bottom, likely obstructions at certain heights (< 2.7 m)

The optimum height for mounting targets would thus be around 2.1 m. The vertical extension of the targets is not restricted, but is around 1 m in the GEC system.

Based upon the above constraints the following columns could be used for mounting facility based targets (Refer to Floor Plan of OPF):

E2, E12, F2, F12, G2, G12, H2A, H11A, I4, I10, J5, J9, L5B, L8E, O5E, O8B, Q6, Q8.

It may not be necessary to mount targets on all of these columns. In addition to the columns, the forward and aft body jackstands could be used for mounting shuttle based targets.

Figure 7-8 Facility based target mounting locations

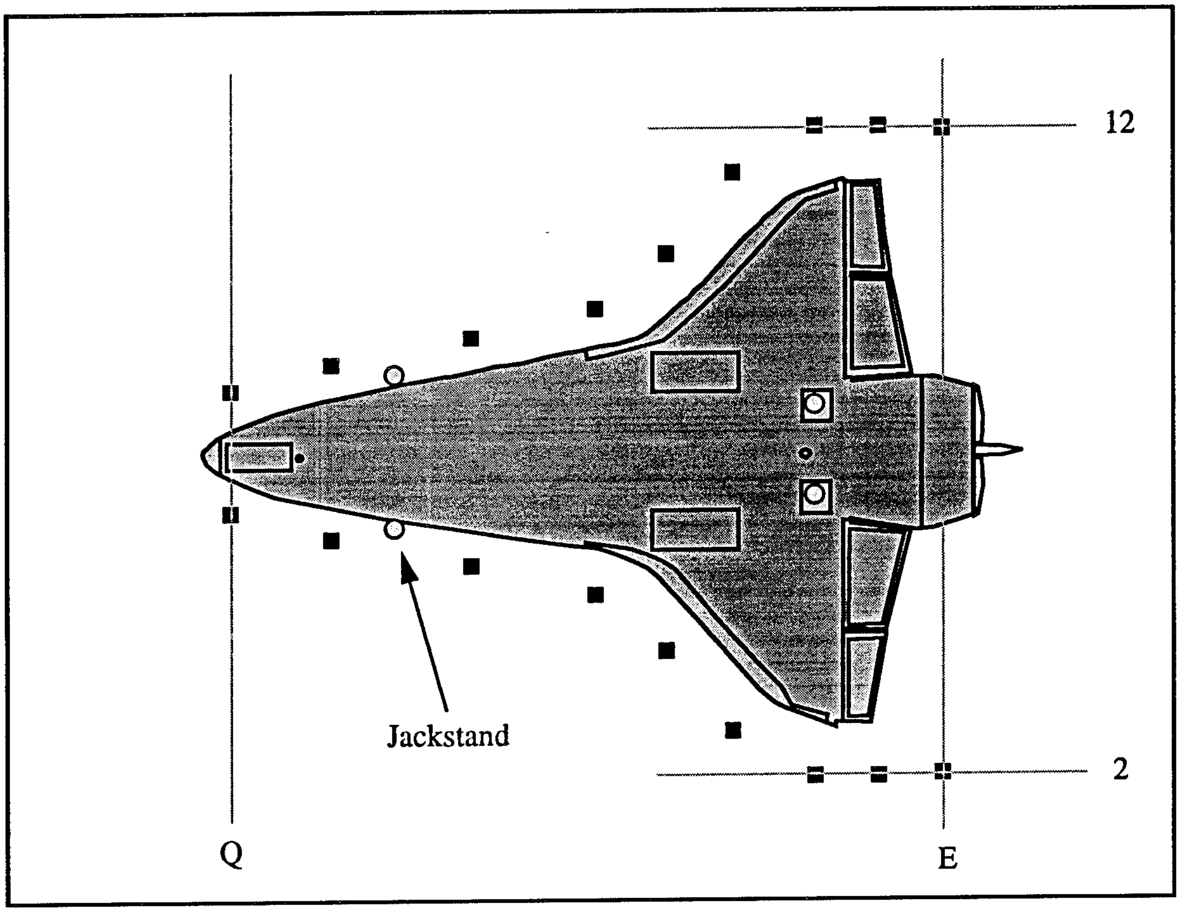

There are several possible mounting locations for the scanner on the robot. It could be mounted in the middle of the base inside the rectangle formed by the four vertical gantry columns at a height of 2.1 m. In this case, problems arise due to interference with the vertical movement of the x-y table, and obstruction of an 82° sector by the vertical columns.

Figure 7-9 Scanner placement.

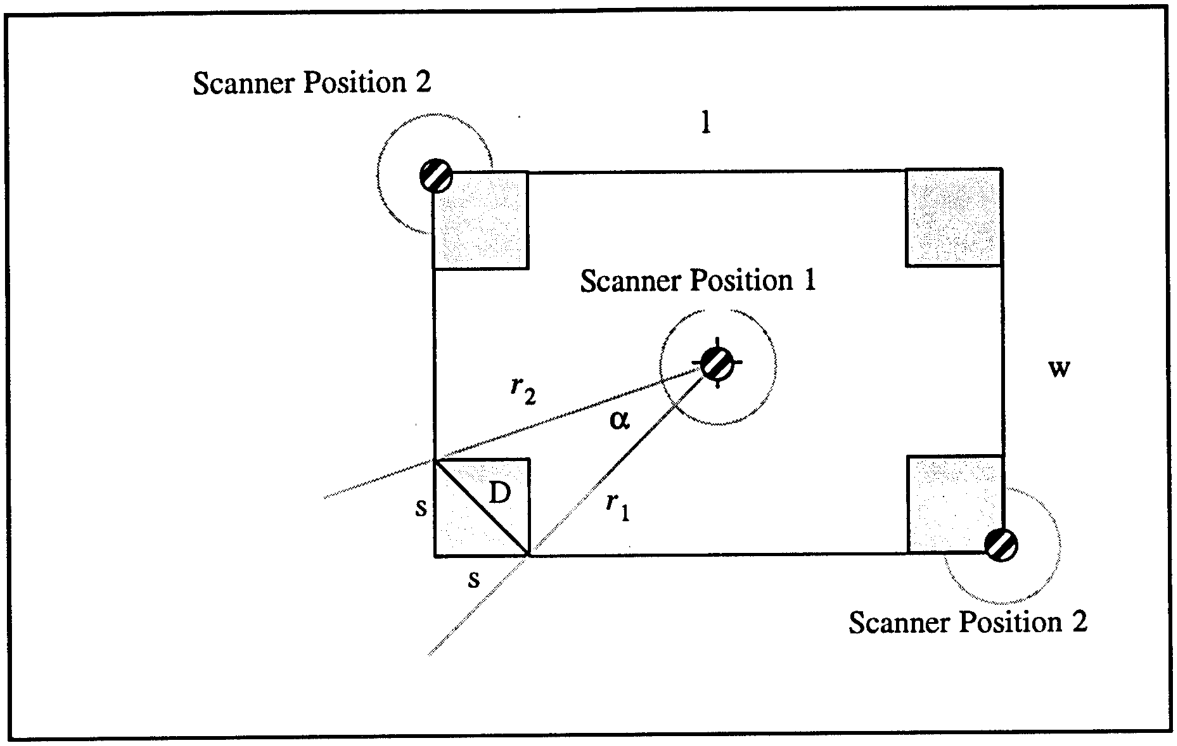

The obscured angle Θ can be calculated by the following formulae:

$$\cos\alpha = \frac{r_1^2 + r_2^2 - D^2}{2r_1r_2} \quad \text{Eq. 7-1}$$

$$r_1 = \frac{1}{2}\sqrt{w^2 + (l-2s)^2} \quad \text{Eq. 7-2}$$

$$r_2 = \frac{1}{2}\sqrt{l^2 + (w-2s)^2} \quad \text{Eq. 7-3}$$

Assuming base dimensions $l \times w = 3m \times 2.1m$ and $D = 0.57m$ ($s = 40.64cm$),we get $\Theta = 4\alpha = 4 \cdot 20.5° = 82°$ for Scanner Position 1.

Another possibility is to mount two scanners on diagonally opposite corners of the mobile base. Readings from both scanners could be combined or only the scanner with the better target selection could be used. Each scanner covers a 270° sector, unobstructed by the vehicle. From past experience with the system at Caterpillar, it may be sufficient to deploy only one scanner in Scanner Position 2 and still attain the desired accuracy. For reasons explained in the previous paragraph, the scanner(s) would be mounted at a height around 2.1 m. For initial deployment, the robot should not exceed a height of 1.83 m. Thus, the scanner would need to be mounted on a telescopic column that would be raised to the scanner's operating height during deployment of the robot. The scanner head should also

be gimbal mounted. This precaution will keep the laser beam in a horizontal plane and thus prevent it from missing a target because of an uneven floor or the robot driving over an obstacle.

Reference Frames

Regardless of where the global positioning targets are mounted, it will be necessary to measure the location of the shuttle within the facility, ${}^{world}T_{shuttle}$, each time the shuttle is parked in the OPF. This transformation can vary by as much as several cetimeters each time the shuttle is parked. The need for this transformation arises due to the existence of databases referenced to both the world and shuttle frames. The facility database, which indicates the current configuration of the OPF, will be world referenced. The tile database, however, will be shuttle referenced. In order to integrate the information from both of these databases, it is necessary to know the relationship between the corresponding reference frames. This relationship is given by ${}^{world}T_{shuttle}$.

Several methods for measuring ${}^{world}T_{shuttle}$ have been studied. The simplest method is to manually survey the shuttle position relative to fixed landmarks in the facility. If this approach could be performed quickly and accurately it might provide an adequate solution. Several schemes for automatically measuring this transformation have also been studied. One approach would be to mount secondary targets at known locations with respect to the shuttle (i.e.: on jackstands which are rigidly attached to the shuttle). Since the locations of the primary targets in the OPF are known with respect to the world, and the location of the secondary targets are known with respect to the shuttle, then measuring both sets of targets from the mobile base will allow the computation of ${}^{world}T_{shuttle}$.

Similarly, another technique for measuring ${}^{world}T_{shuttle}$ would utilize the local position estimation approach discussed in section 7.1. The local position estimation system would be used to locate several known points on the shuttle with respect to the mobile base. By combining the vehicle's world referenced global position estimate with the above mentioned shuttle measurements, the desired transformation could again be calculated.

This section has addressed some of the issues related to the global position estimation problem. In the next section, we address the local position estimation problem.

7.3 Local Position Estimation

This section addresses some details of local position estimation. In particular, we concentrate on two approaches for finding the transformation ${}^{camera}T_{region}$ which was defined in section 7.1.[1] One approach utilizes information from the tile database in order to calculate this transformation, while the other relies only on features from the image

In section 7.1., we assumed that the sensor used to measure the above transformation is a camera. In general, it is important to note that there are several sensor types which could be used to provide an adequate measurement of ${}^{camera}T_{region}$. In the remainder of this section, we concentrate primarily on conventional black and white vision schemes (hence the term "camera"), however investigation of other methods is a part of our continuing study.

Another assumption made in section 7.1. is that the camera will be attached to a point on the manipulator base. In this section we suggest that there are several structures to which the camera can be attached, including: end effector, mobile base, X-Y table frame, or manipulator base. Implications of mounting the sensor in each of these locations will be discussed.

7.3.1 Model Based Vision for Local Position Estimation

In a typical black and white image of a group of shuttle tiles there are several features which are relevant for the purposes of local position estimation. These features include: edges between adjacent tiles, rewaterproofing hole markers (i.e. white painted circles), and tile identification numbers (white painted characters). Each of these features appears with a different degree of visibility/detectability. In some tile regions, certain tile features may be completely missing. Nevertheless, these features provide good "landmarks" for local positioning. In particular, methods for extracting tile edges (i.e. lines) and hole markers (i.e. circles) are fast and well understood.

The transformation ${}^{camera}T_{region}$ is, in general, a 6 degree of freedom transformation. By making some simplifications, however, the dimensionality of this transformation can be reduced to 3. The main simplification is to assume that the camera can always be aligned so that its optical axis is normal to the tile surface. This alignment would require range sensors for measuring the surface, and a pan-tilt mechanism for aligning the camera.[2] When this alignment condition is satisfied, a weak perspective projection can be assumed. Under this assumption, range variations within the scene (i.e.: variations along the tile surface) are negligible with respect to the viewing distance. Therefore, perspective distortion is eliminated except for a scale factor which is uniform over the scene. Thus, finding the transformation, ${}^{camera}T_{region}$, can be reduced to a 2D model based recognition problem. The goal of this type of problem is to determine the position, orientation and scale of a 2D model (i.e. its reference frame) with respect to the sensor reference frame. If the scale is known, then one can roughly determine the distance between the sensor and the tile surface. Conversely, if the distance is known, then the scale can be inferred. By performing an independent distance measurement using range sensors and converting this

1. In this section, we use this transformation to discuss the local position estimation problem. It is important to note, however, that the transformation between camera and tile could also be used without loss of generality.
2. If the camera is mounted on the end effector, an additional mechanism would not be necessary.

distance measurement to scale information, the recognition procedure can be greatly simplified.

The model based local position estimation problem is thus reduced to recovering 4 parameters. The first 3 parameters will be extracted from image information (i.e.: the x and y translational offsets in the plane normal to the optical axis, and the angle of rotation about the optical axis). The 4th parameter will be measured independently using range sensors (i.e: the distance between the tile surface and the image plane). One scheme for finding these parameters can be summarized in the following steps:

1) move the end effector so that the camera's optical axis is aligned normal to the tile surface using range data from several sensors mounted on the end effector;
2) move the camera to a fixed distance from the tile surface;
3) extract primitive image features (i.e. lines, circles);
4) compute model features from features found in step (3) (i.e.: tile vertices, hole marker centroids);
5) compute the transformation between model features stored in the tile database, and model features extracted in step (3).

In our situation, the model is an irregular polygonal grid description of the shuttle tiles which has been pre-compiled into a database. The database will include characteristic features of tiles such as the position of hole centroids, the position of hole marker centroids, and any other relevant information such as tile type or tile identification number.

The first two steps listed above are self-explanatory. In step (3) the image processing scheme should extract edges using a conventional edge detector, and then group these edges into lines (tile edges) and circles (hole markers) using a Hough transform[1]. Assuming that the tile model is stored as a collection of polygon vertices, step (4) should compute intersecting points of the extracted lines and use these points as the measured polygon vertices. Centroids of the circles are also readily computed. In step (5), the model features measured from the image are matched against the database model features, and the transformation is computed.

There are a variety of known approaches for model matching. An important difference among these approaches is their ability to operate on incomplete or uncertain data. In our problem, the model (local tile map) will probably be sufficiently complete and accurate, however the image data may be quite noisy and incomplete. In particular, tile edges and hole markers may not be visible for every tile in the scene due to wear in the marking paint, tile outgassing patterns, imperceptible tile boundaries, etc. We have identified at least one algorithm which is robust with respect to incomplete image data.[2] The philosophy

1. Hough transform does not produce satisfactory results if the number of edge points for a relevant feature is too small. If the magnification/field-of-view is such that the feature (i.e. circle) is distributed over small number of pixels, then it is likely that the contribution to the bins in Hough space will be stronger from the spurious edge points rather than from the feature edge points themselves. For locating hole markers (circle) a template matching is possible, while for tile gaps/edges, more complex alternative (if necessary) is needed.

behind this algorithm is similar to that of the Hough transform[1], and is summarized in the following steps:

- Hypothesize that a pair of model features corresponds to a pair of extracted scene features, and establish a reference frame accordingly.
- Verify correspondence of the remaining features and assign a score to the hypothesis based upon the goodness of correspondence.
- After a sufficient number of hypotheses have been examined, select the most likely correspondence by selecting the one with the highest score. The resulting hypothesis is said to be verified, and the match is found.

This procedure will determine correspondence between model features and image features. Then, the model is "fit" to measured features so that the residual is minimized in the least squares sense. The position of relevant features (i.e.: rewaterproofing hole or hole marker) can be then based upon both image measurements and model descriptions. For features which are not detectable in the image, only model information would be used. In order for this approach to work, however, position uncertainties in the model would need to be within the tolerances required for task completion.

We propose a hierarchical selection of features for model matching. By hierarchical we mean that we will classify features into "levels" and try to match the model using features from one level at the time. If the match is not possible or not good enough, the features from the next level of the hierarchy would be used. The rationale for hierarchically ordering the features is based on following:

- the location of some features is more easily computable than the location of others
- the verification of true/false model match is less computationally intensive if the model is based on certain features[2].

Hole markers belong to the first level since they can be located by simple template matching. In addition, hole markers are printed at more or less random locations with respect to tile edges. Therefore, a polygon formed by several hole markers is expected to be locally unique. Due to this local uniqueness, model fitting error can be used as a measure for determining the correctness of a match; a straightforward thresholding of the model fitting residual (least square error) can be used to decide if a match is correct. Tile edges or vertices are not suitable for this purpose since the pattern of these features may be highly repetitive over some portions of the TPS, resulting in spatial ambiguity. Therefore, tile edges/vertices belong to the next hierarchical level of features[3]. They will be useful when hole markers are not detectable in an image. If tile edges also fail, the next level of

---

2. Y. Lamdan, H. J. Wolfson, Geometric Hashing: A General and Efficient Model-Based Recognition Scheme, IEEE, 1988

1. Recall that the Hough transform can detect lines even if there are numerous points missing along that line.
2. As we mentioned earlier, the model can be described by hole marker positions, or tile vertices and/or edges.
3. In addition to possible spatial confusion using the tile edge/vertex pattern, it is expected that locating tile edges/vertices will be more computationally intensive then the simple template matching applicable to the hole markers. To locate tile edges, one should extract edge pixels, group them into connected lines, and then fit a line to them. This is expected to take longer then locating hole markers.

features would be recognition of the tile ID number. The number of features included in the hierarchy will depend on the availability of computational resources, availability of processing time, and the importance of servicing tiles whose features are difficult to detect.

It is important to note that the first hypothesis for model matching will be based on the output of global position estimation. If this position estimate has large errors, the match will fail. Most of the time we expect the initial correspondence hypothesis will be correct, and will be verified by the first level of features (hole markers) using the simple least squares error thresholding. The primary purpose of the hierarchical feature scheme is to provide an efficient and inexpensive image processing and model matching technique for detecting false model matches. It will provide a safety mechanism for detecting crude errors caused by global positioning system failure.

As we suggested in section 7.1, the success of model matching for local position estimation depends upon the magnitude of errors induced by the various components of the system. The sources of these errors include uncertainty in the tile model, uncertainty in the sensing operation, and uncertainty in manipulator motions. A significant amount of additional study will be required in order to assess the performance of this model based position estimation approach. In the event that this approach is not sufficient to perform the required tile operations, we are investigating a second, complementary scheme which could be built on top of the model based approach.

7.3.2 Visual Servoing Approach to Local Positioning

The visual servoing approach to local position estimation differs from the previously described model based approach in several respects. First, the visual servoing approach would not utilize any information from the tile database, but rather would operate only using image features. Second, while the model based approach can be classified as a static "look-and-move" type strategy, the visual servoing approach would utilize a closed loop servo in order to perform the required positioning task. Third, the region of operation of the visual servoing approach would be limited to a small area near the feature of interest. Thus, it is important that this approach be "bootstrapped" using the model based approach.

In the remainder of this section we assume that the model based approach will provide sufficient accuracy for all tile operations with the exception of the rewaterproofing task. Thus, the primary purpose of the visual servoing approach is to accurately locate the rewaterproofing hole.

In order to locate the rewaterproofing hole, we propose to use a camera positioned very near the tip of the rewaterproofing tool. A conceptual arrangement of the sensor and the required illumination is shown in Figure 7-10. We assume that the camera magnification is adjusted so that the rewaterproofing hole fills most of the field of view. When the hole is illuminated from certain directions, the hole itself will appear dark relative to the surrounding tile surface. There are numerous approaches to tracking parametric contours such as circles and ellipses. One such scheme which has been demonstrated at CMU is based upon a neural net architecture[1]. In this approach, the image is sampled at a coarse resolution (i.e. 30 by 30), and the resulting image is presented as the input layer to the

1. See work of Dean Pomerleau related to the Self-Mobile Space-Manipulator at Carnegie Mellon.

neural net. The net is trained to output (x, y) position corrections (i.e.: servoing errors), which are used to servo the tool position. An alternative approach is to have a set of templates (filter masks) with corresponding (x, y) corrections designed in advanced. The input image is correlated with each of these masks, and the mask and (x, y) pair which result in the highest correlation value are used to update the tool position[1]. Both of these approaches have been successfully demonstrated in Carnegie Mellon projects, one of which was a hole tracking task very similar to the problem considered here. The advantages of these schemes are reflected in fast operation, and robustness to noise, scene texture and image quality.

Figure 7-10 Camera and illumination layout for visual servo based positioning.

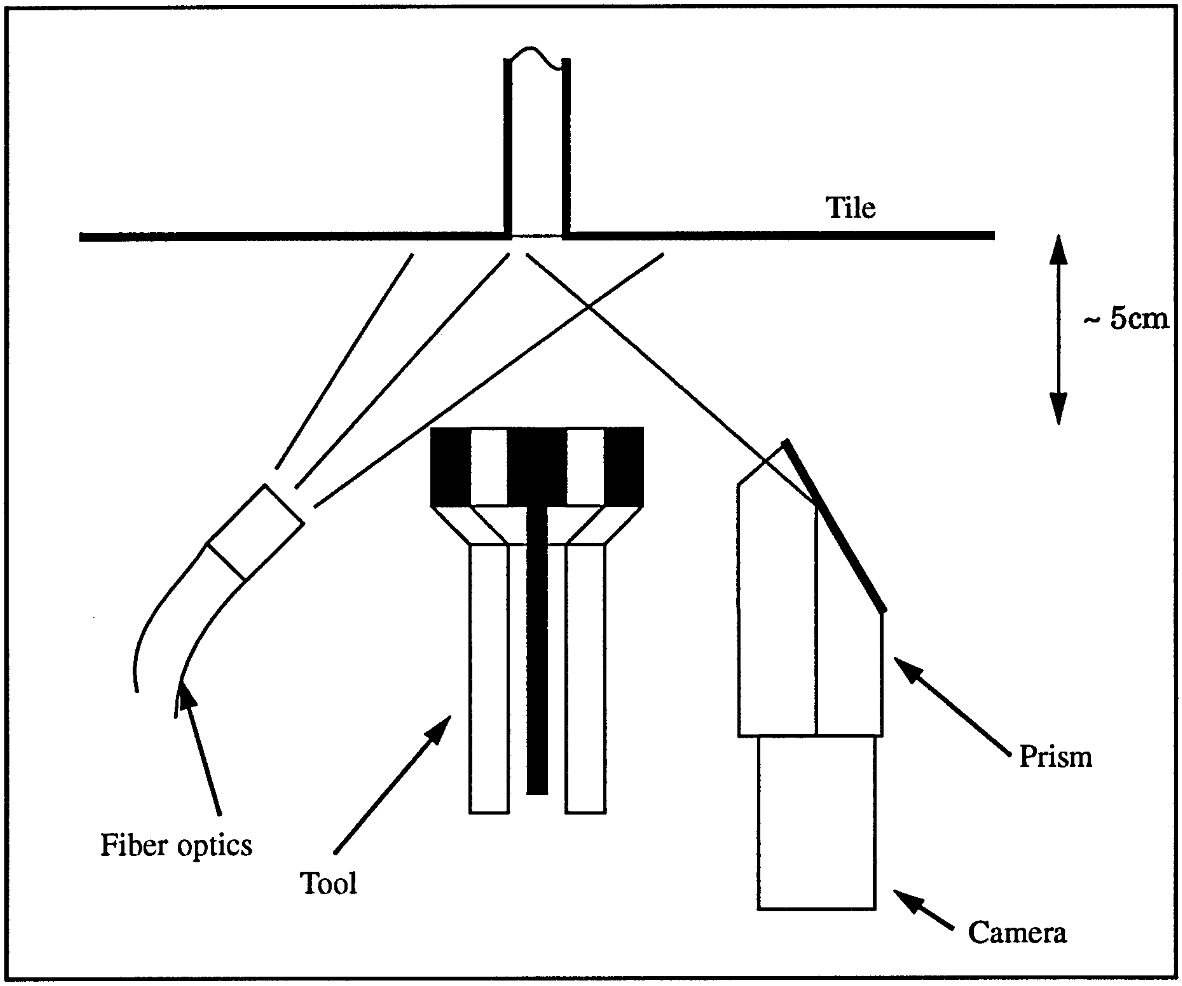

7.3.3 Camera Positioning Issues

This section addresses issues relating to the positioning of the camera which will be used for local position estimation. It is almost certain that the camera used for inspection will be mounted on the manipulator's end effector.

Issues concerning sensor placement for local position estimation include:

1. Note that this is a single point correlation since the size of the image and filter are equal.

1) **Required field-of-view/stand-off-distance.** The field-of-view of the camera determines the number of tiles in a single image. Several tiles in a single image are desirable for two reasons:

   a) More "landmarks" in the field-of-view result in a more robust model matching/fitting, and hence a more accurate feature position estimation.

   b) Using data derived from a single image, several tiles can be serviced. The image processing time per move is the time required for processing one image divided by the number of tiles which can be serviced using the position estimate from this image.

Based on these observations, we expect that the required number of tiles within a single camera image must be greater than four.

2) **Required adjustable orientation of the camera.** As we mentioned earlier, in order to assume a weak perspective projection between the scene and the image (and thus reduce the problem to the 2 dimensional case) the camera must be positioned along the shuttle's local surface normal. This requirement suggests that the manipulator would be a good positioning mechanism for the camera. Other placement alternatives such as on the gantry mechanism or the x-y platform would require an independent orientation adjustment mechanism.

3) **Affect on the planning strategy.** In the present planning strategy, no pipelining of operations is assumed. I.e. acquiring and processing images does not overlap in time with servicing of the tiles. Therefore, the possibility of mounting the camera on the manipulator is permissible. If time efficiency must be improved by pipelining, however, other alternatives for camera placement must be employed. For the system to accommodate pipelining of data acquisition and servicing, the camera has to look "ahead" of the manipulator.

The above requirements are somewhat contradictory: it is hard to satisfy all of them simultaneously for the given mechanical configuration. At this point, it is appealing to mount the camera on the end effector, since the manipulator mechanism could be used for camera positioning. In addition, the camera could be positioned to view all tile sections that are accessible to the end effector itself. On the other hand, the following questions remain:

- Can a sufficiently large field-of-view can be achieved using standard camera lenses when the camera is mounted on the end effector? To illustrate this point, consider the gantry in its low position (1.86m) servicing the lowest portion of the TPS. In this case, the maximum stand-off distance of ~70cm is achieved when the end effector is in its lowest position (z=0). If a 6mm lens and a 1 x 1 cm CCD array are used, the field-of-view is about 30cm square (roughly 4 tiles in a 2x2 grid). If a 3x3 cm CCD is used, then a 6x6 tile grid will be in the camera's field-of-view. However, for the larger CCD optical distortion on the boundary of the image due to aberration may be a problem.

- How much time overhead will be introduced due to the positioning requirement?[1] This issue relates to the portion of the tile servicing cycle required to adequately position the camera. This time can be significant since the manipulator must assume a low vertical (z) position for the purpose of image acquisition, and then return to a high vertical position to accomplish the tile servicing task.

There are a few alternatives for camera placement:

- X-Y platform (manipulator base)
- Several points on the gantry

In either case, an independent 2 degree-of-freedom positioning mechanism would be required. If the camera is positioned on the x-y platform, it is possible that the manipulator would obstruct a significant portion of the field-of-view (unless it is in a low z position). If the camera were mounted on the gantry, most of the waterproofing operation would be open-loop, i.e. based on tile map rather then on "seeing" each feature (hole) first.

At early stages of the project we considered some other possible solutions to sensor placement. One possibility is to scan the entire workspace once per base move. This would be done after the base has been positioned using global position estimate, and could use a sweeping linear CCD array mounted on the x-y translation mechanism. Another possible approach would use an independent x-y positioning platform with the camera positioning mechanism on it. The necessity for additional mechanisms is obvious in these approaches. It should also be noted that the local position measurement and corresponding manipulator move would be significantly separated in time and space. This could potentially reduce the accuracy of the positioning operation. Nevertheless, these alternatives have not been completely eliminated from consideration, and may be reconsidered after initial experiments on local positioning schemes.

1. Note that a z-motion may be required to provide adequate stand-off for image acquisition. Whether or not this is the case depends on which manipulator design is selected.

7.4 Obstacle Detection

For safety reasons, obstacle detection is a very important aspect of robot perception. Proper obstacle detection will prevent damage to the shuttle, humans, and the robot itself. It is assumed that obstacles will be mostly static, except for humans and human driven machines. Expected obstacles include: humans, shuttle tiles, appendages of the shuttle (landing gear doors, protective coverings), scaffolds, work stands, tool boxes, and cables. The primary goal of obstacle detection is to detect the *presence* of obstacles for the purpose of avoiding collisions. An estimate of the distance between the robot and the closest point on an obstacle should be provided by the system. It is not the intent of obstacle detection to be able to identify particular obstacles or to accurately localize an obstacle. While there will be a facility to allow the robot to work in the vicinity of known obstacles, *unexpected* obstacles should be handled as exception conditions requiring the interaction of a human operator.

The following list gives an overview of the sensors which have been considered for use in the obstacle detection system. Advantages and disadvantages are indicated by "+" and "-" respectively.

Piezoelectric Sonars (Closed type)

Electrostatic and *open type* piezoelectric sonars cannot be used because of their susceptibility to dirt and moisture.

\+ Long range detection
0.8 - 6 m: +/- 9 mm max. uncertainty
0.2 - 1 m: +/- 1.5 mm max. uncertainty
Detection of people, scaffolds, jack stands, large objects.

\- Detection of cables, and other low objects difficult with forward looking sonar.
Problems may arise with total coverage of area.
Interference between adjacent sonars.
Poor response for specularly reflecting objects.

Mechanical bumpers, Whiskers

\+ Complete coverage for low obstacles.
Simple fail safe mechanism for direct, low level interaction with actuators.

\- Very short range
Only binary (on/off) type information possible

CCD Camera

\+ Good area coverage
Covers floor area
Simple "light-striping" techniques possible

\- Obstacle detection difficult in cluttered environment
No direct range information
Complex image processing required for general cases.

Lasers (1D, 2D)

+ Accurate, long range
  1D line scanners especially good for detecting low floor based obstacles

- Expensive, technology still in development
  Measures only discrete points

Light Curtains

+ Non mechanical
  Inexpensive
  Good area coverage achievable

- Needs separately mounted reflector or receiver

Optical proximity switches

- Inaccurate
  Short range

Pressure Sensitive Skins

+ Simple, reliable mechanism for contact sensing
  Complete area coverage of critical surfaces

- Requires contact to be activated

Figure 7-11 shows the current design of the obstacle detection system. There are two basic types of sensors in this design: long range and short range. Long range sensors are intended to detect obstacles while the obstacle is still relatively far from the robot. Unfortunately, these sensors may not be able to detect all possible obstacles and some may penetrate the long range perimeter without being detected. A redundant second level of sensing is therefore necessary in order to reliably detect all obstacles which are not detected by the long range sensors. The short range sensors are mostly contact type sensors: obstacles will not be detected until contact has been made with the robot. By providing these contact type sensors with mechanical compliance, the robot will have time to decelerate before any damage is done.

Each of the sensors in Figure 7-11 will now be described, starting with the lowest sensors and working upward. One of the requirements for the mobile base is to have the ability to pass over obstacles less than 5cm in height (hoses, cables, etc.) The downward looking sonar are intended to detect these low obstacles so that the system can be configured to cross over them. Since the mobile base is omni-directional, it is necessary to provide full 360 degree coverage around the perimeter of the vehicle. This reasoning will also apply to many of the other sensors included in the obstacle detection system.

The low mechanical bumper is a last resort contact sensor. The bumper is made of a compliant material which will bend when a force is applied to its surface. Mechanical or optical switches are used to detect contact. The standoff distance between the bumper surface and the robot will be determined by the maximum robot deceleration distance. Bumper height is adjusted so that only obstacles which can be surmounted by the mobile base will fit under the bumper. As suggested above, because the vehicle is omnidirectional the bumper will completely surround the base.

Figure 7-11 Overview of the obstacle detection system

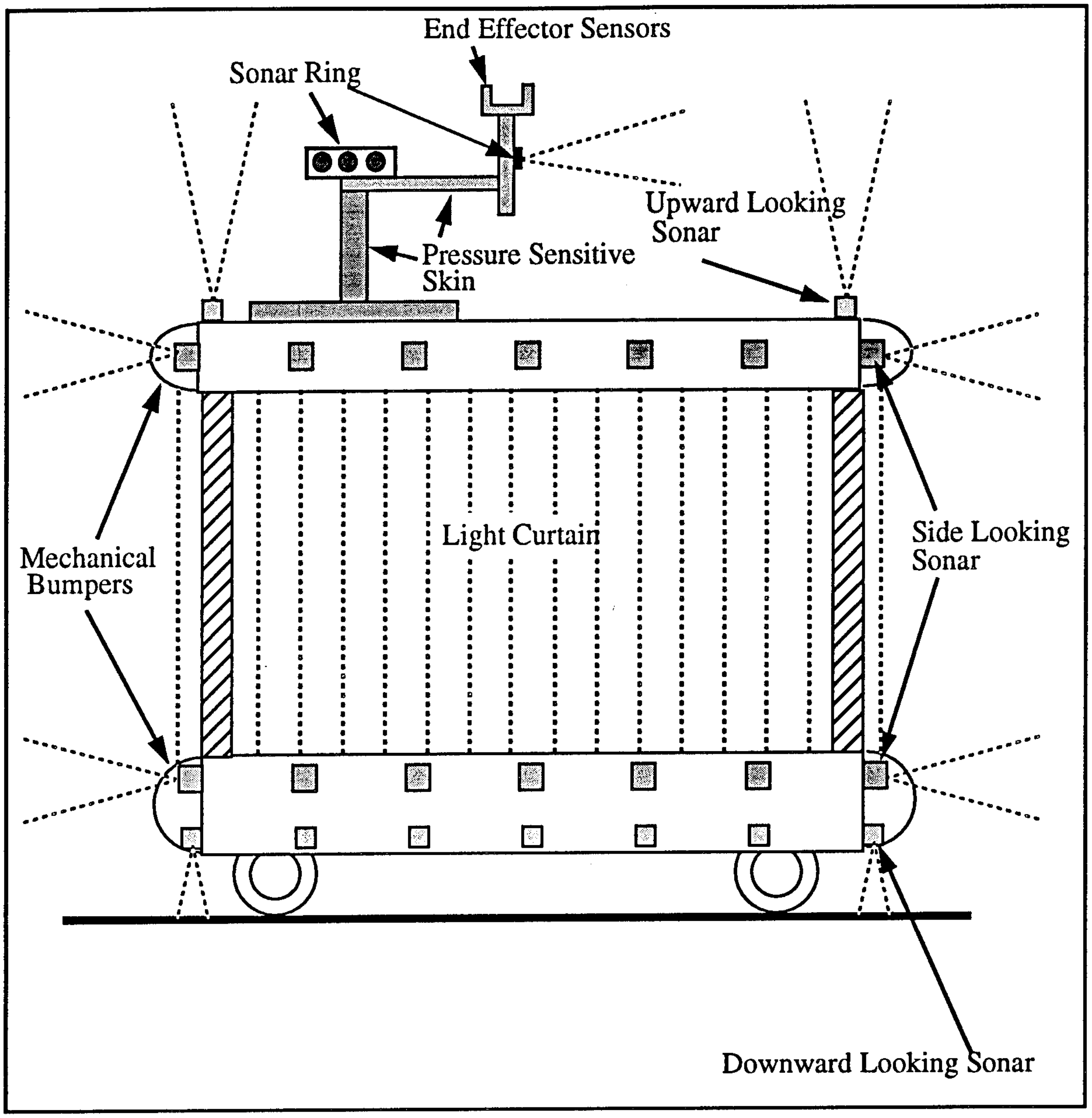

The low side looking sonar are designed to detect floor based obstacles above a given height. These sensors should not detect the very low obstacles which can be surmounted by the mobile base. The side looking sonars will be mounted on the mechanical bumpers such that the front surfaces of the sonars are recessed with respect to the surface of the bumper.

The mechanical bumper and side looking sonar configuration will be repeated at the top of the gantry mechanism. These sensors are intended to detect jackstands, landing gear doors, or any other obstacles which could contact the robot at heights between 1.8m and 3m.

The region between the low mechanical bumper (the mobile base platform) and the high mechanical bumper (the x-y table platform) will not be protected by any of the obstacle detection systems previously discussed. After analyzing the types of obstacles which exist in the robot's operating environment, we decided that it is important to ensure that

obstacles cannot enter the above mentioned region. Protection of this region will consist of an optical light curtain as well as a mechanical covering which completely encloses this region. The covering will probably consist of a rubber or plastic shroud which expands and contracts as the gantry mechanism is raised and lowered. The light curtain will consist of optical transmitter/receiver pairs which detect interruption of a beam of light between the two. In order to reduce the number of receivers and transmitters required, mirrors may be used to provide multiple light beams for each transmitter/receiver pair. The light curtain components will be mounted on the high and low mechanical bumpers, so that sufficient standoff from the vehicle can be achieved.

The upward looking sonar will be mounted on top of the gantry mechanism in each of the four corners of the system. These sensors are not intended to detect all obstacles which might enter the manipulator's workspace. Rather, they will be used to measure the distance between the x-y table platform and the orbiter underside. This information will be used to ensure that the gantry does not get too close to the orbiter, and also to augment the information available to local position estimation.

At heights above the x-y table platform, the only system component which could collide with an obstacle is the manipulator itself. Thus, obstacle detection at these heights is centered around the manipulator mechanism. There are three components of manipulator protection. First, a sonar ring mounted on top of the manipulator's shoulder joint is designed to detect obstacles with which the manipulator could collide. The sonar ring will rotate with the shoulder joint so that individual sensors will always be at a fixed orientation with respect to the manipulator. In order to cover the small region which will be occluded by the manipulator's lower arm, it may be necessary to mount an additional sensor on the arm.

The second component of the manipulator's protection is a compliant, pressure sensitive shroud which completely encloses the manipulator. The shroud will consist of a foam core bonded to the manipulator, and a pressure sensitive skin covering the foam which provides a contact detection mechanism. Since the expected maximum speed of the manipulator is relatively low (about 15cm/sec), this concept should provide a simple, reliable mechanism to ensure that the manipulator does not damage any objects which it may contact. Pressure sensitive skins are currently being evaluated for this purpose.

An alternative to the pressure sensitive skin is an optical proximity skin which would serve the same function. This sensor uses optical reflectance as a means to detect nearby objects. The primary advantage of this skin is that it has the ability to detect obstacles before the obstacle is contacted. A potential problem with this type of sensor is that the ability to sense an object is dependent in part on the object's reflectance properties. Poor reflectors (matte black finishes), or specular reflectors (shiny metal) could be a problem for this type of sensor.

The third component of the manipulator's obstacle detection system consists of a set of sensors mounted on the manipulator's tooling plate. Figure 7-12 shows the various sensors which will be mounted on the end effector.

Figure 7-12 End effector sensors

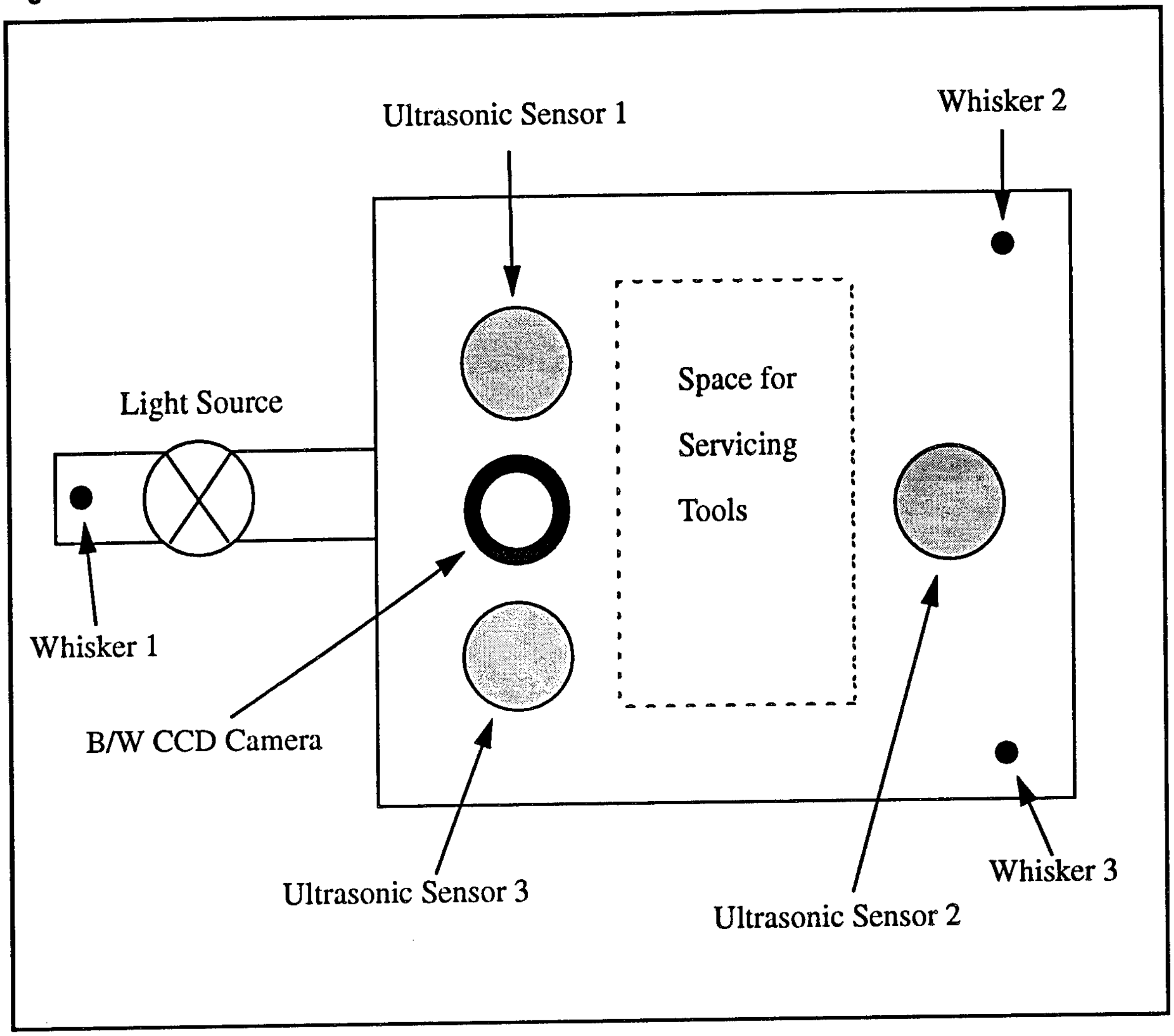

The three ultrasonic sensors will be used for obstacle detection and for local position estimation. These sensors will ensure that the tooling plate does not contact shuttle tiles or other objects in the vicinity of the end effector. They will also be used by local position estimation to measure the local surface orientation of the shuttle tiles. Each mechanical whisker will activate a simple microswitch upon contact. When there is no servicing tool mounted on the tooling plate, these whiskers will be the highest points on the robot. Contact between the whiskers and an object will indicate the presence of an obstacle. The CCD camera and light source will be used for tile inspection and local position estimation. At this time, there is no planned use of this sensor for obstacle detection.

As mentioned above, when a servicing tool (i.e.: rewaterproofing tool) is installed on the tooling plate, it will be the highest point on the robot system. Thus, we feel that an independent set of force/contact sensors should be mounted on all servicing tools, and should be directly interfaced with the obstacle detection system.

Additional Remarks about Sonars

The sonars mounted on the end effector will be close to the injection nozzle. The nozzle uses pressurized air in operation which is one of the worst noise sources for sonars. In order to minimize effects of noise, only high frequency sonars should be used. Noise sources are less common at high frequencies which, due to increased attenuation, do not travel well through air. Sonars are available at 200 kHz and 400 kHz, having a range of ~1 m or ~0.5 m respectively. Another problem when using sonar sensors is their susceptibility to interference between adjacent sensors. Signals transmitted by one sensor may be received by another. Sensors could be triggered sequentially, but this would slow down the data acquisition rate by a large factor.

The downward looking sonars will generally face a flat floor containing few obstacles. Thus, there is little chance of interference if the first echo is the only one evaluated. Therefore, the downward looking sonars can be triggered in parallel. The same reasoning applies to the four upward looking sonars mounted on the gantry and those on the end effector. On the other hand, all side looking sonars may face an unstructured environment and echoes emanating from one sensor may be received by other sensors. The longer range of these sensors also increases the likelihood of interference since echoes are received over a longer period of time. Hence sequential triggering of side looking sonar subsets may be necessary.

Interference can also be avoided by using several different frequencies. This approach will therefore be used between different sensor groups. The following list shows the sonar types deployed at different positions on the vehicle, taking into account the above reasoning. Frequency used, maximum range and triggering mode are given. All sonars are of the sealed piezoceramic type and are commercially available:

- Downward looking (base): 200 kHz; Range 1 m; Trigger parallel
- Side looking (base): 80 or 50 kHz; Range 6 - 10 m; Trigger subsets sequentially
- Side looking (gantry): 80 or 50 kHz; Range 6 - 10 m; Trigger subsets sequentially
- Upward looking (gantry): 80 kHz; Range 6 m; Trigger parallel
- Sonar ring; outward looking (manipulator): 200 kHz; Range 1-1.5 m; Trigger parallel
- Upward looking (end effector): 200 or 400 kHz; 1 m or 0.4 m; Trigger parallel

If the dimension of the base is 2.1 m x 3 m, the total number of sensors needed can be calculated as follows:

1) Base

- Downward looking short range sonar:
  - 1 sonar at each corner. (total = 4)
  - 9 sonars at each 3m side. Spacing between sonars = 0.3 m. (total = 18).
  - 6 sonars at each 2.1m side. Spacing between sonars = 0.3 m. (total = 12).

  Assuming a beam angle of 5 deg. for medium reflecting objects, the diameter of the circular area covered by the sensor = 0.1 m at a height of 0.5 m above the floor.

- Side looking long range sonars:
  - 1 sonar at each corner, looking at 45 deg. (total = 4).
  - 4 sonars at each 3m side. Spacing between sonars = 0.75 m. (total = 8).
  - 3 sonars at each 2.1m side. Spacing between sonars = 0.7 m. (total = 6).

  Assuming a beam angle of 8 deg. for medium reflecting objects, the diameter of the circular area covered by the sensor = 0.42 m at 3m range.

2) Gantry

- Forward looking long range sonars:
  - 1 sonar at each corner, looking at 45 deg. (total = 4)
  - 4 sonars at each 3m side. Spacing between sonars = 0.75 m. (total = 8).
  - 3 sonars at each 2.1m side. Spacing between sonars = 0.7 m. (total = 6).

  Assuming a beam angle of 8 deg. for medium reflecting objects, the diameter of the circular area covered by the sensor = 0.42 m at 3m range.

- Upward looking long range sonars:
  - 1 sonar at each corner (total = 4)

3) Manipulator

- Sonar Ring - To be decided.
  Depends on obstacle size.

- Upward looking short range sonar (end effector):
  - 3 sonars for parallel positioning and shuttle bottom avoidance

8. Conclusion

In this document we have traced a design flow from constraints and specifications to a complete and detailed outline of the configured base and manipulator system. Each of the sections provided strong rationale for decisions and we also provided a look at the final system configuration from mechanics, hardware, sensing and software.

A. Driving and Steering Configuration Evaluation

The following sections examine a variety of wheel steer and drive arrangements.

Figure 8-1 Ackerman steering.

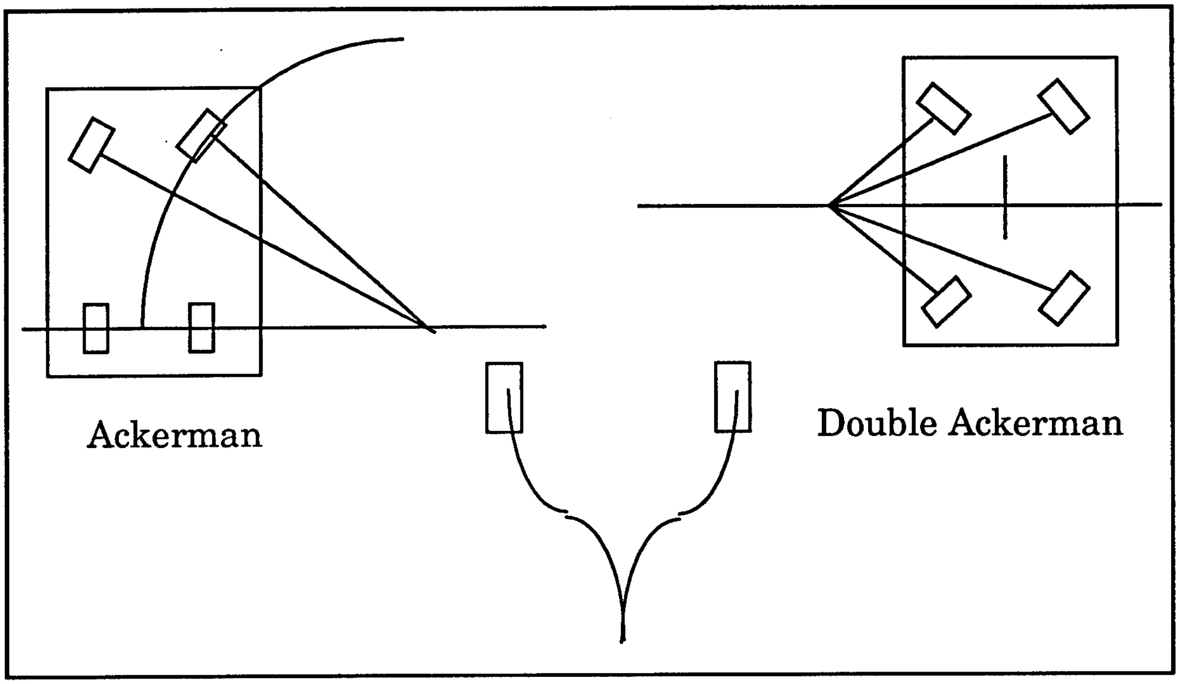

A.1 Ackerman

The Ackerman linkage, first brought to public notice around the turn of the century, uses a mechanical linkage to provide correct steering angles for wheels. The exact relationship is an inverse tangent function of wheel base and wheel separation. Most mechanical linkages are approximations to this function but are close enough and steering angles are small enough that little wheel slip occurs. However, this can affect dead-reckoning for curvilinear vehicle motions over time.

The rear wheels are either independent or require differentials if they are driven. Four wheel drive system can even have three differentials with the third between the front and rear wheel systems. The Ackerman linkage offers a nice decoupling between steer and drive so that distance along a path dictates steering angle rather than wheel. If Ackerman linkages are used for both sets of wheels the turning radius is halved and maneuverability is increased. See Figure 8-1 for examples of Ackerman steering.

Figure 8-2 Synchronous steer and drive mechanism.

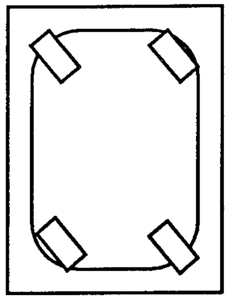

A.2 Synchronous Steering

A synchronous drive is the linking of wheel motions through mechanical means. The first synchronous device was a chain linked wheelchair design in the mid-1970's. A synchronous lawnmower drive which was a belt driven machine was unsuccessfully market it the 1980's. The synchronous drive is a 2DOF system and does not provide reorientation. However, through the use of a rotating turret atop the synchronous mechanism 3DOF can be controlled in a perfect matching of controlled actuations and DOF's required in two-dimensional spaces. I.e. X,Y and Theta.

John Holland of Cybermotion, was the first to mention robots in his patents. He licensed and supplied a synchro-base to Denning using belt drives. His more recent design is an ingenious torque tube design where a coupling between the drive and steering motions prevents the friction-patch that happens when a wheel is turned within it's own width. Another small company, RWI, has built very small 12 inch diameter research bases that are synchronous.

The largest synchro drive is probably Carnegie Mellon's Locomotion Emulator which is 8' in diameter and almost 4' high. Fitzpatrick and Whittaker developed this for the US Bureau of Mines to emulate any vehicle.[1] It has an independent turntable atop the base. Together they provide 3DOF in the plane. The LE uses a belt driven mechanism and uses differentials between wheel pairs to avoid the friction problem of a wheel turning in place.

Advantages of synchronous drive include simple control with a single actuator for steering and another for drive. The turntable provides the rotation to complete the 3DOF in the plane. No coupling between the two occurs except that finite tire diameters often lead to a small wobble for in place direction changes.

Suspension is difficult since the whole base is mechanically coupled. Compliant tires can offset this need but a means to stabilize the vehicle is required. The complex arrangement of belts, actuators and links results in a large amount of space eliminated from packaging considerations.

1. K. Fitzpatrick and J.L. Ladd, "Locomotion Emulator: A Testbed for Navigation Research", in proceedings "1989 World Conference on Robotics Research: The Next Five Years and Beyond", Gaithersburg, Maryland, May 1989

Figure 8-3 Omnidirectional wheels.

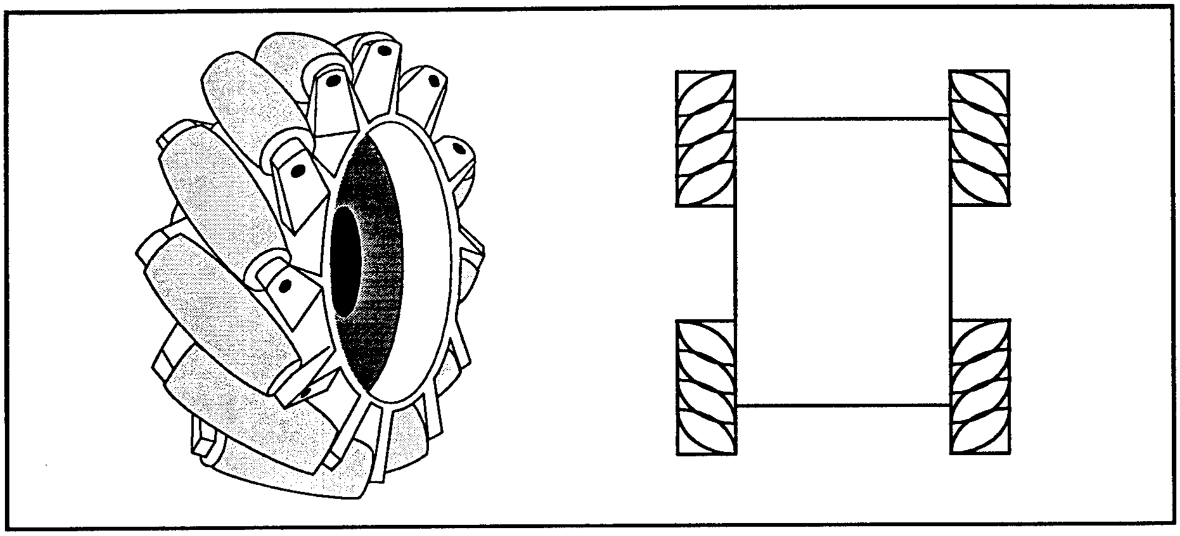

A.3 Omnidirectional Wheels

As shown, synchronous mechanism gives 2DOF. i.e. any path on the floor and if you add an independent turntable it allows any paths at any orientation limited by the dynamics of the vehicle. However, there exist several 3DOF mechanism utilizing rollers on the outside of wheels but these are fairly terrain-limited. i.e. limited by the radius of the small roller.

CMU's Uranus[1] is based upon the Swedish Mechanum wheels invented by Ilon. Another similar development, developed by Bill La, are wheel using rollers on the periphery of the wheels. This configuration utilizes three wheels for 3DOF, a nice coupling with no overconstraints and no elaborate transmissions between wheels. Another advantage of roller wheels is the elimination of steering mechanisms and swept volumes incurred through wheel movements. Control is straightforward and a number of methods have been developed to model and control these systems.[2]

The disadvantage of these systems however is the radius of the small rollers which limit climbing ability in directions lateral to the large diameter of the wheels. Additionally, pinch points between rollers and roller supports may cause problems with local obstacles especially cables and fluid lines obstacles.

1. Blackwell, M., The URANUS Mobile Robot, Robotics Institute Technical Report, CMU-RI-TR-91-06.
2. Muir, P. and Neuman, C.P., Kinematic Modeling of Wheeled Mobile Robots. Robotics Institute Technical Report CMU-RI-TR-86-12, Carnegie Mellon, 1986

Figure 8-4 Differential steering.

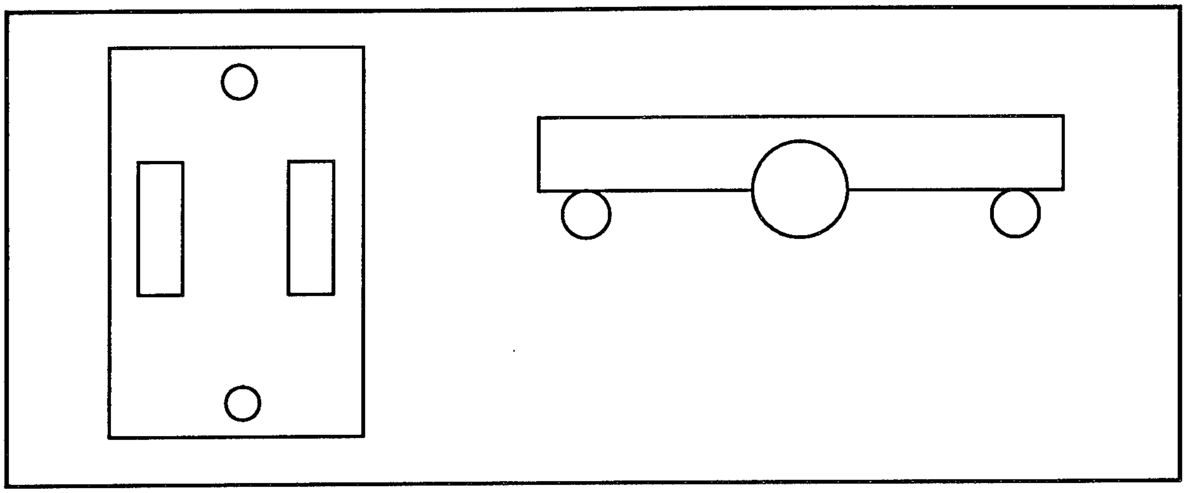

A.4 Differential Steer

As shown in the figure above, differential steer is simply two wheels aligned along the same axis. Both are drive and neither are steered. Although there is strong coupling of drive and steer control is straightforward and any 2D trajectory can be followed limited only by dynamics of the vehicle.

Differential steer does not allow lateral movements without pivoting 90 degrees or making a series of 'parking maneuvers'. For a rectangular vehicle this requires a large swept volume and large excursions of the vehicle to move laterally even short distances.[1] Obviously caster are also required to stabilize the vehicle since the two drive wheels cannot support the load without falling to one side.

Figure 8-5 Independent steer and drive configuration.

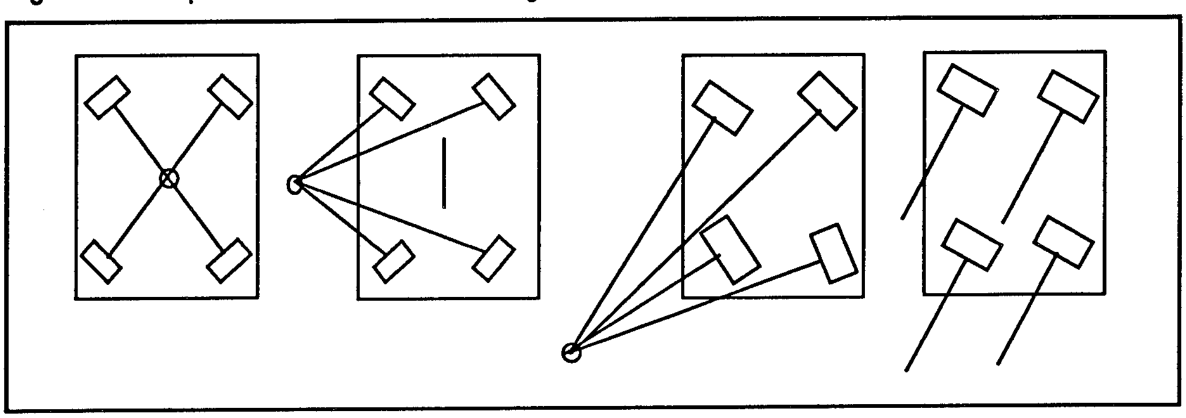

A.5 Independent Drive and Steer

Finally, the last configuration under consideration, is the fully independent drive and steer layout. The primary advantage is the ability to provide complete 3DOF in the plane.

1. An interesting variant of differential steer provides 3DOF by utilizing a turntable atop the base. The axis of rotation can be anywhere but along the line joining the wheel axis, otherwise a singularity occurs.

Simple constraints on wheel steering can provide crabbing motions, rotations, or any rate of curvature. Like the omnidirectional wheel or the synchronous drive with turntable this configuration can follow any path in the plane and rotate along that path. It does not have the climbing limitations of the omnidirectional wheel nor the mechanical packaging issues of the synchronous drive. Another advantage is the redundancy of drive mechanisms. If a drive unit fails that remaining three can still move the vehicle.

The primary disadvantages are control issues of the additional actuated degrees of freedom. It is necessarily an overconstrained system. For a 4 wheel steer and drive a total of 8 degrees of freedom of control are required. Thus, the system is overconstrained by several DOF's and possible control errors will introduce 'floor stretching' or 'isometric exercises' which are internal forces generated through improper control.

Another possible disadvantage is operator input and control without computer control between operator and robot. However, through independent mechanical alignment and then a standard 3DOF joystick such control should be easy to provide.

The existence of precedent or analogous mechanisms is required for a project that is fast tracked. Otherwise assumptions and errors can cause failure.

Examples of Precedent Systems

Unique Mobility, Englewood, Colorado designed and constructed the Full Mobility Robotic Vehicle (FMRV) a four drive and steer vehicle with independent suspension. The vehicle is capable of turning while moving in a fixed direction. The FMRV was developed and successfully tested and then delivered to Missile Command (MICOM) in Hunstville, AL for further evaluation in 1990. Also, a small prototype was first constructed to test concepts.

Ability Technologies of Spencer Iowa, has constructed mobile base systems utilizing three driven and steered wheels and demonstrated the accurate control of the vehicle from a remote link.

The CMU Remote Workhorse Vehicle (RWV) is a remote teleoperated vehicle with independent hydraulic steer and drive that can provide control for crabbing, rotation and describing arcs of any radius.

Examples of Analogous Systems

While a number of overconstrained systems have been developed there are several specifc and relevant examples worth noting. Ambler (12 DOF planar motions) provides body control from 6 legs such that 12 actuated DOF's control 3 body DOF's.

There are many examples of construction machinery capable of crabbing (lateral) motions as well as the short radius turns. These are mostly found in rough-terrain forklifts. Straddle cranes for storage yards and dry-docks are also examples of this high maneuverability.

A.6 Summary

The major differences in configurations are degrees of freedom provided, degrees of freedom controlled, and payload and packaging effects. We've established a need for both lateral and forward translation and tight turning is another requirement.

The controlled degrees of freedom range from two to eight. Mechanical coupling introduces componentry that is not functionally redundant.; i.e. if a single component fails there is no way to then drive the system whereas with multiple drives it is possible to overcome a non-functioning actuator through over-powering or backdrive.

B. Manipulator Evaluation

This appendix details the design synthesis selection for the manipulator configuration. It is divided into sections on the manipulator and related topics:

- Kinematic configurations
- Positioning accuracies
- Workspace
- Stiffness and resonance
- Static and dynamic forces
- Base stability due to manipulator weight and forces
- System weight
- Functional and mechanical components

Each section examines and compares the different design selections. At the end of the manipulator configuration section we have summarized the key points involved in the final design proposal and selection cycle.

B.1 Kinematic Configuration

The comparative analysis focuses on two prime candidates configurations. They are:

- A Mobile Base with a single column elevator and a 2 DOF SCARA manipulator and endeffector
- A Mobile Base with a four column-supported XY gantry and a 1 DOF boom and endeffector

Of all the different configurations considered, these two were the most promising concepts. Such systems as mobile bases with scissor lifts and industrial arm 6 DOF articulated arms, suction-cup style tile-walkers, and bolt-down oversized industrial arms were all rejected based on such criteria as mechanical feasibility, deployment complexity, shuttle and OPF safety requirements, small work envelopes, complex planning/navigation issues, power consumption and other related issues.

Covering a large number of shuttle tiles from a mobile platform with a safe and power efficient mechanism requires a minimum base size, a gravity-decoupled manipulator, and safe deployment scenario. The design was divided into a mobile base, a manipulator and endeffector to be deployed from a minimum collapsed height of 1.83 meters to the lowest working height of 2.87 meters and the maximum working height of 3.96 meters. The system needs to retain a certain minimum positioning accuracy, while being able to sustain contact pressures of 3.4 atm at the rewaterproofing nozzle[1]. The endeffector must have a

1. It is still uncertain whether the 3.5 atm is at the nozzle or at the exit of the DMES tank. We have received notification that the current human rewaterproofing process is claimed to use no more than 20 to 40 N of force to hold the tool in place for a 9.5mm nozzle diameter. Pressures at the delivery tube exit may be as high as 10 atm (tube-sectional area unknown)

full +/- 45 ° range on pitch and yaw, with a full 360 ° roll to access all tiles at any shuttle location, independent of the particular base orientation.

In the fast tile-to-tile transitions, the system can spend no more than a second to traverse 30cm before stopping and acquiring a new tile. The base and manipulator system were required to be as structurally stiff as possible and resonances have to be high frequency with negligibly small settling times. Such timing issues are crucial for successive tile motions, since each second lost per tile due to system damping, cost 4.2 hours over the entire shuttle servicing cycle of 15,000 tiles.

The total system weight, power efficiency, design complexity, and fabrication cost are other issues that were considered at the outset, but which were harder to quantify. The overall convention was to optimize these factors favoring system performance over fabrication costs or design time.

Figure B-1 Kinematic robot configurations

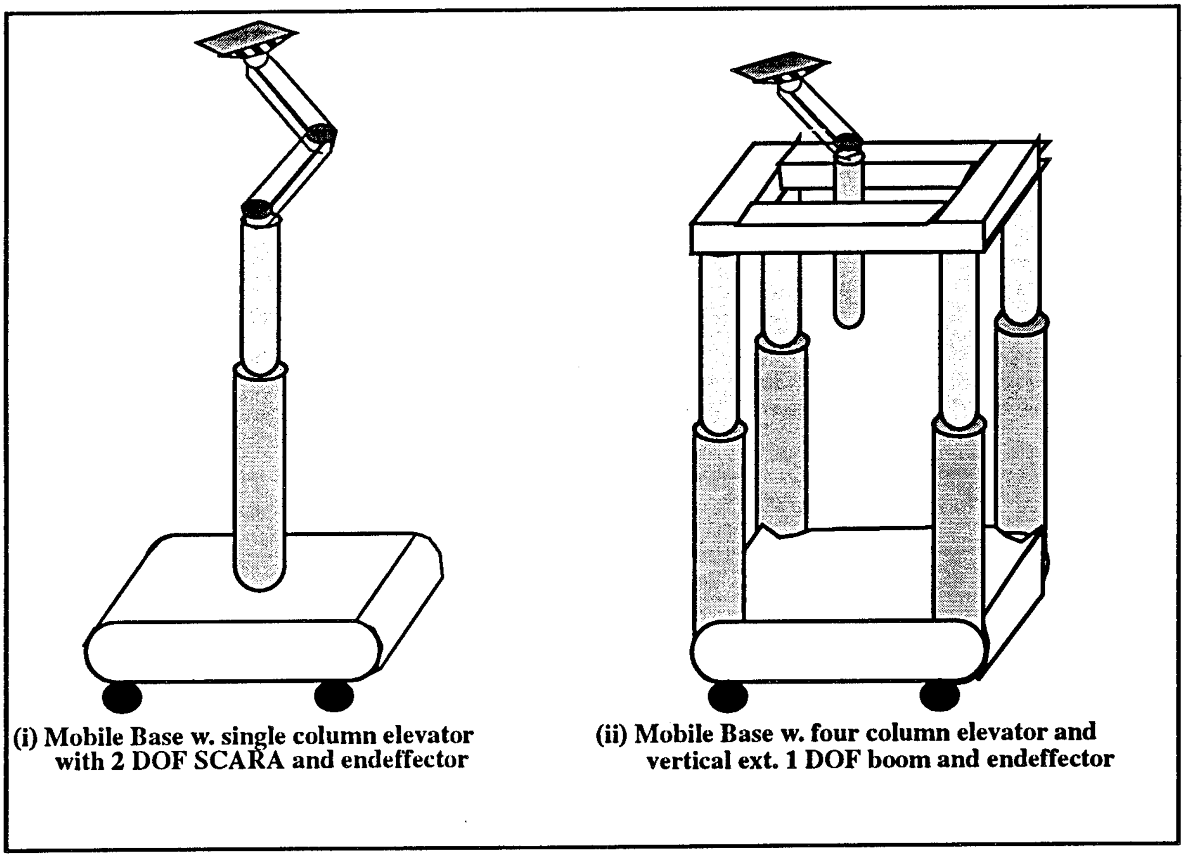

Figure B-1 illustrates the different kinematic and functional characteristics that we decided to analyze and compare.

The main differences among these two designs is the number of vertical columns and the reduced length of the manipulator linkage. These two criteria have a profound effect on system rigidity and resonance. But other criteria had to be analyzed, since we were analyzing systems in a multi-parameter space, where optimal solutions are usually hard to visualize.

The comparative analysis performed was based on several key characteristics. The main kinematic and mechanic differences between these two systems are in the areas of reachable workspace, positioning accuracies, static structure stiffness (deflection under load), dynamic resonances, static and dynamic load sharing, weight, functional and mechanical component simplicity, and ease of implementation and maintenance. Such criteria as cost and design time were deemed marginal and thus considered to be secondary with no real effect on the primary conceptual design decisions.

B.2 Positioning Accuracies

The positioning accuracy required for the end effector was determined to be a function of several key dimensions, as well as the accuracy provided by the vision-based position estimation scheme. These dimensions are based on a nominal 1 cm diameter for the white circle surrounding the rewaterproofing injection hole, a nominal injection hole diameter of 0.1 cm, and the nozzle diameter D. Figure B-2 below illustrates where those dimensions are located.

Figure B-2 Rewaterproofing effector and tile dimensions

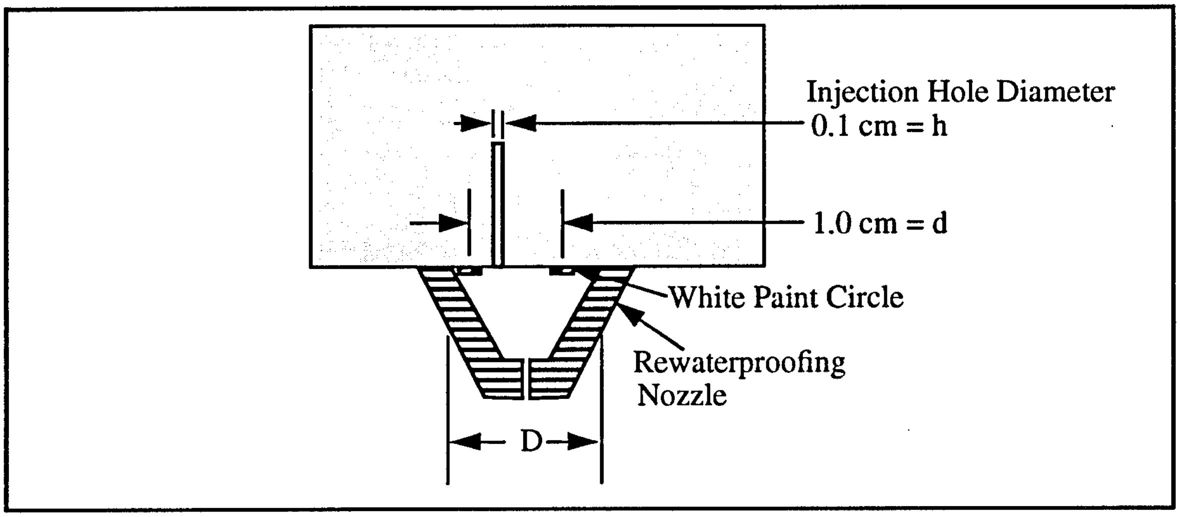

The basic equations governing the feasible mechanical precision, depending on whether one queues off the white circle or the injection hole, are:

The basic equation governing the feasible mechanical precision is:

$$\Delta x_{max} = \Delta_{vision} + \Delta_{mechanical} + \Delta_{CAD} = \frac{1}{2}(D-h) \ldots [cm] \qquad \textbf{Eq. B-1}$$

which indicates the maximum allowable accuracy errors which we can incur while still being able to accomplish the task. This equation assumes that we can detect the injection hole, and do not rely upon the white circle. $\Delta_{\text{mechanical}}$ is the mechanical positioning accuracy of the endeffector, Δ_{vision} is the achievable accuracy of the vision system, and Δ_{CAD} is the error in position of the whole on the tile as given by the database. The

relationship among the variables in this equation is shown in Table 2. We have assumed the following: the hole is located somewhere within the white circle, not necessarily at its center, all accuracies are taken as worst case linear sums, we only open-loop servo after acquiring an image, and do thus NOT servo continuously based on vision data, and that vision-limited accuracies are around 0.2 cm. $\Delta\theta_1$ and $\Delta\theta_2$ are the respective angular positioning resolutions of the two links in the SCARA manipulator configuration.

The accuracy is bounded by the precision of the vision system and the mechanical lash in the system. Achievable accuracy figures are in the +/- 1 to 2mm range and are the figures that we have specified. We considered increasing the nozzle diameter to account for excessive vision inaccuracies or tolerance stackup. The problem is that we have a 3 to 4 second nitrogen purge at 3.4 atm which we have to brace against and that an increased area implies increased holding forces, which drastically affect the mechanical design of the endeffector. We are not prepared at this time to evaluate the issues involved since the exact data for the vision system accuracies have not been determined and it is not clear whether we have to sustain a full 3.4 atm environment inside the nozzle, or whether this number corresponds to the delivery pressure as the nitrogen exits the fine pitot tube at the bottom of the nozzle.

It is clear from this table that certain minimum nozzle diameters are necessary to achieve realistic mechanical accuracies if we intend to cue off the white circle using a certain vision scheme. This constraint can be relaxed at the expense of increased contact forces due to the 4 second long, 3.4 atm nitrogen purge necessary to force the DMES into the tile. A trade-off between nozzle diameter, which determines end effector accuracy, and contact forces is necessary. If we are able to estimate the location of the rewaterproofing hole itself, to within a certain accuracy, the constraints are vastly different. The nozzle diameters can be as low as 0.95 cm and we would still have mechanical accuracy requirements of +/-2 mm, which are indeed quite reasonable. The proposed nozzle diameter of 10mm, require that we locate the location of the rewaterproofing hole itself (to within a certain error of 0.2 cm), with the possible aid of the white circle to narrow down the search area within the acquired image data set.

Such accuracy figures in the horizontal plane are also affected by the amount of mechanical

Table 2 Mechanical Accuracy Requirements

Δx_{max} (cm)	D (cm)	Δ_{vision} (cm)	$\Delta_{mechanical}$ (cm)	Contact Force at **+/- 3.4 atm**
-0.02	0.95	0.2	-0.22	24.5
0.14	1.27	0.2	-0.06	43.7
0.30	1.59	0.2	0.10	68.3
0.45	1.91	0.2	0.25	98.3

slop or 'lost-motion' any mechanism exhibits. The dominating contribution for the 1 DOF

boom and 2 DOF SCARA manipulators are the accuracies of their rotary joints. They will contribute to linear inaccuracies as a function of the overall reach or link-length. In Table 3 below, we have given figures of achievable accuracy for different levels of angular slop.

If we assume a joint-slop of about 1 arc-min ($0.02\,^{o} = 0.0003$ rad) for each joint, with a worst-case assumption that these slops add up as linear vectors, for links of length l_1 and l_2, we have as a worst case:

$$\Delta_{SCARA} = (l_1 + l_2)\,\Delta\theta_1 + l_2\Delta\theta_2 \ldots\ldots \Delta_{BOOM} = l_1\Delta\theta_1 \qquad \textbf{Eq. B-2}$$

If we assume that $l_1=l_2=l$, and we tabulate Δ_{xy} [mm] for different $\Delta\theta_1=\Delta\theta_2=\Delta\theta$, we get the following table.

The black line shows an allowable mechanical accuracy limit of +/- 2mm, indicating a

Table 3 Δ_{xy} for various mechanical slops and boom lengths

	$\Delta\theta$(arc-minutes)				
l (m)	0.5 Δ_{xy} [mm]	1.0	2.0	3.0	4.0
0.25	0.11	0.22	0.40	0.65	1.10
0.50	0.22	0.44	0.87	1.31	2.18
0.75	0.33	0.65	1.31	1.96	3.27
1.00	0.44	0.87	1.75	2.62	4.36
1.25	0.55	1.09	2.18	3.27	5.49
1.50	0.65	1.31	2.62	3.93	6.55

trade-off between positioning accuracy and transmission backlash, motor-position discretization control, etc. It is important to realize that the behavior of the endeffector while moving within this +/- 2mm range is extremely important as it affects the transient response when bang-bang point-to-point motions are performed, and forces are exerted while nitrogen is pumped into the tile. The transmissions capable of delivering such accuracies are available, yet can be extremely expensive and have regrettably large weight and size constraints.

B.3 Workspace

We need to consider the tile acreages covered by the different configurations of a single-column SCARA manipulator and an XY table with a SCARA/Boom manipulator. We compared the different workspaces covered by the different manipulator arrangements and then compared link lengths and coverage. The following analysis looks at the necessary

link and base dimensions to cover a certain number of tiles based on a 100% tiling efficiency and 15cm square tiles. This type of study allows for interesting trade-offs depending on pure acreage criteria.

The analysis reveals that differences between these two configurations depend dramatically on arm length and base size. This type of analysis is only a preliminary look at the issues involved, since we have not considered the effect of reduced tiling efficiency. This reduced efficiency is due to the tessellation necessary to cover the irregular shape of the shuttle underside. Since the shuttle underside does not have two axes of symmetry and contains regions of varying slopes, a study of the true number of base moves and overlap between base moves is necessary to determine the true tiling efficiency for each configuration.

The total areas covered by each manipulator are given by:

$$^{SCARA}A_{circle} = 4\pi L^2 \quad \textbf{Eq. B-3}$$

$$^{XY}A_{circle} = (a+2L)\,(b+2L) + \pi L^2 - 4L^2 \quad \textbf{Eq. B-4}$$

$$^{SCARA}A_{hex} = L^2\sqrt{108} \quad \textbf{Eq. B-5}$$

$$^{XY}A_{rect} \equiv \left(a + 2L\sin\left(\operatorname{atan}\left(\frac{b}{a}\right)\right)\right)\left(b + 2L\cos\left(\operatorname{atan}\left(\frac{b}{a}\right)\right)\right) \quad \textbf{Eq. B-6}$$

Where $^{xy}A_{rect}$ was approximated using a constrained optimization: $^{xy}A_{rect}=(a+2x)(b+2y)$ and $x^2+y^2=L^2$.

Figure B-3 Tile coverage for different vehicle/manipulator configurations

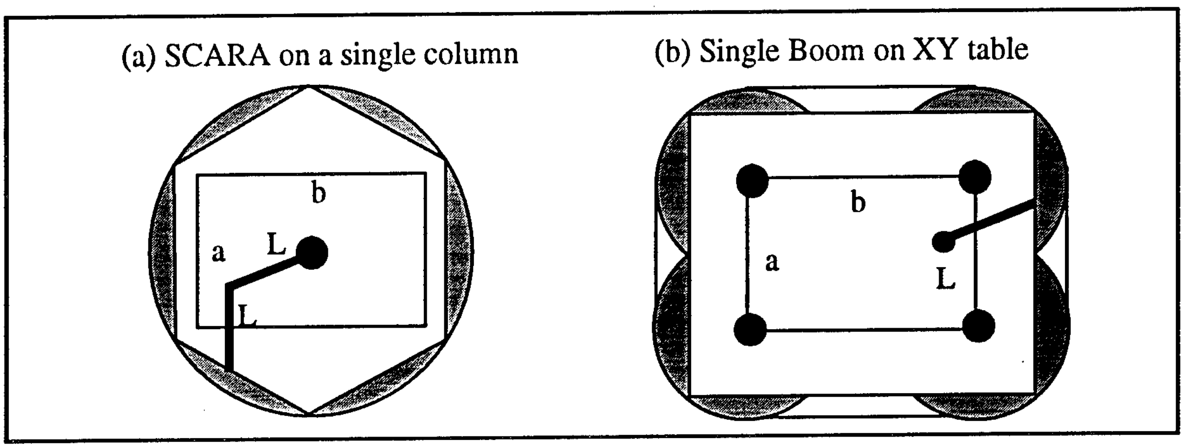

Equation Eq. B-4 and Eq. B-6 compute the area covered by each configuration (Figure B-3) regardless of the overlap that will result in side-by-side base moves (denoted by the outer boundary of the work envelope). These compute the area covered by each configuration

assuming that there will be a minimum overlap in side-by-side base moves These are denoted by the lightly shaded hexagon and rectangles.

The following tables shows the total workspace covered, the number of tiles, N, and assumes an average tile servicing time of 10 secs. N is based on an area 0.023m^2 and 100% tiling efficiency.

Table 4 and Table 5 indicate the minimum horizontal reach for the SCARA on a single

Table 4 Tiling efficiency vs. link length: Single boom on XY table.

	L	a/b					a/b				a/b		
		1	0.8	.67	0.57	0.5	1	0.83	0.71	0.63	1	0.86	0.75
a [m]		1.22	1.22	1.22	1.22	1.22	1.52	1.52	1.52	1.52	1.83	1.83	1.83
b [m]		1.22	1.52	1.83	2.13	2.44	1.52	1.83	2.13	2.44	1.83	2.13	2.44
$^{xy}A_{rect}$ [m^2]	0.5	3.71				6.10	4.96			7.03	6.44		8.00
	0.75	5.20				7.97	6.66			9.03	8.36		10.12
	1	6.94				10.03	8.61			11.25	10.52		12.49
$T_{service}$ [min] / base moves	0.5	27/95				44/58	36/71			50/50	46/54		57/44
	0.75	37/67				57/44	47/53			65/39	60/42		73/35
	1	50/50				72/35	62/41			81/31	76/33		90/28
$^{xy}N_{rect}$	0.5	1592				262	213			302	287		344
	0.75	223				343	286			388	359		435
	1	298				431	370			484	453		537

elevating column to reach a certain number of tiles and is contrasted to the base and boom dimensions necessary for the XY gantry system. Since the base dimensions affect the coverage, the boom lengths can be reduced and the base size can be increased, thus maintaining a constant tile coverage while increasing the speeds and resonant frequencies of the manipulator.

Table 5 Tiling efficiency vs. link lengths: SCARA on Single Column

	L [m]					
	0.25	0.5	0.75	1.0	1.25	1.50
$^{SCARA}A_{hex}$ [m^2]	0.6495	2.598	5.846	10.392	16.238	23.383
$T_{service}$ [min]	5	19	42	75	117	168
No. of Base Moves	536	134	60	34	22	15
$^{SCARA}N_{hex}$	28	112	251	447	699	1007

B.4 Stiffness and Resonances

This criteria offers revealing data by which to compare the two different configurations. The two types of stiffnesses and resonances to consider are structural (horizontal and vertical) and joint-specific (horizontal plane only).

Figure B-4 Single column elevator stiffness and resonance

K_L = Linear Bending [N/m]

Δ = Deflection [m]

P = Side Load [N]

E = Modulus of Elasticity

H = Height

I_o = Area Moment of Inertia

J_o = Polar Area Moment of Inertia

d = Column Diameter [m]

t = wall thickness

W_{COL} = Total weight of all columns

$$W_{COL} = \pi H \rho t(4d - t)$$

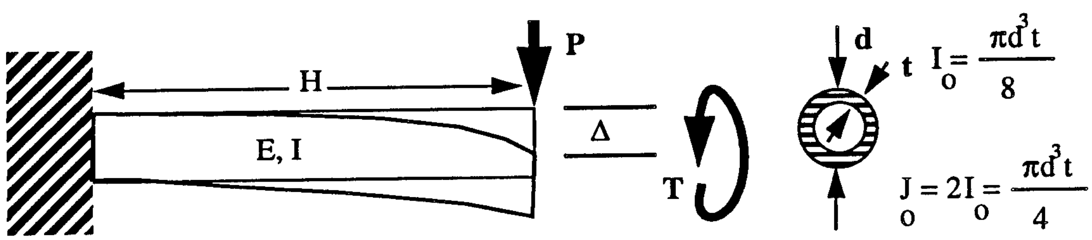

Structural Bending and Torsional Rigidity in the Horizontal Plane - Single Column

The differences in structural resonances for the different elevating mechanisms are substantial. A box-beam arrangement like the xy-gantry on four columns is up to 16 times stiffer with resonance frequencies up to 4 times higher than those for the single-column elevating mechanism. A comparison is given by for structural analysis for the single column and box-beam elevator mechanism. The vertical structural resonance of the 2 DOF SCARA and a 1 DOF boom under realistic loading is of consequence only for excessively long reaches. Deflections and resonances under such loading conditions are negligible compared to the horizontal resonances experienced by the structural elevating mechanisms. The horizontal structural resonance of the 2 DOF SCARA or 1 DOF boom arrangement has resonance frequencies that are factors of 10 to 20 higher than those due to finite joint compliance.

Using the simple bending-beam equation (Eq. B-7) for the situation described in Figure B-4:

$$Bending;\Delta = \frac{PH^3}{3EI_o};and;K_L = \frac{P}{\Delta} \cong \frac{3EI_o}{H^3};Torsion;\phi = \frac{TL}{J_oG};K_\phi = \frac{J_oG}{H} \Rightarrow K_L = \frac{K_\phi}{L^2} = \frac{J_oG}{HL^2} \qquad \text{Eq. B-7}$$

we can generate a table of expected static/dynamic deflections based on estimates of static and dynamic forces. An estimate of "stiffness" of the structure can also be made, approximating the actual stiffness parameter as shown above. Tabulating the expected horizontal deflections as a function of different loads, and circular column diameter and wall thickness, and a natural frequency ω assuming a linear mass equal to the entire maximum moving weight (M_L=100 kgs) at a linear acceleration of 1 m/sec^2, we can get the results given in the table below:

Table 6 Stiffness of Various Manipulator Configurations - Bending Stiffness

		d [m] with H= 4.57 m											
		0.15			0.305			0.457			0.61		
	P	t/d			t/d			t/d			t/d		
	[N]	1/40	1/20	1/10	1/40	1/20	1/10	1/40	1/20	1/10	1/40	1/20	1/10
Δ [m]	45	0.0042	0.002	0.001	0.0002	0.0001	0.00006	0.00009	0.00002	0.00001	0.00001	0.0	0.0
	223	0.0207	0.0104	0.0052	0.0012	0.0006	0.003	0.002	0.0001	0.00006	0.00008	0.00004	0.0
	445	0.0413	0.0207	0.0103	0.0024	0.0012	0.0006	0.0005	0.0002	0.0001	0.0002	0.00008	0.0
	890	0.0827	0.0413	0.027	0.0048	0.0024	0.0012	0.001	0.0005	0.0002	0.0003	0.0002	0.0
	1335	0.124	0.062	0.31	0.0073	0.0036	0.0018	0.0014	0.0004	0.0005	0.0003	0.0001	
	(Column Weight)	15kg	28kg	53kg	60kg	116kg	220kg	124kg	261kg	495kg	239kg	465kg	882kg
K_L^{bend} [N/m]x10^4		1.077	2.153	4.306	18.4	36.8	73.6	92.28	185.5	371	294	589	1178
ω [rad/sec] [Hz] $(K_L^{bend}/M_L)^{.5}$		(1.65) 10.4	(2.34) 14.7	(3.31) 20.8	(6.83) 42.9	(9.66) 60.7	(13.66) 85.8	(15.3) 96.1	(21.7) 136	(30.7) 193	(27.2) 171	(38.7) 243	(54.6) 343

Figure B-5 Quad-column xy-gantry elevator stiffness & resonance

$$W_{COL} = 4\pi H\rho\left(d^2 - (d-2t)^2\right)$$

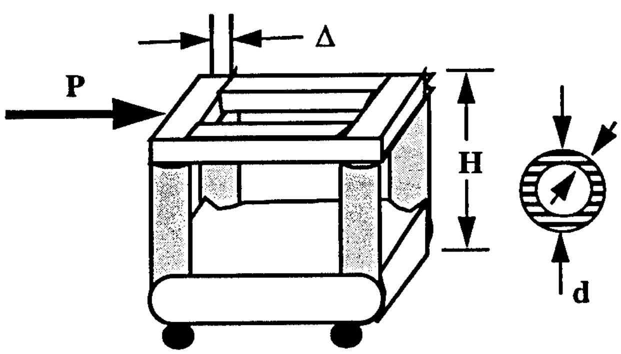

$$I_0 = \frac{\pi d^3 t}{8}$$

$$J_0 = 2 I_0 = \frac{\pi d^3 t}{4}$$

Structural Bending Rigidity in the Horizontal Plane - Four Column Box Beam

Using the simple bending-beam equation (Eq. B-8) for the situation described in Figure B-5 below, we get:

$$Bending;\Delta = \frac{PH^3}{48EI_o};K_L = \frac{P}{\Delta} \cong \frac{48EI_o}{H^3} \qquad \textbf{Eq. B-8}$$

As is evident from the equations of the four column box beam (Eq. B-8), and that of the single column Eq. B-7, the difference in deflections and stiffness is a factor of 16. Hence the above box-beam arrangement will deflect 16 times less and thus be 16 times stiffer than the single column design for comparably sized column diameters and wall thicknesses and identical material properties.

Notice further that neither in the single nor gantry column arrangements have we considered compliance nor slop in the support rails nor bearings due to a multi-stage arrangement of the columns. It is thus necessary to remember that these figures represent best-case scenarios.

We have also assumed a 4.57m reach. In reality the reach is much shorter for the column itself and more in the range of 3.05m. The difference in deflections and stiffness can be simply computed by multiplying (for the stiffness) or dividing (for the deflections) the numbers below by a factor of $(4.57/3.05)^3$=3.364.

On the following table we have given some numerical results for the situations we have considered:

Table 7 Horizontal Plane Stiffness

		d [m] with H = 4.57m											
		0.1524			0.2032			0.254			0.3048		
	P[N] t/d	1/40	1/20	1/10	1/40	1/20	1/10	1/40	1/20	1/10	1/40	1/20	1/10
Δ [m]	45	0.00025	0.00012	0.00006	0.00008	0.00004	0.00002	0.00003	0.00002	0.00001	0.00002	0.00001	0.0
	223	0.0012	0.00061	0.003	0.00038	0.00019	0.0001	0.00016	0.00008	0.00004	0.00008	0.00004	0.0
	445	0.0024	0.0012	0.00061	0.00077	0.00038	0.00019	0.00031	0.00016	0.00078	0.00015	0.00008	0.0
	1335	0.0073	0.0036	0.0018	0.0023	0.0012	0.00058	0.00094	0.00047	0.00024	0.00045	0.00023	0.0001
	$W_{COL}s$ [Kg]	60	116	220	106	207	391	166	323	612	239	465	881
	K_L^{bend} [N/m]x10^4 $48EI_o/H^3$	18.53	36.71	73.40	58.0	116.0	232.0	141.6	283.2	566.5	293.7	587.3	1175

Figure B-6 Simplified model of manipulator

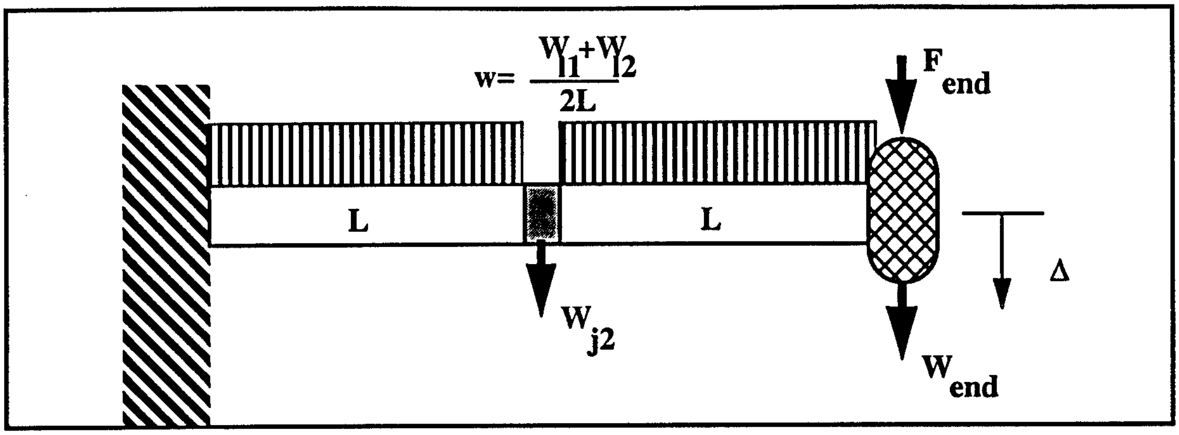

Structural Bending Rigidity in the Vertical Plane - 2DOF Scara and 1DOF Boom

The vertical deflection of the endpoint of the Scara manipulator is also affected by the loads applied to the structure itself. Below (Figure B-6) we have illustrated the deflection computation using the link weights, joint weights, endeffector weight, and a maximum endpoint force applied during the rewaterproofing process

The total deflection and stiffness at the endpoint can be computed by linear superposition to give:

$$\Delta = \left(\frac{2wL^4}{EI} + \frac{5W_{j2}L^3}{6EI} + (W_{end} + F_{end})\left(\frac{16L^3}{6EI}\right)\right); K_\Theta = \frac{w\frac{L^2}{2} + W_{j2}L + 2(W_{end} + F_{end})L}{\frac{\Delta}{2L}} \qquad \text{Eq. B-9}$$

$$K_L = \frac{K_\Theta}{L^2}; \omega = \sqrt{\frac{K_L}{I_{links} + (W_{j2} + 4(F_{end} + W_{end}))L^2}} \qquad \text{Eq. B-10}$$

The resulting vertical deflection can then be tabulated as a function of the individual manipulator link length L, the aspect ratio of the square link cross-section (assuming b = 0.15m), wall thickness t=a/5=width/5, with an endeffector weight W_{end}=25kgs, endpoint force F_{end}=15 kgs, and an individual joint weight of W_{j2}=10kgs. The weight per unit link length w is computed based on a rectangular x-sectional area (A=ab-(a-2t)(b-2t), with t fixed to t=a/5) and the density of AL T7075 (ρ_{al}=2750kg/m^3) (Table 8):

Table 8 Vertical Deflection

	a/b b=0.15m, t=a/5									
	1.5		1.25		1.0		0.75		0.5	
L[m]	Δ[mm]	ω [Hz]	Δ	ω	Δ	ω	Δ	ω	Δ	ω
0.25	0.0065	810	0.0006	758	0.0008	686	0.001	589	0.002	465
0.5	0.006	122	0.0067	117	0.008	109	0.01	96	0.016	78

Table 8 Vertical Deflection

	a/b b=0.15m, t=a/5									
	1.5		1.25		1.0		0.75		0.5	
L[m]	Δ[mm]	ω [Hz]	Δ	ω	Δ	ω	Δ	ω	Δ	ω
0.75	0.02	39	0.025	38	0.03	36	0.038	33	0.058	27
1.0	0.06	17	0.07	16.9	0.077	16.2	0.097	14.9	0.146	12.6
1.25	0.136	8.9	0.145	8.87	0.165	8.64	0.205	8.06	0.3	6.95
1.50	0.26	5.25	0.278	5.23	0.311	5.13	0.381	4.84	0.55	4.24

Structural Bending Rigidity in the Horizontal Plane - 2DOF SCARA and 1DOF Boom

No matter which configuration we choose, we will still need to use a horizontal reach extension. Positioning performance is limited by resonances due to finite joint/transmission stiffness. We have used realistic transmission stiffness values and analyzed resonance frequencies and settling times based on link and joint weights. The results confirm intuition, in that a range of resonance frequencies from 5 to 30 Hz are expected for 2 DOF SCARA arms with link lengths from 1.5 (3m reach) to 0.25 m (0.5m reach), and a 1 DOF boom with reach of 1.5m to 0.25m. The 1 DOF boom had up to 50% higher resonance frequencies and 10% lower settling times than the 2 DOF SCARA with links of similar length and weight. These figures illustrate that the system performance in tile-to-tile moves is dominated by joint compliance, endeffector and joint weights and the link lengths and weights.

We must also consider the structural stiffness of the link assembly itself. In the horizontal plane, the worst case is when both links are colinear and at the edge of the work envelope. A simple bending beam stiffness relation can express the beam deflection equation so that one solves for the linear stiffness, translates it into a rotational stiffness at the fixed end, and use a simple natural frequency and settling-time relation. As seen in the previous example, such an estimate is usually about a 10% to 20% overestimate on the real natural frequency, yet it provides an estimate for further calculations. Also, for the 2DOF SCARA and 1DOF booms the equations are no different, except for the variation in length. The equations used for estimating the tabulated parameters are given below.

Linear Endpoint Stiffness Estimate (w=weight/unit_length, W_{end}=Endeffector Weight)

$$y = \frac{wL^4}{8EI_a} + \frac{W_{end}L^3}{3EI_a},\ \text{since};K_L \approx \frac{wL + W_{end}}{y} \Rightarrow K_L \approx \frac{24EI(wL + W_{end})}{3wL^4 + 8W_{end}L^3} \qquad \textbf{Eq. B-11}$$

Rotational Stiffness:

$$K_{\Theta} = \frac{\tau}{\Theta} \approx \frac{w\frac{L^2}{2} + W_{end}L}{\frac{y}{L}} = \frac{24EI\left(w\frac{L^2}{2} + W_{end}L\right)}{3wL^3 + 8W_{end}L^2} \qquad \textbf{Eq. B-12}$$

Natural Frequency and settling time:

$$\omega = \sqrt{\frac{K_{\Theta}}{I_m}} \text{---} T_s \cong \frac{4}{\zeta\omega} \qquad \textbf{Eq. B-13}$$

where I_m is given by:

$$I_m = \frac{1}{12}\rho_{AL}L\left[ab - (a-2t)(b-2t)\right]\left\{\frac{L^2}{4} + \left[a^2 + b^2 - (a-2t)^2\left(b-2t^2\right)\right]\right\} + W_{end}L^2 \qquad \textbf{Eq. B-14}$$

These equations can be used to tabulate horizontal structural resonances and settling times: (Table 9)

Figure B-7 Scara and boom linkage dynamic parameters

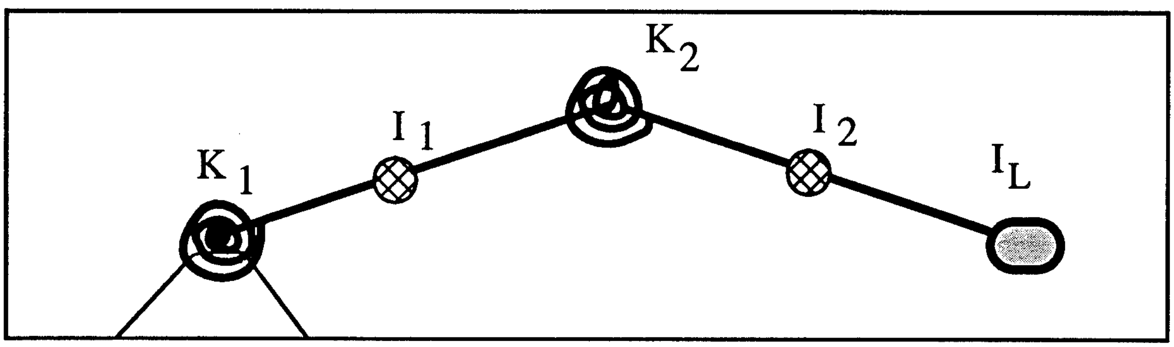

Table 9 Horizontal Resonances and Settling Times

	2DOF SCARA ω_j [Hz]					$\zeta=0.7$	1DOF BOOM ω_j [Hz]					$\zeta=0.7$
l [m]	1.5	1.25	1.0 [a/b]	0.75	0.5	T_s (sec)	1.5	1.25	1.0	0.75	0.5	T_s (sec)
0.25	433	332	239	155	85	0.01	1225	941	677	439	239	0.004
0.5	144	112	82	54	30	0.03	419	324	234	153	84	0.01
0.75	74	58	43	28	16	0.06	219	170	124	82	45	0.02
1.0	45	36	27	18	10	0.09	136	107	79	52	29	0.03
1.25	31	24	18	13	7	0.13	94	74	55	37	20	0.04
1.5	22	18	14	10	5	0.17	69	55	41	27	15	0.06

Joint Compliance in the Horizontal Plane - 2DOF SCARA and 1DOF Boom

Since transmissions have a finite stiffness, we must also look at the resonant modes induced by joint compliance. A simple SCARA model illustrated below shows the abstraction with all the necessary physical parameters that are needed. It can be shown that the equation to determine the two resonant modes of vibration for such a system is:

$$\omega_{1,2} = \sqrt{\frac{K_2(I_1+I_2+I_L)+K_1I_1}{2I_1(I_2+I_L)}\left\{1 \pm \sqrt{1-\frac{4K_1K_2I_1(I_2+I_L)}{[K_2(I_1+I_2+I_L)+K_1I_1]^2}}\right\}} \qquad \textbf{Eq. B-15}$$

with the variables taken from Figure B-7 (we are using the smallest ω value).

The resulting lowest joint-resonance frequency ω_j [Hz] for horizontal motions can then be tabulated for a Scara arm with $l_1=l_2=l$, and similarly for a single boom of length l, with similar cross-sections (a, b=0.15m, t=a/5) and carrying the same load $I_L(25kg*l_2^2)$, $K_1=K_2=50{,}000$ Nm/rad, with $T_s=4/(\zeta\omega)$ (similar results are obtainable for a 1 DOF boom of length L; $\omega^2=K_1/(I_1+I_L)$):

The overall conclusion is that the xy-gantry box-beam elevating structure provides

Table 10 Resonant frequencies for SCARA and Boom arms

l [m]	2DOF SCARA a/b(t=a/5, b=.15m)					ζ=0.7 T_s	1DOF BOOM (Length l) a/b(t=a/5, b=.15m)					ζ=0.7 T_s
	1.5	1.25	1.0	0.75	0.5	[sec]	1.5	1.25	1.0	0.75	0.5	[sec]
0.25	22	24	25	26	27	0.03	25	26	27	27	28	0.03
0.50	10	11	12	13	13	0.07	12	12	13	13	14	0.07
0.75	6	7	7	8	8	0.11	7	8	8	8	9	0.10
1.0	4	4	5	6	6	0.15	5	5	6	6	7	0.14
1.25	3	3	4	4	5	0.20	4	4	4	5	5	0.18
1.50	2	3	3	3	4	0.25	3	3	4	4	4	0.22
	ω_j [Hz]						ω_j [Hz]					

substantially stiffer support at large reaches, and allows for a horizontal boom structure with reduced link length. The resulting resonances are thus higher (by as much as 50%), anywhere from 10 to 30 Hz, than for a single-column elevating mechanism with a 2 DOF SCARA with comparable tile acreage (5 to 15 Hz), and the settling times are also reduced for the gantry-boom combination (0.05 to 0.2 sec as compared to 0.1 to 0.35 sec).

B.5 Inertial Forces/Torques

Acceleration

An important aspect of dynamic behavior is the presence of inertial forces due to linear and angular accelerations during tile-to-tile transitions. These inertial effects excite system resonances and in turn determine the speed of response, material strengths, bearing selection, and power requirements for the entire manipulator system.

For moves from one tile to the next, the shortest average distance is 15cm, while the largest is about 30cm. If we assume a linear constant acceleration and a constant deceleration phase with a triangular velocity profile, we can calculate the necessary acceleration to perform any such move within a given time T.

Figure B-8 Tile-to-tile acceleration profile

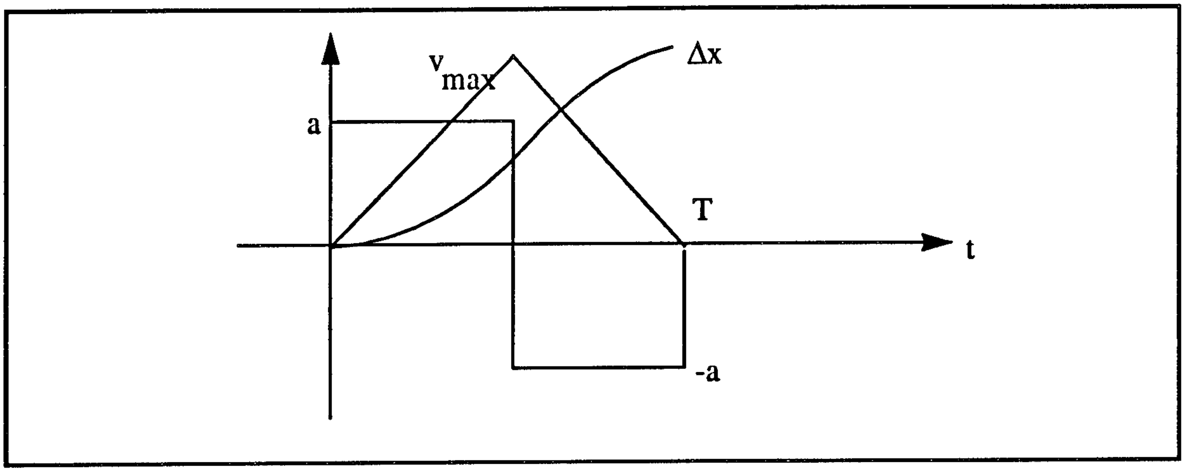

If T=1sec, and Δx=30cm, then 30cm=v_{max}*.5sec or a=1.25m/sec^2. Thus a good estimate of maximum accelerations is about a_{max}=1.5 m/sec^2

Dynamics, Inertial Forces and Torques

The dynamic forces and torques experienced during a move are an important aspect of the design phase. They not only make mechanical design issues clear for component selection, but they also provide a good estimate of loading and associated deflections. These deflections can then be used to generate dynamic accuracy figures and also estimates of dynamic stiffness, which when used with the appropriate inertia figures and damping ratios, yields data for expected system bandwidth.

We explored the inertial torques and linear side forces exerted on a 2 DOF SCARA and 1 DOF boom of varying lengths and different cross-sections and weights per unit length. This allows a comparison between a 2-link versus a 1-link manipulator configuration. The inertial forces exerted by motions of the XY-gantry system due to boom, manipulator and XY-shuttle motions are then calculated to estimate additional linear forces on the manipulator and xy-gantry structures. These forces and torques determine the dynamic deflections from the stiffness and resonance tables presented earlier.

The results indicate that, depending on the size of the manipulator boom(s), the motors and transmission will have to be properly sized to achieve such endpoint accelerations. This data will be used to select motors, bearings, transmissions, and power components for the base.

Figure B-9 Manipulator acceleration distribution

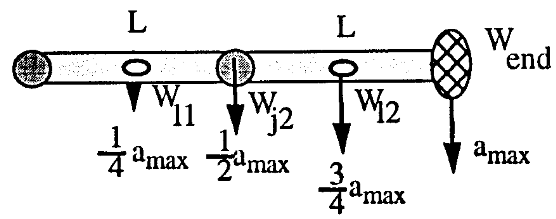

2DOF Scara and 1DOF boom & Endeffector

For the SCARA arm, we can thus envision, seeing torques that are in the linear horizontal plane depending on the angular acceleration (α=a/r).

$$\Gamma_{dyn} \equiv \left(\frac{W_{l1}}{4} + \frac{W_{j2}}{2} + \frac{3W_{l2}}{4} + W_{end}\right)a_{max} \qquad \textbf{Eq. B-16}$$

Using aluminum and a rectangular cross-section (b=.15m,t=a/5), and a_{max}=1.5m/sec^2, we get (equivalent linear forces are computed by ${}^{SCARA}F_{dyn}=\Gamma_{dyn}/2L$ and ${}^{boom}F_{dyn}=\Gamma_{dyn}/L$):

Table 11 Manipulator Inertial Forces and Torques

l [m]	2DOF SCARA a/b(b=.15m, t=a/5)					1DOF BOOM(Length l) a/b(b=.15m, t=a/5)				
	1.5	1.25	1.0	0.75	0.5	1.5	1.25	1.0	0.75	0.5
0.25	71.5	65.3	59.9	55.1	51.0	50.7	47.7	44.9	42.5	40.5
0.5	97.9	85.6	74.7	65.2	57.1	63.9	57.8	52.4	47.6	43.5
0.75	124.4	105.9	89.6	75.3	63.1	77.2	67.9	59.8	52.6	46.5
1.0	150.8	126.2	104.4	85.4	69.1	90.4	78.1	67.2	57.7	49.6
1.25	177.3	146.5	119.3	95.5	75.2	103.6	88.3	74.6	62.7	52.6
1.50	203.7	166.8	134.1	105.6	81.2	116.9	98.4	82.1	67.8	55.6
	Γ_{dyn} [Nm]					Γ_{dyn} [Nm]				

XY Shuttle

The forces required to move the entire shuttle assembly at 1.5m/sec^2 from one tile to the next, depend on the overall mass being moved. In the following table (Table 12) we have given some estimates of linear inertia present in the manipulator/endeffector design, and the associated dynamic side-loads for different accelerations.

Table 12 Mass Moved by XY table

PART	WEIGHTS [kg]
Endeffector and Wrist	40
Tooling	10
Vertical Z	50

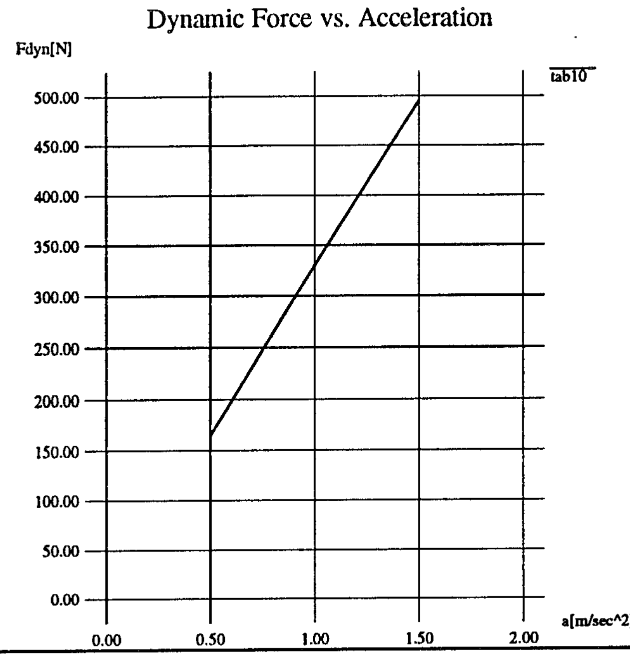

Manipulator and Endeffector

Since we will not necessarily use the XY table to do ALL the tile-to-tile motions, but instead use a simple horizontal boom with a 360 ^{o} rotation in the horizontal plane. We had previously estimated the necessary joint and link weight for such a boom, but are giving such figures again to tabulate the differences. Expected linear stiffnesses due to link and vertical short-column stiffness have to be considered as two springs in series with endpoint loads and distributed loads. The table below (Table 13) breaks out the different components and their weights:

Table 13 Masses Moved by Manipulator

PART	WEIGHTS [kg]
Endeffector Tooling	5
(Plate, Sensors, Conn.)	10
Instrumented Rot. Compliance	2.5
Force/Torque Sensor	2.5
Wrist Roll	5
Pitch	5
Yaw	5
Endeffector Extension	5

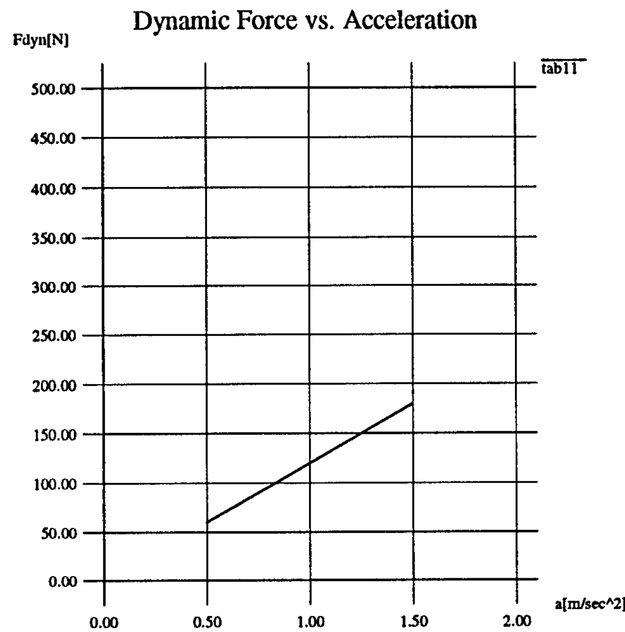

Figure B-10 System candidate weights and stability

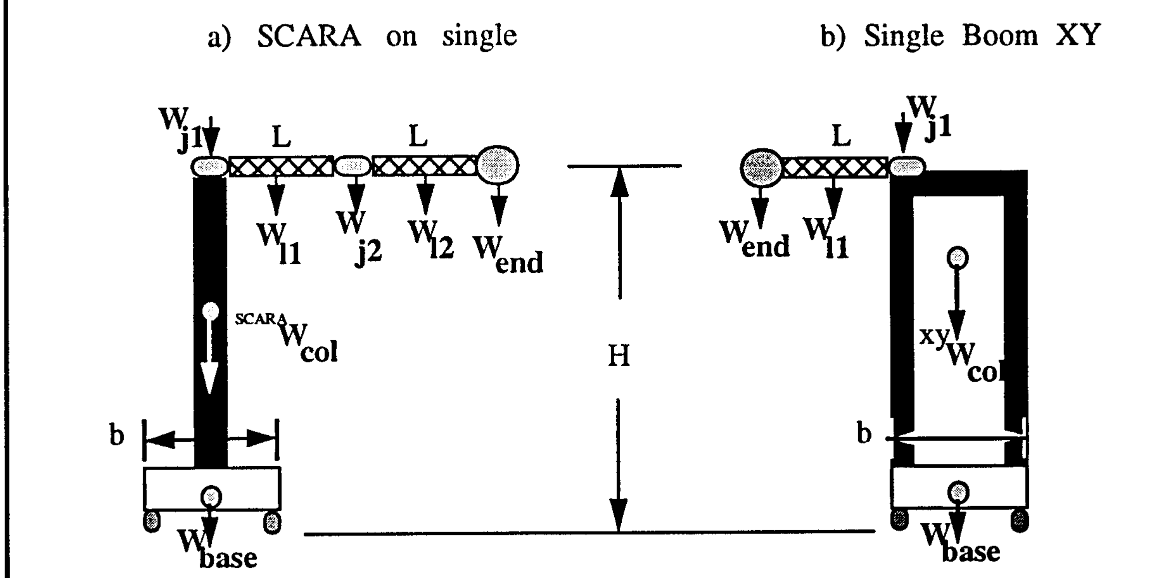

B.6 Tip-over stabilities

Tip-over stability properties are criteria used to compare the two different designs. It is quite clear that the XY base is more stable not only due to its reduced overhang because of reduced manipulator length necessary to reach the same number of tiles, but also because

of its increase in structural mass necessary to support and raise the XY table and manipulator assemblies. Even though the difference is not dramatic, the additional safety margin provided by the gantry design is worth noting.

The tip-over stability properties are another criteria by which to compare the two different designs. We have tabulated the required base and vertical column extension weight necessary to support a manipulator structure with a given weight distribution and a function of link length and base dimensions. It is quite clear that the XY-gantry system is inherently more stable.

In the stability analysis we assume b<=a, manipulators with differing lengths L, weights of the column structures, with W_{end}=25kgs, $W_{j1}=W_{j2}$=10kgs, h=0.15m, w/h=2/3, t=w/5, and H=4.25m, with $^{xy}W= {}^{xy}W_{base}+{}^{xy}W_{col}$ and $^{SCARA}W= {}^{SCARA}W_{base}+{}^{SCARA}W_{col}$ to be determined (Figure B-10).

The resulting base dimension a, and weights ^{xy}W and $^{SCARA}W$ as a function of link lengths L and base width b, stabilizes in the vertical plane as follows (Table 13):

Table 14 Base Tipover Parameters

	L $w/h\|_{manip}$=2/3, t=w/5, h=0.15m											
	0.5			0.75			1.00			1.25		
b [m]	1.22	1.52	1.83	1.22	1.52	1.83	1.22	1.52	1.83	1.22	1.52	1.83
^{xy}W [kg]	25.2	20.25	16.82	41.39	33.22	27.59	59.92	48.09	39.95	80.81	64.86	53.9
^{CARA}W [kg]	0.05	-13.4	-22.7	36.72	13.75	-2.07	82.89	48.54	24.87	138.5	90.92	58.1

B.7 Weight Estimates

System Mass

We have provided comparative weight estimates of the two systems between the large vertical column and the manipulation mechanism. The weight of the base is excluded in this part of the analysis. The relative contribution to the overall weight of the XYZ table to the manipulator linkage, motor, and endeffector structure is about 80%. The current estimate of endeffector weight is about 10 kgs, the 3 DOF wrist assembly and sensing platforms is about 15 kgs. The linkage structure weighs about 35 kgs, and the vertical Z extension is around 50 kgs. The total manipulator weight of around 110 kgs, comparing favorably with the 90 kg estimate for the XY table components and structures. Thus the entire XYZ and manipulator assembly is currently estimated to weigh around 200 kgs. The vertical gantry elevating mechanism has to raise a total mass of no more than 230 kgs; incorporating a safety factor of about 15%.

We have broken down a comparative weight estimate of the two systems into the weight of the large vertical column extension hardware, and the manipulation mechanism. The weight of the base is excluded in this part of the analysis.

2 DOF SCARA and 1 DOF Boom

The first clear difference in system weight is the actual weight of the 2 DOF SCARA and the 1 DOF boom. We assume a dual-link configuration, with rectangular cross-section, different width/height ratios, different lengths, and we set the motor/transmission/bearings/ sensor arrangement to weigh about 10 kgs. The endeffector is assumed to weigh no more than 25 kgs. This includes material, bearings, motors, transmissions, bearings, fasteners, interface plate, change-out mechanism, force sensor, cameras, rewaterproof tooling, and miscellaneous hardware.

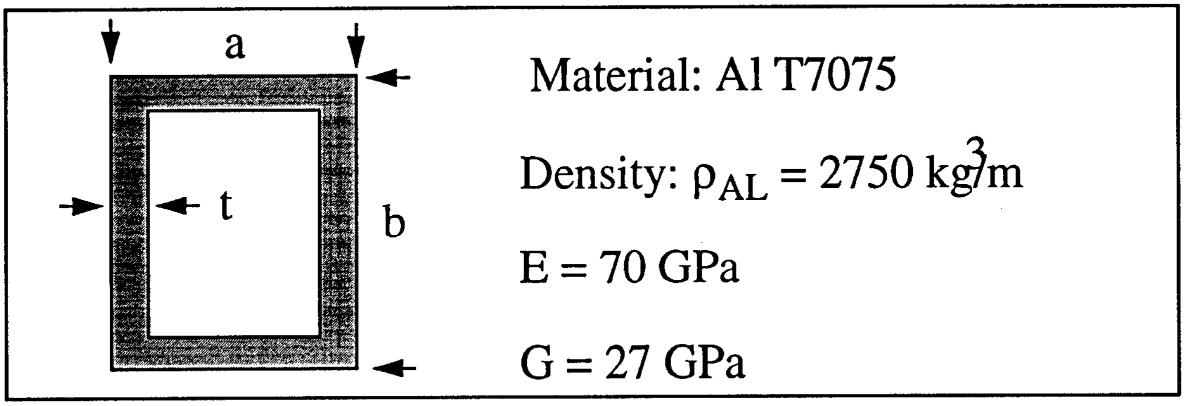

Figure B-11 Manipulator link cross section.

The assumed SCARA Link configuration with link lengths l_1=l_2, link-weights W_{l1} and W_{l2}, joint-weights W_{j1} and W_{j2}, and endeffector weight W_{end} is given in Figure B-12:

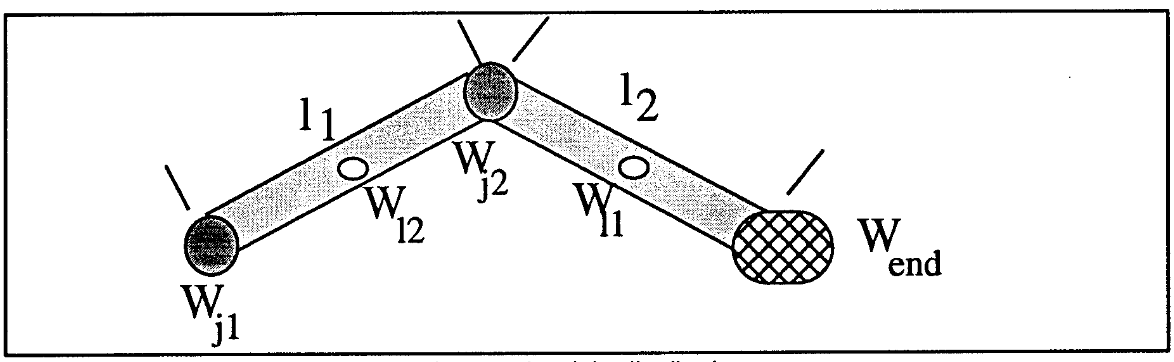

Figure B-12 Manipulator link dimensions and weight distribution.

For the 1DOF boom analysis, we assumed a single link of length l, with only a single joint at the shoulder with weight W_{j1}, similar individual link length l to the 2DOF SCARA with analogous weight W_{l1}, and the same endeffector weight W_{end}.

The resulting dual-link weights [kgs] for different a/b ratios, link height b, with t=a/5, l_1=l_2=l, and $w/l = \rho_{AL}(ab-(a-2t)(b-2t))$, yields:

Notice that the weight savings for a 1 DOF boom over a 2 DOF Scara of equivalent

Table 15 Manipulator Weight Estimates

a/b w/l[kg/m]	**b** [0.1m] 1.5 31.4	1.0 17.6	0.5 7.2	**b** [0.15m] 1.5 70.5	1.0 39.6	0.5 16.1	**b** [0.2m] 1.5 125.4	1.0 70.4	0.5 28.6
lam	**Weight** [kgs] - 2 DOF SCARA: Links, Joints, Endeffector								
0.25	60.7	53.8	48.6	80.3	64.8	53.0	107.7	80.2	59.3
0.5	76.4	62.6	52.2	116	84.6	61.1	170	115.4	73.6
0.75	92.0	71.4	55.7	151	104	69.1	233	151	87.9
1.0	108	80.2	59.3	186	124	77.2	296	186	102
1.25	123	89.0	62.9	221	144	85.2	359	221	117
1.50	139	97.8	66.5	257	164	93.3	421	256	131
lam	**Weight** [kgs] - 1 DOF Boom: Link, Joint, Endeffector								
0.25	42.8	39.4	36.8	52.6	44.9	39.0	66.4	52.6	42.2
0.5	50.7	43.8	38.6	70.3	54.8	43.0	97.7	70.2	49.3
0.75	58.5	48.2	40.4	87.9	64.7	47.1	129	87.8	56.5
1.0	66.4	52.6	42.2	106	74.6	51.1	160	105	63.6
1.25	74.2	57.0	43.9	123	84.5	55.1	192	123	70.8
1.50	82.0	61.4	45.7	141	94.4	59.1	223	141	77.9

individual length is substantial, as the link weight begins to dominate the overall weight budget for increasingly large work envelopes.

XY Table and Z extension

Based on actual weights of different table sizes from a commercial manufacturer, including the vertical travel with a weight of approximately 50 kgs., we can tabulate the XY weight and the overall weight (Table 15). The estimate below does NOT include the single or four-column elevating mechanism, but it does include 10kg per motor added to each DOF:

Table 16 System Weights

	BASE SIZE [m]			
Weight[kg]	1.82x1.22	2.13x1.52	2.43x1.82	2.74x2.13
XY	103.8	113.6	123.5	133.2
Z	50	50	50	50
Total	154	164	174	183

B.8 XY Table

X/Y TABLE COMPARISONS (HAUSER)

Table Size meters		Stage Length cm	Travel cm	Deflection cm	Weight kg	Cost dollars	XY Table # Tiles	Arm Length cm
1.82 X 1.22							12	
	X	183	98	0.22	55.7	10,925.55	101	
	Y	122	30	0.11	28.1	7,925.03		
2.13 X 1.52							33	
()	X	213	128	0.38	61.8	11,153.98		69.3
	Y	152	60	0.24	31.8	8,085.53		
2.43 X 1.82							61	
0	X	244	159	0.59	67.9	11,382.41		45.9
	Y	183	91	0.44	35.6	8,246.04		
2.74 X 2.13							98	
0	X	274	189	0.88	73.9	11,610.84		24.1
	Y	213	121	0.73	39.3	8,406.55		

NOTE:
- X deflection assumes 136kg. vertical load. Y deflection assumes 200lb. load vertical load.
- Arm length allows coverage of 3.48 m2 which equates to 150 tiles at 0.0232 m2/tile.
- Weights include 9kg per axis for motor and transmission.
- $2900.00 has been added to the price of the X/Y carriages to cover planetary gear, limit switches, cable carrier, misc. hardware.
- Number of tiles covered by XY Table based on acreage covered through stage travel only.
- Linear Lip seals rated to 50K km (estimated XY travel per single orbiter flow is about 5km for a 1.5x2m travel)

X/Y TABLE COMPARISONS (THOMSON)

Table Size meters		Stage Length cm	Travel cm	Deflection mm	Weight kg	Cost dollars
1.82 X 1.22						
	X	183	81.3	0.5	56.8	$3226.00
	Y	122	48.2	0.1	40.0	$2893.00
2.13 X 1.52						
	X	213	101.6	0.8	69.6	$3386.00
	Y	152	68.6	0.2	48.4	$3057.00
2.43 X 1.82						
	X	244	121.9	1.22	73.7	$3546.00
	Y	183	88.9	0.34	56.8	$3226.00
2.74 X 2.13						
	X	274	142.2	1.74	82.0	$3716.50
	Y	213	109.2	0.55	65.3	$3386.00

NOTE:
- X deflection assumes 136kg. vertical load. Y deflection assumes 90kg. load vertical load.
- Cost includes steel lead screw and shaft (not corrosion proof), shaft supports, and bearing pillow blocks.
- Weights include shaft support base. Base is Aluminum, 90mm square with 5mm wall. Aluminum weight/length = w = 6g/mm. Total weight is w times the total stage lengths
- Travel allows room for shaft-rail protective nylon/neoprene bellows (consume 17% of travel at either end).
- Extra set-up, assembly, AL support base material, and engineering costs are NOT included in the above estimate (add 200%)

Functional and Mechanical Components

The most important requirements for the horizontal 1 DOF boom or 2 DOF SCARA manipulator configuration are that the joint compliance be kept to a minimum, and that the system have extremely small, if not zero, backlash. Commonly available transmissions that fulfill such requirements include high precision planetary gear-boxes. Manufacturers include: Neugart, Bayside Controls, and Micron. Suitable variants of cycloidal reducers include those made by Harmonics Drive, Dojen, Kamo, and Sumitomo. The choice will be made based on failure rates and relative performance differences. A tentative selection is a Dojen cycloidal cam reducer. Their availability in a large variety of power and reduction sizes makes them even more attractive. These transmissions can be optimized upon assembly to have a minimum of friction while retaining zero backlash and extreme rigidity.

The motors will be brushless DC motors with multiple power windings and resolvers and an absolute encoder. There are many manufacturers that can deliver brushless DC motors, but none that has redundancy in terms of windings or electronics. E.g Moog, PS, Seiberco, Inland, MFM, Schaffer Magnetics, Hathaway, Pittman and others. We will also include a brake in the horizontal manipulator mechanism to lock the arm during servicing resulting in small power requirements, and providing added safety levels during an emergency. Such companies are numerous, but they differ mainly in the quality, packaging and pricing of their products. A comparison evaluation will be performed in order to select the most appropriate product and manufacturer.

The materials to be used as structural elements for the link(s) will most probably be Al 7075 or an anodized AL 6061 alloy. We will select a rectangular cross-section with a certain wall-thickness to minimize weight and maximize structural rigidity. Statically due to gravity, and dynamically due to accelerations in the horizontal plane. Joints will be machined separately and become a single piece to be attached to the structural link via a mechanical fit secured by pins and other fasteners. No welding is planned which will reduce warping and the introduction of residual stresses.

All electronic connections can be run on the inside of the manipulator links to reduce clutter and snagging of wires. The fluid (DMES) provided to the endeffector will be routed on the outside of the structure to ease access and removal. Collision detection and avoidance sensors such as piezo-electric, infrared and acoustic, will be placed in several spots on the outside of the manipulator link structure. Cabling will be run internally to the manipulator link, with partial processing of such sensor data to be performed by electronics located within the link structure. Such local processing reduces wire count, data corruption and allows the addition of other sensors. These sensors might provide additional safety and collision detection/avoidance through such devices as mechanical 'whiskers' or force-threshold strain-gauge measurement inputs.

B.9 Reach and Dexterity

Table 17: Reach and Dexterity

			10 deg tangent plane					45 deg tangent plane					
X	S	L_{ii}	D_{ii}	L_i	D_i	O	P	D_{ii}	L_i	D_i	O	P	
a	0 6 12	50	0.83 12.8	50.2 52.3	0.84 13.0	-39.8 -39.8	-21.4 -19.3	7.9 20.0	58.0 70.0	11.2 28.2	-24.2 -24.2	2.0 14.0	NOSE
b	0 6 12	50	3.0 15.0	50.5 52.3	3.1 15.3	-11.0 -11.0	-41.5 -39.4	16.0 28.0	66.0 78.0	22.6 39.6	22.3 22.3	7.3 19.3	
c	0 6 12	50	4.0 16.0	50.7 52.3	4.1 16.3	6.9 6.9	-47.3 -45.2	18.3 30.3	68.3 80.3	25.8 42.8	47.0 47.0	10.4 22.4	
d	0 6 12	50	5.1 17.1	50.9 53.0	5.2 17.4	18.3 18.3	-59.0 -57.9	21.5 33.5	71.5 83.5	30.5 47.4	73.6 73.6	16.9 28.9	MID
e	0 6 12	50	5.6 17.6	51.0 53.1	5.7 17.9	33.5 33.5	-62.9 -60.8	20.4 32.4	70.4 82.4	28.9 45.8	96.4 96.4	19.4 31.4	
f	0 6 12	50	6.6 18.6	51.2 53.3	6.7 18.9	61.9 61.9	-57.9 -55.7	15.3 27.3	65.3 77.3	21.6 38.6	119 119	13.7 25.7	
g	0 6 12	50	6.9 18.9	51.2 53.3	7.0 19.2	120 120	-41.7 -39.6	13.6 25.6	63.6 75.6	19.3 36.2	161 161	11.6 23.6	WING
h	0 6 12	50	9.2 21.2	51.6 53.7	9.3 21.5	261 261	-30.5 -28.4	13.5 25.5	63.5 75.5	19.1 36.1	292 292	12.4 24.4	
i	0 6 12	50	10.1 22.1	51.8 53.9	10.3 22.5	390 390	-14.7 -12.5	15.2 27.2	65.2 77.2	21.5 38.5	404 404	13.7 25.7	
j	0 6 12	50	15.3 27.3	52.7 54.8	15.6 27.8	408 408	-8.0 -5.9	17.3 29.3	67.3 79.3	24.5 41.5	419 419	17.3 29.3	TAIL

B.10 Power Analysis

To facilitate a power analysis for the XY gantry manipulator, a free-body model, which simulates the manipulator as a series of point masses connected by massless joints, has been constructed. This model is shown below

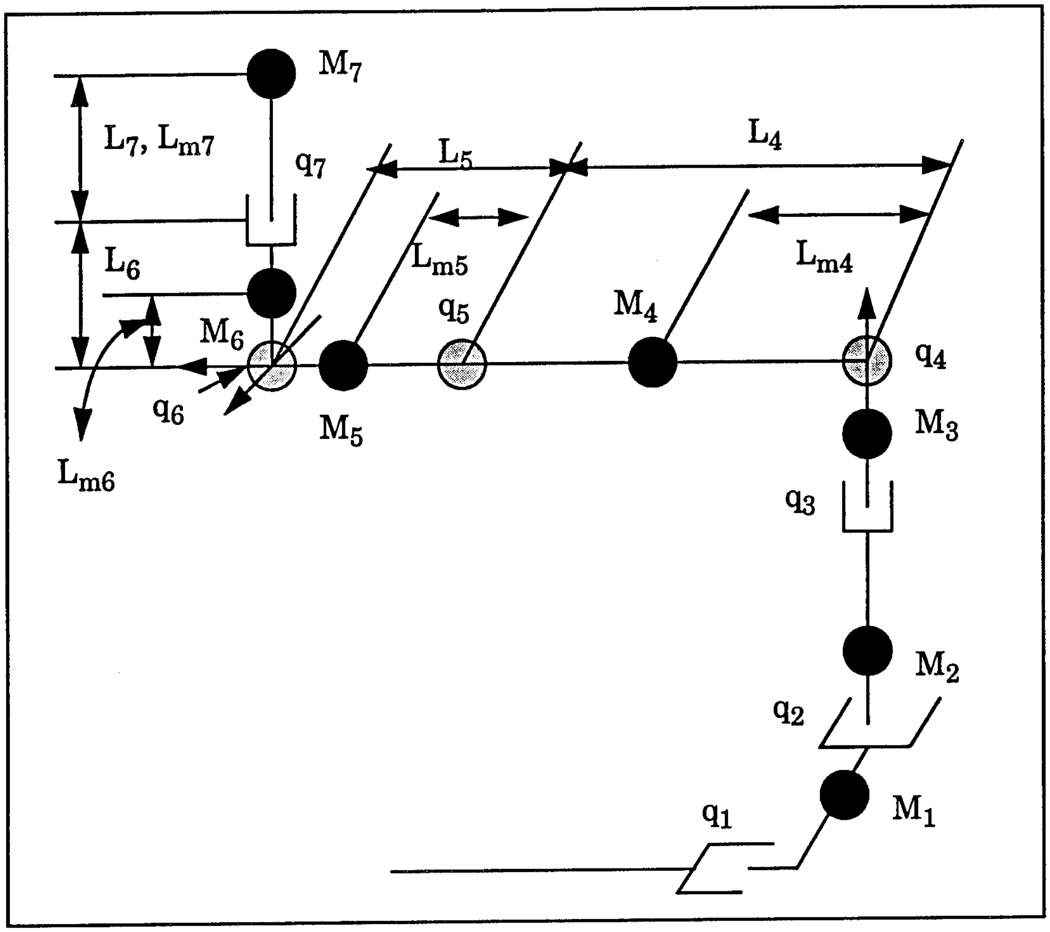

Figure B-13 XYZ gantry and manipulator schematic.

Since the first three joints of the manipulator are orthogonally-acting prismatic actuators, their lengths are irrelevant as far as total system power is concerned, although proper sizing of these actuators is critical to performance.

We will divide this analysis into roughly two parts. For joints which act in the horizontal plane (q_1, q_2, q_4), we will compute work performed by each joint using a constant acceleration profile. For joints which operate primarily in the vertical plane (q_3, q_5, q_6, q_7) we will compute work performed by each joint based on change in potential energy over time. For simplicity, we will make the following assumptions:

- the workspace of the manipulator is evenly covered with tiles.
- the rotational inertia about the shoulder is constant; it actually changes with wrist-forearm actuation, but this effect is negligible.
- the major Z motion is mechanically locked in place for the duration of the task; all other joints will be constantly servoed.
- the system is non-regenerative; i.e. energy exerted to raise a given mass is not recovered when that mass is lowered.
- multi-joint coupling and frictional forces are minimal.

- times for various moves are those reflected in the task scenarios described earlier.

Given the free-body model, and the assumptions above, we can calculate the masses and inertias which must be moved by the actuators. This is reflected in the table below:

- q_1 (x Motion) ->M_1+M_2+M_3+M_4+M_5+M_6+M_7
- q_2 (y motion) ->M_2+M_3+M_4+M_5+M_6+M_7
- q_3 (major z motion) ->M_3+M_4+M_5+M_6+M_7
- q_4 (shoulder rotation) ->I_4+I_5+I_6+I_7
- q_5 (wrist pitch) ->I_5+I_6+I_7
- q_6 (wrist yaw) ->I_6+I_7
- q_7 (minor z motion) ->I_7

The analysis is as follows: given a basically flat area of the shuttle bottom, how much energy is expended to service all tiles in the manipulator's workspace. The horizontal workspace of the manipulator forms a rectangle with rounded corners and its area is given by:

$$A_{reach} = L_x \cdot L_y + L_x \cdot (L_4 + L_5) + L_y \cdot (L_4 + L_5) + \pi (L_4 + L_5)^2 \qquad \textbf{Eq. B-17}$$

If we divide this area by the mean area of a tile, we get the number of service cycles performed. The power required per service cycle is broken up into the power required to position the manipulator end effector normal to the tile, and the power necessary to raise the tooling into contact with the shuttle bottom.

Tile coverage during a servicing task is depicted in Figure B-14 below. First, tiles in region I are covered in a raster scan manner, from top to bottom, with no shoulder actuation. A 90° shoulder rotation is then performed, and region II is serviced from bottom to top. Region III is then serviced using a series of sweeping shoulder motions. the manipulator then translates to region IV, and services this using sweeping shoulder motions. Region V is then serviced from top to bottom, using raster motions. Region VI is then serviced using sweeping motions, region VII with raster motions, and region VIII with sweeping motions.

The energy necessary to raise tooling into contact is constant for the flat acreage region we are considering. It is determined by the stand-off distance we maintain for the tooling, and the mass of the payload

$$U_{tool} = 2M_7 \cdot g \cdot D_{stand} \qquad \textbf{Eq. B-18}$$

The energy necessary for manipulator positioning is computed separately for each region.

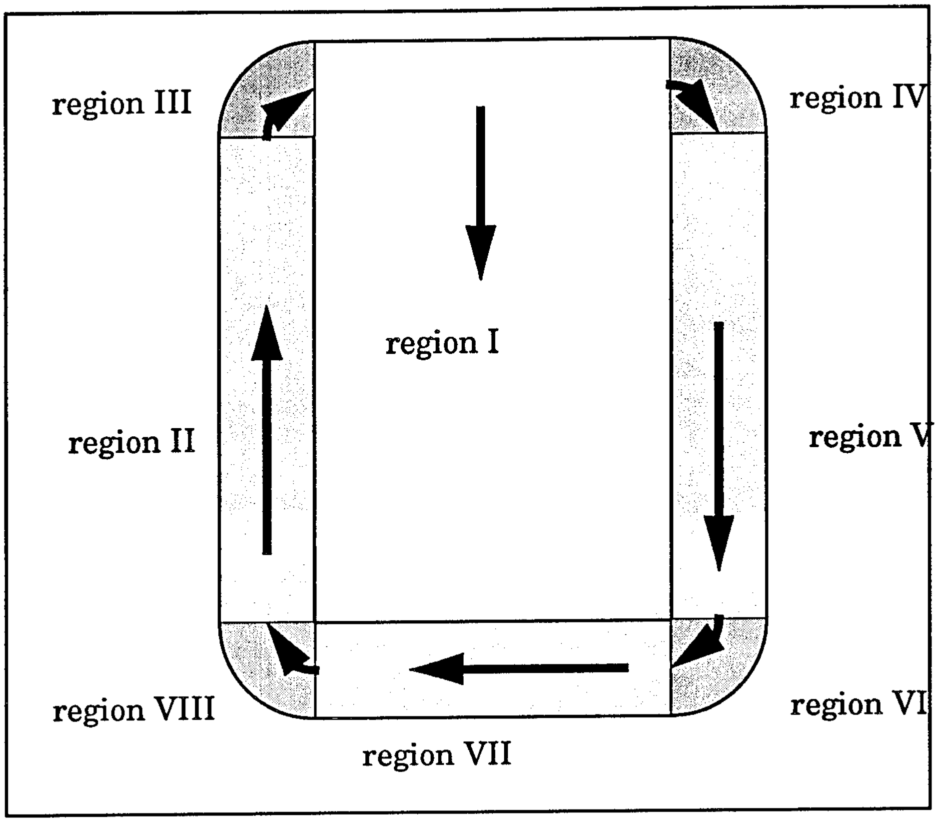

Figure B-14 Workspace coverage scheme.

For the rectangular regions, no shoulder actuation is performed. The manipulator is simply scanned back and forth across the shuttle surface. The energy necessary to perform this operation (per tile) is given by the force required to achieve the desired acceleration, multiplied by the distance over which this force operates. This is given by

$$U_{xy} = M_{xy} \cdot \frac{D^2_{tile-to-tile}}{t^2_{tile-to-tile}} \qquad \textbf{Eq. B-19}$$

where M_{xy} is the sum of the masses moved by the gantry

For the circular regions, shoulder actuation must be performed in addition to XY motion. Since the region will be serviced in a series of sweeping motions with XY moves in between, the number of XY moves is given by the radius of the sweep, divided by the diagonal distance across a tile:

$$N_{xy} = \frac{(L_4 + L_5)}{\sqrt{A_{tile}} \cdot 2} \qquad \textbf{Eq. B-20}$$

The amount of energy necessary to move the manipulator is given the previous expression for XY move energy, except we are now moving diagonally

$$U_{xy_{diag}} = M_x \cdot \frac{D^2_{tile-to-tile}}{t^2_{tile-to-tile}} \sqrt{2} \qquad \textbf{Eq. B-21}$$

The amount of energy necessary to sweep the manipulator from one tile to an adjacent tile is given by the torque required to accelerate the mass, multiplied by the radial length of the arm

$$U_{sweep} = I_{shoulder} \cdot \frac{A_{tile}}{(L_4 + L_5)\, t^2_{tile-to-tile}} \qquad \textbf{Eq. B-22}$$

where $I_{shoulder}$ is the inertia about the shoulder axis.

With these equations, we can compute the amount of energy necessary to perform servicing. For each region, we can compute the number of tiles which would are serviced for a given region:

$$N_{tiles_i} = \frac{Area_{region_i}}{Area_{tile}} \qquad \textbf{Eq. B-23}$$

This number, multiplied by the energy-per-tile for that region, gives us the energy required. We are now at a point where can begin to determine the actual power draws for a given manipulator. Realistic masses and lengths have been selected for the various elements of the manipulator, and are shown in Table 18. The tile area has been fixed at 232.26cm^2, and the distance between tiles at 31 cm. Tile-to-tile transition time is set at 2.0 seconds, and standoff distance is set at 15.24cm. The various energies are calculated below:

$$U_{tool} = 29.87j$$
$$U_{xy} = 2.8j$$
$$U_{xy_{diag}} = 4.07j$$
$$U_{sweep} = 1.11j$$
$$A_{rect} = 11.68m^2$$
$$A_{circle} = 4.83m^2$$

Table 18 Parametric Variables and Numerics

Parameter	Quantity	Units
M_1	36	Kg
M_2	11	Kg
M_3	30	Kg
M_4	50	Kg
M_5	7.4	Kg
M_6	7.4	Kg
M_7	10	Kg
L_4	1.0	m
L_{m4}	0.5	m
L_5	.24	m
L_{m5}	.125	m
L_6	.24	m
L_{m6}	.125	m
L_7	.30	m
L_{m7}	.30	m
L_x	1.4	m
L_y	2.0	m
$I_{shoulder}$	48.2	Kgm^2
M_{xy}	152.8	Kg

A total of 6.3kW-h is required to service all of the tiles in the manipulator's workspace,. The total number of tiles serviced using this energy is about 710, which is about 3.3 Kw per service cycle (per base move) - this translates to a total of 69.7kW per entire shuttle tile rewaterproofing flow (15,000 tiles in 40 hrs.).

This is a first cut at a power consumption estimate and to be conservative a safety factor of 2 to 4 is used. Thus, the maximum continuous power consumption of 350 to 400 Watts is realistic with peak power requirements not exceeding 500 Watts.

We can refine this estimate by thinking in terms of the torque requirements for the various tasks, rather than the changes in energy. Motor speed, measured in revolutions per minute, is more a function of voltage, while the torque produced is basically a function of current. For a constant voltage, a higher current produces higher torques, which produce accelerations in the system. This type of analysis requires us to assign some gearing ratios to the various actuators to determine the torque referred to the shaft, as well as deciding on some of the inner workings of the various actuators. For this next analysis, we will use timing-belt style drives for the XYZ motion as well as the minor Z motion. It should be mentioned that the actual mechanisms for actuation have not been decided upon; we use these types of mechanisms only to help us estimate the various torques and power draws of the system.

For the rotary actuators, rotary servo motors with a 100:1 reduction gearing are used; friction and gearing losses are modelled by a mechanical transfer efficiency, while

electrical to mechanical conversion is modelled by an electrical transfer efficiency or impedance match. This is illustrated by the simple plant model shown below, which transfers an input current, through a motor and gearbox, into an output torque.

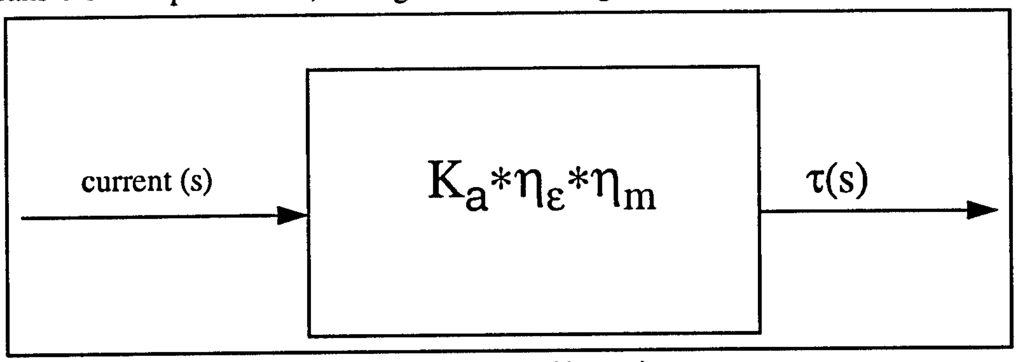

Figure B-15 Model of linear motor with gearbox.

The timing belt drive linear actuators are modelled by a linear motor model with a pulley coupled to the output shaft. Linear forces are tangential to the pulley. This is shown by the plant model below:.

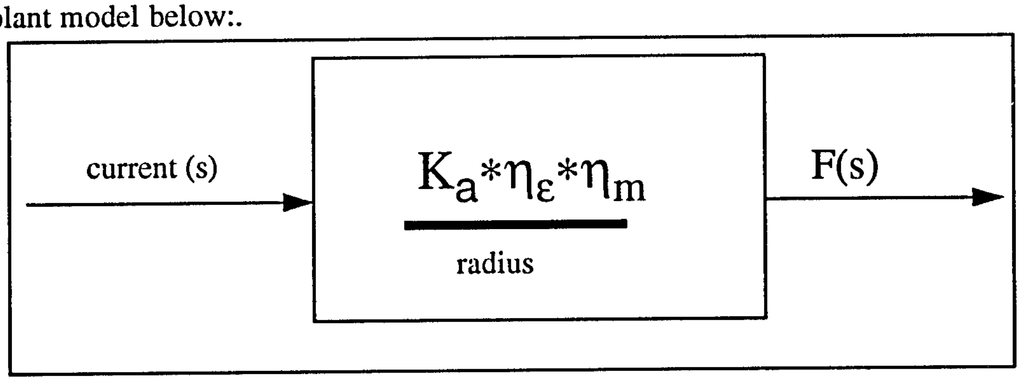

Figure B-16 Model of linear motor with pulley and gearbox

The Major-Z axis motion at the shoulder has a 100:1 reduction, while the Minor-Z axis motion at the wrist goes through a 10:1 reduction. This prevents an excessive force at the toolpoint of the robot.

By assuming constant acceleration during various portions of the task, we can determine the total amount of torque, and from this, the total amount of current, drawn by the motors. Since voltage is kept constant, we can determine how much power the system is drawing. We use the same values for tooling stand-off distance (15.24 cm) and tile-to-tile distance (31 cm.).

In order to raise the tooling into place, a linear force is needed to overcome the gravitational force on the tooling. The value of this force depends on how quickly the

tooling must be moved; faster moves require larger accelerations, which in turn require larger forces. The acceleration required to raise the tooling into place is given by:

$$a_{tool} = \frac{4D_{stand}}{t_{raise}^2} \qquad \text{Eq. B-24}$$

The force required to raise the tooling is:

$$F_{raise} = M_7(a_{tool} + g) \qquad \text{Eq. B-25}$$

where g is the acceleration due to gravity. The motor current necessary to achieve this linear force can be calculated by using the motor models previously described. Since the minor z motion has a 10:1 reduction between the motor and the actual linkage, only 1/10th of this force is referred to the pulley. The overall motor power necessary to achieve this force is thus given by:

$$P_{raise} = \frac{F_{raise} \cdot gearing \cdot r_{pulley}}{K_a \eta_e \eta_m} v_{motor} \qquad \text{Eq. B-26}$$

Once the tooling is in contact with the shuttle, it must be held there while servicing is performed. Servicing itself produces its own set of forces, since liquids and gases are forced against the shuttle surface. The power necessary to perform this portion of the task is given by:

$$P_{service} = \frac{(M_7 g + F_{contact}) gearing \cdot r_{pulley}}{K_a \eta_e \eta_m} v_{motor} \qquad \text{Eq. B-27}$$

The force necessary to lower the tooling is given by:

$$F_{lower} = M_7(a_{tool} - g) \qquad \text{Eq. B-28}$$

and the power to lower the tooling is computed in the same manner as the lifting power.

We can compute similar power measures for the rotary shoulder and XY gantry motions. For the XY gantry, the entire mass of the manipulator must be moved from one service

station to another service station in a given amount of time. The acceleration for this maneuver is determined by the distance to be moved, and the time allotted for the move:

$$a_{manip} = \frac{4D_{tile-to-tile}}{t^2_{tile-to-tile}} \qquad \textbf{Eq. B-29}$$

The force and power necessary for this move are calculated as shown previously, except that there are no forces due to gravity since the motion is horizontal.

The angular acceleration needed for shoulder rotations is determined by the length of the arm, and the time allotted for a tile-to-tile move:

$$\frac{\phi}{2} = \frac{1}{2} \cdot \frac{s}{r} = \frac{1}{2}\ddot{\omega}\left(\frac{t}{2}\right)^2 \Rightarrow \ddot{\omega} = \frac{4D_{tile-to-tile}}{t^2_{tile-to-tile}(l_4 + L_5)} \qquad \textbf{Eq. B-30}$$

The product of this acceleration and the rotational inertia of the arm give us the torque necessary to accelerate and decelerate the arm.

In the following table is a breakdown of the various types of maneuvers which the manipulator must perform, along with force/torque requirements at the motor shafts, toolpoint accelerations, masses/inertias which must be accelerated, gearing ratios, and the respective power draws in the system during a typical service cycle.

NOTE - torques for motors are actual torques referred to motor. They take into account a 75% electrical transfer efficiency η_e and 75% mechanical transfer efficiency η_m. The armature constant K_a is 1.5 Nm/A.

Table 19 Power an Torque Requirements for various Maneuvers

Task Description	Torque at Motor (Nm)	time (s)	gear ratio	power (W) @24 V	energy (W-s)	η_e,η_m	K_a (N-m/A)
Vertical lift of tooling (5.24cm lift of 10kg)	2.8@elbow lift	0.5	10:1	269	134.4	0.75,0.75	0.25
Hold tooling in place against 30N contact force	2.8@ elbow lift	3.0	10:1	269	806.2	75,75	0.25
Retraction of tooling (15.24cm drop of 10kg)	68@elbow lift	0.5	10:1	161.3	80.6	75,75	0.25

Table 19 Power an Torque Requirements for various Maneuvers

Task Description	Torque at Motor (Nm)	time (s)	gear ratio	power (W) @24 V	energy (W-s)	η_e, η_m	K_a (N-m/A)
Lateral move of manipulator using only XY base (31cm move of 128kg)	0.088@ XY gantry	2.0	100:1	8.4	16.9	75,75	0.25
Diagonal move of manipulator using only XY base (44cm move of 128kg	0.128@ XY gantry	2.0	100:1	12.3	24.576	75,75	0.25

B.11 Fault Tolerance and Redundancy

There are several components and subsystems that are crucial in the performance and safing of the eventual rewaterproofing contact task(s) on the shuttle tiles. Below is a list of those components and the associated steps deemed necessary to introduce levels of redundancy and fault tolerance in order to guarantee performance in the face of probable failures and insure safety to the shuttle in case of an unexpected failure or situation. The individual components in need of such considerations are:

Table 20 Components and fault tolerance features

Component	Effect and Corrective Action
Motor	• Brushless DC motor to avoid sparks and wear • Multiple (dual/triple) windings for power redundancy • Hall Effect, Resolver (optical, inductive) for sensing redundancy • Multi-layered hardware controller for redundant power windings and sensor types
Actuator	• Maximized rigidity to avoid deflection and failure • Mechanical factor of safety (2 to 4) to increase MTBF and probability of failure. • Added input brake to avoid uncontrollable runaway • No real intention yet to parallel-up dual drives as parts are humanly serviceable and mainly in need of safing
Tool Extender	• Light-weight and rigid to provide fast dynamic response • Highly backdriveable to increase accuracy and response of force tool-tip interaction force control • Single/dual base-mount force sensors between actuator and tool • Force measurement and control at endeffector nozzle-tip via strain-gauged nozzle extension

Table 20 Components and fault tolerance features

Component	Effect and Corrective Action
Proximity Sensors - electronic	• Light-weight and rigid to provide fast dynamic response • Highly backdriveable to increase accuracy and response of force tool-tip interaction force control • Single/dual base-mount force sensors between actuator and tool •Force measurement and control at endeffector nozzle-tip via strain-gauged nozzle extension
Collision Sensors - mechanical	• Multiple cantilevered spring-loaded limit-switch whiskers to detect shuttle contact and cut power, apply brakes and emergency tool retract • Light-weight contact switch skirt around links to safe against hard collisions

B.12 Discussion

The design is a single shoulder -jointed 1 DOF horizontal boom mounted on an elevated gantry-style XYZ-table. The length of the boom will be determined by the amount of necessary overhang and reach required to cover a minimum number of tiles and reach into cluttered or confined workspaces. Issues and conclusions drawn from each specific analysis include:

- Horizontal Boom or SCARA Manipulator Configuration
- Positioning Accuracies of +/- 2mm are necessary and feasible and largely dominated by vision accuracies, mechanical lash, and affects the requirements for injection tooling dimensioning.
- The workspace covered by a 2 DOF SCARA on a single elevating column is markedly smaller compared to an XY table with a horizontal boom of identical individual link length.
- Joint compliance dominates the resonance of the manipulator system (<35 Hz). Structural vertical and horizontal resonances for the XY gantry (400 Hz) are much higher frequencies than for the single elevator 2 DOF SCARA configuration (100 Hz). Single link boom configurations for the XY gantry should have a maximum length to minimize effects of joint compliance.
- Dynamic and static forces during moves and servicing are not excessive and are necessary to size components. A typical 1 second transition time from tile to tile is physically achievable with accelerations below 1.5m/sec^2.
- Base stability will not be as important for the XY gantry robot due to reduced overhang of manipulator and payload.
- Typical arm weights for 1 DOF booms are around 40 kgs, versus 70 kgs. for the 2 DOF SCARA to cover similar workspaces.

- Mechanical component selection is not too critical, as most components will be commercially available. Special attention will have to be given to redundant and fault-tolerant motors and actuators (transmissions), and the related sensing and computing hardware and software requirements.

The conclusion is that mechanical implementation of either design is feasible and can meet the design specs. On the other hand, we felt it was important to favor a more robust, rigid and large work envelope design requiring less design time and effort. An effort which could meet and exceed the required design specs to result in an inherent design specification safety margin or to meet future TPS servicing specs which have not been finalized or formulated.

The moderate number of additional parts does not imply increased complexity since it will use proven technologies. Selecting an existing single-column elevating mechanism with mechanical integrity, reach, integrity and feasible precedence proved to be difficult, yielding only a single component manufacturer whose product was new and lacked a track record and reliability data. Other conventional mechanisms required overly increased levels of mechanical complexity and packaging. The issues led to to the selection of a single boom manipulator with a sensing and tooling endeffector positioned by an XYZ linear stage device mounted on a four-column elevator gantry which was part of the mobile base.

C. System Inputs and Outputs

The inputs and outputs necessary for each of the system functions is listed below.

In addition, the bandwidth requirements, expected frequency, and necessary reaction latency time are listed. Low, Medium and High in the table are defined as:

- Bandwidth:
  - Low: under 10kbps (kilo bits per second)
  - Medium: 10kbps - 100kbps
  - High: above 100kbps
- Frequency:
  - Low: up to 1Hz or for signals that are very rarely generated
  - Medium: 1Hz - 10Hz
  - High: above 10Hz
- Latency:
  - Low: under 50ms
  - Medium: 50ms - 500ms
  - High: above 500ms

These estimates were used to determine the degree of concurrency and number of processors needed to meet these requirements, as described in section 6..

Health Maintenance:

Inputs	Bandwidth/Frequency/Latency
Temperature	low/low/large
Roll and Pitch	low/low/large
DMES level	low/low/large
Communications link status (radio and/or tether)	low/low/large
Hardware heartbeat	low/low/large
Software heartbeat	low/low/large

Outputs	Bandwidth/Frequency/Latency
Signal to operator terminal	low/low/large
Audible alarm at robot	low/low/large
Motor shutoff	low/low/medium

Configuration Control:

Outputs	Bandwidth/Frequency/Latency
Wheel motor commands	medium/high/small
Manipulator actuator commands	medium/high/small
Effector commands	medium/high/small
Sensor commands	medium/high/small

Planning:

Inputs	Bandwidth/Frequency/Latency
Encoder readings	low/high/small
Global position of base	low/low/large
Current location (operator input)	low/low/large
Tile map	high/low/large
Tile ID	low/medium/medium
Desired base position (operator input)	low/low/large
Permanent obstacle locations	medium/low/large
Joystick control	low/low/small
Detected obstacles for mobile base	low/low/medium
Detected obstacles for manipulator	low/low/small

Database Access / Manager / Communication:

Input	Bandwidth/Frequency/Latency
Pre-existing tile images	high/low/medium
Newly sensed tile images	high/low/medium

Outputs	Bandwidth/Frequency/Latency
Damaged tile reports	low/low/large
Newly sensed tile images	high/low/large
Unreachable/serviced/unserviced tiles	low/low/large

Human Interface:

Inputs	Bandwidth/Frequency/Latency
Orbiter configuration	low/low/small
Mission specs	medium/low/small

Tile surface	high/low/small
Force feedback	low/high/small
DMES leak detection	low/low/medium
Limit switches	low/low/small
Bump sensors	low/low/small
Whiskers	low/low/small
Operator kill switch	low/low/small
Operator inputs (joystick/mouse)	low/low/medium

Outputs	Bandwidth/Frequency/Latency
Mobile base location	low/low/large
Arm configuration	low/low/medium
Obstacle locations	low/low/large
Tile partitioning map	low/low/large